

Copyright
by
Katherine Alexis Crawford
2014

**The Dissertation Committee for Katherine Alexis Crawford Certifies that this is the
approved version of the following dissertation:**

**Direct Comparison of Homogeneous and Heterogeneous Palladium(II)
Catalysts for Suzuki-Miyaura Cross-Coupling Reactions**

Committee:

Alan H. Cowley, Supervisor

Simon M. Humphrey, Co-Supervisor

Richard A. Jones

Bradley J. Holliday

Ben A. Shoulders

John G. Ekerdt

**Direct Comparison of Homogeneous and Heterogeneous Palladium(II)
Catalysts for Suzuki-Miyaura Cross-Coupling Reactions**

by

Katherine Alexis Crawford, B.S. Chem

Dissertation

Presented to the Faculty of the Graduate School of

The University of Texas at Austin

in Partial Fulfillment

of the Requirements

for the Degree of

Doctor of Philosophy

The University of Texas at Austin

May 2014

Dedication

To my family-

This is *for* you. This is *because* of you. It wouldn't mean anything *without* you.

Acknowledgements

Thank you, first of all, to my research adviser, Professor Alan Cowley, whose dedication to the field has been a constant inspiration for me. His passion for chemistry is contagious; Sundays in the laboratory were surprisingly enjoyable because he was always there to keep me company. I will be forever grateful for this experience and consider it a great honor to have worked for Professor Cowley, the “Main Group King”.

I would also like to thank Professor Simon Humphrey, who allowed me to become a member of his group four years into my graduate studies. His expertise on catalysis was invaluable and I am extremely thankful for his assistance on my research projects. Thank you for challenging me.

To the Inorganic Professors, Richard Jones, Bradley Holliday, and Michael Rose, thank you very much for your suggestions and critiques during Saturday morning chalk talks. The experience was completely terrifying, but I am unbelievably appreciative for the opportunity to develop the necessary skills to properly present a research project. I would specifically like to thank Professor Jones and Professor Holliday for agreeing to serve on my committee.

I am indebted to the Cowley group, both past and present group members, especially Sarah, Dan, and Owen Maria. Thank you for all your Borat impressions and Q’doba Mondays. I would also like to thank Lauren, Beth, Kelly, and Stephany for their constant support and encouragement. I feel privileged to have made life-long friends with each and every one of you.

I am so thankful that I have such an incredible family. Thank you, Mom, Dad, Brittany and Brendan, for always supporting me, and for giving me strength when I wanted to quit. I am extremely grateful for your unconditional love. I would also like to thank Chelsea and Caitlin for being my best friends, and for forgiving me when I let too much time pass between conversations. To the Smoz girls, “come and knock on my door” always and forever.

Lastly, to the best thing that has ever happened to me, thank you for encouraging me during the hard times, for the cheesecake during the happy times, but most importantly, for the laughter every time in between. I love you, Joshua David.

Direct Comparison of Homogeneous and Heterogeneous Palladium(II) Catalysts for Suzuki-Miyaura Cross-Coupling Reactions

Katherine Alexis Crawford, Ph.D.

The University of Texas at Austin, 2014

Supervisors: Alan H. Cowley and Simon M. Humphrey

Abstract: The syntheses and catalytic properties of four new 1,2-acenaphthenyl *N*-heterocyclic carbene-supported palladium(II) catalysts are presented. The acenaphthenyl carbene can be prepared using either mesityl or 2,6-diisopropyl *N*-aryl substituents. In addition, two new heterogeneous analogs were synthesized with 2,6-diisopropyl *N*-aryl substituents that were anchored through the backbone to an insoluble silica-support. Comprehensive catalytic studies of the Suzuki coupling of aryl halides with aryl boronic acids were carried out. In general, the homogeneous diisopropyl-functionalized catalyst was found to exhibit superior selectivity and reactivity. A comparison of the performances of the aforementioned catalysts in toluene, dichloromethane and aqueous solutions are also presented. In organic solvents, the catalysts were found to be proficient for the homogeneous Suzuki coupling of aryl iodides, bromides and chlorides with boronic acids at low temperatures (35–40 °C). Similar reactions that were carried out in aqueous media resulted in the formation of insoluble colloidal catalytic species. Nevertheless, these species still retained high activities in terms of in the Suzuki reaction with aryl chlorides. Moreover, the heterogeneous Pd precipitates can be easily recovered for subsequent use by means of filtration. The activation energies that were determined

for the aryl bromide-based Suzuki reactions were found to fall in the range, 159.2–171.2 kJ mol⁻¹ in organic solvents and 111.3–115.9 kJ mol⁻¹ in water. The corresponding activation energy for the aryl chloride was found to be 321.8 kJ mol⁻¹ in aqueous media using the homogeneous diisopropyl-functionalized carbene catalyst. Conversely, the heterogeneous catalyst exhibited reactivity toward aryl iodides and bromides exclusively, and required significantly higher temperatures and catalyst loadings in both toluene and water. Additional experimental trials that were performed in tetrahydrofuran solution at lower temperatures resulted in substantially larger catalytic conversions. The heterogeneous catalyst allowed for easy separation and recovery. However, the catalyst exhibited a significant decrease in reactivity toward the aryl halides after two consecutive trials.

Table of Contents

List of Tables	xiii
List of Figures	xxiv
List of Schemes	xxxv
Chapter 1: Suzuki-Miyaura Coupling: <i>a broad overview of homogeneous and heterogeneous Suzuki-Miyaura cross-coupling catalysis</i>	1
1.1 Introduction	1
1.1.1 History	1
1.1.2 Mechanism	4
1.1.3 Current Applications	11
1.2 Homogeneous Catalysis	16
1.2.1 Ligands	16
1.2.1.1 Phosphine Ligands	17
1.2.1.2 N-Heterocyclic Carbene Ligands	30
1.2.1.3 Mixed Phosphine and NHC Ligands	44
1.2.2 Media	52
1.3 Heterogeneous Catalysis	57
1.3.1 Polystyrene and Other Polymer Supports	58
1.3.1.1 Polymer-supported Phosphine Ligands	58
1.3.1.2 Polymer-supported N-Heterocyclic Carbene Ligands	65
1.3.2 Silica	68
1.3.2.1 Silica-supported Phosphine Ligands	68
1.3.2.2 Silica-supported N-Heterocyclic Carbene Ligands	72
1.3.3 Media	78
1.4 Homogeneous vs. Heterogeneous Catalysis	82
1.4.1 Identification of the Active Species	83
1.4.2 Homoeopathic Systems	85

Chapter 2: <i>Bis(imino)acenaphthene</i> (BIAN)-supported palladium(II) carbene complexes as effective C–C coupling catalysts and solvent effects in organic and aqueous media	88
2.1 Abstract	88
2.2 Introduction	88
2.3 Results and Discussion	91
2.3.1 Catalyst synthesis and structures	91
2.3.2 Suzuki coupling by catalysts 1 and 2 with aryl iodide, bromide and chloride precursors	93
2.3.3 A quantitative assessment of the effect of solvent system upon Suzuki coupling by catalysts 1 and 2	101
2.4 Conclusions	126
2.5 Summary of Key Results	127
2.6 Acknowledgements	127
2.7 Experimental	127
2.7.1 General Procedures	127
2.7.2 Physical Measurements	127
2.7.3 Preparations	128
2.7.3.1 IMes(BIAN)[AgCl]	128
2.7.3.2 (IMes)PdCl ₂ PPh ₃ (1)	129
2.7.3.3 (IPr)PdCl ₂ PPh ₃ (2)	129
2.7.4 General Procedure for Suzuki Cross-Coupling Reactions	130
Chapter 3: Direct comparison of <i>bis(imino)acenaphthene</i> (BIAN)-supported palladium(II) <i>mono</i> - and <i>bis(carbene)</i> complexes as catalysts for Suzuki-Miyaura cross-coupling reactions	131
3.1 Abstract	131
3.2 Introduction	131
3.3 Results and Discussion	133
3.4 Conclusions	145
3.6 Summary of Key Results	146
3.6 Acknowledgements	146

3.7 Experimental	146
3.7.1 General Procedures	146
3.7.2 Physical Measurements.....	146
3.7.3 Preparations.....	147
3.7.3.1 (IMes) ₂ PdCl ₂ (3)	147
3.7.3.2 (IPr) ₂ PdCl ₂ (4).....	148
3.7.4 General Procedure for Suzuki Cross-Coupling Reactions.....	148
Chapter 4: Suzuki-Miyaura cross-coupling reactions performed with silica-anchored <i>bis</i> (imino)acenaphthene (BIAN)-supported palladium(II) carbene complexes	150
4.1 Abstract	150
4.2 Introduction.....	150
4.3 Results and Discussion	154
4.3.1 Synthesis of 5	154
4.3.2 Characterization of 5.....	156
4.3.3 Optimization of the catalytic activity of 5	158
4.3.4 Catalytic activity of 5	164
4.3.5 Recyclability of 5	169
4.3.6 Synthesis and characterization of 6.....	173
4.3.7 Catalytic activity of 6	176
4.3.8 Final optimization of 5	178
4.4 Conclusions.....	181
4.5 Summary of Key Results	182
4.6 Acknowledgements.....	182
4.7 Experimental	182
4.7.1 General Procedures	182
4.7.2 Physical Measurements.....	182
4.7.3 Preparations.....	183
4.7.3.1 1-methylacenaphthenequinone (A-I)	183
4.7.3.2 1-ethylacenaphthenequinone (B-I).....	184
4.7.3.3 1-methyl(dipp)BIAN (A-II)	185

4.7.3.4 1-ethyl(dipp)BIAN (B-II)	185
4.7.3.5 [1-methyl(IPr)BIAN]Cl (A-III)	186
4.7.3.6 [1-ethyl(IPr)BIAN]Cl (B-III).....	187
4.7.3.7 [1-bromomethyl(IPr)BIAN]Cl (A-IV).....	187
4.7.3.8 [1-bromoethyl(IPr)BIAN]Cl (B-IV)	188
4.7.3.9 Functionalized Silica (C)	188
4.7.3.10 [1-methyl(IPr)BIAN]Cl@SiO ₂ (A-V)	189
4.7.3.11 [1-ethyl(IPr)BIAN]Cl@SiO ₂ (B-V).....	189
4.7.3.12 [1-methyl(IPr)BIAN]AgCl@SiO ₂ (A-VI)	189
4.7.3.13 [1-ethyl(IPr)BIAN]AgCl@SiO ₂ (B-VI)	190
4.7.3.14 [1-methyl(IPr)BIAN]PdCl ₂ PPh ₃ @SiO ₂ (A-VII)	190
4.7.3.15 [1-ethyl(IPr)BIAN]PdCl ₂ PPh ₃ @SiO ₂ (B-VII).....	190
4.7.4 General Procedure for Suzuki Cross-Coupling Reactions.....	191
Appendix A: X-Ray Tables.....	192
Appendix B: UV-vis Spectroscopy.....	235
Appendix C: NMR spectra.....	238
Glossary	248
References.....	250
Vita	273

List of Tables

Table 1.1: Reaction conditions: 3 mol% Pd ₂ (dba) ₃ , 6 mol% P-donor ligand, 2 equivalents K ₃ PO ₄ , dioxane, 95 °C, 8 h.....	19
Table 1.2: Reaction conditions: 1.5 mol% Pd ₂ (dba) ₃ , 3.6 mol% phosphane, 2 equivalents Cs ₂ CO ₃ , dioxane, 80 °C, 5 h.	20
Table 1.3: Reaction conditions: Pd(OAc) ₂ :P (2:1), K ₃ PO ₄ , toluene, 100 °C, 20 h.	21
Table 1.4: Reaction conditions: Pd(OAc) ₂ :L•HCl, Cs ₂ CO ₃ , dioxane, 80 °C, 1.5-39 h; (a) Pd ₂ (dba) ₃ was used in these reactions.	35
Table 1.5: Buried volume calculated for a Pd–C _{carbenic} bond length of (a) 2.0 Å or (b) experimental values based on crystallographic data (<i>S</i> indicates a saturated C–C backbone).	38
Table 1.6: Pertinent results obtained from Suzuki coupling with sterically-hindered (NHC)Pd(allyl)Cl complexes; Reaction conditions: Pd (1 mol%), NaO ^t Bu, dioxane, 80 °C, 20 min.	39
Table 1.7: Saturated and unsaturated <i>biscarbene</i> complexes along with the corresponding yields obtained from the Suzuki coupling of <i>p</i> -chlorotoluene and phenylboronic acid (<i>a</i>) a mixture of <i>cis</i> - and <i>trans</i> -isomers; Reaction conditions: Pd (1 mol%), (<i>t</i> -Bu ₃)P (2 mol%), H ₂ O, reflux, 24 h.	43
Table 1.8: Suzuki coupling of aryl bromides and chlorides with phenylboronic acid using <i>trans</i> -NHC-phosphine catalysts; Reaction conditions: Pd (1.0 mol%), 130 °C.	46
Table 1.9: The thermal analysis data for mixed PR ₃ /NHC complexes.....	49

Table 1.10: Turnover numbers for Heck reactions of iodobenzene and methyl acrylate; Reaction conditions: Pd (0.25 mol%), 60-95 °C.....	53
Table 1.11: Suzuki coupling of <i>m</i> -chlorobenzoic acid and phenylboronic acid with ligand A or B in various solvent systems; Reaction conditions: Pd (2 mol%).....	57
Table 1.12: Suzuki coupling of several bromoaromatics with phenylboronic acid utilizing catalyst A (0.2 mol%), B (3 mol%), or Pd(PPh ₃) ₄ (3 mol%) in Tol:EtOH:H ₂ O (10:1:1).	59
Table 1.13: Microwave irradiation of the Suzuki coupling of 2-bromonaphthalene and sodium tetraphenylborate in H ₂ O at 120 °C for 15 min.	60
Table 1.14: Surface areas, pore volumes and catalytic activities of five phosphine-palladium heterogeneous catalysts on silica.	72
Table 1.15: Yields of Pd(OAc) ₂ -BOX-MPSG catalyst for toluene, DMAc, NMP, DMF (DMF at 150 °C).	79
Table 1.16: Suzuki coupling of a few heterogeneous catalysts using Et ₃ N or Na ₂ CO ₃ ; Reaction conditions: Pd (2 mol%), μ w-oven assisted reactions (26-89 °C).....	79
Table 2.1: Selected bond distances and angles of 2	93
Table 2.2: Suzuki-Miyaura biaryl coupling of aryl iodides by 1 and 2 ; Reaction conditions: aryl iodide (0.216 mmol), phenylboronic acid (0.259 mmol), K ₂ CO ₃ (0.647 mmol), 1 or 2 (1.0 mol % Pd), solvent (a-toluene, b-CH ₂ Cl ₂ , c-H ₂ O; 3.0 mL), 40 °C, 20 h; all reactions were monitored by GC.....	95

Table 2.3: Suzuki-Miyaura biaryl coupling of aryl bromides by **1** and **2**; Reaction conditions: aryl bromide (0.270 mmol), phenylboronic acid (0.324 mmol), K₂CO₃ (0.811 mmol), **1** or **2** (1.0 mol % Pd), solvent (a-toluene, b-CH₂Cl₂, c-H₂O; 3.0 mL), 40 °C, 20 h; all reactions were monitored for conversion by GC. ^a 0.1 mol % Pd.....98

Table 2.4: Suzuki-Miyaura biaryl coupling of aryl chlorides by **1** and **2**; Reaction conditions: aryl chloride (0.357 mmol), phenylboronic acid (0.429 mmol), K₂CO₃ (1.07 mmol), **1** or **2** (1.0 mol % Pd), solvent (a-toluene, b-CH₂Cl₂, c-H₂O; 3.0 mL), 40 °C, 48h; all reactions were monitored by GC. ^a 2.0 mol% Pd ^b 79.3% selectivity for bifunctionalized *homo*-coupled biaryl product.100

Table 2.5: Recyclability of **1** and **2** in Suzuki-Miyaura biaryl coupling of the *p*-bromobenzaldehyde supernatant (*sup*) and precipitate (*ppt*); Reaction conditions: *p*-bromobenzaldehyde (0.270 mmol), phenylboronic acid (0.324 mmol), K₂CO₃ (0.811 mmol), Pd (1 mol%), solvent (a-toluene, b-CH₂Cl₂, c-H₂O; 3.0 mL), 40 °C, 20 h; all reactions were monitored by GC. ^a % Pd of supernatant and precipitate determined by ICP-MS. ^b *p*-bromobenzaldehyde (0.270 mmol), phenylboronic acid (0.324 mmol), K₂CO₃ (0.811 mmol), H₂O (3.0 mL), Pd-PVP (0.537 mmol), 40 °C, 20 h.....103

Table 2.6: Rate constants for **1** and **2** for *p*-bromobenzaldehyde in H₂O; Reaction conditions: *p*-bromobenzaldehyde (3.24 mmol), phenylboronic acid (3.89 mmol), K₂CO₃ (9.73 mmol), H₂O (15.0 mL), 40 °C; all reactions were monitored by GC.....107

Figure 2.7: Conversion of <i>p</i> -bromobenzaldehyde with phenylboronic acid as a function of time for Suzuki-Miyaura cross-coupling reactions by 1 and 2 at 40 °C with 0.10, 0.25, and 0.50 mol % catalyst loading in H ₂ O; all reactions were monitored by GC.	107
Table 2.7: Rate constants of 1 and 2 for <i>p</i> -bromobenzaldehyde; Reaction conditions: <i>p</i> -bromobenzaldehyde (3.24 mmol), phenylboronic acid (3.89 mmol), K ₂ CO ₃ (9.73 mmol), solvent (a-toluene, b-CH ₂ Cl ₂ , c-H ₂ O; 15.0 mL); all reactions were monitored by GC.	109
Table 2.8: Activation energies for 1 and 2 for <i>p</i> -bromobenzaldehyde; Calculated from the slope of the Arrhenius plots in Figures 2.18-19.....	115
Table 2.9: Rate constants of 1 and 2 of <i>p</i> -chlorobenzaldehyde in H ₂ O; Reaction conditions: <i>p</i> -chlorobenzaldehyde (4.28 mmol), phenylboronic acid (5.14 mmol), K ₂ CO ₃ (12.86 mmol), H ₂ O (15.0 mL); all reactions were monitored by GC. ^a mol %.	118
Table 2.10: Rate constants for 2 using <i>p</i> -chlorobenzaldehyde in H ₂ O; Reaction conditions: <i>p</i> -chlorobenzaldehyde (4.28 mmol), phenylboronic acid (5.14), K ₂ CO ₃ (12.86 mmol), H ₂ O (15.0 mL), 40 °C; all reactions were monitored by GC.....	125
Table 3.1: Selected bond distances and angles for 3 and 4	135
Table 3.2: Suzuki-Miyaura biaryl coupling of aryl iodides by 3 and 4 ; Reaction conditions: aryl iodide (0.216 mmol), phenylboronic acid (0.259 mmol), K ₂ CO ₃ (0.647 mmol), 3 or 4 (1.0 mol % Pd), solvent (a-toluene, b-CH ₂ Cl ₂ , c-H ₂ O; 3.0 mL), 40 °C, 20 h; all reactions were monitored by GC.	137

Table 3.3: Suzuki-Miyaura biaryl coupling of aryl bromides by 3 and 4 ; Reaction conditions: aryl bromide (0.270 mmol), phenylboronic acid (0.324 mmol), K ₂ CO ₃ (0.811 mmol), 3 or 4 (1.0 mol % Pd), solvent (a-toluene, b-CH ₂ Cl ₂ , c-H ₂ O; 3.0 mL), 40 °C, 20 h; all reactions were monitored for conversion by GC.	139
Table 3.4: Suzuki-Miyaura biaryl coupling of aryl chlorides by 3 and 4 ; Reaction conditions: aryl chloride (0.357 mmol), phenylboronic acid (0.429 mmol), K ₂ CO ₃ (1.07 mmol), 3 or 4 (1.0 mol % Pd), solvent (a-toluene, b-CH ₂ Cl ₂ , c-H ₂ O; 3.0 mL), 40 °C, 48h; all reactions were monitored by GC.	141
Table 3.5: Recyclability of 3 and 4 in Suzuki-Miyaura biaryl coupling of the <i>p</i> -bromobenzaldehyde supernatant (<i>sup</i>) and precipitate (<i>ppt</i>); Reaction conditions: <i>p</i> -bromobenzaldehyde (0.270 mmol), phenylboronic acid (0.324 mmol), K ₂ CO ₃ (0.811 mmol), Pd (1 mol%), solvent (a-toluene, b-CH ₂ Cl ₂ , c-H ₂ O; 3.0 mL), 40 °C, 20 h; all reactions were monitored by GC. ^a % Pd of supernatant and precipitate determined by ICP-MS. ^b <i>p</i> -bromobenzaldehyde (0.270 mmol), phenylboronic acid (0.324 mmol), K ₂ CO ₃ (0.811 mmol), H ₂ O (3.0 mL), Pd-PVP (0.537 mmol), 40 °C, 20 h.	143
Table 4.1: IR peak assignments for APTES@SiO ₂ , Imidazolium@SiO ₂ (A-V), and (NHC)PdCl ₂ (PPh ₃)@SiO ₂ (5).	157

Table 4.2: Suzuki-Miyaura biaryl coupling of aryl bromides by 5 ; Reaction conditions: aryl bromide (0.270 mmol), phenylboronic acid (0.324 mmol), K ₂ CO ₃ (0.811 mmol), 5 (1.0 mol% Pd), solvent (a-toluene, b-CH ₂ Cl ₂ , c-H ₂ O; 3.0 mL), 40 °C, 20 h; all reactions were monitored for conversion by GC.	160
Table 4.3: Suzuki-Miyaura biaryl coupling of aryl bromides by 5 ; Reaction conditions: aryl bromide (0.270 mmol), phenylboronic acid (0.324 mmol), K ₂ CO ₃ (0.811 mmol), 5 (5.0 mol% Pd), solvent (CH ₂ Cl ₂ ; 3.0 mL), 40 °C, 20 h; all reactions were monitored for conversion by GC.	161
Table 4.4: Suzuki-Miyaura biaryl coupling of aryl bromides by 5 ; Reaction conditions: aryl bromide (0.270 mmol), phenylboronic acid (0.324 mmol), K ₂ CO ₃ (0.811 mmol), 5 (5.0 mol% Pd), solvent (toluene; 3.0 mL), 65 °C, 20 h; all reactions were monitored for conversion by GC.	162
Table 4.5: Suzuki-Miyaura biaryl coupling of aryl bromides by 5 ; Reaction conditions: aryl bromide (0.270 mmol), phenylboronic acid (0.324 mmol), K ₂ CO ₃ (0.811 mmol), 5 (5.0 mol% Pd), solvent (a-toluene, c-H ₂ O; 3.0 mL), 100 °C, 20 h; all reactions were monitored for conversion by GC.	163

Table 4.6: Suzuki-Miyaura biaryl coupling of aryl bromides by 5 ; Reaction conditions: aryl bromide (0.270 mmol), phenylboronic acid (0.324 mmol), K ₂ CO ₃ (0.811 mmol), 5 (10.0 mol% Pd), solvent (a-toluene, c-H ₂ O; 3.0 mL), 100 °C, 20 h; all reactions were monitored for conversion by GC.....	164
Table 4.7: Suzuki-Miyaura biaryl coupling of <i>p</i> -bromobenzaldehyde by SiO ₂ , APTES@SiO ₂ or A-V ; Reaction conditions: aryl bromide (0.270 mmol), phenylboronic acid (0.324 mmol), K ₂ CO ₃ (0.811 mmol), compound (10.0 mol% Pd), solvent (a-toluene, b-THF, c-H ₂ O; 3.0 mL), 100 °C, 20 h; all reactions were monitored for conversion by GC.....	165
Table 4.8: Suzuki-Miyaura biaryl coupling of aryl iodides by 5 ; Reaction conditions: aryl iodide (0.216 mmol), phenylboronic acid (0.259 mmol), K ₂ CO ₃ (0.647 mmol), 5 (10.0 mol% Pd), solvent (a-toluene, c-H ₂ O; 3.0 mL), 40 °C, 20 h; all reactions were monitored by GC.....	166
Table 4.9: Suzuki-Miyaura coupling by 5 ; Reaction conditions: aryl bromide (0.270 mmol), phenylboronic acid (0.324 mmol), K ₂ CO ₃ (0.811 mmol), 5 (10.0 mol% Pd), solvent (a-toluene, c-H ₂ O; 3.0 mL), 40 °C, 20 h; all reactions were monitored for conversion by GC.....	167
Table 4.10: Suzuki-Miyaura biaryl coupling of aryl chlorides by 5 ; Reaction conditions: aryl chloride (0.357 mmol), phenylboronic acid (0.429 mmol), K ₂ CO ₃ (1.07 mmol), 5 (10.0 mol% Pd), solvent (a-toluene, c-H ₂ O; 3.0 mL), 40 °C, 48h; all reactions were monitored by GC....	169

Table 4.11: Recyclability of **5** in Suzuki-Miyaura biaryl coupling of the *p*-bromobenzaldehyde supernatant (*sup*) and precipitate (*ppt*); Reaction conditions: *p*-bromobenzaldehyde (0.270 mmol), phenylboronic acid (0.324 mmol), K₂CO₃ (0.811 mmol), Pd (10 mol%), solvent (a-toluene, c-H₂O; 3.0 mL), 40 °C, 20 h; all reactions were monitored by GC. ^a % Pd of supernatant and precipitate determined by ICP-MS. ^b *p*-bromobenzaldehyde (0.270 mmol), phenylboronic acid (0.324 mmol), K₂CO₃ (0.811 mmol), H₂O (3.0 mL), Pd-PVP (0.537 mmol), 40 °C, 20 h.....170

Table 4.12: Recyclability of **5** in Suzuki-Miyaura biaryl coupling of the *p*-bromobenzaldehyde supernatant (*sup*) and precipitate (*ppt*); Reaction conditions: *p*-bromobenzaldehyde (0.270 mmol), phenylboronic acid (0.324 mmol), K₂CO₃ (0.811 mmol), Pd (10 mol%), solvent (toluene, H₂O; 3.0 mL), 40 °C, 20 h; all reactions were monitored by GC...172

Table 4.13: IR peak assignments for APTES@SiO₂, Imidazolium@SiO₂ (**B-V**), and (NHC)PdCl₂(PPh₃)@SiO₂ (**6**).....175

Table 4.14: Suzuki-Miyaura biaryl coupling of aryl bromides by **6**; Reaction conditions: aryl bromide (0.270 mmol), phenylboronic acid (0.324 mmol), K₂CO₃ (0.811 mmol), **6** (5.0 mol% Pd), solvent (toluene; 3.0 mL), 100 °C, 20 h; all reactions were monitored for conversion by GC.177

Table 4.15: Suzuki-Miyaura biaryl coupling of aryl bromides by 6 ; Reaction conditions: aryl bromide (0.270 mmol), phenylboronic acid (0.324 mmol), K ₂ CO ₃ (0.811 mmol), 6 (10.0 mol% Pd), solvent (toluene; 3.0 mL), 100 °C, 20 h; all reactions were monitored for conversion by GC.	178
Table 4.16: Optimization of 5 in N-methyl-2-pyrrolidone (NMP), tetrahydrofuran (THF), dimethoxyethane (DME), and ethanol:water (EtOH:H ₂ O 1:1); Reaction conditions: <i>p</i> -bromobenzaldehyde (0.270 mmol), phenylboronic acid (0.324 mmol), K ₂ CO ₃ (0.811 mmol), 5 (10 mol%), solvent (3.0 mL), 100 °C, 20 h; all reactions were monitored by GC.	179
Table 4.17: Suzuki-Miyaura biaryl coupling of aryl bromides by 5 ; Reaction conditions: aryl bromide (0.270 mmol), phenylboronic acid (0.324 mmol), K ₂ CO ₃ (0.811 mmol), 5 (10.0 mol % Pd), THF (3.0 mL), 80 °C, 48 h; all reactions were monitored for conversion by GC.	180
Table 4.18: Suzuki-Miyaura biaryl coupling of aryl bromides by 5 ; Reaction conditions: aryl chloride (0.357 mmol), phenylboronic acid (0.429 mmol), K ₂ CO ₃ (1.07 mmol), 5 (10.0 mol % Pd), THF (3.0 mL), 80 °C, 48h; all reactions were monitored by GC.	181
Table A1: Crystal data and structure refinement for 2 .	192
Table A2: Atomic coordinates (× 10 ⁴) and equivalent isotropic displacement parameters (Å ² × 10 ³) for 2 . U(eq) is defined as one third of the trace of the orthogonalized U ^{ij} tensor.	196
Table A3: Bond lengths [Å] and angles [°] for 2 .	207

Table A4: Anisotropic displacement parameters ($\text{\AA}^2 \times 10^3$) for 2 . The anisotropic displacement factor exponent takes the form: $-2\pi^2 [h^2 a^{*2} U_{11} + \dots + 2 h k a^* b^* U_{12}]$	211
Table A5: Torsion angles [$^\circ$] for 2	217
Table A6: Crystal data and structure refinement for 3	218
Table A7: Atomic coordinates ($\times 10^4$) and equivalent isotropic displacement parameters ($\text{\AA}^2 \times 10^3$) for 3 . $U(\text{eq})$ is defined as one third of the trace of the orthogonalized U_{ij} tensor.....	219
Table A8: Bond lengths [\AA] and angles [$^\circ$] for 3 . Symmetry transformations used to generate equivalent atoms: #1 $-x, y, -z+1/2$ #2 $-x+1/2, -y, z$ #3 $-x+0, -y+1/2, z$	221
Table A9: Anisotropic displacement parameters ($\text{\AA}^2 \times 10^3$) for 3 . The anisotropic displacement factor exponent takes the form: $-2\pi^2 [h^2 a^{*2} U_{11} + \dots + 2 h k a^* b^* U_{12}]$	222
Table A10: Torsion angles [$^\circ$] for 3 . Symmetry transformations used to generate equivalent atoms: #1 $-x, y, -z+1/2$ #2 $-x+1/2, -y, z$ #3 $-x+0, -y+1/2, z$	223
Table A11: Crystal data and structure refinement for 4	224
Table A12: Atomic coordinates ($\times 10^4$) and equivalent isotropic displacement parameters ($\text{\AA}^2 \times 10^3$) for 4 . $U(\text{eq})$ is defined as one third of the trace of the orthogonalized U_{ij} tensor.....	226
Table A13: Bond lengths [\AA] and angles [$^\circ$] for 4 . Symmetry transformations used to generate equivalent atoms: #1 $-x+1, -y, -z$	230

Table A14: Anisotropic displacement parameters ($\text{\AA}^2 \times 10^3$) for 4 . The anisotropic displacement factor exponent takes the form: $-2\pi^2 [h^2 a^{*2} U^{11} + \dots + 2 h k a^* b^* U^{12}]$	232
Table A15: Torsion angles [$^\circ$] for 4 . Symmetry transformations used to generate equivalent atoms: #1 $-x+1, -y, -z$	234

List of Figures

Figure 1.1: The rate determining step of the Suzuki-Miyaura reaction is determined by the ratio of the concentration of the hydroxide ion to the phenylboronic acid.	8
Figure 1.2: The structure of the antibiotic Vancomycin synthesized by Nicolaou <i>et al.</i>	12
Figure 1.3: The molecular orbital diagram of PR_3 ; R = C, N, O, F derived by Dias <i>et al.</i>	18
Figure 1.4: Two illustrations of <i>cis,cis,cis</i> -1,2,3,4- <i>tetrakis</i> (diphenylphosphinomethyl)-cyclopentane, Tedicyp.	22
Figure 1.5: Common dialkylbiarylphosphine ligands with their associated monikers.	24
Figure 1.6: A concise summary of the benefits of dialkylbiarylphosphine ligands in the Suzuki-Miyaura cross-coupling reaction presented by Buchwald <i>et al.</i>	26
Figure 1.7: (a) Bicyclic triaminophosphine ligand presented by Urgaonkar <i>et al.</i> (b) aminophosphine ligand introduced by Cheng <i>et al.</i> (c) phosphinoimidazole established by Harkal <i>et al.</i>	28
Figure 1.8: bidentate ligands (a) 1,3-bis(diphenylphosphino)propane (b) <i>cis</i> -1,3-(Ph_2PCH_2) $_2C_6H_{10}$ (c) 1,4-bis(diphenylphosphino)-1,3-butadiene); R = Ph, Me.	29
Figure 1.9: Bidentate ligands (a) 2-(2'-dicyclohexylphosphinophenyl)-1,3-dioxolane; R = Me, H (b) pyrazole-tethered triarylphosphine; R = CH_3 , <i>t</i> Bu, Ph, Mes.	30

Figure 1.10: Illustration of PR_3 and NHC steric characteristics presented by Fortman <i>et al.</i>	31
Figure 1.11: A simple picture of the frontier orbitals involved in three distinct M–NHC interactions.	32
Figure 1.12: The relative stabilities of three diaminocarbene ligands.	33
Figure 1.13: The first NHC ligands reported by Arduengo <i>et al.</i>	33
Figure 1.14: Imidazolium salts investigated for activity in the Suzuki coupling reaction.....	35
Figure 1.15: Viciu's (NHC)Pd(allyl)Cl complexes.	36
Figure 1.16: Visual representation of buried volume.	37
Figure 1.17: <i>Mono</i> - and <i>bis</i> carbene complexes designed by McGuinness <i>et al.</i>	40
Figure 1.18: Six active <i>bis</i> (carbene) catalysts synthesized by Fu <i>et al.</i>	43
Figure 1.19: Additional <i>trans</i> -NHC-phosphine catalysts presented by Weskamp <i>et al.</i> ; R = C_6H_5 , 2- $(\text{CH}_3)\text{C}_6\text{H}_4$, <i>cyclo</i> - C_6H_{11} , $\text{C}(\text{CH}_3)_3$	46
Figure 1.20: Saturated and unsaturated mixed <i>cis</i> -NHC- PR_3 catalysts for Suzuki coupling.....	48
Figure 1.21: Six new mixed PR_3 /NHC complexes synthesized for a detailed thermal stability study.	49
Figure 1.22: Two <i>N</i> -heterocyclic carbene-phosphine Pd(II) complexes prepared by Xu <i>et al.</i>	50
Figure 1.23: Structural isomers of <i>cis</i> – and <i>trans</i> –(NHC)(PPh_3)(Br) $_2$ Pd.	50
Figure 1.24: Ellul's timteb ^{<i>t</i>-Bu} and timteb ^{dipp} palladium phosphine species.	52
Figure 1.25: The first example of air- and moisture-stable polystyrene-supported catalysts for Suzuki coupling.	59

Figure 1.26: The air- and moisture- stable polystyrene catalyst reported by Inada <i>et al.</i>	60
Figure 1.27: FibreCat TM -1001, FibreCat TM -D8, FibreCat-Pd(MeCN) and TunaCat as examples of insoluble palladium catalysts.....	61
Figure 1.28: Polymer-bound phosphine, PS-Pd(0).	62
Figure 1.29: Polymer-supported dialkylphosphinobiphenyl ligands.	63
Figure 1.30: Monomethyl polyethyleneglycol-supported dialkylphosphinobiphenyl and MeOPEG-BnP-(1-Ad) ₂ ligands presented by Plenio <i>et al.</i>	64
Figure 1.31: Poly(methyl)styrene-supported BnP-(1-Ad) ₂ ligand system presented by Plenio <i>et al.</i>	64
Figure 1.32: Heterogeneous NHC-Pd catalysts presented by Schwarz <i>et al.</i> (left) and Byun <i>et al</i> (right).	66
Figure 1.33: Polystyrene-supported NHC-Pd catalyst reported by Lee <i>et al.</i>	67
Figure 1.34: <i>Bis</i> (NHC)-Pd catalysts synthesized from theobromine.	67
Figure 1.35: Silica-supported <i>cis</i> -phosphine-palladium heterogeneous catalyst. ...	70
Figure 1.36: Silica-supported <i>trans</i> -phosphine-palladium heterogeneous catalyst. ...	70
Figure 1.37: Five organic-functionalized silica materials with various palladium-silica linkers.....	71
Figure 1.38: The first example of an NHC-silica ligand.	72
Figure 1.39: Silica-imidazoline-palladium complex active for aryl chlorides.	73
Figure 1.40: Pd-NHC-silica complex described by Gürbüz <i>et al.</i>	74
Figure 1.41: (a) <i>cis</i> -Pd-NHC-silica complex presented by Karimi (b) <i>trans</i> -Pd-NHC- silica complex presented by Aksin.	75

Figure 1.42: Illustration of several palladium complexes anchored to a silica particle as reported by Lee <i>et al.</i>	76
Figure 1.43: NHC-Pd-OSO ₂ R heterogeneous catalysts active for both the Suzuki and Heck reactions.....	77
Figure 1.44: Pd(OAc) ₂ -BOX-MPSG catalyst presented by Gruber-Woelfler <i>et al.</i>	78
Figure 1.45: Polystyrene-supported palladium catalysts for the Suzuki reaction.....	80
Figure 1.46: 3-D Pd-phosphine network reported by Yamada and Uozimi <i>et al.</i>	81
Figure 1.47: PS-PEG-NHC-Pd complex synthesized by Kim <i>et al.</i>	82
Figure 2.1: Crystal structure of 2	92
Figure 2.2: Absorption spectrum of 1 in CH ₂ Cl ₂ with $\lambda_{\text{max}} = 308$ nm. Beer's law was used to determine ϵ from a calibration curve created with ten data points in 10 μL increments ranging 10-100 μL ($\epsilon = 29,646 \text{ M}^{-1} \text{ cm}^{-1}$, $R^2 = 0.9918$).....	94
Figure 2.3: The absorption spectrum of 2 in CH ₂ Cl ₂ with $\lambda_{\text{max}} = 309$ nm. Beer's law was used to determine ϵ from a calibration curve created with ten data points in 10 μL increments ranging 10-100 μL ($\epsilon = 36,868 \text{ M}^{-1} \text{ cm}^{-1}$, $R^2 = 0.9997$).....	94
Figure 2.4: TEM images of Pd-PVP (50 nm scale).....	105
Figure 2.5: TEM images of Pd-PVP (100 nm scale).....	105
Figure 2.6: Particle size distribution of Pd-PVP.....	106
Figure 2.8: Conversion of <i>p</i> -bromobenzaldehyde with phenylboronic acid as a function of time in Suzuki-Miyaura coupling by catalyst 2 at 40°C with 0.05 mol% catalyst loading ($k^2 = 0.8427$).....	108

Figure 2.9: Reaction of <i>p</i> -bromobenzaldehyde with phenylboronic acid as a function of time in Suzuki-Miyaura coupling by 0.5 mol % of 1 at 30 °C...	109
Figure 2.10: Reaction of <i>p</i> -bromobenzaldehyde with phenylboronic acid as a function of time in Suzuki-Miyaura coupling by 0.5 mol % of 1 at 35 °C...	110
Figure 2.11: Reaction of <i>p</i> -bromobenzaldehyde with phenylboronic acid as a function of time in Suzuki-Miyaura coupling by 0.5 mol % of 1 at 40 °C...	110
Figure 2.12: Reaction of <i>p</i> -bromobenzaldehyde with phenylboronic acid as a function of time in Suzuki-Miyaura coupling by 0.5 mol % of 2 at 30 °C...	111
Figure 2.13: Reaction of <i>p</i> -bromobenzaldehyde with phenylboronic acid as a function of time in Suzuki-Miyaura coupling by 0.5 mol % of 2 at 35 °C...	111
Figure 2.14: Reaction of <i>p</i> -bromobenzaldehyde with phenylboronic acid as a function of time in Suzuki-Miyaura coupling by 0.5 mol % of 2 at 40 °C...	112
Figure 2.15: Reaction of <i>p</i> -bromobenzaldehyde with phenylboronic acid as a function of time in Suzuki-Miyaura coupling by 0.5 mol % of 1 and 2 at 30 °C. A comparison of total conversion and coupling selectivity (solid <i>versus</i> open bars).....	112
Figure 2.16: Reaction of <i>p</i> -bromobenzaldehyde with phenylboronic acid as a function of time in Suzuki coupling by 0.5 mol % of 1 and 2 at 35 °C. A comparison of total conversion and coupling selectivity (solid <i>versus</i> open bars).....	113
Figure 2.17: Reaction of <i>p</i> -bromobenzaldehyde with phenylboronic acid as a function of time in Suzuki coupling by 0.5 mol % of 1 and 2 at 40 °C. A comparison of total conversion and coupling selectivity (solid <i>versus</i> open bars).....	113

Figure 2.18: Arrhenius plot for the activation of <i>p</i> -bromobenzaldehyde by 1 in toluene, CH ₂ Cl ₂ , and H ₂ O.....	115
Figure 2.19: Arrhenius plot for the activation of <i>p</i> -bromobenzaldehyde by 2 in toluene, CH ₂ Cl ₂ , and H ₂ O.....	116
Figure 2.20: Conversion of <i>p</i> -chlorobenzaldehyde with phenylboronic acid as a function of time in Suzuki-Miyaura coupling by catalysts 1 at 40 °C in H ₂ O.	117
Figure 2.21: Conversion of <i>p</i> -chlorobenzaldehyde with phenylboronic acid as a function of time in Suzuki-Miyaura coupling by catalysts 2 at 40 °C in H ₂ O.	117
Figure 2.22: Conversion (solid squares) and selectivity (open circles) of <i>p</i> -chlorobenzaldehyde with phenylboronic acid as a function of time in Suzuki-Miyaura coupling at 40 °C with 0.5 mol % of 1 in H ₂ O. Dashed and solid lines through open circles denote selectivities of the <i>hetero</i> - and <i>homo</i> -coupled products, respectively.....	119
Figure 2.23: Conversion (solid squares) and selectivity (open circles) of <i>p</i> -chlorobenzaldehyde with phenylboronic acid as a function of time in Suzuki-Miyaura coupling at 40 °C with 1.0 mol % of 1 in H ₂ O. Dashed and solid lines through open circles denote selectivities of the <i>hetero</i> - and <i>homo</i> -coupled products, respectively.....	119

Figure 2.24: Conversion (solid squares) and selectivity (open circles) of *p*-chlorobenzaldehyde with phenylboronic acid as a function of time in Suzuki-Miyaura coupling at 40 °C with 1.5 mol % of **1** in H₂O. Dashed and solid lines through open circles denote selectivities of the *hetero*- and *homo*-coupled products, respectively.....120

Figure 2.25: Conversion (solid squares) and selectivity (open circles) of *p*-chlorobenzaldehyde with phenylboronic acid as a function of time in Suzuki-Miyaura coupling at 40 °C with 0.5 mol % of **2** in H₂O. Dashed and solid lines through open circles denote selectivities of the *hetero*- and *homo*-coupled products, respectively.....120

Figure 2.26: Conversion (solid squares) and selectivity (open circles) of *p*-chlorobenzaldehyde with phenylboronic acid as a function of time in Suzuki-Miyaura coupling at 40 °C with 1.0 mol % of **2** in H₂O. Dashed and solid lines through open circles denote selectivities of the *hetero*- and *homo*-coupled products, respectively.....121

Figure 2.27: Conversion (solid squares) and selectivity (open circles) of *p*-chlorobenzaldehyde with phenylboronic acid as a function of time in Suzuki-Miyaura coupling at 35 °C with 0.25 mol % of **2** in H₂O. Dashed and solid lines through open circles denote selectivities of the *hetero*- and *homo*-coupled products, respectively.....121

Figure 2.28: Conversion (solid squares) and selectivity (open circles) of <i>p</i> -chlorobenzaldehyde with phenylboronic acid as a function of time in Suzuki-Miyaura coupling at 30 °C with 0.25 mol % of 2 in H ₂ O. Dashed and solid lines through open circles denote selectivities of the <i>hetero</i> - and <i>homo</i> -coupled products, respectively.....	122
Figure 2.29: Reaction of <i>p</i> -chlorobenzaldehyde with phenylboronic acid as a function of time for Suzuki-Miyaura coupling at 40 °C with 0.5 and 1.0 mol % of 1 in H ₂ O.	123
Figure 2.30: Reaction of <i>p</i> -chlorobenzaldehyde with phenylboronic acid as a function of time for Suzuki-Miyaura coupling at 40 °C with 0.5 and 1.0 mol % of 2 in H ₂ O.	123
Figure 2.31: Conversion of <i>p</i> -chlorobenzaldehyde as a function of time in Suzuki-Miyaura coupling at 40 °C in H ₂ O with 0.5 mol % of 2 under varying conditions of phenylboronic acid and K ₂ CO ₃ (legend denotes stoichiometric equivalents of phenylboronic acid : K ₂ CO ₃)......	124
Figure 2.32: Suzuki-Miyaura coupling of <i>p</i> -chlorobenzaldehyde with phenylboronic acid as a function of time using 0.25 mol % of 2 at 24, 30, 35, and 40 °C in H ₂ O.	124
Figure 2.33: Arrhenius plot for the activation of <i>p</i> -chlorobenzaldehyde by 2 in H ₂ O.	125
Figure 3.1: Crystal structure of 3 showing the mean plane angle of 46.3° through two different orientations.....	134
Figure 3.2: Crystal structure of 4 showing the mean plane angle of 0.2° through two different orientations.....	134

Figure 3.3: The absorption spectrum of 3 in dichloromethane with $\lambda_{\text{max}} = 293$ nm. Beer's law was used to determine the molar absorptivity from a calibration curve created with ten data points in 10 μL increments ranging 10-100 μL ($\epsilon = 102,736 \text{ M}^{-1} \text{ cm}^{-1}$, $R^2 = 0.998$).....	136
Figure 3.4: The absorption spectrum of 4 in dichloromethane with $\lambda_{\text{max}} = 295$ nm. Beer's law was used to determine the molar absorptivity from a calibration curve created with ten data points in 10 μL increments ranging 10-100 μL ($\epsilon = 100,498 \text{ M}^{-1} \text{ cm}^{-1}$, $R^2 = 0.9415$).....	136
Figure 4.1: Metallopolymer based on bifunctional BIAN ligand based on the 3-D polymer presented by Karimi <i>et al</i>	152
Figure 4.2: Design of 1-D metal organic polymer of Pd(II) BIAN species incorporating organic linkers.	153
Figure 4.3: Design of asymmetrical silica-anchored BIAN catalyst.	154
Figure 4.4: Design of silica-anchored catalyst using the BIAN backbone.	154
Figure 4.5: UV-vis spectra of (NHC)(PPh ₃)PdCl ₂ (2 , dark grey), Imidazolium@SiO ₂ (A-V , light grey), and (NHC)PdCl ₂ (PPh ₃)@SiO ₂ (5 , black).	157
Figure 4.6: TGA for (NHC)(PPh ₃)PdCl ₂ (2 , dark grey), Imidazolium@SiO ₂ (A-V , light grey), and (NHC)PdCl ₂ (PPh ₃)@SiO ₂ (5 , black).....	158
Figure 4.7: Recyclability for (NHC)PdCl ₂ (PPh ₃)@SiO ₂ (5) in toluene (grey) and H ₂ O (black) over four consecutive trials.....	172
Figure 4.8: UV-vis spectra of (NHC)(PPh ₃)PdCl ₂ (2 , dark grey), Imidazolium@SiO ₂ (B-V , light grey), and (NHC)PdCl ₂ (PPh ₃)@SiO ₂ (6 , black).	175
Figure 4.9: TGA for (NHC)(PPh ₃)PdCl ₂ (2 , dark grey), Imidazolium@SiO ₂ (B-V , light grey), and (NHC)PdCl ₂ (PPh ₃)@SiO ₂ (6 , black).....	176

Figure B1: Absorption spectrum of **1** in dichloromethane with $\lambda_{\text{max}} = 308$ nm.

Beer's law was used to determine the molar absorptivity from a calibration curve created with ten data points in 10 μL increments ranging 10-100 μL ($\epsilon = 29,646 \text{ M}^{-1} \text{ cm}^{-1}$, $R^2 = 0.9918$).....235

Figure B2: The absorption spectrum of **2** in dichloromethane with $\lambda_{\text{max}} = 309$ nm.

Beer's law was used to determine the molar absorptivity from a calibration curve created with ten data points in 10 μL increments ranging 10-100 μL ($\epsilon = 36,868 \text{ M}^{-1} \text{ cm}^{-1}$, $R^2 = 0.9997$).....235

Figure B3: The absorption spectrum of **3** in dichloromethane with $\lambda_{\text{max}} = 293$ nm.

Beer's law was used to determine the molar absorptivity from a calibration curve created with ten data points in 10 μL increments ranging 10-100 μL ($\epsilon = 102,736 \text{ M}^{-1} \text{ cm}^{-1}$, $R^2 = 0.998$).....236

Figure B4: The absorption spectrum of **4** in dichloromethane with $\lambda_{\text{max}} = 295$ nm.

Beer's law was used to determine the molar absorptivity from a calibration curve created with ten data points in 10 μL increments ranging 10-100 μL ($\epsilon = 100,498 \text{ M}^{-1} \text{ cm}^{-1}$, $R^2 = 0.9415$).....236

Figure B5: UV-vis spectra of (NHC)(PPh₃)PdCl₂ (**2**, dark grey), Imidazolium@SiO₂

(**A-V**, light grey), and (NHC)PdCl₂(PPh₃)@SiO₂ (**5**, black)237

Figure B6: UV-vis spectra of (NHC)(PPh₃)PdCl₂ (**2**, dark grey), Imidazolium@SiO₂

(**B-V**, light grey), and (NHC)PdCl₂(PPh₃)@SiO₂ (**6**, black)237

Figure C1: ¹H NMR of **1**.....238

Figure C2: ¹³C NMR of **1**.....239

Figure C3: ³¹P NMR of **1**240

Figure C4: ¹H NMR of **2**.....241

Figure C5: ^{13}C NMR of 2	242
Figure C6: ^{31}P NMR of 2	243
Figure C7: ^1H NMR of 3	244
Figure C8: ^{13}C NMR of 3	245
Figure C9: ^1H NMR of 4	246
Figure C10: ^{13}C NMR of 4	247

List of Schemes

Scheme 1.1: The original Suzuki-Miyaura cross-coupling reaction.....	1
Scheme 1.2: A generic Suzuki-Miyaura cross-coupling reaction.....	2
Scheme 1.3: A generic Suzuki-Miyaura cross-coupling mechanism.	3
Scheme 1.4: Generic representation of Nobel Prize winning cross-coupling reactions.	4
Scheme 1.5: Four postulated transmetallation steps for the original Suzuki mechanism; R = alkyl, H and L = PPh ₃ for A and B ; R = H and L = PPh ₃ , PR" ₃ for C and D	5
Scheme 1.6: Generic reaction of aryl halides with phenylboronic acids reported by Amatore and co-workers.....	6
Scheme 1.7: The Suzuki-Miyaura mechanism involving the base OH ⁻ devised by Amatore <i>et al.</i> (L = PPh ₃).	7
Scheme 1.8: The Suzuki-Miyaura mechanism with the base OH ⁻ and counteraction M ⁺ as proposed by Amatore <i>et al.</i> (L = PPh ₃).	9
Scheme 1.9: The Suzuki-Miyaura mechanism using the base CO ₃ ²⁻ and the counteraction M ⁺ as presented by Amatore <i>et al.</i> (L = PPh ₃).	10
Scheme 1.10: The <i>homo</i> -coupled mechanism of the Suzuki-Miyaura reaction devised by Amatore <i>et al.</i> (L = PPh ₃).	11
Scheme 1.11: The eleventh step in the total synthesis of Vancomycin is the Suzuki coupling of an asymmetrical aryl iodide with a functionalized boronic acid. The reaction mixture was heated to 90 °C for 2 h and the products were isolated in a combined 80% yield.....	12

Scheme 1.12: The Suzuki cross-coupling reaction was heated at reflux for 0.5-18 h, thereby affording the asymmetrical product in 83% yield.....	13
Scheme 1.13: The Suzuki cross-coupling reaction was heated overnight at 100 °C, thereby affording the <i>hetero</i> -coupled product in 74% yield.	13
Scheme 1.14: The Suzuki cross-coupling reaction was heated to reflux for 5 h, thereby affording the trisubstituted imidazole in 68% yield.	14
Scheme 1.15: The Suzuki cross-coupling reaction was heated to reflux for 4 h, thereby affording the luminescent imidazopyrazine system in 96% yield.	15
Scheme 1.16: The direct synthesis of the desired hetarylene building block presented by Manickam and Schlüter utilizing two Suzuki and one Stille cross- coupling reactions.	16
Scheme 1.17: Synthesis of a generic trisubstituted-dialkylbiarylphosphine ligand.	24
Scheme 1.18: Reaction conditions: 1 mol% Pd, 4 mol% ligand, toluene, 90 °C, 16 h, K ₃ PO ₄ or CsF.	27
Scheme 1.19: The first Suzuki reaction carried out with an NHC ligand (80 °C, 1.5 h).	34
Scheme 1.20: Unique Suzuki coupling of <i>m</i> -chloropyridine with (NHC)Pd(allyl)Cl.	37
Scheme 1.21: Suzuki coupling with (NHC)Pd(allyl)Cl reported by Navarro <i>et al.</i> ; Reaction conditions: 80 °C, 20 min.	39
Scheme 1.22: Suzuki-Miyaura coupling optimized by Böhm <i>et al.</i> for aryl chlorides; R = Mes, <i>t</i> -Bu, <i>i</i> -Pr, Cy.....	41

Scheme 1.23: Asymmetric catalyst for Suzuki-Miyaura coupling developed by Lebel <i>et al.</i>	42
Scheme 1.24: The first stable mixed PR ₃ /NHC complexes; R = Me, Et, <i>p</i> -ClC ₆ H ₄ , <i>p</i> - CH ₃ OC ₆ H ₄	44
Scheme 1.25: The <i>trans</i> -NHC-phosphine ligand presented by Weskamp <i>et al.</i> ...	45
Scheme 1.26: The first example of coupling an unactivated aryl chloride with phenylboronic acid at room temperature.	47
Scheme 1.27: Suzuki coupling of bromobenzene with phenylboronic acid in an imidazolium ionic liquid.	51
Scheme 1.28: Aqueous-phase Suzuki coupling presented by Shaughnessy <i>et al.</i> ...	55
Scheme 1.29: Ultrasound assisted syntheses of polystyrene-tethered Pd(II) catalysts.	60
Scheme 1.30: Synthesis of Yamada's self-assembled palladium non-cross-linked amphiphilic copolymer.	65
Scheme 1.31: Grating vs. sol-gel method for the synthesis of supported imidazolium salts presented by Ranganath <i>et al.</i>	68
Scheme 1.32: Synthesis of a bidentate phosphine ligand tethered to silica.	69
Scheme 1.33: Homeopathic mechanism presented by De Vries <i>et al.</i>	86
Scheme 1.34: Mechanism of the cocktail of molecular complexes, metal clusters, and metal nanoparticles as presented by Ananikov <i>et al.</i>	87
Scheme 2.1: Syntheses of palladium catalysts 1 and 2	92
Scheme 3.1: Syntheses of BIAN palladium catalysts 3 and 4	133
Scheme 4.1: (a) Synthesis of silica-anchored BIAN palladium catalyst 5 (b) Synthesis of functionalized silica.	156

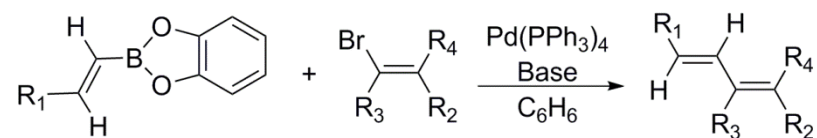
Scheme 4.2: (a) Synthesis of silica-anchored BIAN palladium catalyst 6 (b) Synthesis of functionalized silica	174
--	-----

Chapter 1: Suzuki-Miyaura Coupling: *a broad overview of homogeneous and heterogeneous Suzuki-Miyaura cross-coupling catalysis*

1.1 INTRODUCTION

1.1.1 History

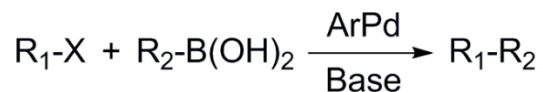
The Suzuki-Miyaura cross-coupling reaction was first published in 1979. This publication described the synthesis of a few conjugated dienes using palladium *tetrakis*(triphenylphosphine) as the catalyst (Scheme 1.1).¹ At the time, this reaction was unique since the coupling of alkenylboranes with alkenyl halides had yet to be accomplished without the addition of stoichiometric amounts of an organometallic species (*e.g.* Rh, Ir, etc.). Furthermore, an aqueous solution of sodium hydroxide in THF or sodium ethoxide in ethanol was added to assist in the stereo- and regioselectivity of the catalyst. It was also discovered that the reaction would not proceed without the presence of a base to promote the cross-coupling reaction. The reaction was further optimized by using 1 mol% catalyst loading relative to the alkenyl halide in the presence of a slight excess of the organoborane. Ultimately, Suzuki *et al.* concluded this work with the speculation that this technique may someday be applicable to allyl, benzyl, and aryl halides.



Scheme 1.1: The original Suzuki-Miyaura cross-coupling reaction.

Subsequently, the previous reaction conditions have been extended to include functionalized starting materials (both organoboranes and halogenated reagents) and new

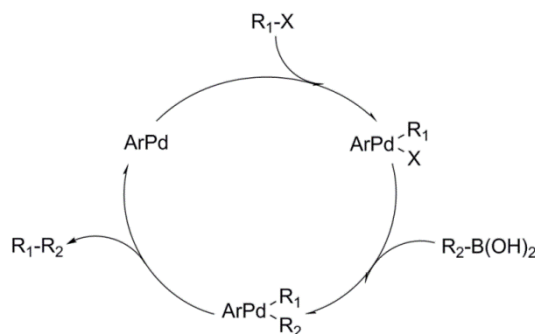
palladium catalysts in order to form symmetrical and asymmetrical biaryls.² A generic Suzuki-Miyaura cross-coupling reaction is presented in Scheme 1.2. These homogeneous catalysts (ArPd) were typically four-coordinate square planar complexes with phosphine-type ligands.³ More recent research has shown that the substitution of phosphine ligands by *N*-heterocyclic carbenes (NHC) permits less ligand-to-metal π -backbonding, thus increasing the stabilities of the resulting complexes. In turn, the lack of π -backbonding from the metal to the NHC ligands results in less metal-ligand degradation than those of the analogous phosphine ligands. This was an extremely desirable characteristic from the point of view of cross-coupling reactions.⁴ Originally, these catalysts were only capable of activating aryl iodides and aryl bromides. However, eventually new catalysts were developed that were capable of activating aryl chlorides.⁵ This development was particularly noteworthy since the chlorinated reagents are more abundant and less expensive than the corresponding brominated and iodinated analogs. On the other hand, the former typically have a larger bond dissociation energy, thus requiring an efficient catalyst for activation of the thermodynamically more stable C–Cl bond.⁶



Scheme 1.2: A generic Suzuki-Miyaura cross-coupling reaction.

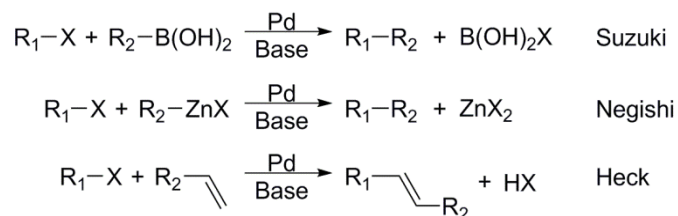
The role of the palladium catalyst was examined meticulously and resulted in the development of the generic catalytic cycle presented in Scheme 1.3.⁴ The palladium species typically undergoes oxidative addition of an aryl/alkenyl halide followed by transmetallation with an organoborane. The final step is generally the reductive

elimination of the *hetero*-coupled product. Interestingly, the role of the base was not thoroughly examined until the twenty-first century.⁷



Scheme 1.3: A generic Suzuki-Miyaura cross-coupling mechanism.

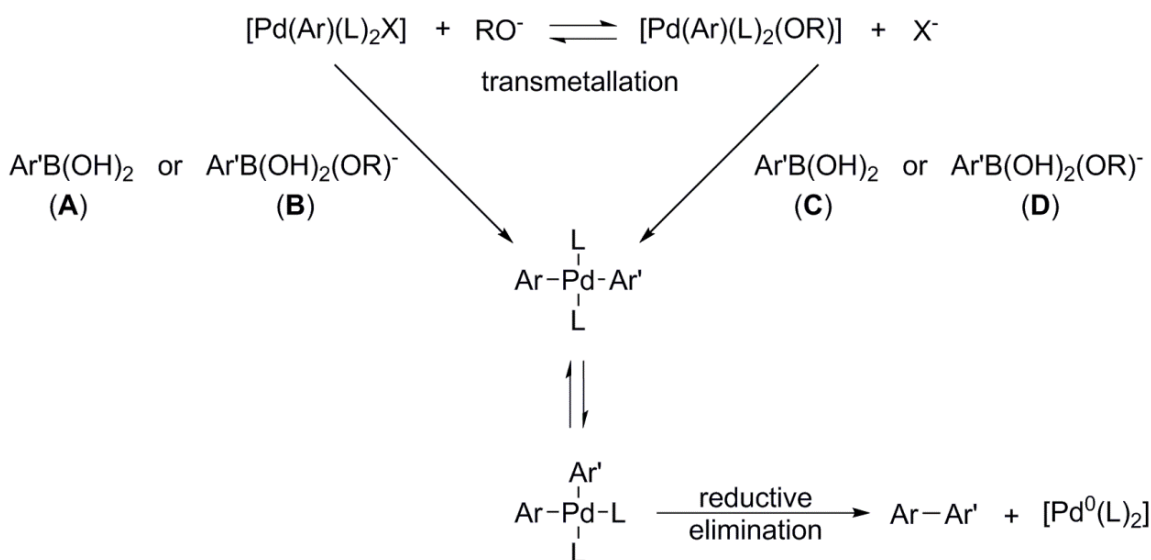
In less than forty years, the Suzuki-Miyaura cross-coupling reaction has become one of the most convenient methods for the creation of C–C bonds. Indeed, this reaction has become the focus of a large number of research groups, since it is a simple, yet very efficient chemical reaction. Moreover, an array of substrates, bases, ligands and transition metals have been used successfully in this cross-coupling reaction. Not surprisingly, Akira Suzuki (University of Hokkaido), Ei-ichi Negishi (Purdue University) and Richard Heck (University of Delaware) were jointly awarded the Nobel Prize in Chemistry for their work on C–C bond formation, using a palladium catalyst (Scheme 1.4).⁸ Subsequent research has been focused on performing coupling reactions in green solvents such as ethanol or water using a heterogeneous catalyst. Typically, these heterogeneous catalysts consist of an optimal homogenous catalyst that has been anchored to an appropriate solid support. Ideally, the heterogeneous catalyst can be extracted from the resulting reaction mixture and replenished with fresh reagents without any significant loss of catalytic activity.



Scheme 1.4: Generic representation of Nobel Prize winning cross-coupling reactions.

1.1.2 Mechanism

In their initial publication Suzuki and Miyaura asserted that the presence of a base was absolutely necessary for the cross-coupling reaction to occur.¹ In the years following this unusual proclamation, the catalytic cycle has been systematically investigated by a large number of research groups.⁹⁻¹⁴ Originally, Suzuki *et al.* postulated that the first step of the mechanism involved the oxidative addition of the aryl halide to produce *trans*-[Pd(Ar)(L)₂X]. The formation of this four-coordinate square planar Pd(II) species was generally accepted in the scientific community. However, the precise details of the mechanism became a topic of vigorous debate. Four separate mechanisms for this transmetallation step were proposed and are displayed in Scheme 1.5.¹⁵

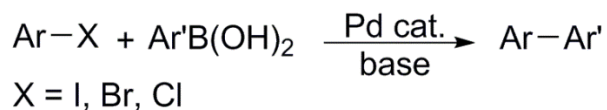


Scheme 1.5: Four postulated transmetallation steps for the original Suzuki mechanism; R = alkyl, H and L = PPh₃ for **A** and **B**; R = H and L = PPh₃, PR''₃ for **C** and **D**.

Suzuki *et al.* suggested pathway **A**, in which the palladium intermediate species *trans*-[Pd(Ar)(L)₂X] underwent reaction with an organoborane (Ar'B(OH)₂) to form a *trans*-[Pd(Ar)(L)₂(Ar')] product.¹⁶ However, these authors also hypothesized an additional pathway **B**, in which the organoborane was treated with an alkoxide (RO⁻, R = Me, Et) to generate Ar'B(OH)₂(OR⁻) prior to undergoing transmetallation.¹⁷ At this time, it was believed that the anionic phenylboronic acid was more reactive than the corresponding neutral species during the transmetallation process. Moreover, Suzuki *et al.* followed these two proposals by suggesting pathway **D**, in which it was shown that an X/OR exchange occurred with *trans*-[Pd(Ar)(L)₂X] to afford *trans*-[Pd(Ar)(L)₂(OR)]. The latter newly formed palladium complex then underwent transmetallation with Ar'B(OH)₂(OR⁻), ultimately producing the desired *trans*-[Pd(Ar)(L)₂(Ar')] intermediate. Concurrently, Matos and Soderquist proposed pathways **B** and **C** with the analogous

alkylboranes,¹⁸ and Smith *et al.* presented alternative pathway **B** with the base OH⁻.¹⁹ Interestingly, Braga *et al.* published DFT calculations that revealed the existence of competing pathways (**B** and **C**) when OH⁻ was employed as the base.²⁰ In the case of pathway **B**, [Pd(Br)(Ph)(L)_n] (n = 1, 2; L = PH₃, PR''₃) reacted with PhB(OH)₃⁻,^{21,22} whereas [Pd(OH)(L)₂(Ph)] (L = PH₃) reacted with PhB(OH)₂ via pathway **C**.²⁰ Regardless of the particular pathway, *trans*-[Pd(Ar)(L)₂(Ar')] always rearranged to form *cis*-[Pd(Ar)(Ar')(L)₂], followed by reductive elimination of the anticipated *hetero*-coupled Ar–Ar' product. The catalyst was generally believed to complete the catalytic cycle as Pd(0) in the form of [Pd⁰(L)₂].

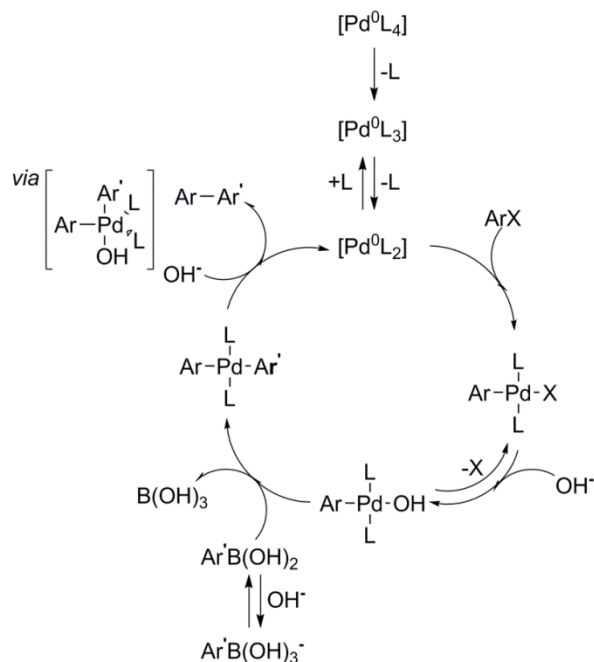
Consideration of pathways **A–D** was finally concluded when Amatore and co-workers began focusing on the coupling of *aryl* halides with organoboranes (Scheme 1.6). Remarkably, the majority of the scientific advances in this field have been performed by his research group in the past five years.^{7,23–26} In 2009, Amatore *et al.* initiated an investigation of the role of the base in the Suzuki-Miyaura reaction mechanism. On the basis of concrete kinetic data, Amatore *et al.* were able to support their views on the rate determining step.



Scheme 1.6: Generic reaction of aryl halides with phenylboronic acids reported by Amatore and co-workers.

By means of kinetic experiments, Amatore *et al.* has developed a new and currently accepted Suzuki-Miyaura mechanism.⁷ In this work, [*n*Bu₄N]OH was employed as the base, and thereby three separate roles of the newly-formed hydroxide ions were

observed (Scheme 1.7). The initial role of the anion was to assist the formation of the *trans*-[(Ar)Pd(OH)(PPh₃)₂], thereby forming a more reactive intermediate for subsequent transmetallation with Ar'B(OH)₂. Interestingly, the hydroxide ion unexpectedly promoted the reductive elimination of the disubstituted biaryl product from *trans*-[(Ar)Pd(Ar')-(PPh₃)₂].



Scheme 1.7: The Suzuki-Miyaura mechanism involving the base OH⁻ devised by Amatore *et al.* (L = PPh₃).

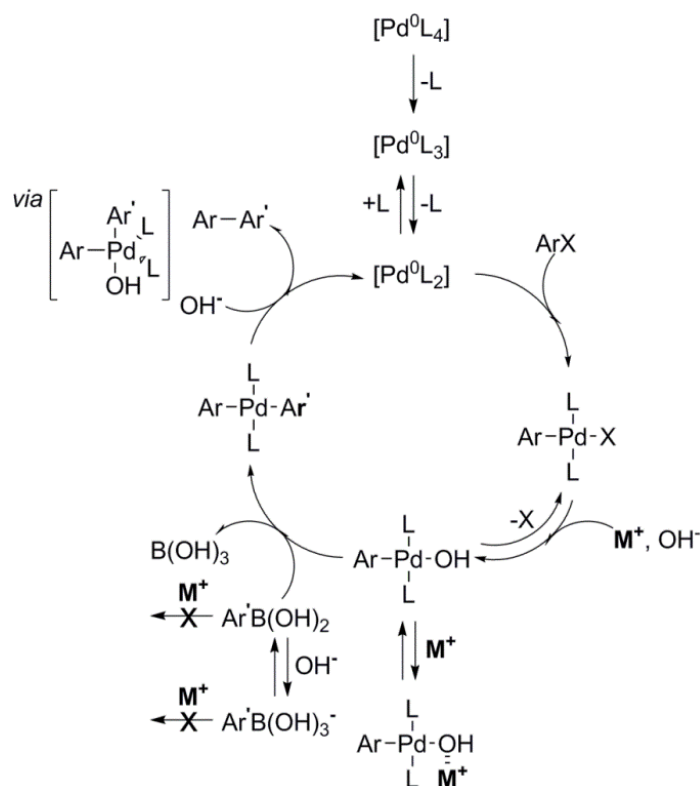
Although the hydroxide anion assisted in two of the major steps in the cross-coupling reaction, the anion unfortunately had a notable adverse impact on the Suzuki-Miyaura catalytic cycle. The hydroxide ion rapidly formed Ar'B(OH)₃⁻, which is a particularly unreactive type of phenylboronic acid. The same product was originally believed by Suzuki to be the more desirable form of organoborane. However, Amatore *et*

al. reported that this competitive cycle adversely affected the rate of reaction. In all the cases studied, the rate determining step was found to be the reaction of *trans*-[(Ar)Pd(OH)(PPh₃)₂] with ArB'(OH)₂ and can be calculated by the ratio of [OH⁻] and [Ar'B(OH)₂] (Figure 1.1). Interestingly, the rate of transmetallation was slightly slower than the corresponding rate of reductive elimination. On the other hand, the addition of OH⁻ increased this rate of reductive elimination significantly due to the formation of the intermediate *trans*-[(Ar)Pd(Ar')(OH)(PPh₃)₂].

$$\text{Rate determining step} = \frac{[\text{OH}^-]}{[\text{Ar}'\text{B}(\text{OH}_2)]}$$

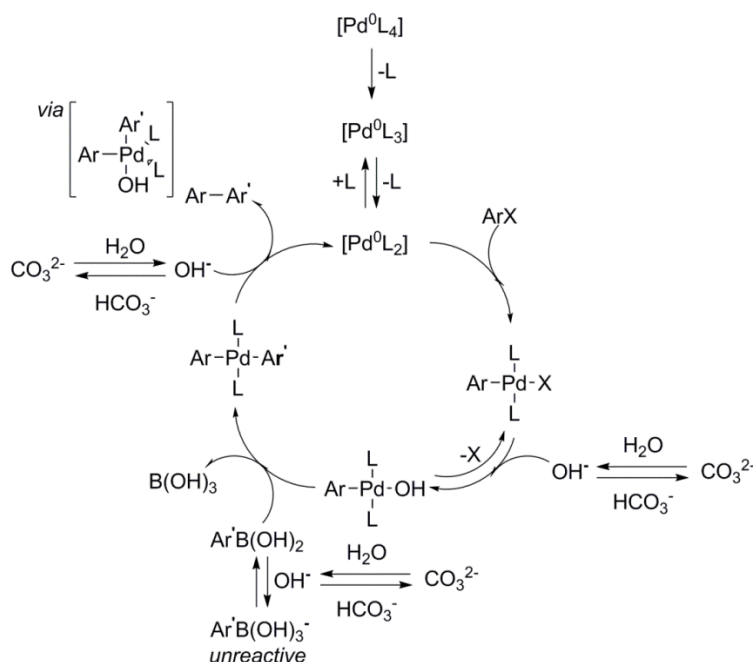
Figure 1.1: The rate determining step of the Suzuki-Miyaura reaction is determined by the ratio of the concentration of the hydroxide ion to the phenylboronic acid.

Amatore and co-workers intentionally utilized [nBu₄N]OH as the base in their original kinetic studies to avoid any undesirable interactions between the palladium catalyst and the counteranion of the base. Nevertheless, within a year, Amatore *et al.* reported a supplementary Suzuki mechanism in order to establish the role of this counteranion (Scheme 1.8).²⁷ It was concluded that the counteranion was never directly coordinated to a boronic acid. However, it was detected to be in a dynamic equilibrium with *trans*-[Pd(Ar)(L)₂(OH)]. Furthermore, this innovative equilibrium step had a decelerating effect on the rate of transmetallation. The most suitable base for the Suzuki reaction was established to be [nBu₄N]OH, followed in succession by KOH, CsOH, and NaOH. Finally, the overall rate of reaction was not affected by the presence of the counteranion.



Scheme 1.8: The Suzuki-Miyaura mechanism with the base OH^- and counteraction M^+ as proposed by Amatore *et al.* ($L = PPh_3$).

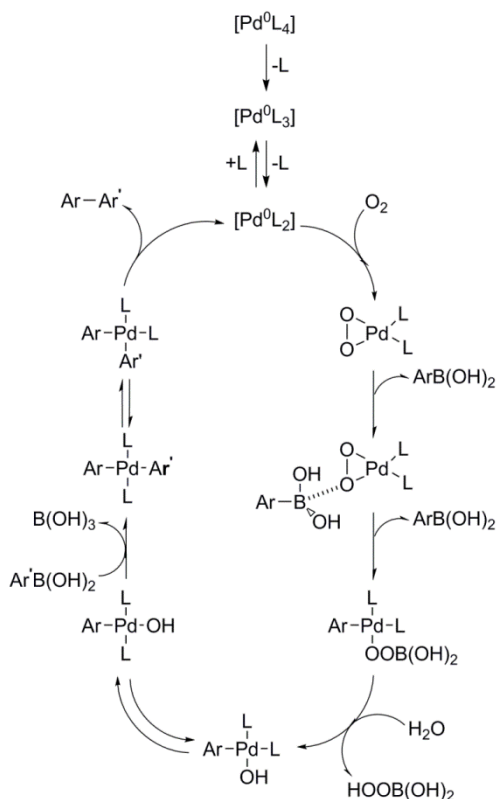
The final investigation by Amatore *et al.* into the Suzuki reaction mechanism was to examine the most commonly used bases Na_2CO_3 and K_2CO_3 in order to explore their roles in the cross-coupling reaction. It was proposed that in aqueous media or “wet” solvents, the carbonate base accepted a proton to form HCO_3^- , and thereby produced the necessary OH^- (Scheme 1.9).²³ Interestingly, CO_3^{2-} directly influenced the concentration of OH^- , thus inevitably controlling the overall rate of reaction (Figure 1.1). It could be argued that the aforementioned mechanism is Amatore’s most significant contribution to the understanding of the complexity of the Suzuki-Miyaura reaction.



Scheme 1.9: The Suzuki-Miyaura mechanism using the base CO_3^{2-} and the counteraction M^+ as presented by Amatore *et al.* ($L = PPh_3$).

As an addendum to the multiple *hetero*-coupling mechanisms explored by Amatore *et al.*, he also investigated the *homo*-coupling mechanism. It was confirmed that the *homo*-coupled product was derived exclusively from the presence of multiple organoboranes and that the catalytic cycle was entirely independent of the presence of the aryl halide. Furthermore, the coupling of two phenylboronic acids was found to proceed in the presence of dioxygen. The proposed mechanism is displayed in Scheme 1.10.²⁵ The peroxo complex $[(\eta^2-O_2)Pd(L)_2]$ was generated by the addition of dioxygen to the $Pd(0)$ species. This step was followed promptly by the activation of one of the $Pd-O$ bonds by treatment with an arylboronic acid. However, a second phenylboronic acid was necessary to complete the subsequent transmetalation step. In successive steps, the boronic acid was displaced by the pertinent OH^- , followed by a second transmetalation step with an

additional organoborane. The final step consisted of the reductive elimination of the *homo*-coupled biaryl product.



Scheme 1.10: The *homo*-coupled mechanism of the Suzuki-Miyaura reaction devised by Amatore *et al.* ($\text{L} = \text{PPh}_3$).

1.1.3 Current Applications

The Suzuki-Miyaura reaction represents one of the most industrially important methods for the generation of C–C bonds. The formation of such bonds is of critical importance for the synthesis of both natural products and pharmaceuticals.²⁸ Recently, Nicolaou *et al.* reported the synthesis of Vancomycin, an antibiotic capable of treating the penicillin-resistant *Staphylococcus Aureus*, in which a Suzuki coupling was

performed for the asymmetric construction of the bicyclic structure (Figure 1.2).²⁹ In this case, the parent boronic acid was coupled to the asymmetric aryl iodide to produce a single compound with atropisomers. The pertinent step is depicted in Scheme 1.11.

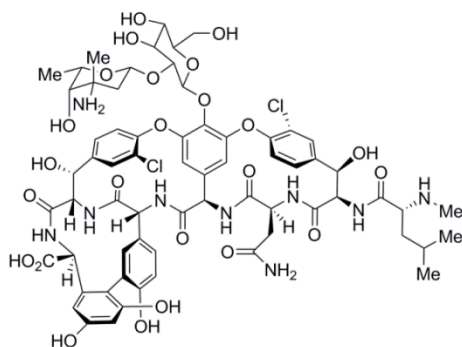
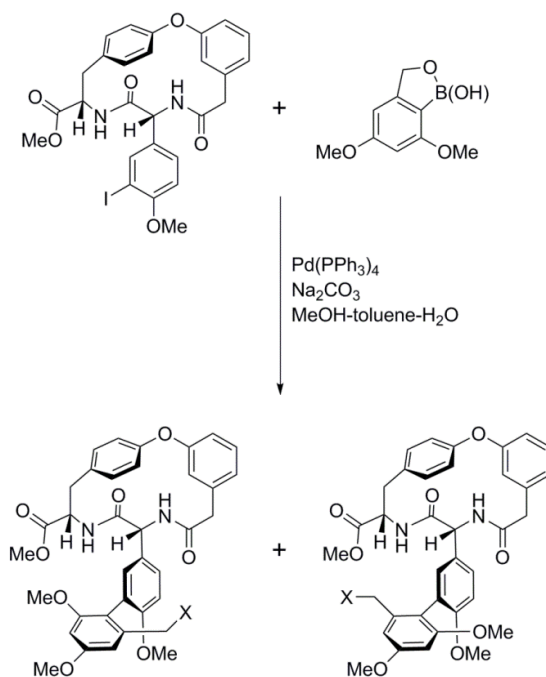
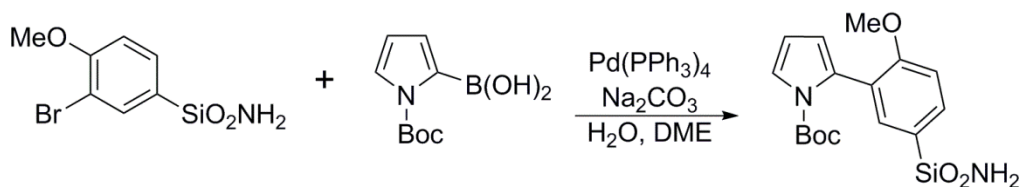


Figure 1.2: The structure of the antibiotic Vancomycin synthesized by Nicolaou *et al.*



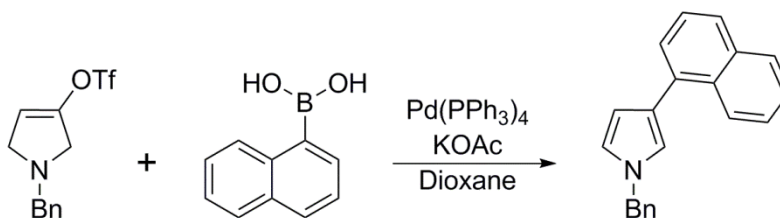
Scheme 1.11: The eleventh step in the total synthesis of Vancomycin is the Suzuki coupling of an asymmetrical aryl iodide with a functionalized boronic acid. The reaction mixture was heated to 90 °C for 2 h and the products were isolated in a combined 80% yield.

The preparation of Vancomycin was particularly significant as it was one of the first examples of an application for the Suzuki cross-coupling reaction. In the ensuing decade, a plethora of novel applications have been developed.^{30–34} The development of aryl 2,5-disubstituted pyrroles has been examined extensively, due to their selective dopamine D₃ receptor antagonist properties. For example, Johnson *et al.* examined 2-arylpyrroles that were capable of a one-step conversion to produce 2,5-disubstituted pyrroles (Scheme 1.12).³⁰ The Boc protecting group was removed by treatment with sodium methoxide in methanol at room temperature.



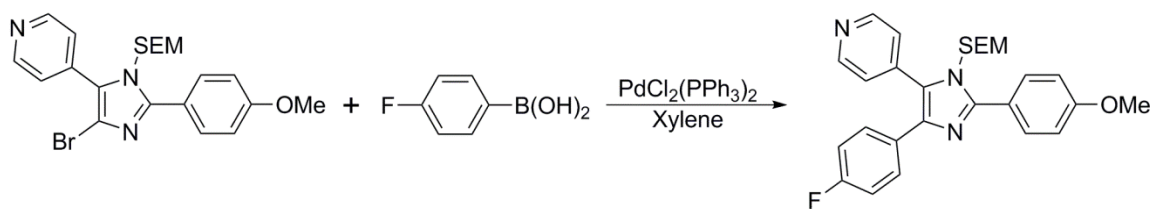
Scheme 1.12: The Suzuki cross-coupling reaction was heated at reflux for 0.5–18 h, thereby affording the asymmetrical product in 83% yield.

Lee and co-workers also pursued the synthesis of 2,5-disubstituted pyrroles with bulkier phenylboronic acids (Scheme 1.13). Interestingly, they observed a tandem Suzuki-dehydrogenation reaction, in which the Suzuki reaction was immediately followed by a dehydrogenative aromatization of the pyrroline to form 3-arylpyrrole.³¹



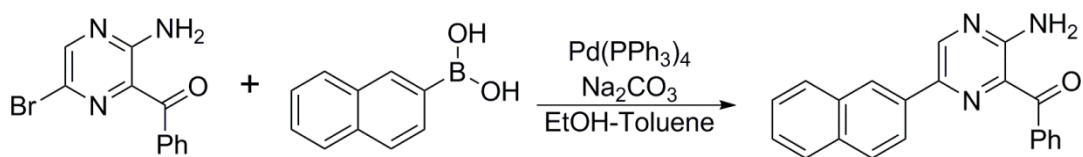
Scheme 1.13: The Suzuki cross-coupling reaction was heated overnight at 100 °C, thereby affording the *hetero*-coupled product in 74% yield.

The Suzuki-Miyaura cross-coupling reactions presented by Johnson and Lee were enhanced by Revesz and co-workers for the construction of trisubstituted imidazoles. These imidazoles have been found to be invaluable for the natural synthesis of anti-inflammatory pharmaceuticals. It was determined that the coordination of an anisole directly to an imidazole provided optimal reaction conditions (Scheme 1.14).³² Revesz also noted that the coupling of the aryl bromide with fluorophenylboronic acid would not proceed without the SEM (2-(trimethylsilyl)ethoxymethyl) protecting group. Upon completion of the reaction, the SEM group was removed by the addition of a 1:1 EtOH:HCl_{conc} mixture at room temperature.



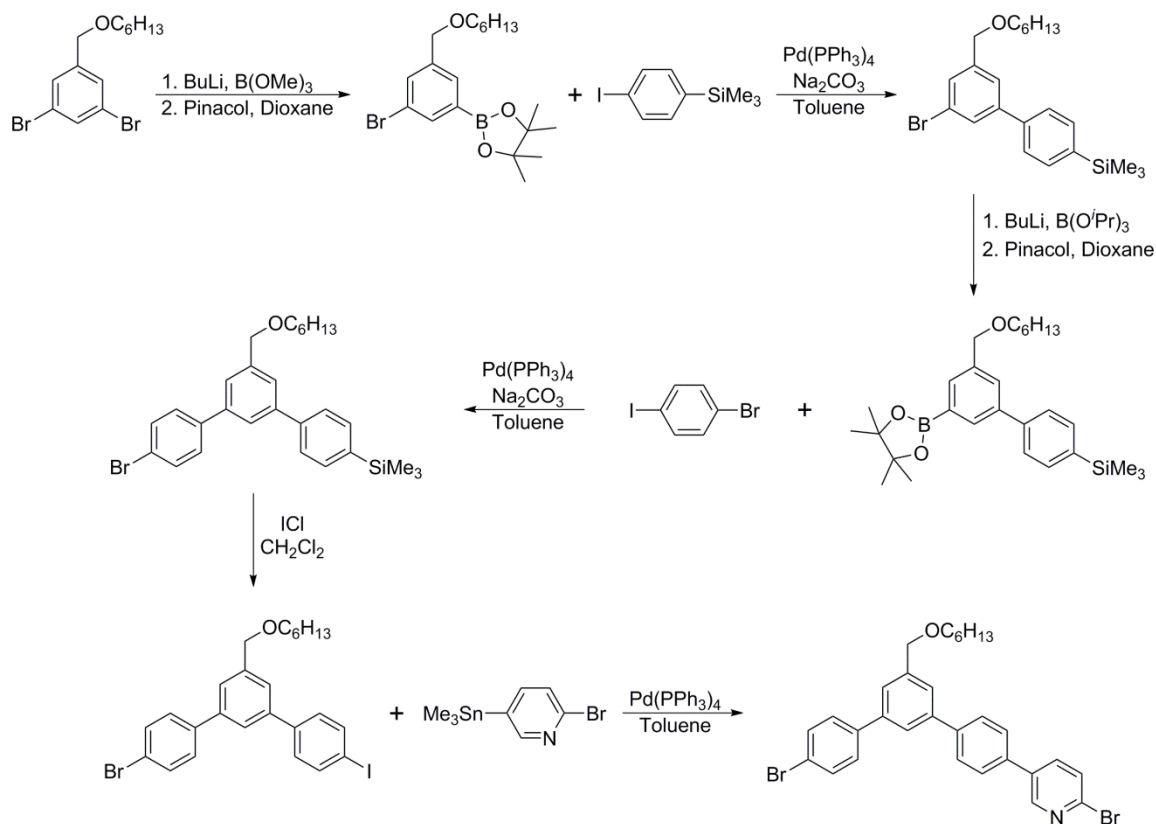
Scheme 1.14: The Suzuki cross-coupling reaction was heated to reflux for 5 h, thereby affording the trisubstituted imidazole in 68% yield.

Furthermore, the Suzuki reaction was found to be essential for the production of imidazopyrazine ring systems. A significant effort was made to develop such systems due to their luminescent properties that are common to those of several marine organisms. Jones *et al.* expanded the scope of the Suzuki reaction by coupling naphthalene-2-boronic acid to a functionalized aryl bromide in an ethanol-toluene mixture (Scheme 1.15).³³ Interestingly, this particular Suzuki coupling reaction proceeded to almost complete conversion.



Scheme 1.15: The Suzuki cross-coupling reaction was heated to reflux for 4 h, thereby affording the luminescent imidazopyrazine system in 96% yield.

Although the previous examples are definitely noteworthy, it can be argued that the most significant application of the Suzuki-Miyaura cross-coupling reaction relates to Manickam and Schlüter's modular chemistry. These authors devised a beautiful example of a six-step synthesis to produce the hetarylene building block, in which two Suzuki coupling reactions were partnered with a Stille reaction. The order of the Suzuki couplings was crucial in terms of the overall yields of these targeted building blocks. The order of Suzuki reactions displayed in Scheme 1.16 afforded a yield of 63%, while the reverse order of Suzuki couplings resulted in only a 16% yield³⁴



Scheme 1.16: The direct synthesis of the desired hetarylene building block presented by Manickam and Schlüter utilizing two Suzuki and one Stille cross-coupling reactions.

1.2 HOMOGENEOUS CATALYSIS

1.2.1 Ligands

Prior to the publication of the original Suzuki-Miyaura reaction, Richard Heck and Tsutomu Mizoroki separately pioneered the first palladium catalyzed cross-coupling reaction of an aryl halide with an olefin to afford a 70% yield of *cis/trans* isomers.^{35,36} In the following year, Heck and Dieck supplemented the reaction with triphenylphosphine, which subsequently produced comparable yields of stereospecific alkenes.³⁷ It was determined that the optimum ratio of phosphine ligand to palladium metal was 2:1, since

the use of all other ratios resulted in slower rates. Furthermore, Heck and co-workers used triphenyl phosphite, tri-*n*-butylphosphine, and trimethylolpropane phosphite as ligands for their experiments. However, in each case the ligand was found to be less selective and significantly slower than triphenylphosphine.

The modified Heck-Mizoroki reaction presented by Heck and Dieck generated significant interest in the field of palladium-catalyzed cross-coupling reactions. One of the first variations was accomplished by Sonogashira in the coupling of an aryl halide with acetylene.³⁸ Although the addition of cuprous iodide was necessary, triphenylphosphine was still used as the primary ligand. In 1977, Negishi employed triphenylphosphine as a ligand for the coupling of aryl halides with organozinc compounds, and shortly thereafter Stille described a similar reaction with organotin reagents and aryl halides.^{39,40} Interestingly, Sonogashira, Negishi, and Stille all utilized the optimal 2:1 PPh₃:Pd ratio that had been first used by Heck. In the following year, Suzuki presented the first Suzuki-Miyaura cross-coupling reaction. In this case, four triphenylphosphine ligands were attached to the palladium(0) metal center in the form of palladium *tetrakis*(triphenylphosphine).¹

1.2.1.1 Phosphine Ligands

In the years following the original Suzuki publication, a significant number of other phosphine ligands have been investigated for their efficacy in the palladium-catalyzed homogeneous cross-coupling reaction. Tertiary phosphines, PR₃, were of particular interest due to their ability to be tuned both sterically and electronically by changing the R group. Moreover, these phosphine ligands were also able to confer stability on the corresponding palladium complexes, (R₃P)_{*n*}M–L. In most cases, this extra stability was due to the π -acidity of the phosphine ligands.⁴¹ Furthermore, Dias and co-

workers studied the electronic properties of several PR_3 ligands, and thereby derived a representative molecular orbital diagram based on the various R groups (Figure 1.3).⁴² It was observed that the metal donated electrons directly into the empty σ^* orbital of the P–R bond. However, the stability of this orbital only corresponded to the electronic properties of the R group. As the electronegativity of the R group increased, the σ^* orbital became lower in energy, thus providing more stability to the system. Furthermore, the electronegativity of the R group provided an increased electronic contribution from the phosphorus center, which, in turn, resulted in a larger σ^* orbital. Dias *et al.* established that both of the above factors promoted more back donation from the palladium metal center, and provided the following ranking of frequently used phosphine ligands based on observed π -acidity: $\text{PF}_3 > \text{PCl}_3 > \text{P}(\text{OAr})_3 > \text{P}(\text{OMe})_3 > \text{PAr}_3 > \text{PMe}_3$.

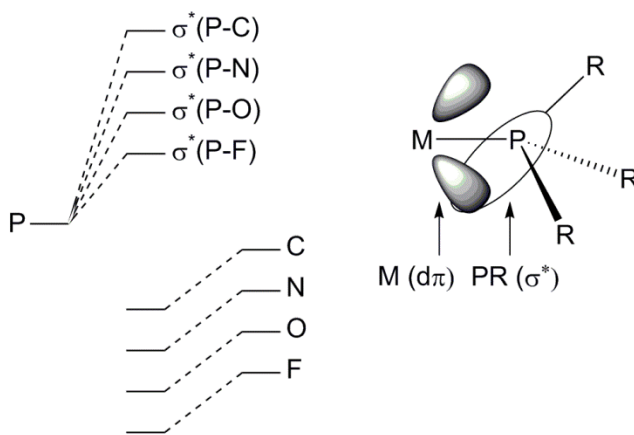
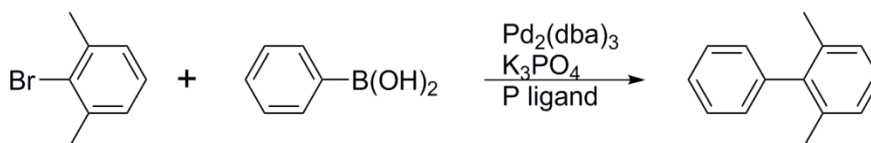


Figure 1.3: The molecular orbital diagram of PR_3 ; R = C, N, O, F derived by Dias *et al.*

In addition to σ -orbital back donation, tertiary phosphines have also been evaluated from the standpoint of cone angles. For example, Griffiths and Leadbetter studied the effect of the PR_3 cone angle on the Suzuki coupling of sterically hindered 2,5-

dibromobenzene with phenylboronic acid. Several phosphine and phosphite ligands were treated with *bis*(dibenzylideneacetone)palladium(0) ($\text{Pd}_2(\text{dba})_3$), which revealed a direct correlation between the cone angles and the overall reaction yields. It was postulated that a phosphine ligand with a small cone angle allowed for an easier access of the resulting phosphine complex to the sterically hindered C–X bond. The forgoing hypothesis was supported when $\text{P}(\text{OMe})_3$ and PPh_3 were employed as ligands for the Suzuki reaction. The former ligand resulted in 82% conversion to the *hetero*-coupled product, while PPh_3 ligands resulted in no conversion. The large difference in yields may be attributed to the small cone angle of 107° in the case of trimethylphosphite. By way of comparison, triphenylphosphine has a cone angle of 145° . (Table 1.1).⁴³

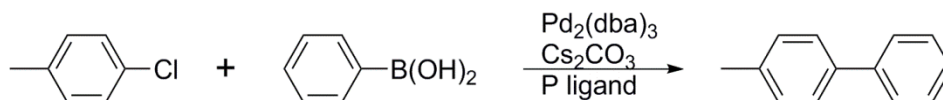


P-donor Ligand	Yield (%)	Cone Angle ($^\circ$)
PPh_3	0	145
PEt_3	30	132
$\text{P}(\text{OEt})_3$	37	110
$\text{P}(\text{OMe})_3$	82	107

Table 1.1: Reaction conditions: 3 mol% $\text{Pd}_2(\text{dba})_3$, 6 mol% P-donor ligand, 2 equivalents K_3PO_4 , dioxane, 95°C , 8 h.

Although Griffiths *et al.* demonstrated an indirect relationship between cone angle and yield in the case of the sterically hindered coupling of aryl bromides and boronic acids, Littke *et al.* published a contradictory trend for the activation of simple aryl chlorides. In fact, only phosphine ligands with significant steric bulk and higher pK_a were

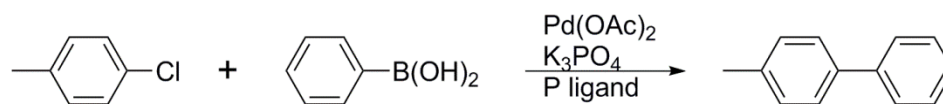
capable of assisting the oxidative addition of the aryl halide (Table 1.2). The optimum ratio of $\text{Pd}_2(\text{dba})_3:\text{P}(t\text{-Bu}_3)$ was found to be 1.0:2.4, which afforded yields of 82-92%.⁴⁴



Phosphane	Yield (%)
PPh_3	0
BINAP	0
dppf	0
$\text{P}(o\text{-tol})_3$	10
$\text{Ph}_2\text{P}(\text{CH}_2)_3\text{PPh}_2$	0
$\text{Cy}_2\text{P}(\text{CH}_2)_3\text{PCy}_2$	0
PCy_3	75
$\text{P}(t\text{-Bu}_3)$	86

Table 1.2: Reaction conditions: 1.5 mol% $\text{Pd}_2(\text{dba})_3$, 3.6 mol% phosphane, 2 equivalents Cs_2CO_3 , dioxane, 80 °C, 5 h.

In an effort to develop a more industrially viable catalytic system, Zapf and co-workers expanded the work presented by Littke *et al.* to include significantly larger phosphine ligands. For example, the use of Littke's $\text{P}(t\text{-Bu}_3)$ ligand with 0.01 mol% $\text{Pd}(\text{OAc})_2$ resulted in a 92% conversion. However, the use of BuPAd_2 and 0.005 mol% $\text{Pd}(\text{OAc})_2$ afforded the desired *hetero*-coupled product in 87% yield (Table 1.3).⁴⁵ The data presented by Zapf *et al.* provided additional support for the proposal that large, bulky phosphine ligands were ideal for the Suzuki-Miyaura cross-coupling reaction.



Phosphane	Pd [mol %]	Yield [%]	TON
PPh ₃	0.1	5	50
PhPCy ₂	0.1	23	230
(<i>o</i> -tol)PCy ₂	0.1	49	490
(<i>o</i> -anisyl)PCy ₂	0.1	42	420
(<i>o</i> -biph)PCy ₂	0.05	93	1860
(<i>o</i> -biph)PCy ₂	0.01	47	4700
PCy ₃	0.1	23	230
P(<i>t</i> -Bu) ₃	0.01	92	9200
P(<i>t</i> -Bu) ₃	0.005	41	8200
BuPAd ₂	0.01	94	9400
BuPAd ₂	0.005	87	17,400

Table 1.3: Reaction conditions: Pd(OAc)₂:P (2:1), K₃PO₄, toluene, 100 °C, 20 h.

Taking into account the results presented in Table 1.3, Feuerstein *et al.* prepared a bulky tetrapodal phosphine ligand, namely *cis,cis,cis*-1,2,3,4-*tetrakis*(diphenylphosphinomethyl)-cyclopentane (Tedicyp) in an attempt to couple heteroaromatic substrates.⁴⁶ It was anticipated that the large phosphine ligand could possibly assist in the oxidative addition of the C–X bond, due to the positioning of all four diphenylphosphinoalkyl groups on the same face of the cyclopentane ring (Figure 1.4). In 2001, Feuerstein *et al.* disclosed the unusually high activity of Tedicyp in the presence of palladium. The Tedicyp–[PdCl(C₃H₅)]₂ complex successfully activated a large number of aryl halides and heteroaromatics in high yields with appreciable turnover numbers.^{2,46–52} In the case of 4-bromobenzophenone, a turnover number of 28,000,000 was achieved using a catalyst loading of 0.00001%.⁴⁷ As a consequence of the significant bond dissociation energy of the C–Cl bond, Feuerstein *et al.* reached a lower turnover

number of 21 with the deactivated 4-chloroanisole. Nevertheless, with 0.000005% catalyst loading and 2-chloro-5-(trifluoromethyl)nitrobenzene, a turnover number of 6,800,000 was achieved.⁴⁸ Interestingly, comparable turnover numbers were reported with β - and γ -substituted bromopyridines (2,500,000 and 810,000, respectively). However, in this case, due to a negative interaction between the nitrogen atom in α -substituted bromopyridines and the palladium metal center on the catalyst resulted in significantly lower turnover numbers (62,000).⁵³

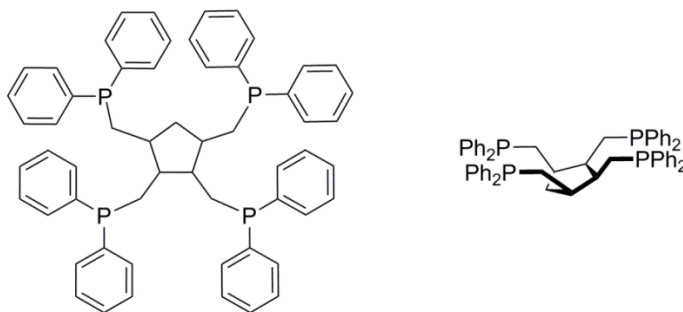
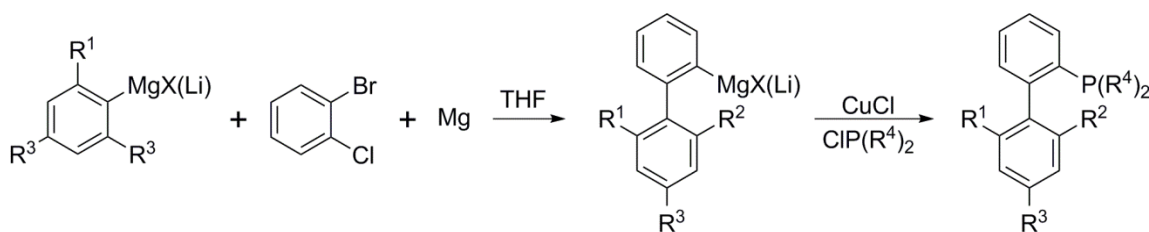


Figure 1.4: Two illustrations of *cis,cis,cis*-1,2,3,4-*tetrakis*(diphenylphosphinomethyl)-cyclopentane, Tedicyp.

The Suzuki-Miyaura cross-coupling reaction catalyzed by Tedicyp-[PdCl(C₃H₅)]₂ was subsequently extended to include vinyl bromides by Berthiol *et al.* With the use of only 0.001% of the catalyst in the reaction mixture, it was found that α -bromostyrene was able to generate 1,1-biarylethylene in 92% yield.⁵⁴ Furthermore, Chahen and co-workers enhanced the Suzuki coupling of benzylic halides with functionalized phenylboronic acids at catalyst loadings of as small as 0.0001% Tedicyp-[PdCl(C₃H₅)]₂. Furthermore, in the case of deactivated 3,5-dinitrobenzyl chloride, complete conversion was achieved with a relative turnover number of 840.⁵⁵

Although the Tedicyp ligand provided stability and readily enhanced the activity of the palladium catalyst, the sensitivity of this ligand to air and moisture rendered these catalysts inappropriate for industrial use. Nevertheless, the advantageous properties of Tedicyp were found to fortuitously exist in dialkylbiarylphosphine and trialkylphosphine ligands that maintained the steric bulk and electron-rich character of Tedicyp. Subsequently, Buchwald *et al.* presented the following five advantages of employing dialkylbiarylphosphine ligands for the Suzuki reaction: (i) they are crystalline materials; (ii) they are air stable; (iii) they are thermally stable; (iv) they are predominantly commercially available; and (v) they are utilized in atmospheric conditions without a glovebox.⁵⁶ These ligands have also been synthesized in a one-pot procedure using an aryl Grignard (Scheme 1.17),⁵⁷ the ligands for which are depicted in Figure 1.5. Remarkably, the tunable steric and electronic properties on the biarylphosphine ligands have allowed for significantly enhanced activity and selectivity of the corresponding palladium complexes. The steric bulk and electron-rich character of these ligands have been found to provide stability to the monoligated L_1Pd intermediates in the catalytic cycle.⁵⁸ Moreover, the rate of oxidative addition of aryl halides to $L_1Pd(0)$ has been found to be considerably faster than the that of analogous $L_2Pd(0)$ species.^{59,60} This result can be attributed directly to the difference in size between the mono- and biligated species. Thus, the aryl halide is capable of accessing the palladium intermediate more easily in $L_1Pd(0)$. Although no experimental evidence has been presented, the rate of transmetallation is presumed to operate in a similar manner. In fact, the rate of reductive elimination has been confirmed to proceed significantly faster with a monoligated compound relative to the corresponding biligated analogue.^{61,62} The individual rates in the catalytic cycle were enhanced by the addition of a substituent in the *ortho* position

relative to the lower aryl ring due to the substantial increase in the concentration of the L_1Pd intermediate. It was also determined that a larger group in the *ortho* position would prevent palladacycle formation.⁶³



Scheme 1.17: Synthesis of a generic trisubstituted-dialkylbiarylphosphine ligand.

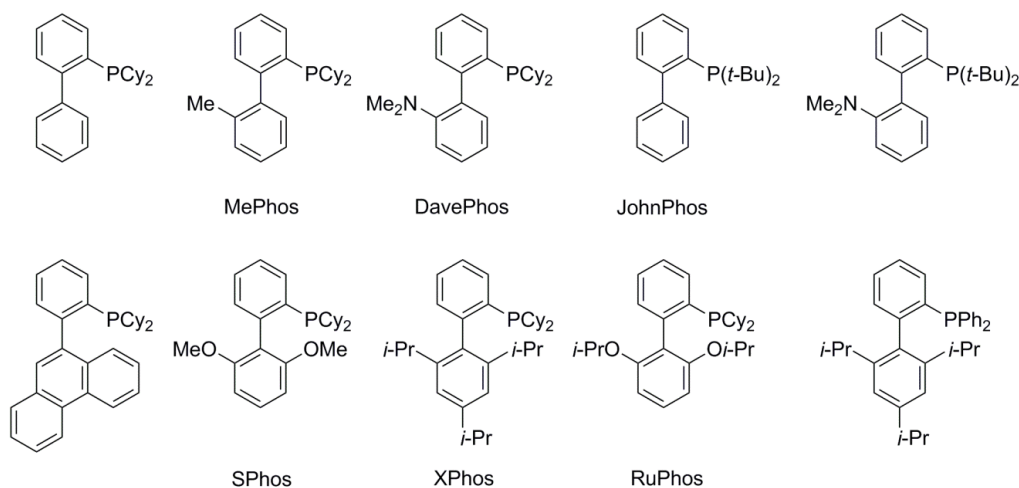


Figure 1.5: Common dialkylbiarylphosphine ligands with their associated monikers.

The biarylphosphines were probed initially with $Pd(OAc)_2$ for their activities in the Suzuki reaction with the specific objective of coupling hindered substrates. It was discovered that the presence of a small functional group in the *ortho*-position of the lower benzene ring resulted in a significant increase in the activity of the palladium catalyst.

For example, the ligand ‘DavePhos’ was found to facilitate C–X activation, which was attributed to the addition of a dimethylamino functional group.⁶⁴ Simultaneously, Fu *et al.* exploited the use of $P(t\text{-Bu})_3$ as a ligand and reported a slight increase in activity.⁴⁴ In turn, the latter development resulted in the design of the ligand ‘JohnPhos’, in which PCy_3 was replaced by $P(t\text{-Bu})_3$, in addition to the removal the dimethylamino functional group.⁶⁵ Remarkably, the JohnPhos–Pd system was even more reactive at room temperature. The increase in activity was believed to be due to higher $L_1Pd(0)$ and $L_1Pd(Ar)Cl$ concentrations than those used in the analogous L_2Pd intermediates.

Although JohnPhos significantly enhanced the coupling of aryl halides with phenylboronic acids, it was not particularly useful for the production of unsymmetrical *tetra-ortho*-substituted biaryls. The desired product was eventually prepared by Buchwald *et al.* using the new bi-*ortho*-substituted biarylphosphine ligand, SPhos.^{66,67} Interestingly, the SPhos ligand conferred unprecedented stability on the L_1Pd system, which, in turn, resulted in the promotion of unactivated aryl bromides and chlorides using only 0.0005 mol% Pd. The final successful modification of the dialkylbiarylphosphine ligand class involved the addition of a bulky substituent to the *para*-position of the lower biaryl ring. The resulting XPhos ligand featured the presence of isopropyl groups in the *ortho*- and *para*-positions of the lower biaryl ring.⁶⁸ Although XPhos was unable to provide a more active catalyst than SPhos using the standard Suzuki-Miyaura reaction conditions, the XPhos–Pd catalyst efficiently coupled thiophenes and pyridylboronic acids with low catalyst loading. This accomplishment was unparalleled, particularly in the presence of highly basic aminopyridines and heteroaryl chlorides due to the predisposition of such compounds to undergo protodeboronation. It has also been demonstrated that XPhos and SPhos are both capable of aryl chloride borylation.⁶⁹ A

useful summary of the pertinent characteristics of the dialkylbiarylphosphine ligands was published recently by Buchwald *et al.* (Figure 1.6).⁵⁶

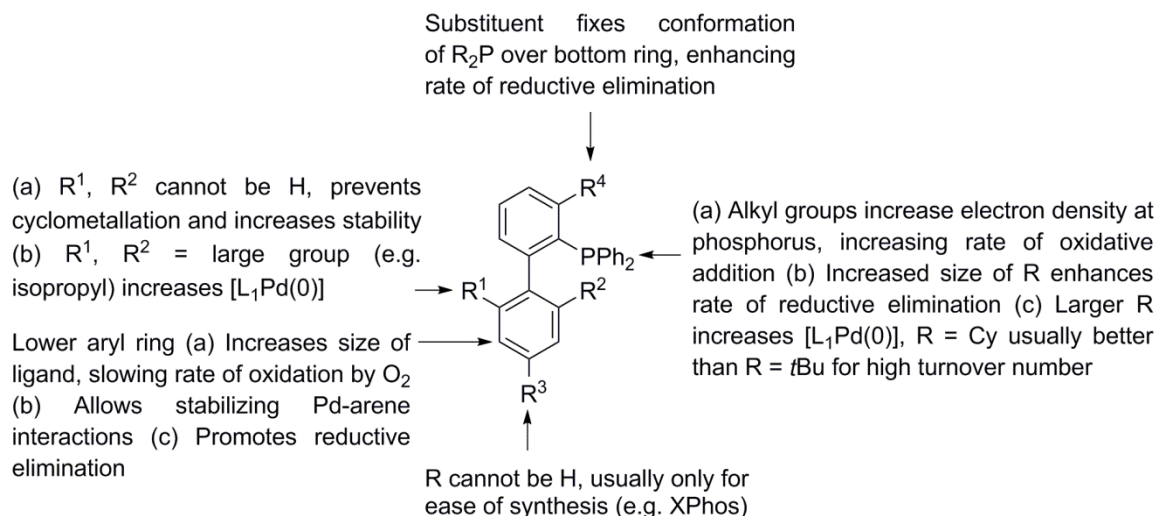


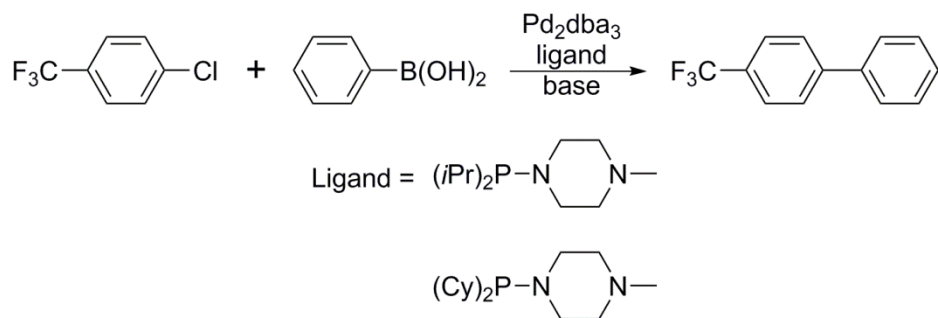
Figure 1.6: A concise summary of the benefits of dialkylbiarylphosphine ligands in the Suzuki-Miyaura cross-coupling reaction presented by Buchwald *et al.*

Buchwald *et al.* presented a compelling argument for the advantages of using biarylphosphine ligands; nevertheless, a significant amount of interest has been generated on the use of smaller air stable variations of triphenylphosphine. Initially, many research groups attempted to couple deactivated aryl chlorides with phenylboronic acids by the use of sterically hindered phosphite-palladium systems. Unfortunately however, the cross-coupling reactions would not proceed without the addition of calcium fluoride. Nevertheless, under optimum conditions a turnover number of 820,000 can be achieved.⁷⁰

Li *et al.* discovered the first air stable phosphine-palladium systems that were active for Suzuki-Miyaura cross-coupling reactions. These phosphine oxide precursors ($RR'P(O)H$) were converted to phosphinous acid ($RR'POH$)-metal complexes that regioselectively activated aryl and vinyl chlorides with thiols, olefins, and amines.⁷¹⁻⁷³

Kayaki expanded this idea by the design and synthesis of $\text{Pd}[\text{P}(\text{OC}_6\text{H}_5)_3]_4$, which is capable of converting allylic alcohols to phenylbutenes in thirty minutes in a 67% yield.⁷⁴

A few aminophosphines have also been proposed as potentially valuable ligands for the Suzuki reaction on the basis that the donating character of the amine substituent would assist the activation of the C–X bond. The first functional example was introduced by Clarke *et al.*, and featured a phosphine functional group attached to a methylpiperazine (Scheme 1.18).⁷⁵ Although this ligand system resulted in 100% conversions for several aryl chlorides; the reaction appeared to be heavily base-dependent. Furthermore, if the aminophosphine ligand was attached to an $(i\text{-Pr})_2\text{P}$ group, the Suzuki coupling reaction required the addition of potassium phosphate. On the other hand, when PCy_2 was used, the highest reactivity occurred with cesium fluoride.



Scheme 1.18: Reaction conditions: 1 mol% Pd, 4 mol% ligand, toluene, 90 °C, 16 h, K_3PO_4 or CsF.

Initially, Urgaonkar used commercially available bicyclic triaminophosphine ligands to create unsymmetrical biaryls from aryl chlorides in high yields (Figure 1.7a).⁷⁶ In the following year, Cheng *et al.* developed air stable aminophosphine ligands, in which two amino functional groups were tethered to a phosphine ligand (Figure 1.7b).⁷⁷ Although these ligands activated the aryl chlorides adequately, the desired biaryl products

were only produced in low yields. One of the most innovative modifications of this reaction was reported by Harkal and co-workers (Figure 1.7c). In this approach, a functionalized *N*-heterocyclic carbene was directly coordinated to a phosphine.⁷⁸ All four variations of this ligand were found to react with palladium (II) acetate in the Suzuki-Miyaura cross-coupling reaction. However, only the unsubstituted phenyl substituent gave reproducible results with aryl chlorides at low catalyst loadings. No explanation for this outcome was provided.

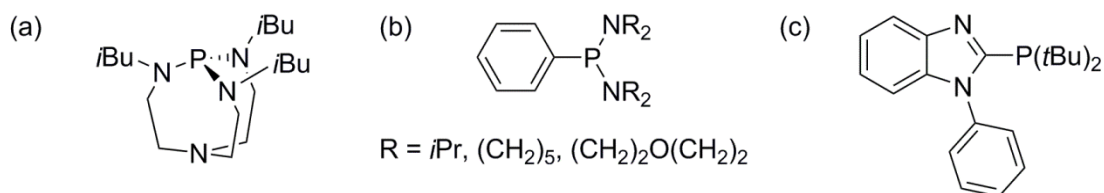


Figure 1.7: (a) Bicyclic triaminophosphine ligand presented by Urgaonkar *et al.* (b) aminophosphine ligand introduced by Cheng *et al.* (c) phosphinoimidazole established by Harkal *et al.*

These ligand modifications were carried out with the objective of enhancing the stabilities of several of the palladium intermediates in the catalytic cycle of the Suzuki reaction by taking advantage of the steric bulk and electron rich character of the aminophosphine and phosphite ligands. In addition to the introduction of oxygen and nitrogen chelating groups into the parent phosphine ligands, a few research groups prepared ligands that contained multiple phosphine sites. For example, Shen and co-workers employed the bidentate ligand 1,3-bis(diphenylphosphino)propane (dppp) and palladium (II) acetate for the activation of aryl chlorides with *ortho*- and *para*-electron withdrawing substituents with high efficiency (Figure 1.8a).⁷⁹ Interestingly, when Sjovalld *et al.* replaced the central carbon of dppp with a benzene ring, the resulting chelating

diphosphane ligand proved to be an adequate catalyst for the vinylation of aryl bromides and iodides in the Heck reaction (Figure 1.8b).⁸⁰ In turn, the success of these bidentate phosphine ligands inspired Doherty *et al.* to combine the ligands developed by Shen and Sjovall to produce 1,3-butadiene bridged diphosphine ligands, specifically for the design of 1,4-bis(diphenylphosphino)-1,3-butadiene) or the ligand ‘NUPHOS’ (Figure 1.8c).⁸¹ The unique invention of NUPHOS permitted $\text{Pd}_2(\text{dba})_3$ to facilitate the Suzuki coupling of aryl bromides and phenylboronic acids with two chelating sites on the Pd(II) metal center with a turnover number of 1,000,000 at 0.0001 mol% Pd.

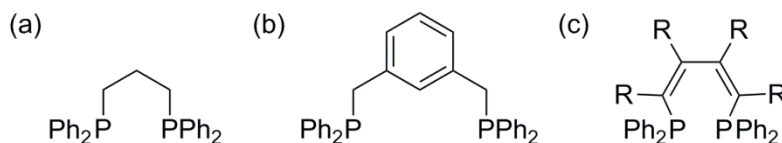


Figure 1.8: bidentate ligands (a) 1,3-bis(diphenylphosphino)propane (b) *cis*-1,3- $(\text{Ph}_2\text{PCH}_2)_2\text{C}_6\text{H}_4$ (c) 1,4-bis(diphenylphosphino)-1,3-butadiene); R = Ph, Me.

In summary, the originally used phosphine ligand, PPh_3 , has been optimized by two major modifications, namely the introduction of (1) an oxygen or nitrogen containing functional groups or (2) the addition of phosphine groups. The foregoing alterations were particularly useful for the Suzuki-Miyaura cross-coupling reaction with functionalized aryl halides and phenylboronic acids through extra stability afforded to various palladium intermediates, $\text{L}_1\text{Pd}(0)$. A few research groups have successfully combined the previously cited modifications to produce bidentate (P,O)– or (P,N)–chelating ligands. Interestingly, the backbone-derived P,O–ligands synthesized by Bei *et al.* were not sensitive to air and moisture.⁸² Moreover, these ligands were capable of activating aryl halides with *ortho*-substituents and electron poor/rich systems with only 1 mol% $\text{Pd}_2(\text{dba})_3$ in ~90% yields.

(Figure 1.9a).⁸³ Furthermore, Mukherjee and co-workers derived a similar system with pyrazole-based bidentate P,N-donor phosphine ligands. However, this approach resulted in lower yields than those of those of the analogous Bei process. The pyrazole system was capable of activating simple aryl chlorides in four hours using 1 mol% Pd (Figure 1.9b).⁸⁴

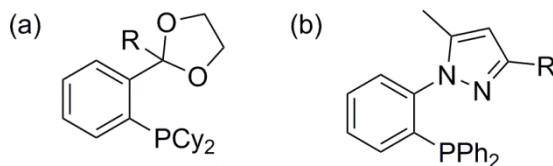


Figure 1.9: Bidentate ligands (a) 2-(2'-dicyclohexylphosphinophenyl)-1,3-dioxolane; R = Me, H (b) pyrazole-tethered triarylphosphine; R = CH₃, *t*Bu, Ph, Mes.

1.2.1.2 *N*-Heterocyclic Carbene Ligands

Although a few cases of air stable phosphine ligands have been highlighted in this review, the majority of these compounds have been found to be air- and moisture-sensitive. In an attempt to circumvent these drawbacks, a new type of ligand was designed as a tertiary phosphine mimic.⁸⁵ This particular *N*-heterocyclic carbene (NHC) ligand was introduced originally by Hermann *et al.* using a Heck olefination reaction. The new NHC ligand was found to possess exceptionally high thermal stability. In the ensuing twenty years, the NHC ligand became the third most popular ligand after bulky dialkylbiaryl- and trialkylphosphines for the Suzuki-Miyaura cross-coupling reaction.⁵⁶

Both the phosphine and the NHC ligands were considered to function as two-electron donors. However, the steric and electronic properties of each ligand system were distinctly different. One of the most attractive properties of the phosphine ligands is typically described from the standpoint of Tolman parameters or cone angles.⁸⁶ The cone angle terminology was derived from the shape of the phosphine ligand, in which the

steric bulk was directed away from the metal center of the catalyst.⁸⁷ Conversely, the R groups on the NHC ligand were often located within the coordination spheres of the palladium complexes (Figure 1.10).⁸⁸ As a consequence, the R groups had a profound influence on the outcome of catalysis utilizing NHC-based complexes.⁸⁵

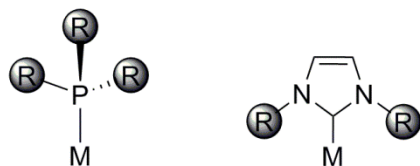


Figure 1.10: Illustration of PR_3 and NHC steric characteristics presented by Fortman *et al.*

The R groups on the NHC ligands were postulated to have a negative steric influence on the corresponding palladium catalysts, although they were also attributed to the unusually strong M–C bond. As a consequence, a molecular orbital diagram was generated in an effort to explain the unique electronic properties of this ligand class. Particular emphasis was placed on the distinction between the strengths of the analogous M–NHC and M– PR_3 bonds (Figures 1.3 & 1.11). The primary component of the M–NHC bond was observed to be $\text{L} \rightarrow \text{M}$ σ -dative bonding, followed in order of weakening bonding component by $\text{M} \rightarrow \text{L}$ π^* -backbonding and $\text{L} \rightarrow \text{M}$ π -donation. Furthermore, the M–NHC bonds were found to possess as much as 20% of π -interactions in the case of d^{10} metals and 15% for the corresponding d^8 metals. The $\text{M} \rightarrow \text{L}$ π^* -backbonding was found to be a direct result of an orbital overlap of the π^* -orbital between the carbonyl carbon and the HOMO of the metal center. On the other hand, the $\text{L} \rightarrow \text{M}$ π -donation was found to result from an overlap of the filled NHC π -orbital with an empty metal d -orbital.⁸⁹

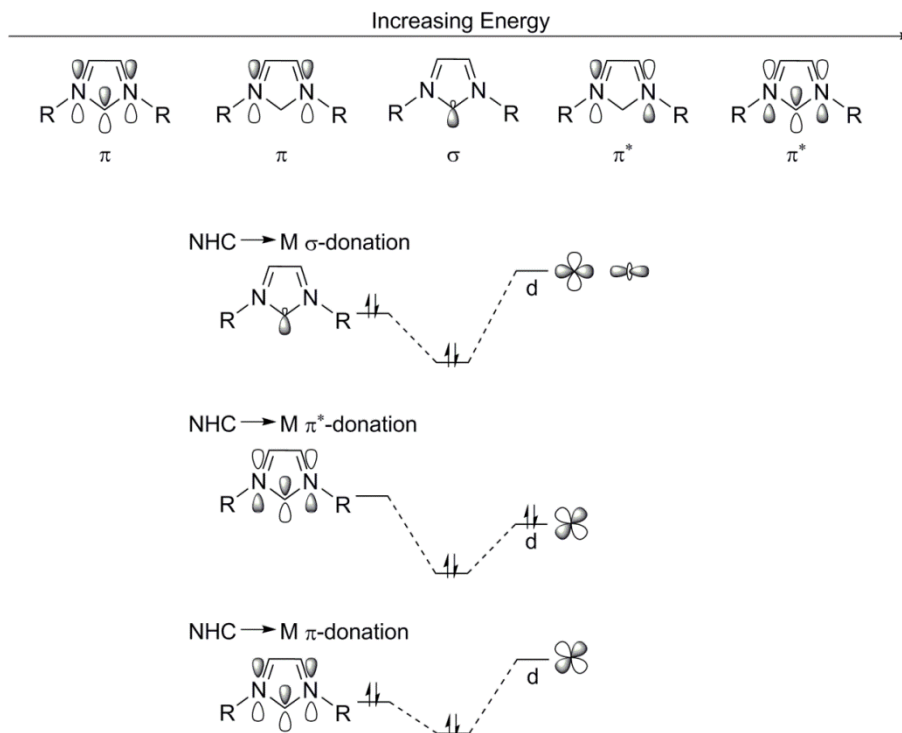


Figure 1.11: A simple picture of the frontier orbitals involved in three distinct M–NHC interactions.

Subsequently, the interesting properties of the NHC ligand have been enhanced by manipulation of the C–C backbone. It was discovered that the bulky R groups with an unsaturated NHC backbone were more capable of protecting the active site on the Pd metal center. Furthermore, fusing the NHC moiety to a benzene ring provided additional stability to an otherwise somewhat sensitive ligand system. It has been proposed that this stabilization effect arises from the presence of a delocalized electron π -cloud above or below the ligand structure. Unfortunately, however the steric bulk of the benzene ring has a tendency to reduce the activities of NHC-based catalysts. Furthermore, the presence of a saturated NHC backbone was found to decrease the overall rate of reaction, due the

difficulty in detachment from the metal center.⁹⁰ The relative thermodynamic stabilities of these NHC ligands are presented in Figure 1.12.^{91,92}

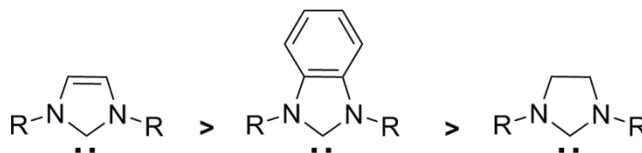


Figure 1.12: The relative stabilities of three diaminocarbene ligands.

The first examples of nucleophilic carbenes were isolated and characterized by Arduengo *et al.* in 1992.⁹³ The four new free carbenes were found to be relatively stable due to a combination of electronic and steric influences (Figure 1.13). Subsequently, the “phosphine mimic” was determined to be effective for numerous hydrosilylation, olefin metathesis, and Heck reactions by a number of research groups.^{94–98} One of the major outcomes of these syntheses was the synthesis of the first NHC–Pd homogeneous catalyst for the Suzuki-Miyaura cross-coupling reaction by Zhang *et al.*⁹⁹ It was found that the presence of $\text{Pd}_2(\text{dba})_3$ and Cs_2CO_3 , IMes successfully activated *p*-chlorotoluene, thereby forming *p*-phenyltoluene with 59% selectivity for the *hetero*-coupled product (Scheme 1.19).

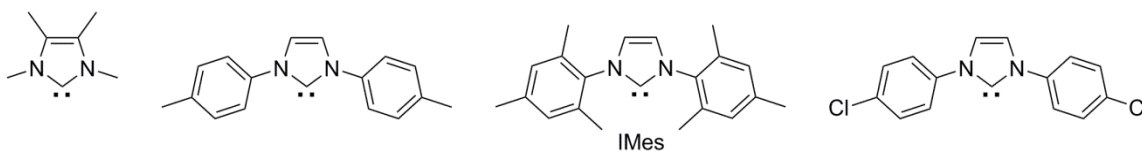
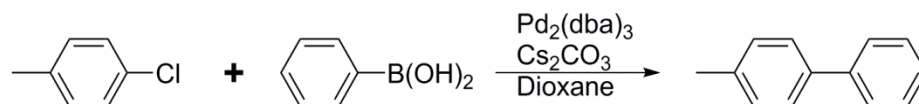


Figure 1.13: The first NHC ligands reported by Arduengo *et al.*



Scheme 1.19: The first Suzuki reaction carried out with an NHC ligand (80 °C, 1.5 h).

In addition to activating the C–Cl bond with a free carbene, they also introduced Zhang *et al.* discovered the first example of a Suzuki coupling reaction by an imidazolium salt. Under otherwise identical reaction conditions, the related reaction with IMes•HCl afforded the desired *hetero*-coupled product in 96% yields. Interestingly, this stable NHC precursor was found to be appreciably more active than that of the corresponding free carbene. This approach also achieved high activity with respect to functionalized phenylboronic acids. For example, it was possible to couple *p*-chlorotoluene to *o*-, *m*-, and *p*-methoxyphenylboronic acids in 88, 91, and 99% yields, respectively.⁹⁹

A more thorough examination of the use of imidazolium salts as ligands for the Suzuki-Miyaura reaction was carried out by Grasa *et al.*, using an assortment of ligands with various steric and electronics effects (Figure 1.14).¹⁰⁰ Interestingly, the ligands featuring smaller aromatic substituents resulted in lower turnover numbers. In the case of ITol, the *hetero*-coupled product *p*-biphenyltoluene was produced only in low yield (5%). However, when additional bulky substituents were attached to the aromatic rings, the biphenyl products were generated in yields as high as 99%. Furthermore, Grasa *et al.* discovered that the use of bulky R groups significantly enhanced the efficiency of the coupling of aryl halides to phenylboronic acids, particularly in the cases of IXy and IMes. A summary of the previous results is presented in Table 1.4.

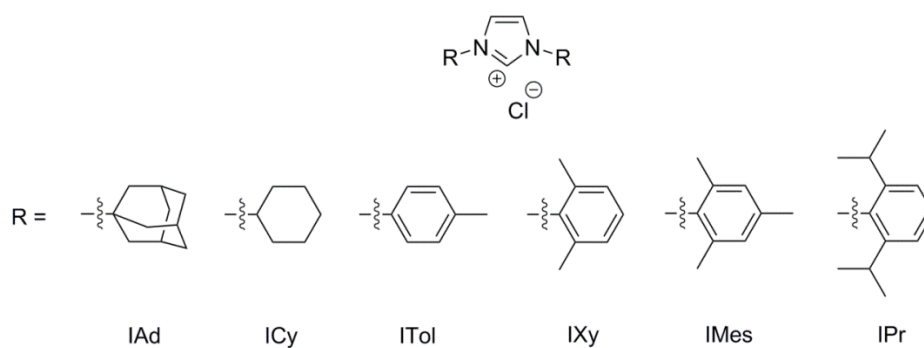
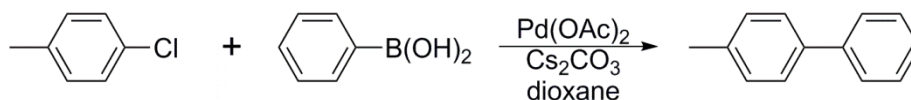


Figure 1.14: Imidazolium salts investigated for activity in the Suzuki coupling reaction.



Ligand	Time [h]	Isolated Yield [%]
None	24	NR
IAd	2	44
ICy	2	14
ITol	2	5
IXy	2	51
IXy	1.5	90 ^a
IMes	2	99
IMes	1.5	90 ^a
IPr	2	53
IPr	1.5	9 ^a

Table 1.4: Reaction conditions: $\text{Pd}(\text{OAc})_2 \cdot \text{L} \cdot \text{HCl}$, Cs_2CO_3 , dioxane, 80 °C, 1.5-39 h; (a) $\text{Pd}_2(\text{dba})_3$ was used in these reactions.

The imidazolium/palladium system was further investigated by Mathews and co-workers, in order to further advance the optimization of the Suzuki reaction. In contrast to Grasa *et al.*, Mathews *et al.* examined a series of commercially-available imidazoles in

the presence of $(\text{CH}_3\text{CN})_2\text{PdCl}_2$ and Na_2CO_3 , and completed these reactions by treatment with tolylboronic acid. Use of the foregoing reaction conditions afforded the desired *hetero*-coupled products with an average turnover frequency of 240 h^{-1} for each aryl iodide and bromide that was studied. Unfortunately, the aryl chlorides exhibited a wide range of turnover frequencies ($0\text{--}140\text{ h}^{-1}$) and yields ($0\text{--}56\%$). Nevertheless, these results were noteworthy for the absence of the undesired *homo*-coupled product. In summary, this novel approach generated *in situ* catalysts that were active for Suzuki coupling. Unfortunately, however, it was extremely difficult to identify the molecular species that were active in the catalytic cycle.

Concurrently, Viciu attempted to circumvent the catalyst ambiguity by development of new molecular NHC–Pd catalysts. The syntheses of several air- and moisture-stable $(\text{NHC})\text{Pd}(\text{allyl})\text{Cl}$ complexes were described (Figure 1.15), along with a few examples of successful Suzuki transformations with $(\text{IMes})\text{Pd}(\text{allyl})\text{Cl}$ and $(\text{IPr})\text{Pd}(\text{allyl})\text{Cl}$ (Scheme 1.20).¹⁰¹ The authors noted a strong dependence of the coupling reactions on the base NaO^tBu . Interestingly, all other bases were found to be ineffective for these coupling reactions. However, both catalysts activated the C–Cl bond in the unique substrate *m*-chloropyridine in 1.5 hours with yields of 95–97%.

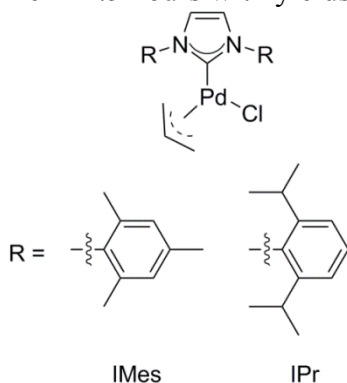
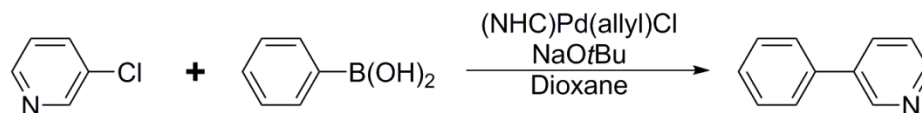


Figure 1.15: Viciu's $(\text{NHC})\text{Pd}(\text{allyl})\text{Cl}$ complexes.



Scheme 1.20: Unique Suzuki coupling of *m*-chloropyridine with (NHC)Pd(allyl)Cl.

In the following year, Viciu *et al.* proposed an innovative method for identification of the steric factor of each NHC ligand. The concept of buried volume was initially introduced by Hillier *et al.* in an attempt to elucidate the environment around a ruthenium metal center relative to that of an NHC ligand.¹⁰² The ‘buried volume’ was defined as a 3.0 Å sphere centered on a noble metal on which the NHC ligand has been confined (Figure 1.16).

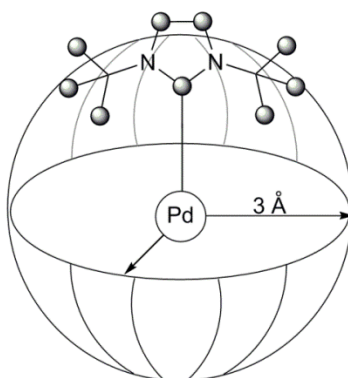


Figure 1.16: Visual representation of buried volume.

Viciu *et al.* expanded the theory of buried volume to evaluate the various (NHC)Pd(allyl)Cl complexes, and thereby calculated the buried volume of a plethora of saturated and unsaturated NHC ligands (Table 1.5). In order to determine the tabulated buried volume values, calculations were carried out with a constrained Pd–C_{carbenic} bond length of 2.0 Å. The second calculation utilized the actual experimental data from the X-

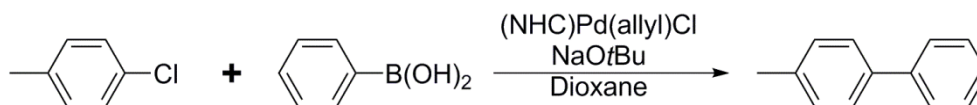
ray crystal structures involving the Pd–C_{carbenic} bond length. The most sterically demanding ligands were found to be *It*Bu, IAd, and SIPr.

Complex	Buried Volume [%]^a	Buried volume [%]^b
(IPr)Pd(allyl)Cl	26.10	24.99
(SIPr)Pd(allyl)Cl	33.03	32.27
(IMes)Pd(allyl)Cl	26.50	25.87
(SIMes)Pd(allyl)Cl	27.49	26.91
(<i>It</i> Bu)Pd(allyl)Cl	33.37	32.25
(ICy)Pd(allyl)Cl	25.17	23.90
(IAd)Pd(allyl)Cl	33.56	32.20
(IBn)Pd(allyl)Cl	23.61	22.93

Table 1.5: Buried volume calculated for a Pd–C_{carbenic} bond length of (a) 2.0 Å or (b) experimental values based on crystallographic data (*S* indicates a saturated C–C backbone).

The information gleaned by Viciu *et al.* prompted Navarro and co-workers to undertake a thorough study of the activities of multiple sterically-hindered (NHC)Pd(allyl)Cl complexes for the Suzuki-Miyaura cross-coupling reactions. The ligands IMes, SIMes, IPr, SIPr, and *It*Bu were used for this purpose and treated with NaO^tBu in dioxane at high temperatures.¹⁰³ Remarkably, the reactions proceeded to completion after twenty minutes compared to previously reported reactions which required a minimum of 1.5 hours (Scheme 1.21 & Table 1.6). Viciu *et al.* predicted the greatest protection of the catalytically active site on the palladium metal center using bulkier aromatic substituents (*It*Bu, IAd, and SIPr) based only on buried volumes, while on the other hand, Navarro *et al.* reported the highest *hetero*-coupled yields using IMes and IPr. Furthermore, when the IPr ligand was employed for the coupling of functionalized aryl chlorides with phenylboronic acids, the yields were at least 94%.

However, slightly lower yields were observed for the coupling of functionalized phenylboronic acids with *p*-chlorotoluene. Finally, the consequences of placing an allyl ligand in the *trans* position relative to the NHC ligand were analyzed by Marion and co-workers. The corresponding yields were significantly improved by the use of larger leaving groups: such as crotyl, prenyl, and cinnamyl ligands.¹⁰⁴



Scheme 1.21: Suzuki coupling with (NHC)Pd(allyl)Cl reported by Navarro *et al.*;
Reaction conditions: 80 °C, 20 min.

Catalyst	Yield
(IPr)Pd(allyl)Cl	80
(SIPr)Pd(allyl)Cl	62
(IMes)Pd(allyl)Cl	80
(SIMes)Pd(allyl)Cl	70
(ItBu)Pd(allyl)Cl	68

Table 1.6: Pertinent results obtained from Suzuki coupling with sterically-hindered (NHC)Pd(allyl)Cl complexes; Reaction conditions: Pd (1 mol%), NaO^tBu, dioxane, 80 °C, 20 min.

An alternative catalyst system was designed by McGuinness and co-workers for C–X activation in the Heck reaction. The methyl-palladium carbene complexes were shown to be capable of producing turnover frequencies as high as 24,000.⁹⁵ Each *mono*- and *bis*(carbene) catalytic systems incorporated simple imidazole ligands attached to a palladium(II) metal center (Figure 1.17). Interestingly, the observed turnover frequencies for the *bis*(carbene) ligands were significantly higher than those of the corresponding

mono(carbene) ligands. McGuinness and co-workers also discovered that only the *mono*(carbene) system became quickly deactivated in solution, and as a consequence the *bis*(carbene) catalysts were able to produce larger concentrations of product.

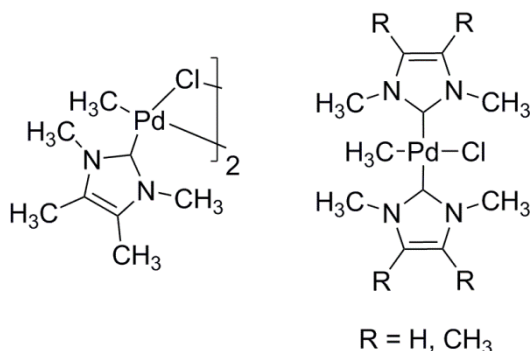
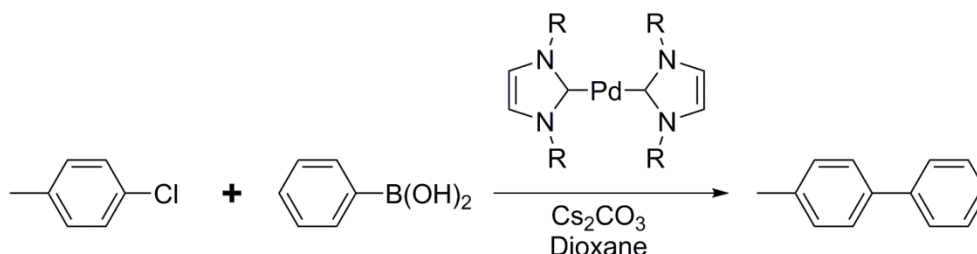


Figure 1.17: *Mono*- and *bis*carbene complexes designed by McGuinness *et al.*

In an attempt to expand their inventory of homogenous catalysts, McGuinness *et al.* utilized silver transfer reagents to generate a variety of unique bidentate carbene systems, in addition to several *bis*(carbene) ligands with C₂ symmetry that were produced from asymmetrical carbene ligands.¹⁰⁵ Both *cis* and *trans* catalysts were synthesized and subsequently employed in Heck, Suzuki, and Sonogashira reactions. In the case of Suzuki coupling, *p*-bromoacetophenone was successfully converted to the *hetero*-coupled biaryl product with a turnover number of 5,500. However, with an increase in reaction time from one hour to twenty-four hours, the turnover number improved dramatically to 109,900. The reaction conditions for the *bis*(carbene) systems were optimized and required forty-eight hours to achieve complete conversion. Shortly thereafter these results were published, McGuinness *et al.* presented a thorough examination of the M–C bond in an attempt to explain the high reactivities that were observed with the high carbene impact.¹⁰⁶ These authors proposed that the strength of the M–L bond was a consequence

of the strong σ -donation from the NHC ligand in concert with the lack of π -backbonding from the metal to the carbene.

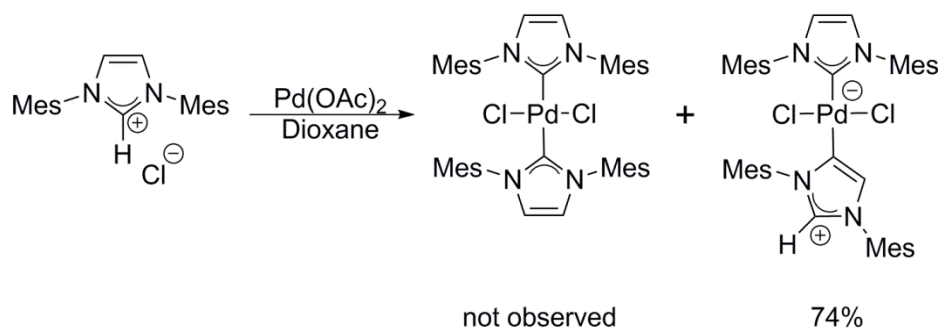
Almost simultaneously, Böhm and co-workers developed a new *bis*(carbene) complex with bulky aromatic groups containing high buried volumes.¹⁰⁷ After the four new catalysts were prepared, the *bis*(carbene) complexes were examined for their activity in terms of C–X bond activation (Scheme 1.22). Intriguingly, a range of yields between 7-68% was measured for the conversion of *p*-chlorotoluene to *p*-methylbiphenyl. The cyclohexyl and *tert*-butyl functional groups afforded the lowest and highest yields, respectively. The authors speculated that this synthetic approach might represent a new method for the creation of mixed NHC-phosphine complexes.



Scheme 1.22: Suzuki-Miyaura coupling optimized by Böhm *et al.* for aryl chlorides; R = Mes, *t*-Bu, *i*-Pr, Cy.

Over the past decade, a number of unique NHC complexes have been prepared in order to investigate their various steric and electronic properties. A particularly unusual result was reported by Lebel *et al.* when two equivalents of IMes were treated with $\text{Pd}(\text{OAc})_2$ in dioxane solution (Scheme 1.23).¹⁰⁸ The anticipated symmetrical $(\text{IMes})_2\text{PdCl}_2$ complex was not obtained even as a minor product, while the asymmetrical *bis*(carbene) ligand was produced in a 74% yield. Furthermore, this distorted catalyst

activated the C–Cl bond in Suzuki and Heck coupling reactions in yields of 44% and 77%, respectively.



Scheme 1.23: Asymmetric catalyst for Suzuki-Miyaura coupling developed by Lebel *et al.*

Subsequently, a more thorough examination of these NHC ligands was performed by Fu *et al.* in 2009. This examination involved a comprehensive inspection of saturated and unsaturated carbene ligands. In particular, Fu *et al.* presented six new *bis*(carbene) ligands and explored their Suzuki coupling activities (Figure 1.18 & Table 1.7).⁹⁰ It was discovered that the saturated NHC ligands remained strongly bonded to the metal center in solution, and consequently exhibited greater activity in the Suzuki-Miyaura cross-coupling reaction than those of the analogous unsaturated NHC ligands. More importantly, it was discovered that the addition of (*t*-Bu₃)P significantly increased the overall yields of the *hetero*-coupled product. These results further supported Böhm's initial theory¹⁰⁷ of combining *N*-heterocyclic carbene and phosphine ligands to form a new class of mixed-ligand system.

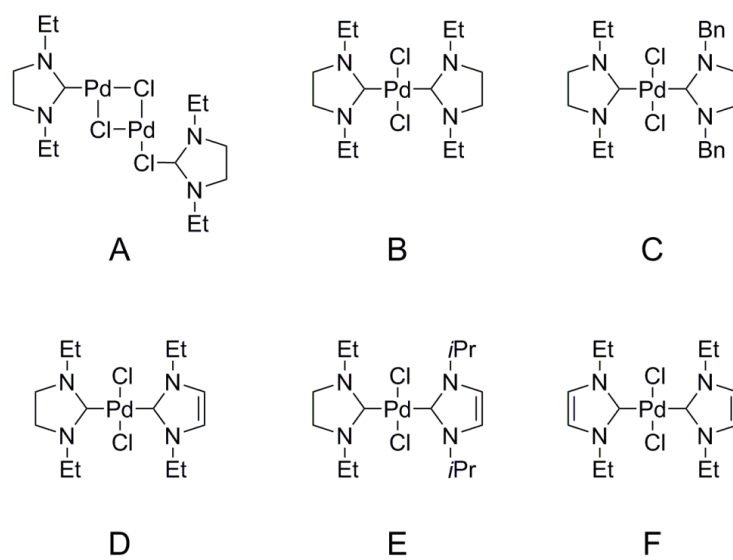
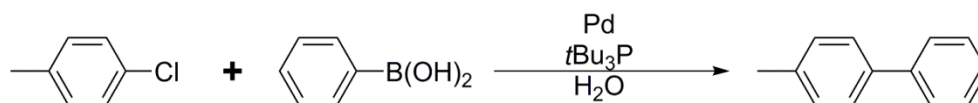


Figure 1.18: Six active *bis*(carbene) catalysts synthesized by Fu *et al.*



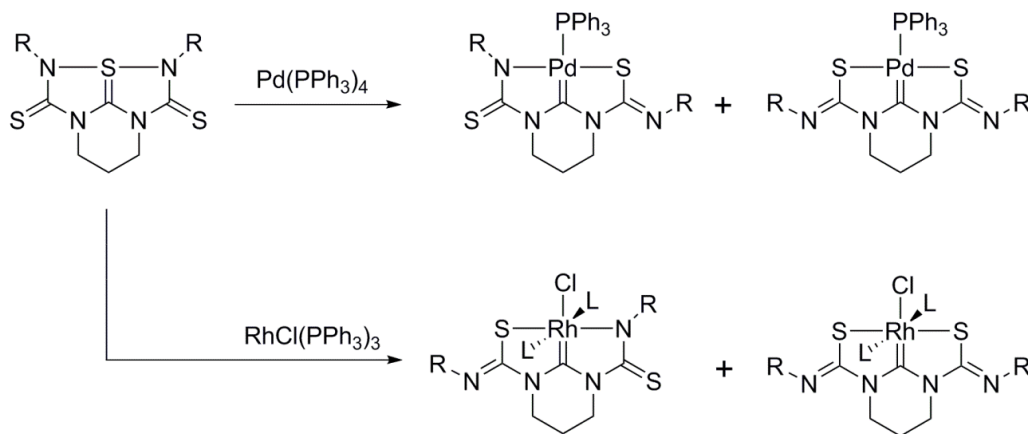
Complex	Yield [%]
A	50
<i>trans</i> -B	>99
<i>cis</i> -B	>99
C	95
D ^a	81
<i>trans</i> -E	74
F	47

Table 1.7: Saturated and unsaturated *bis*carbene complexes along with the corresponding yields obtained from the Suzuki coupling of *p*-chlorotoluene and phenylboronic acid (*a*) a mixture of *cis*- and *trans*-isomers; Reaction conditions: Pd (1 mol%), (*t*-Bu₃)P (2 mol%), H₂O, reflux, 24 h.

1.2.1.3 Mixed Phosphine and NHC Ligands

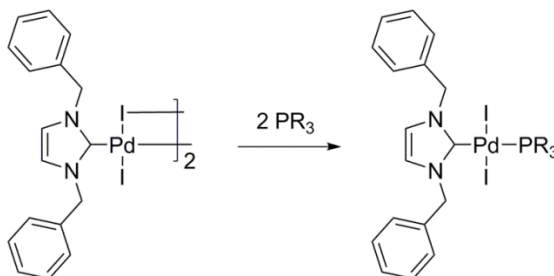
Several of the catalysts that have been designed for the Suzuki-Miyaura cross-coupling reactions consist of either a phosphine ligand or an *N*-heterocyclic carbene. Interestingly, however, there are relatively few examples in the literature of complexes that feature both components. This observation is particularly noteworthy since a mixed PR_3/NHC system could be an ideal candidate as a catalyst for Suzuki coupling, due to the strong σ -donation of the NHC ligand and the labile character of the phosphine ligand. Furthermore, it is possible that the *trans*-influence would be present in these types of systems, in which case the phosphine ligand would dissociate from the metal center in order to create a catalytically active site.

One of the first examples of a mixed PR_3/NHC system was presented by Matsumura and co-workers. In this case, the Pd and Rh carbene complexes were generated from 10-S-3 tetrazapentalene derivatives. The pertinent reaction schemes are presented in Scheme 1.24. The mixed complexes were found to be stable to air and moisture. However, they became unstable when dissolved in organic solvents.¹⁰⁹



Scheme 1.24: The first stable mixed PR_3/NHC complexes; R = Me, Et, *p*-ClC₆H₄, *p*-CH₃OC₆H₄.

Shortly thereafter, Weskamp *et al.* developed a similar mixed PR_3/NHC system for use in the Suzuki-Miyaura cross-coupling reaction. The *trans*-NHC-phosphine catalyst was synthesized from the complex di(μ -iodo)-bis(1,3-di(1'-(*R*)-phenylethyl)imidazolin-2-ylidene)dipalladium(II) by the addition of either PPh_3 or PCy_3 (Scheme 1.25). At that time, the Weskamp catalysts were the most active Pd(II) compounds for effecting Suzuki coupling. With 0.1-1.0 mol% Pd, the C–Br bonds could be activated in >99% yields with PPh_3 or PCy_3 . Alternatively, the activation of aryl chlorides was entirely dependent on the addition of PCy_3 and 1.0 mol% Pd. This catalyst afforded yields of 90, 87, and 69% for activated, unactivated, and deactivated substrates, respectively. Weskamp *et al.* also examined the activity of the Pd(II) precursor. However, this catalyst was found to be completely inactive.⁹⁶



Scheme 1.25: The *trans*-NHC-phosphine ligand presented by Weskamp *et al.*

In the following year, Weskamp *et al.* expanded the simple catalyst structure in order to examine the steric and electronic effects of the functional groups on the NHC and PR_3 ligands. The resulting twelve new mixed PR_3/NHC catalysts were investigated for their abilities to couple aryl bromides and chlorides with phenylboronic acid (Figure 1.19).¹¹⁰ The reactivities of these catalysts depended primarily on the size of the NHC substituents. Bulky NHC ligands were found to provide the highest turnover numbers. On

the other hand, the ideal phosphine ligand varied for each system (Table 1.8). The highest catalytic activities were observed with catalysts that featured PCy₃ located in a *trans* position with respect to the NHC ligands with 1-PhEt.

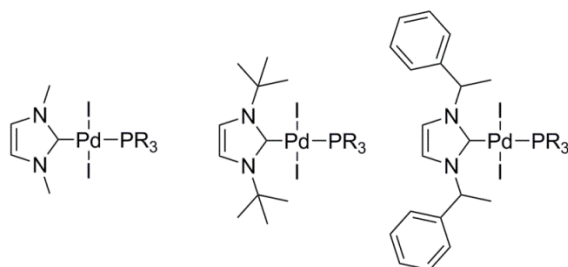
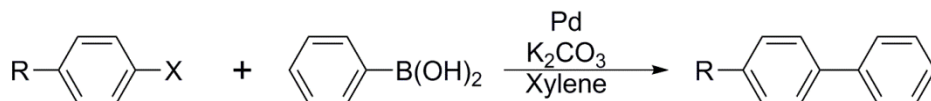


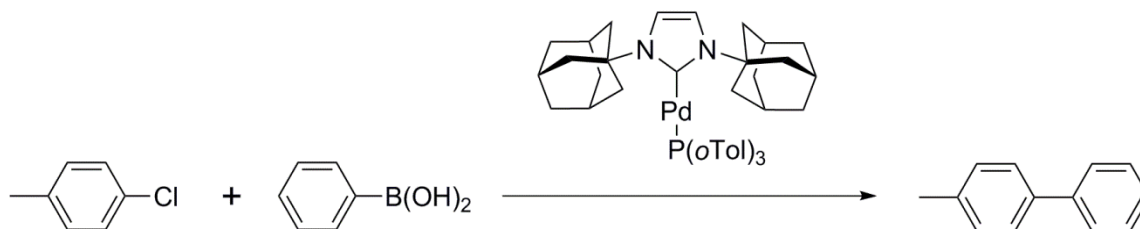
Figure 1.19: Additional *trans*-NHC-phosphine catalysts presented by Weskamp *et al.*;
R = C₆H₅, 2-(CH₃)C₆H₄, *cyclo*-C₆H₁₁, C(CH₃)₃.



X	R	R_{NHC}	PR₃	Yield [%]
Br	C(O)CH ₃	1-PhEt	PPh ₃	100
Br	H	1-PhEt	PPh ₃	100
Br	OCH ₃	1-PhEt	PPh ₃	100
Br	OCH ₃	1-PhEt	P(<i>o</i> -Tol) ₃	95
Br	OCH ₃	1-PhEt	P(<i>t</i> -Bu) ₃	99
Br	OCH ₃	1-PhEt	PCy ₃	100
Br	OCH ₃	<i>t</i> -Bu	PCy ₃	55
Br	OCH ₃	Me	PCy ₃	31
Cl	C(O)CH ₃	1-PhEt	PCy ₃	90
Cl	H	1-PhEt	PPh ₃	7
Cl	H	1-PhEt	PCy ₃	87
Cl	OCH ₃	1-PhEt	PCy ₃	69

Table 1.8: Suzuki coupling of aryl bromides and chlorides with phenylboronic acid using *trans*-NHC-phosphine catalysts; Reaction conditions: Pd (1.0 mol%), 130 °C.

Herrmann and co-workers expanded the mixed PR_3/NHC complex to probe the catalytic activities of the Stille and Heck reactions. During the optimization process, it was determined that bulky adamantyl groups facilitated the coupling of unactivated aryl chlorides with phenylboronic acids. They ultimately presented the first example of the coupling of *p*-chlorotoluene with phenylboronic acid at ambient temperature (Scheme 1.26). These catalyst systems were believed to facilitate the dissociation of *bis*(phosphines), yet retain the stability of *bis*(carbene) complexes.



Scheme 1.26: The first example of coupling an unactivated aryl chloride with phenylboronic acid at room temperature.

Although the NHC backbone had already been thoroughly examined by Fu⁹⁰, Alder⁹¹, and Denk⁹², Liao and co-workers undertook a detailed investigation of the saturated *vs.* unsaturated mixed PR_3/NHC complexes (Figure 1.20).¹¹¹ Moreover, they also explored the role of the phosphine ligand. Each of the catalysts showed high activity with aryl bromides. However, only the catalysts with PCy_3 exhibited any activity with the aryl chlorides. This difference in promotion may be due to the more rapid dissociation of PCy_3 in comparison with the analogous PPh_3 ligand. Furthermore, Liao *et al.* observed similar reactivities for the complexes with saturated and unsaturated NHC backbones, thus implying that either complex would be appropriate for Suzuki coupling.

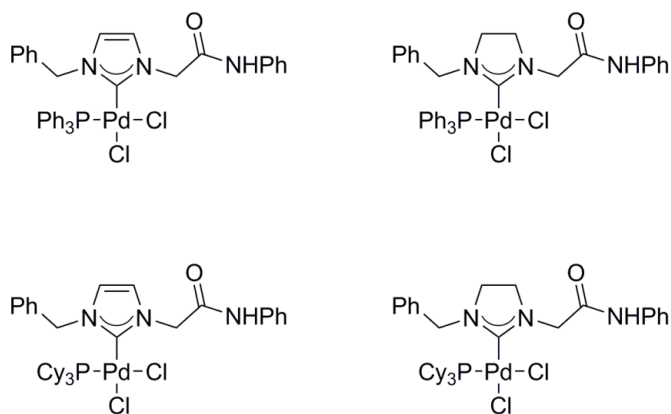


Figure 1.20: Saturated and unsaturated mixed *cis*-NHC-PR₃ catalysts for Suzuki coupling.

The thermal stability of these mixed systems was also investigated by Türkman *et al.* who reported the syntheses of five new palladium(II) complexes along with the necessary thermal analysis data.¹¹² The pertinent data are presented in Figure 1.21 and Table 1.9. In each case, the phosphine ligand was dissociated initially, followed by the NHC ligand. Türkman *et al.* hypothesized that the Pd–PR₃ bond was weaker than that of the corresponding Pd–NHC bond. In fact, the Pd–NHC bond was found to be thermally stable above 300 °C. This high stability was directly correlated with the properties of the substituent in the *para*-position (relative to that of the NHC). Furthermore, in a direct comparison of the *bis*(carbene) and mixed PR₃/NHC systems, Türkman *et al.* observed a significantly higher reaction rate for complexes that incorporated both ligand systems, thus implying a higher thermal stability for *bis*(carbene) complexes in comparison with those of the mixed PR₃/NHC analogues.

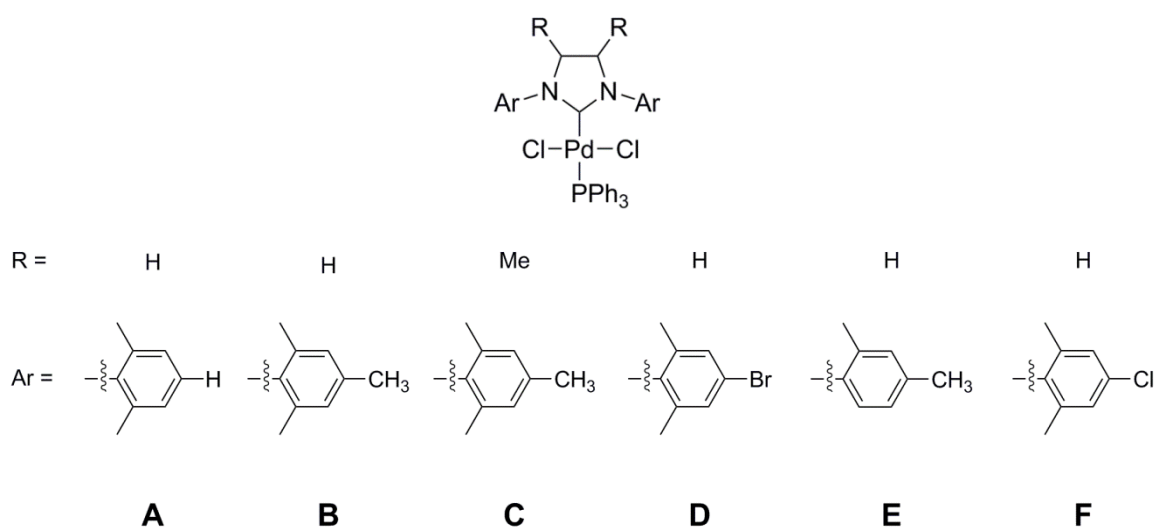


Figure 1.21: Six new mixed PR_3/NHC complexes synthesized for a detailed thermal stability study.

Complex	Peak Temperature [°C]
A	334, 362
B	232, 329, 371
C	339, 354
D	323, 371
E	322, 354
F	330, 350

Table 1.9: The thermal analysis data for mixed PR_3/NHC complexes.

In an attempt to determine the relationship between PR_3/NHC structural conformations and catalytic activity, Xu *et al.* synthesized two new *cis/trans*-NHC-phosphine complexes (Figure 1.22).¹¹³ The *cis* palladium catalyst was found to be slightly more active with respect to simple aryl bromides at 0.5 mol% Pd than those of the corresponding *trans* catalyst. Moreover, only the *cis* catalyst activated the C–Cl bonds of

p-chlorobenzene and *p*-nitrochlorobenzene. Unfortunately, a direct comparison of the *cis/trans* configurations cannot be accomplished due to the paucity of data.

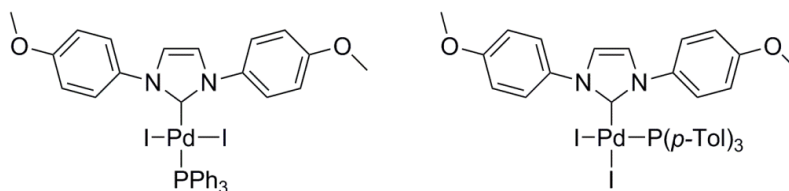


Figure 1.22: Two *N*-heterocyclic carbene-phosphine Pd(II) complexes prepared by Xu *et al.*

Fortunately, a comprehensive study of the structural isomers of *cis*- and *trans*-(NHC)(PPh₃)(Br)₂Pd has been carried out by Huynh *et al.* (Figure 1.23).¹¹⁴ By means of NMR and single-crystal XRD analyses, it was determined that the *trans* product was formed initially. Interestingly, the *trans* complex isomerized to the *cis* complex over a period of 46 hours. Furthermore, Huynh *et al.* observed that the Pd–C bond lengths and C–H...Pd interactions were longer in the case of mixed PR₃/NHC complexes than those in the parent *bis*(carbene) complexes. This observation may be attributed to the lower catalytic activity of the mixed PR₃/NHC complexes.

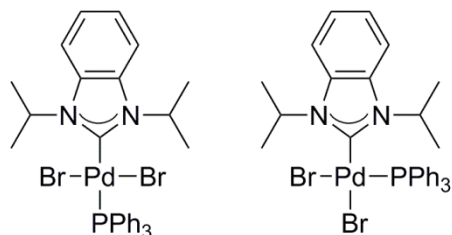
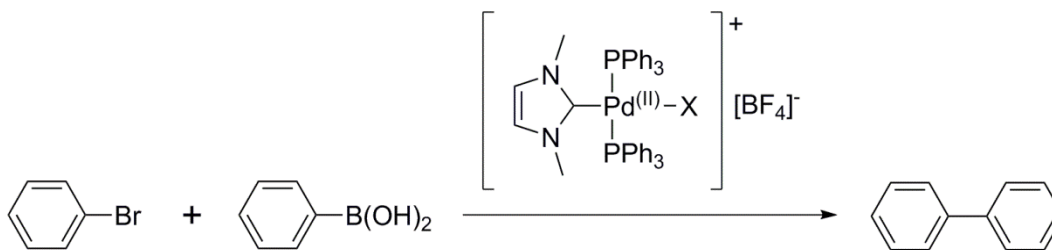


Figure 1.23: Structural isomers of *cis*- and *trans*-(NHC)(PPh₃)(Br)₂Pd.

Mathews and co-workers developed a contrasting mixed PR_3/NHC complex, in which the palladium center contained two PPh_3 ligands in addition to an NHC ligand located *trans* to a halide. On the basis of the strong electrostatic interaction between the Pd(II) center and $[\text{BF}_4]^-$ counteranion was suggested that this complex would be a strong candidate for carrying out Suzuki couplings in imidazolium ionic liquids.¹¹⁵ In fact, Mathews *et al.* reported the Suzuki coupling of bromobenzene and phenylboronic acid in a 95% yield and with a turnover frequency of 930 h^{-1} (Scheme 1.27).



Scheme 1.27: Suzuki coupling of bromobenzene with phenylboronic acid in an imidazolium ionic liquid.

Several other mixed PR_3/NHC complexes have been designed and synthesized in an attempt to further optimize the Suzuki-Miyaura cross-coupling reaction by altering the ratios of NHC to PR_3 in these mixed ligands. A similar palladium(II) complex has been prepared by Baker *et al.* However, in this case two NHC ligands and one phosphine ligand were employed.¹¹⁶ Shortly thereafter, Yang *et al.* designed a *cis*-NHC-phosphine complex. However, it proved to be only an active catalyst for the Heck reaction.¹¹⁷ A particularly unique example of mixed PR_3/NHC complexes was reported by Ellul and co-workers (Figure 1.24), following which a few Suzuki-Miyaura cross-coupling reactions were performed.¹¹⁸ This exceptional catalyst activated aryl iodides and bromides in dioxane at 120°C with 48-100% conversion. Moreover, Marshall¹¹⁹ and Fantasia¹²⁰

independently explored the mechanistic properties of such complexes, subsequently concluding that the labile phosphine ligands were advantageous for both the oxidative addition and reductive elimination steps in the Suzuki catalytic cycle.

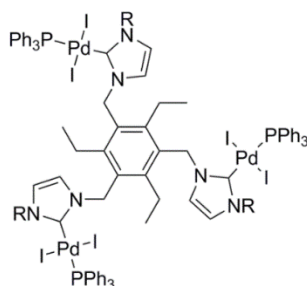


Figure 1.24: Ellul's $\text{timteb}^{t\text{-Bu}}$ and $\text{timteb}^{\text{dipp}}$ palladium phosphine species.

1.2.2 Media

The original Suzuki-Miyaura cross-coupling reaction was performed in tetrahydrofuran (THF) solution. However, Suzuki noted that the addition of aqueous 2N-sodium hydroxide increased the yield of the *hetero*-coupled product significantly.¹ In the ensuing years, the Suzuki reaction was performed in wide range of reaction conditions that included a wide variety of organic solvents, each of which had been optimized based on the characteristics of the palladium catalyst. In the case of similar cross-coupling reactions (*e.g.* the Heck reaction) substantial interest was generated in the nature of the solvent employed to facilitate C–C bond formation. One of the first comparative studies was achieved by Zhao and co-workers in their examination of different solvents for the Heck reaction of iodobenzene with methyl acrylate.¹²¹ The turnover numbers of several solvents with respect to their dielectric constants are presented in Table 1.10. In the case of the optimum Pd:PPh₃ ratio of 1:2, the highest turnover number resulted from palladium catalysts employed in polar solvents. Interestingly, the reaction rates increased

with the increase of the concentration of PPh_3 in nonpolar solvents. The production of $\text{Pd}(\text{PPh}_3)_4$ in nonpolar solvents was believed to deter the rate of reaction. On the other hand, the opposite trend was observed in the case of polar solvents. The conclusions presented by Zhao *et al.* were subsequently supported by means of computational studies reported by Proutiere.¹²²

Solvent	Dielectric Constant	Dipole Moment [D]	TON [mol mol ⁻¹ Pd]
Octane	1.948	0	45
Toluene	2.379	0.37	159
Ethanol	24.55	1.66	97
Propionitrile	27.2	3.57	333
NMAc	-	3.79	380
NMP	31.5	4.09	296
Acetonitrile	37.5	3.44	262

Table 1.10: Turnover numbers for Heck reactions of iodobenzene and methyl acrylate; Reaction conditions: Pd (0.25 mol%), 60-95 °C.

Recent exploration in this field has been focused on the development of catalysts effective in green chemistry, specifically in environmentally benign solvents. Navarro *et al.* successfully activated the C–Cl bond in sterically hindered aryl chlorides with technical grade isopropanol to generate tri-*o*-substituted biaryls. Eleven palladium catalysts containing at least one NHC ligand were employed in 2-propanol at 50 °C and ambient temperature that resulted in conversions as high as 96% in one hour.¹²³ Remarkably, the solvent system was not pre-dried or purified prior to introduction to the reaction mixture.

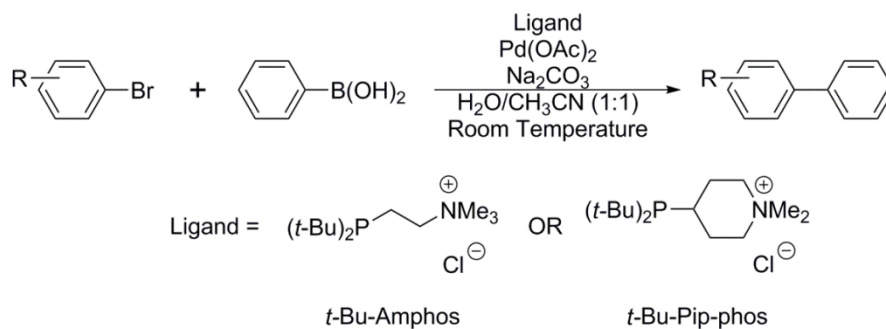
The C–C bond formation performed in isopropanol was particularly noteworthy for the development of green reaction conditions for Suzuki couplings, although the primary emphasis remained on the generation of palladium(II) systems that are operational in aqueous media. The first effective Suzuki coupling in aqueous solutions was reported by Casalnuovo and co-workers in which a few activated aryl iodides and bromides were treated with functionalized boronic acids. Additionally, the solvent system was optimized for each aryl halide, which resulted in a few unusual conditions. For example, *p*-iodotoluene was used in a 1:1 mixture of H₂O and CH₃CN, whereas *p*-bromopyridine provided the highest yields in a 7:1.5:1.5 H₂O:CH₃OH:C₆H₆ mixture.¹²⁴

Genet *et al.* expanded on the above mentioned solvent investigation to include 1:1 mixtures of H₂O:CH₃CN or H₂O:CH₃OH in order to carry out the vinylation or arylation of alkenes with *tris*(3-sulfophenyl)phosphine trisodium salt (TPPTS) and Pd(OAc)₂.¹²⁵ These reactions proceeded satisfactorily under mild conditions and afforded relatively high product yields. Genet and co-workers continued to probe C–C cross-coupling reactions, and thereby identified the optimal reaction conditions for the coupling of iodoalkenes with alkenyl boron reagents. In this context, CH₃CN:H₂O (3:1) was found to be an ideal solution mixture in conjunction with *i*Pr₂NH as a suitable base for the selective formation of the *Z*-isomers of unsaturated esters.¹²⁶

The Suzuki-Miyaura cross-coupling reaction conditions were transformed by pioneering work that was carried out by Zhao,¹²¹ Casalnuovo,¹²⁴ and Genet.^{125,126} Each of these research groups reported a catalytic system that was active in miscible aqueous solvent mixtures. In 1999, Paetzold *et al.* explored the case of 1:1:1 H₂O:EtOH:Tol as a two-phase solvent system for an array of aryl halides. The aryl iodides and bromides

were converted quantitatively to the functionalized biaryl products within a few hours. Typically, the sterically-hindered substrates required reaction times of 24 h.¹²⁷

In an attempt to probe both miscible and biphasic aqueous solvent mixtures, Shaughnessy and co-workers synthesized bulky, water-soluble alkylphosphine ligands for the formation of C–C bonds. The pertinent reaction scheme is presented in Scheme 1.28. Both ligands formed *in situ* palladium species that were extremely active as Suzuki catalysts, particularly in the case of sterically-hindered aryl bromides. This successful outcome represented the first example of room temperature Suzuki couplings in aqueous solutions.¹²⁸ Upon the addition of heat (80 °C), the turnover numbers increased from approximately 10,000 to 95,000 mmol of product per mmol of palladium.



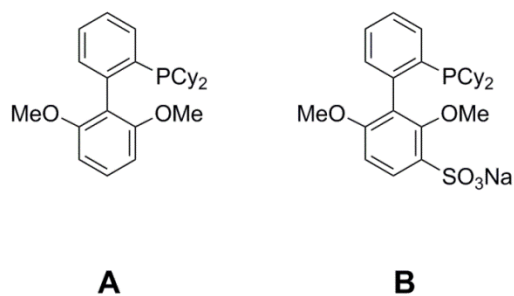
Scheme 1.28: Aqueous-phase Suzuki coupling presented by Shaughnessy *et al.*

Although the active catalysts operated satisfactorily in 1:1 H₂O:CH₃CN solution, Shaughnessy *et al.* subsequently discovered that these catalysts functioned predominantly in the organic phase of the solution. This finding was disappointing, particularly in the context of the original objective of the research. In order to overcome this issue, Shaughnessy *et al.* examined several new biphasic aqueous systems. The optimal reaction conditions for the desired Suzuki couplings included a 1:1 H₂O:Tol solution along with *t*-

Bu-Amphos and Na_2PdCl_4 . Remarkably, these conditions also resulted in the production of *p*-biphenylnitrile from *p*-chlorobenzonitrile. In solely aqueous solution, both activated and deactivated aryl bromides were converted into the desired *hetero*-coupled product in high yields at ambient temperature.¹²⁹

Concurrently, Najera and co-workers investigated the activation of several aryl chlorides in aqueous solvent mixtures. Although the miscible aqueous solvent mixtures facilitated complete conversion, it was determined that pure water afforded the highest turnover numbers. In the case of *p*-bromoacetophenone, turnover numbers of 9,700 and 79,000 were measured for toluene and water, respectively, in otherwise identical reaction conditions.¹³⁰ A similar trend was observed during the investigation of *p*-chloroacetophenone, for which the turnover number for water was over one hundred times larger than that for toluene. The high activity in aqueous media was attributed to the presence of the electron deficient ligand-catalyst system, *di*(2-pyridyl)methylamine-derived palladium(II) chloride.

In 2005, Buchwald *et al.* reported the syntheses of two water-soluble biaryl phosphine ligands, each of which contained the essential sulfonate group. It can be argued that the work presented by Buchwald and co-workers transformed the scope of Suzuki couplings in aqueous media. A direct comparison of the biaryl phosphine ligand with and without the sulfonate group was completed in various solvents (Table 1.11). In contrast to the Shaughnessy approach, Buchwald's system efficiently activated an array of highly functionalized aryl chlorides with excellent yields. Furthermore, these reactions proceeded at room temperature to afford quantitative yields, using 2 mol% Pd. Similar results were obtained at reflux using 0.1 mol% Pd in aqueous media.¹³¹



Ligand	Solvent	Temperature [°C]	Conversion [%]	Yield [%]
A	<i>n</i> BuOH	100	77	75
A	<i>n</i> BuOH:H ₂ O (5:1)	100	27	26
A	CH ₃ CH ₂ CN:H ₂ O (1:1)	100	>99	96
A	DMF:H ₂ O (1:1)	100	>99	94
A	CH ₃ CN:H ₂ O (1:1)	RT	17	12
A	H ₂ O	100	22	20
B	H ₂ O	RT	>99	97

Table 1.11: Suzuki coupling of *m*-chlorobenzoic acid and phenylboronic acid with ligand **A** or **B** in various solvent systems; Reaction conditions: Pd (2 mol%).

1.3 HETEROGENEOUS CATALYSIS

The literature examples discussed so far established the high activities and selectivities of several homogeneous catalysts that are useful for Suzuki-Miyaura cross-coupling reactions. These palladium complexes have proved to be capable of generating highly functionalized biaryl products at large turnover frequencies, most of which are capable of operating at low catalyst loadings and low temperatures. Unfortunately, however, the exclusive use of these methods of C–C bond formation is limited due to the inability to recycle these expensive homogeneous catalysts.

One of the primary techniques that has been introduced to circumvent this problem was first reported by Jang in 1997, who carried out the synthesis of the first

polymer-bound Pd(0) complex. As well as affording higher yields than Pd(PPh₃)₄, this novel anchored-catalyst produced diphenylbutadienes with retention of the original stereochemistry.¹³² Although some homogeneous catalysts have been shown to lose activity upon tethering to a solid-support, recent research has been focused on the development of new heterogeneous catalysts that can be easily separated, recovered, and recycled. Furthermore, the ideal heterogeneous system would maintain activity and selectivity upon subsequent reuse, in addition to reproduction of the original activity of the parent homogeneous compound.

1.3.1 Polystyrene and Other Polymer Supports

1.3.1.1 Polymer-supported Phosphine Ligands

The polymer-bound palladium compound presented by Jang *et al.* provided the parent homogeneous catalyst with heterogeneous-type character, thus allowing for its recovery and reuse for the Suzuki reaction. In the following year, Fenger developed a similar catalyst system, in which the diphenylphosphinated divinylbenzene cross-linked polystyrene palladium complexes were not only synthesized *in situ*, but were also found to be stable toward air and moisture (Figure 1.25).¹³³ Moreover, the new heterogeneous catalysts were highly active throughout a second trial using identical reaction conditions. More importantly, the reactivity of these systems was comparable to that of the parent homogeneous catalyst (Table 1.12). In the case of 4-bromoaniline, catalyst **A** activated the C–Br bond more efficiently than Pd(PPh₃)₄. On the other hand, Akiyama *et al.* reported a similar system comprising of a microencapsulated triphenylphosphane palladium complex that was also more stable than the analogous homogeneous system.

However, this system provided less catalytic activity than those of the analogous $\text{Pd(PPh}_3)_4$.¹³⁴

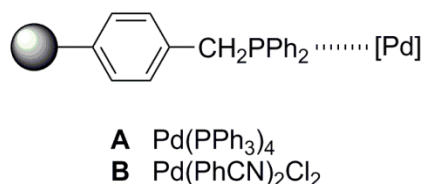


Figure 1.25: The first example of air- and moisture-stable polystyrene-supported catalysts for Suzuki coupling.

Bromoaromatic	A	B	$\text{Pd(PPh}_3)_4$
2-Bromo-5-nitropyridine	90	44	93
3-Bromoquinoline	78	60	93
4-Bromoaniline	56	36	39
4-Bromoanilide	76	65	77
1-Bromo-4-methoxybenzene	80	59	80
4-Bromoacetophenone	98	58	92

Table 1.12: Suzuki coupling of several bromoaromatics with phenylboronic acid utilizing catalyst **A** (0.2 mol%), **B** (3 mol%), or $\text{Pd(PPh}_3)_4$ (3 mol%) in Tol:EtOH:H₂O (10:1:1).

A related heterogeneous system was found to be active for the Suzuki coupling of aryl chlorides (specifically chloropyridines) with tolyboronic acids. However, this catalyst lacked the conjugation provided by the benzene ring in the analogous Fenger system (Figure 1.26).¹³⁵ When this catalyst was employed in air under mild conditions, the *hetero*-coupled biaryl product was produced in high yields. Furthermore, yields of 86-96% were measured for repeat reactions that used the recovered catalyst.

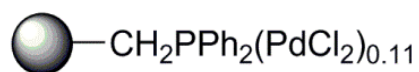
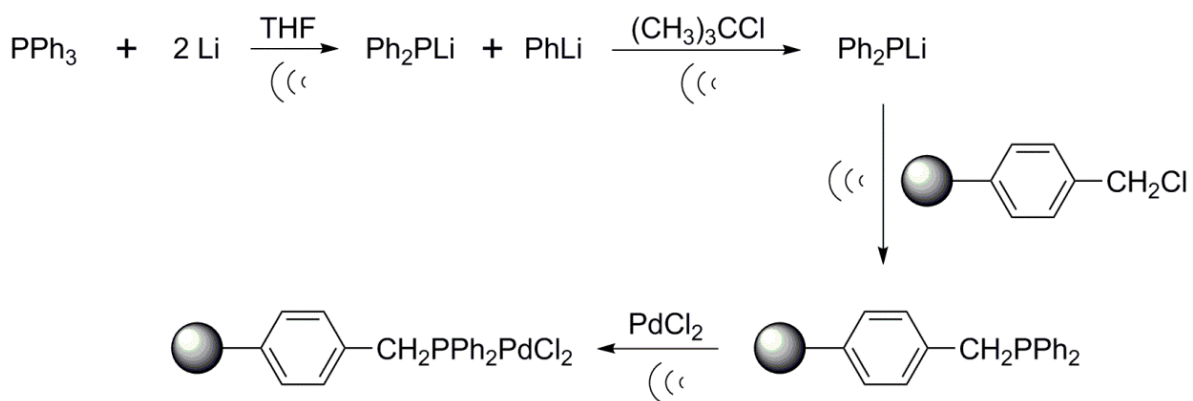


Figure 1.26: The air- and moisture- stable polystyrene catalyst reported by Inada *et al.*

The synthesis of this type of catalyst was optimized by Bai *et al.* by introducing ultrasound into the standard protocol. The new methodology is summarized in Scheme 1.29.¹³⁶ Moreover, the catalysts were easily filtered and reused five times with retention of catalytic activity. Further optimization of the reaction conditions resulted in high yields from aqueous mixtures. Indeed, a yield of 93% was achieved for the reaction of 2-bromonaphthalene with sodium tetraphenylborate in pure H₂O (Table 1.13).¹³⁷



Scheme 1.29: Ultrasound assisted syntheses of polystyrene-tethered Pd(II) catalysts.

Solvents	Ratio	Yield [%]
Benzene:H ₂ O	5:1	48
Toluene:H ₂ O	5:1	32
H ₂ O	-	96
Ethanol:H ₂ O	5:1	82
Solvent-Free	-	40

Table 1.13: Microwave irradiation of the Suzuki coupling of 2-bromonaphthalene and sodium tetraphenylborate in H₂O at 120 °C for 15 min.

Although the catalysts were exceptionally stable, the majority of them were significantly less active than those of the corresponding homogeneous catalysts. A remedy to this problem was to locate a (*t*-Bu₂)P ligand equatorially on the palladium metal center. Colacot and co-workers successfully performed an ancillary ligand exchange with a FibreCat derivative in order to generate a new catalyst, TunaCat (Figure 1.27).¹³⁸ Unlike the commercially-available FibreCats, TunaCat activated the C–Cl bond of *p*-chloroacetophenone selectively with minimal leaching. Shortly thereafter, Wang *et al.* used TunaCat (renamed FibreCat-1032) for the Suzuki coupling of aryl halides with a variety of functionalized phenylboronic acids.¹³⁹ The *hetero*-coupled product was formed after ten minutes of microwave irradiation, and subsequently purified through a Si-Carbonate solid-phase extraction plug for removal of the excess boronic acid.

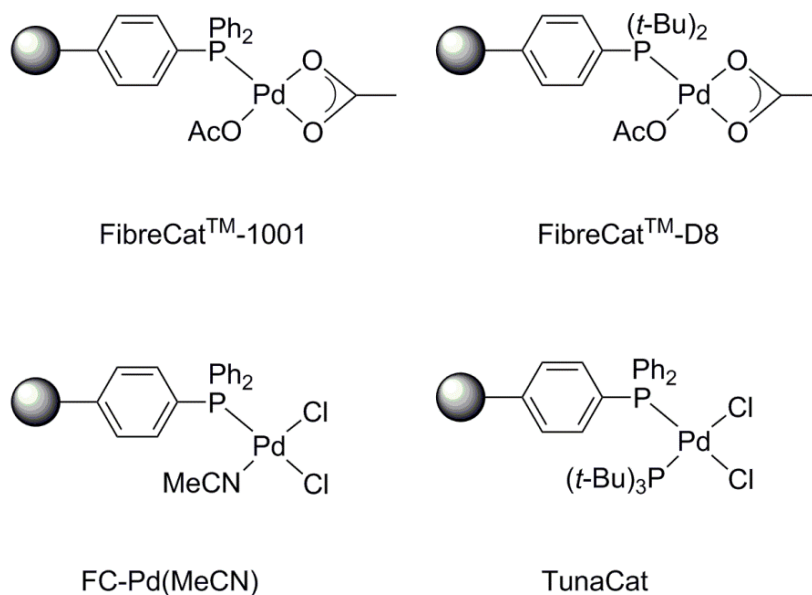


Figure 1.27: FibreCat[™]-1001, FibreCat[™]-D8, FibreCat-Pd(MeCN) and TunaCat as examples of insoluble palladium catalysts.

In an attempt to tune the parent polystyrene palladium heterogeneous catalyst, Shieh and co-workers successfully tethered two polystyrene-bound triphenylphosphine ligands to one palladium metal center (Figure 1.28).¹⁴⁰ This catalyst activated *o*-bromoanisole in five consecutive cycles with 0.006-0.025% Pd leaching in EtOH:H₂O mixtures. Remarkably, when the catalyst was used in toluene solution, even fewer palladium species were detected in the supernatant. However, the overall turnover frequency was significantly suppressed.

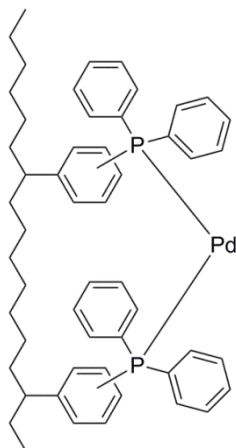


Figure 1.28: Polymer-bound phosphine, PS-Pd(0).

An alternative method for converting homogeneous catalysts directly into heterogeneous catalysts was optimized by Buchwald *et al.* when the synthesis of a few polymer-supported dialkylphosphinobiphenyl ligands was reported. In this case, the resin-bound dicyclohexylphosphine ligands provided the first examples of successful activations of an aryl chloride with a solid-supported catalyst for the Suzuki-Miyaura cross-coupling reaction (Figure 1.29).¹⁴¹ Moreover, this catalyst system could be recycled

effectively four times. However, extended reaction times were necessary for consecutive trials.

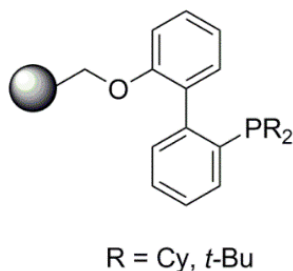


Figure 1.29: Polymer-supported dialkylphosphinobiphenyl ligands.

Plenio and co-workers also synthesized a few insoluble dialkylphosphinobiphenyl ligands as monomethyl polyethyleneglycol tagged phosphonium salts. Concurrently, the synthesis of MeOPEG-BnP-(1-Ad)₂ was also reported, thus permitting for a direct comparison of the two bulky phosphine-palladium systems (Figure 1.30). The Buchwald type catalysts turned out to be more active than the robust catalyst, MeOPEG-BnP-(1-Ad)₂. Both systems were highly active toward aryl chlorides under mild reaction conditions and each of them maintained their activity with negligible leaching after subsequent reuse.¹⁴² Plenio *et al.* also investigated the use of soluble supports on BnP(1-Ad)₂, in which the ligand was anchored to poly(methyl)styrene (Figure 1.31). The corresponding palladium catalyst exhibited high activity toward activated aryl chlorides, and afforded yields as high as 86% even after separation, recovery, and reuse.¹⁴³ Shortly thereafter, the Suzuki reaction conditions were expanded to include functionalized phenylboronic acids. Plenio applied nanofiltration techniques that allowed the catalyst to be successfully recycled nine times.¹⁴⁴

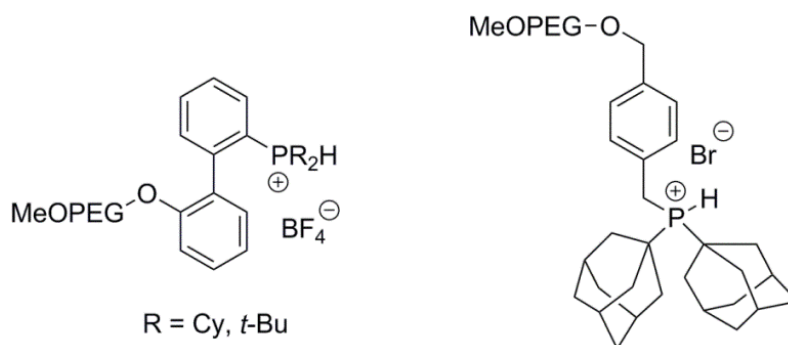


Figure 1.30: Monomethyl polyethyleneglycol-supported dialkylphosphinobiphenyl and MeOPEG-BnP-(1-Ad)₂ ligands presented by Plenio *et al.*

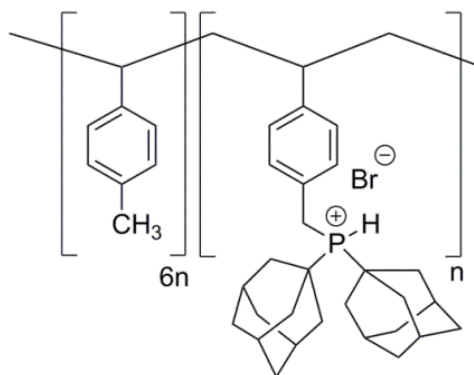
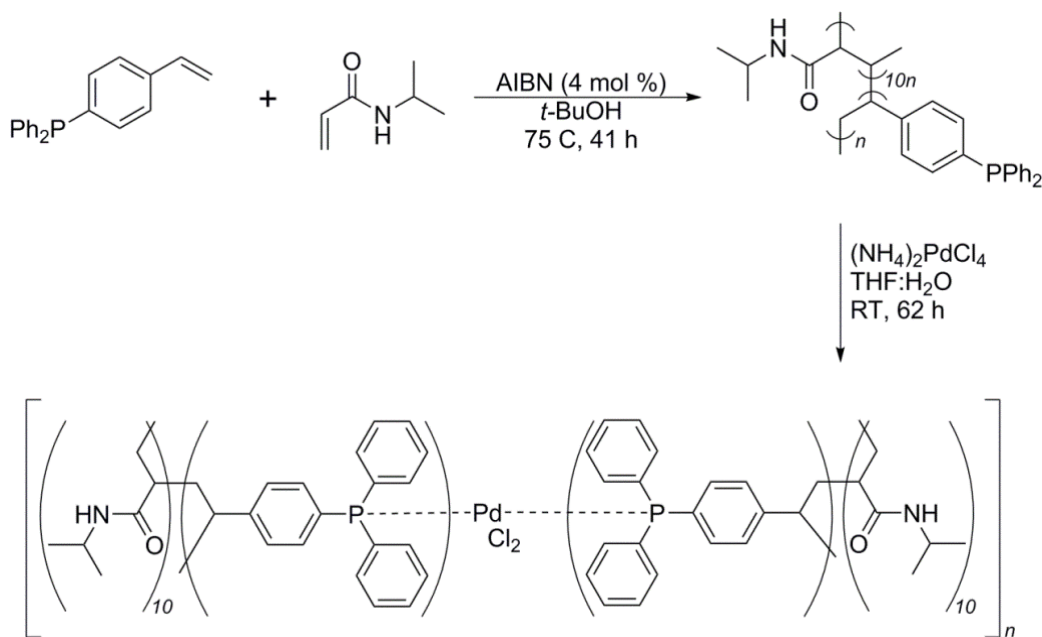


Figure 1.31: Poly(methyl)styrene-supported BnP-(1-Ad)₂ ligand system presented by Plenio *et al.*

These heterogeneous catalysts presented in Figures 1.30 and 1.31 were found to be incredibly stable toward air and moisture, thus generating interest in the development of similar insoluble catalytic systems. For example, Yamada *et al.* developed a procedure for the self-assembly of such catalysts, in which the coupling of a non-cross-linked amphiphilic copolymer was attached to an inorganic entity. This process was designed originally for the production of tungsten catalysts for the epoxidation of allylic alcohols¹⁴⁵, and Yamada *et al.* also expanded this protocol to include inorganic palladium

precursors (Scheme 1.30).¹⁴⁶ In the following year, the catalytic activity of these reusable catalysts for the Suzuki coupling of alkenyl halides and alkenylboronic acids was presented. Substantial turnover numbers were evident when the reactions were carried out in organic or aqueous media. Moreover, these catalysts could be recycled ten times without loss of activity.¹⁴⁷



Scheme 1.30: Synthesis of Yamada's self-assembled palladium non-cross-linked amphiphilic copolymer.

1.3.1.2 Polymer-supported N-Heterocyclic Carbene Ligands

The majority of the heterogeneous catalysis exploration was performed on phosphine-based ligands, although a few examples have been reported for NHC-based catalysts that are insoluble. One of first examples of such catalysts was reported for the Heck reaction by Schwarz and co-workers. The catalyst was particularly active toward aryl bromides, and very little leaching was evident when the catalysts were recycled.¹⁴⁸

Shortly thereafter, Byun *et al.* designed a new polymer-supported Pd–NHC complex that satisfactorily generated C–C bonds.¹⁴⁹ Unfortunately, however, this catalyst was only consistently active for aryl bromides with electron-donating substituents under optimized reactions conditions in a 1:1 DMF:H₂O solution. These catalysts are illustrated in Figure 1.32.

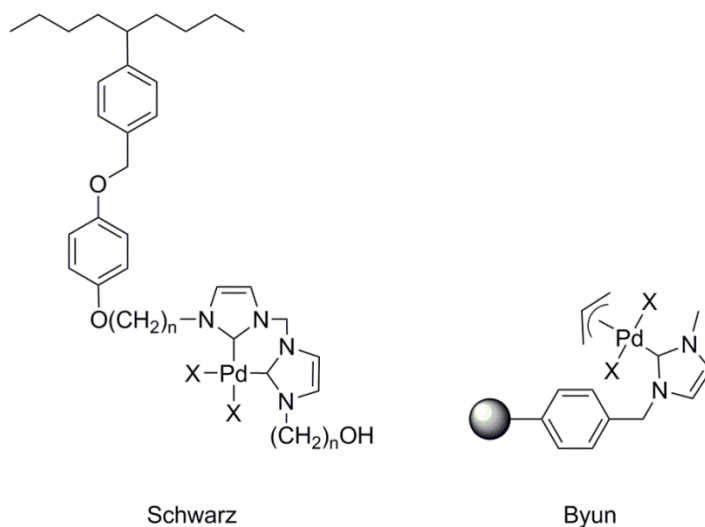


Figure 1.32: Heterogeneous NHC–Pd catalysts presented by Schwarz *et al.* (left) and Byun *et al.* (right).

Kim and co-workers reported an interesting protocol for the generation of heterogeneous NHC systems on polystyrene.¹⁵⁰ A poly(imidazoliummethyl styrene)-*surface grafted*-polystyrene catalyst was developed for the Suzuki-Miyaura cross-coupling reaction. The catalyst was explored in DMF:H₂O (1:1) solution at 50 °C along with phenylboronic acid and several aryl iodides. The anticipated biphenyl products were able to be isolated in reasonable yields.

In an effort to model an insoluble Pd–NHC heterogeneous catalyst that was analogous to the phosphine systems (FibreCat), Lee *et al.* designed a new highly active

macroporous polystyrene-supported 1-mesitylimidazolium chloride resin catalyst (Figure 1.33).¹⁵¹ This catalyst was capable of deactivating aryl chlorides to the desired *hetero*-coupled products in DMF:H₂O (2:1) in moderate yields. At the time, no other solid-supported catalyst had oxidatively added the C–Cl bond in substrates that contained electron-donating groups.

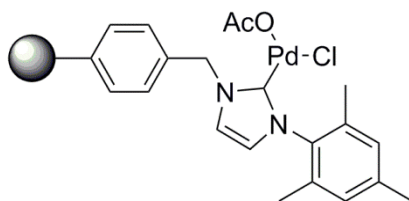


Figure 1.33: Polystyrene-supported NHC–Pd catalyst reported by Lee *et al.*

One of the more unique examples of this type of heterogeneous catalyst was derived from theobromine *via* a four-step synthesis that resulted in the *bis*(carbene)–Pd complex (Figure 1.34). The catalyst was capable of activating the C–Br bond in *m*- and *p*-bromotoluene, which resulted in moderate yields of the biphenyl products when carried out in water. Interestingly, this catalyst could be recycled three times with only a slight decrease in catalytic activity. However, no leaching experiments were reported by the authors.

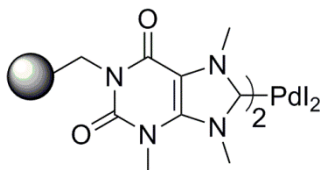
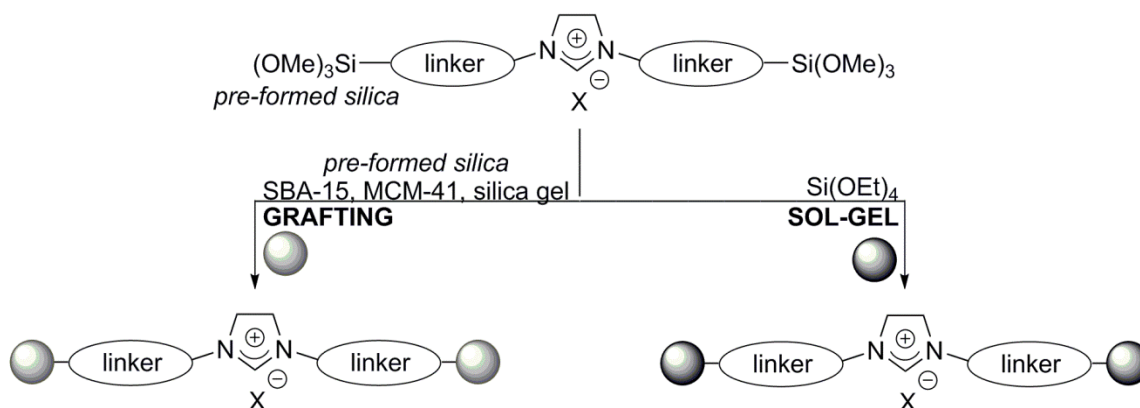


Figure 1.34: *Bis*(NHC)–Pd catalysts synthesized from theobromine.

1.3.2 Silica

Silica has also been used as a solid support material for the heterogenization of homogeneous catalysts. Recently, the previously optimized homogeneous systems have been covalently bonded to the hydroxide groups on the silica surface, thus creating an extremely stable insoluble catalyst.¹⁵² This cost-effective solid support permits facile catalyst synthesis *via* either a sol-gel or a grafting procedure. The former method entails the hydrolysis-polycondensation of a functionalized trialkoxysilane with a silica source, whereas the latter method involves grafting the functionalized trialkoxysilane onto the silica source (Scheme 1.31).¹⁵³ The commonly used silica precursors for the grafting method are SBA-15 (Santa Barbara Amorphous type material, no. 15), MCM-41 (Mobile Composition of Matter, no. 41), and commercially available silica.^{154,155}



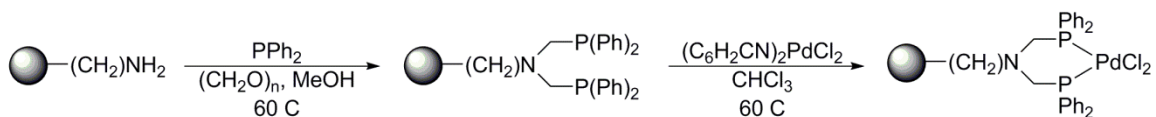
Scheme 1.31: Grafting vs. sol-gel method for the synthesis of supported imidazolium salts presented by Ranganath *et al.*

1.3.2.1 Silica-supported Phosphine Ligands

Cai *et al.* made significant contributions to this area of research in the late 1990s when they tethered several palladium compounds to silica supports using various terminal atoms. While the most active system was designed with an arsine linker,¹⁵⁶ Cai

et al. also developed similar catalysts with selenium, sulfur, and phosphorus linkers.^{157,158} The so-called 'Si'-P-Pd⁰ system performed the Suzuki coupling of activated aryl iodides with sodium tetraphenylborate in DMF solution in moderate yields. However, these heterogeneous species failed to couple either aryl chlorides or bromides.¹⁵⁹ In the following year, Cai *et al.* expanded this approach include organotin and organomagnesium reagents.¹⁶⁰

Further exploration of similar phosphorus-palladium supported catalysts was carried out by Tyrrell and co-workers using a bidentate phosphine ligand (Scheme 1.32). The two-step synthesis resulted in a catalyst with an average loading of 0.4 mmol g⁻¹, that successfully activated the C-I bond of a few different iodobenzenes in the Sonogashira reaction.¹⁶¹ The foregoing reaction conditions were later expanded to include aryl bromides, for which the catalyst remained active for four consecutive catalytic cycles.¹⁶² In contrast to the analogous polystyrene-tethered system, Tyrrell's catalyst did not require pre-swelling of the catalytic entity, thus rendering the silica-based catalytic systems more efficient than the corresponding polystyrene-based systems.



Scheme 1.32: Synthesis of a bidentate phosphine ligand tethered to silica.

A similar Pd-phosphine complex was designed by Chen and co-workers, in which the tether length of the previous example was extended significantly (Figure 1.35). This complex was found to be a highly active catalyst for the Suzuki-Miyaura cross-coupling reaction, particularly when employed at ambient temperature in aqueous media.

Moreover, the catalyst was easily separated and recovered and could be successfully reused ten times with negligible loss of reactivity. The aryl chlorides that were investigated never fully converted to the desired *hetero*-coupled product.¹⁶³ Concurrently, Wang *et al.* developed a *trans*-analog of Chen's catalyst with a smaller tether length (Figure 1.36). This catalyst activated aryl iodides and bromides in dioxane solution at 80 °C. However, there was only poor reactivity with chlorobenzene.¹⁶⁴

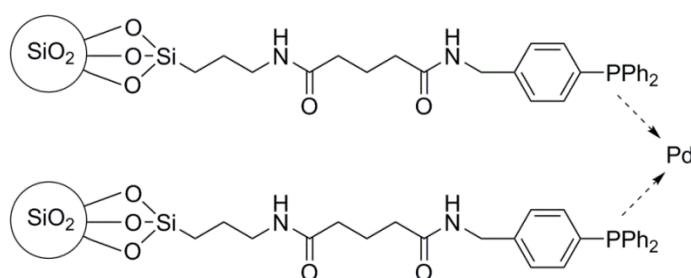


Figure 1.35: Silica-supported *cis*-phosphine-palladium heterogeneous catalyst.

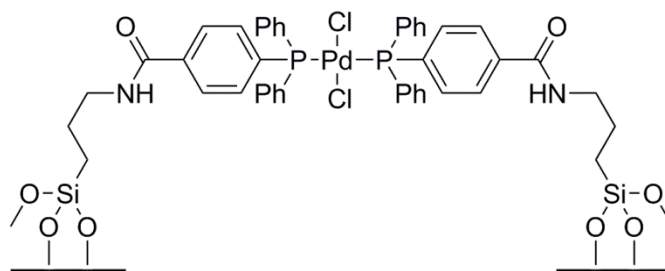


Figure 1.36: Silica-supported *trans*-phosphine-palladium heterogeneous catalyst.

In an attempt to develop a new methodology for the activation of aryl chloride substrates in the Suzuki reaction, Fukaya *et al.* investigated the relationship between the catalytic activity and the properties of the palladium-silica linker. Five different catalysts were produced with various connectivities to the Pd-silica tether, in addition to the

synthesis of $\text{SiO}_2\text{-Pd}$ as a heterogeneous control catalyst (Figure 1.37). The surface area and pore volume of each complex were found to be inversely proportional to the number of linkers in each complex (Table 1.14). However, the opposite trend was observed for the catalytic activities of these complexes in the Suzuki coupling of *p*-chlorobenzoic acid ethyl ester and phenylboronic acid. The catalysts with a tripodal linker exhibited high reactivity and underwent considerably less leaching than those of the analogous trialkoxy-type complexes.¹⁶⁵

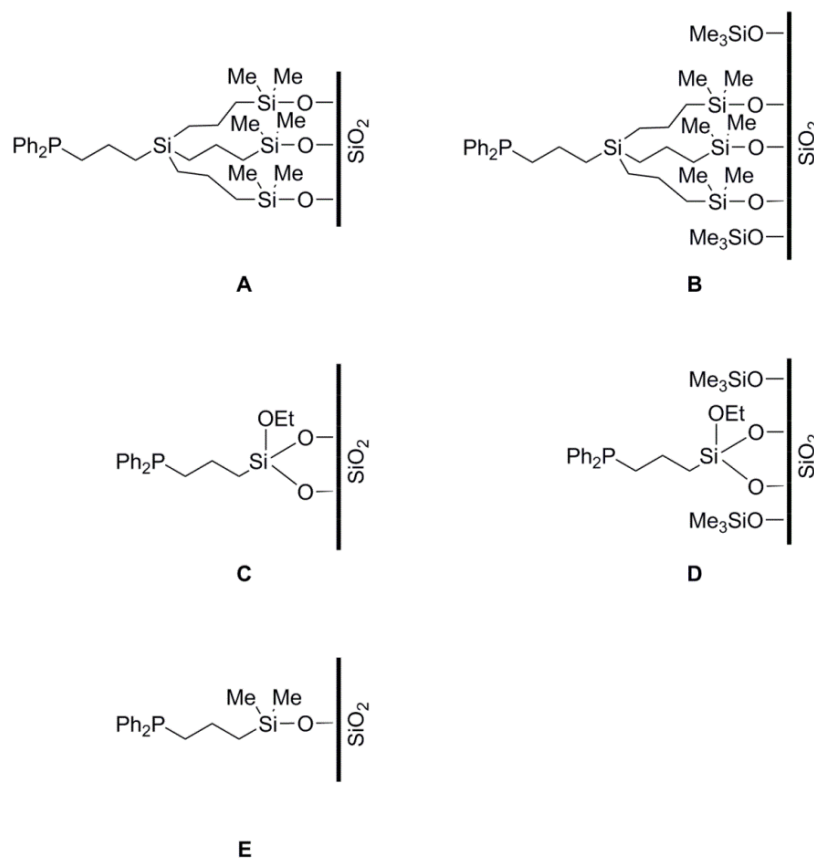
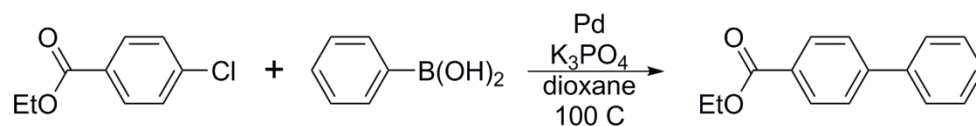


Figure 1.37: Five organic-functionalized silica materials with various palladium-silica linkers.



Catalyst	Surface area [m ² g ⁻¹]	Pore Volume [cm ³ g ⁻¹]	Yield [%]
A	603	0.84	23
B	676	0.88	74
C	993	1.26	13
D	705	0.84	23
E	980	1.31	11
SiO₂-Pd	956	1.39	-

Table 1.14: Surface areas, pore volumes and catalytic activities of five phosphine-palladium heterogeneous catalysts on silica.

1.3.2.2 Silica-supported N-Heterocyclic Carbene Ligands

In 2003, Zhao *et al.* tethered the first NHC ligand to a silica-support (Figure 1.38).¹⁶⁶ This ligand was treated with palladium(II) acetate in order to form catalytically active species *in situ* for the Suzuki reaction. In ethanol solution, the ligand-Pd system coupled sterically-hindered aryl bromides with functionalized organoboranes at ambient temperature in high yields. Moreover, this heterogeneous system was easily synthesized and was found to be air and moisture stable.

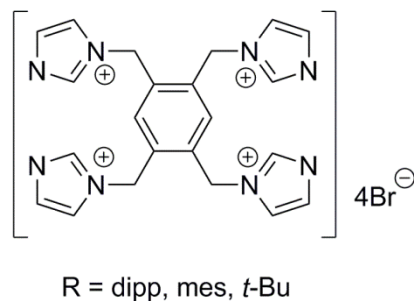


Figure 1.38: The first example of an NHC-silica ligand.

Shortly thereafter, Gürbüz and co-workers designed a Pd-imidazoline complex that was tethered to silica. The *trans*-NHC-palladium complex was produced utilizing the sol-gel method, in which tetraethoxysilane was prepared by means of hydrolysis in an assortment of organic reagents (Figure 1.39).¹⁶⁷ This complex was surprisingly active for the Suzuki-Miyaura reaction. In the case of *p*-chlorotoluene, the heterogeneous catalyst promoted the activity of the C–Cl bond and afforded the functionalized biphenyl product in 82% yield. Furthermore, the catalyst was shown to retain activity after five consecutive trials in contrast to the deactivation of Pd/C after three subsequent cycles.

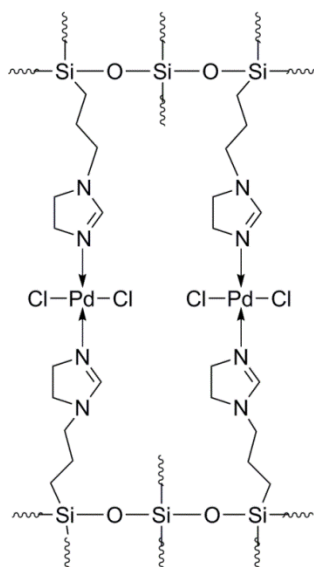


Figure 1.39: Silica-imidazoline-palladium complex active for aryl chlorides.

In an attempt to optimize their catalyst, Gürbüz and co-workers synthesized a *cis*-NHC–Pd analog. Interestingly, this catalyst employed strong Pd–C bonds instead of the previously favored Pd–N bonds (Figure 1.40).¹⁶⁸ All of the aryl chlorides were activated by this heterogeneous catalyst and the desired *hetero*-coupled products were produced in

high yields. Unfortunately, this catalyst could only be active for four cycles of subsequent use and recovery.

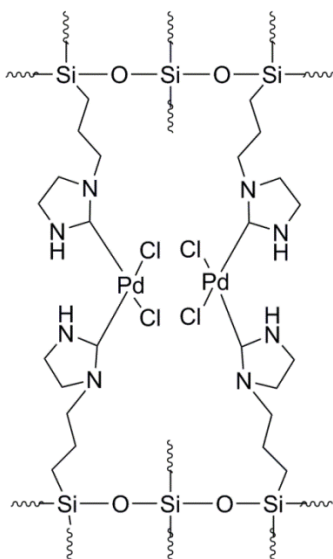


Figure 1.40: Pd-NHC-silica complex described by Gürbüz *et al.*

An alternative method for grafting palladium complexes onto silica was developed by Karimi and Enders. In this case, the catalyst was generated from a Pd–NHC/ionic liquid matrix (Figure 1.41a).¹⁶⁹ This catalyst maintained thermal stability up to 280 °C, in addition to producing turnover numbers of 36,600 for the Heck reaction. Furthermore, the catalyst was reused in four subsequent trials. A similar catalyst was presented by Aksin and co-workers and afforded comparable turnover numbers of 10^4 – 10^5 in DMF solution at 140 °C (Figure 1.41b).¹⁷⁰ It was determined by means of hot filtration and poisoning tests that Aksin’s compound was producing leached catalysts for the Heck reaction.

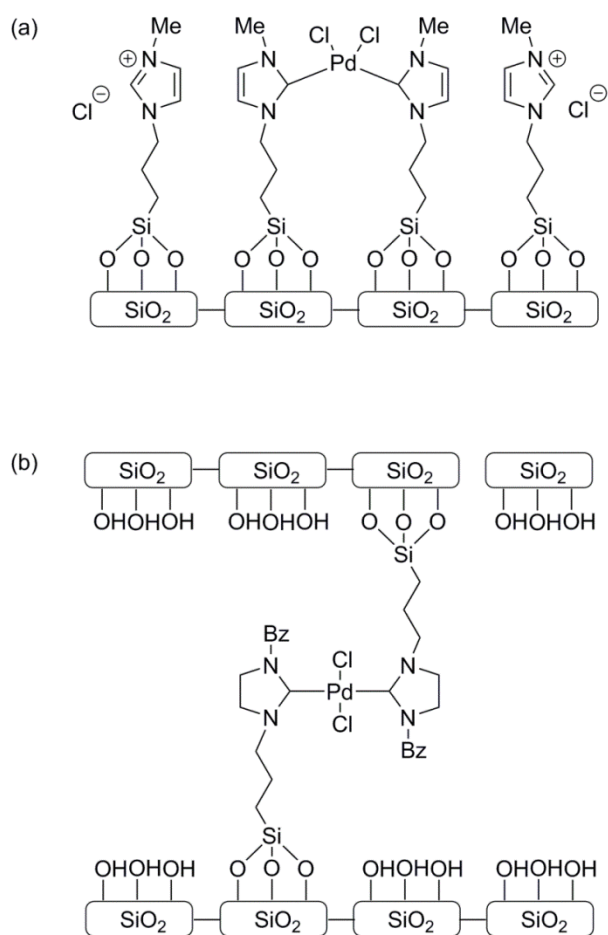


Figure 1.41: (a) *cis*-Pd-NHC-silica complex presented by Karimi (b) *trans*-Pd-NHC-silica complex presented by Aksin.

The results reported by Karimi and Aksin for the Heck reaction stimulated the interest of other research groups, particularly those of Qiu and Lee. The latter authors were interested in developing analogous systems to those described for Karimi and Enders's original Pd-NHC-silica catalyst. In fact, Qiu replicated the *cis* catalyst and optimized the Suzuki-Miyaura reaction conditions for reactivity in aqueous media. This catalyst operated extremely well with aryl iodides and bromides, but only produced moderate yields in the case of aryl chlorides. Moreover, the catalyst could be reused six

times in succession.¹⁷¹ On the other hand, Lee *et al.* isolated the *trans* isomer and proposed a structure for this novel system (Figure 1.42). The resulting heterogeneous catalyst exhibited high activity with aryl bromides at ambient temperature. Moreover, the reaction was complete after only two hours and the catalyst could be reused four times.¹⁷²

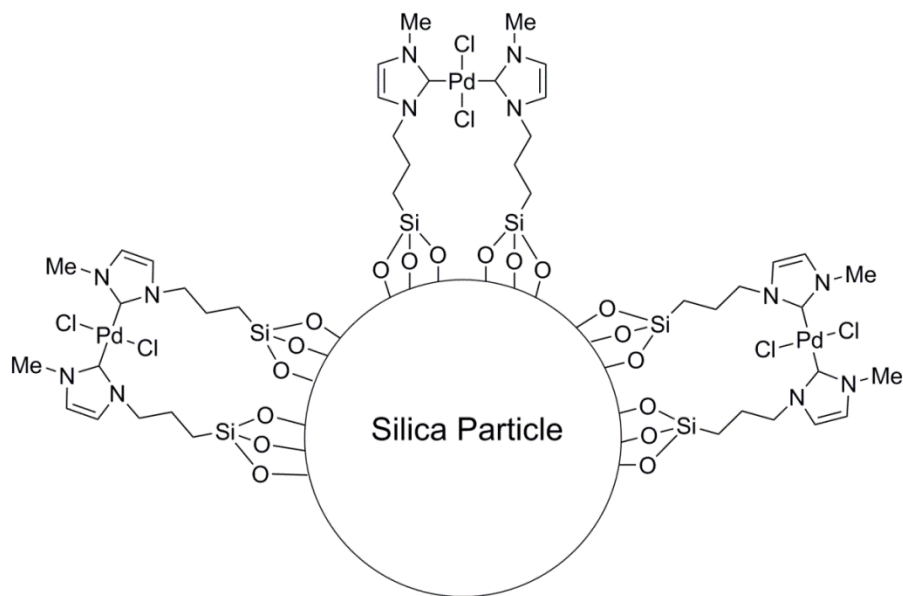


Figure 1.42: Illustration of several palladium complexes anchored to a silica particle as reported by Lee *et al.*

The *bis*(carbene) catalysts were believed to provide optimal reaction conditions for Suzuki couplings. However, the role of the chloride ions on the palladium metal center was still being investigated. Tandukar and co-workers performed an ancillary ligand exchange in order to coordinate either dodecane sulfonate or *p*-toluene sulfonate groups to the palladium metal center of the heterogeneous catalyst (Figure 1.43). Both aryl iodides and aryl bromides were converted to the biphenyl product in moderate yields in 1:1 IPA:H₂O solution. The nanoparticles were easily removed and recycled five times

with retention of catalytic activity. Interestingly, the catalyst was also highly active in the Heck reaction.¹⁷³

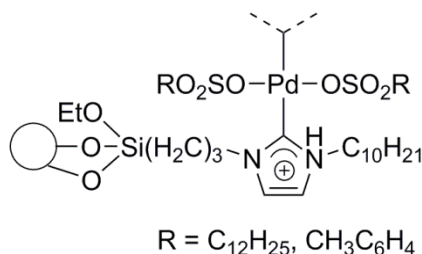


Figure 1.43: NHC-Pd-OSO₂R heterogeneous catalysts active for both the Suzuki and Heck reactions.

Following the success of Tandukar, Polshettiwar *et al.* replaced the originally used chloride substituent with iodide ligands in their heterogeneous catalyst design. The sol-gel method was employed for the production of these catalysts, thus this system was to be the first Pd-NHC complex attached to an organic-silica. An array of aryl bromides was activated by means of microwave irradiation which resulted in turnover numbers up to 16,385. This catalyst was recycled five times without detectable leaching.¹⁷⁴

Tyrrell and co-workers employed bromide ligands in the *trans* catalyst, and discovered a direct correlation between the size of the heterogeneous catalyst and the catalytic activity. For the first time, direct evidence was obtained to support the hypothesis that bulkier systems were advantageous for these types of C–C cross-coupling reactions. Interestingly however, this catalyst was never found to be primarily selective for the *hetero*-coupled product in the presence of aryl chlorides.¹⁷⁵

1.3.3 Media

The standard reaction conditions for the heterogeneous Suzuki-Miyaura coupling of aryl halides with organoboranes typically includes an organic solvent and temperatures in the range of 80-150 °C. Normally, toluene and *N*-methyl-2-pyrrolidone (NMP) are employed as the principal solvents, even though high catalytic activities have been measured for polar organic solvents. The high selectivity of the anchored catalysts in such solvents has been attributed to leaching of Pd metal from the heterogeneous system. In order to negate excessive characterization of the active species, organic solvents have been favored for these types of C–C bond forming reactions.

Gruber-Woelfler and co-workers examined the activity of the Pd(OAc)₂-BOX-MPSG ligand system with several common organic solvents at various temperatures (Figure 1.44 & Table 1.15).¹⁷⁶ In all the solvents that were studied, an insignificant amount of palladium leaching into the reaction solution was measured. This observation remained consistent even for systems that were examined at high temperature, thus demonstrating the substantial thermal stability of the heterogenised Pd complex. The latter catalyst was recycled successfully ten times with full retention of catalytic activity.

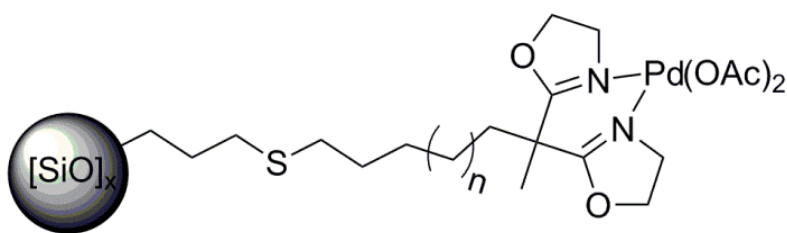
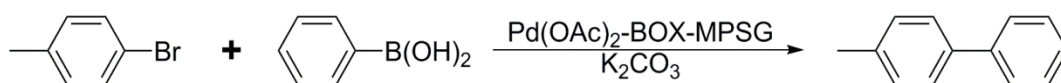


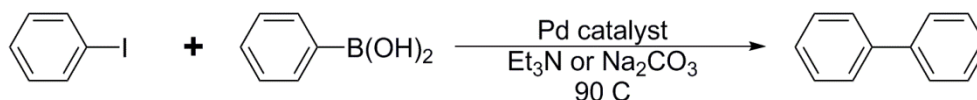
Figure 1.44: Pd(OAc)₂-BOX-MPSG catalyst presented by Gruber-Woelfler *et al.*



Temperature [°C]	Toluene [%]	DMAc [%]	NMP [%]	DMF [%]
110	96	23	No reaction	No reaction
160	98	75 ^a	62	75

Table 1.15: Yields of Pd(OAc)₂-BOX-MPSG catalyst for toluene, DMAc, NMP, DMF (DMF at 150 °C).

In an attempt to perform a Suzuki-Miyaura reaction in a green solvent, Wolfson *et al.* investigated the catalytic properties of several heterogeneous Pd species in glycerol. Interestingly, the catalysts were more active for the Heck reaction than the analogous Suzuki reaction. The pertinent reaction data are presented in Table 1.16.¹⁷⁷ When PdCl₂(TPPTS)₂ was employed in the presence of Na₂CO₃, the biphenyl product was produced in the highest yields. Finally, Glycerol was found to be the most appropriate solvent for both the Suzuki and Heck cross-coupling reactions.



Catalyst	Base	Yield [%]
PdCl ₂ (TPPTS) ₂	Et ₃ N	83
PdCl ₂ (TPPTS) ₂	Na ₂ CO ₃	94
Pd(OAc) ₂ (TPPTS) ₂	Et ₃ N	66
Pd(OAc) ₂ (TPPTS) ₂	Na ₂ CO ₃	75
PdCl ₂ (DPPF) ₂	Na ₂ CO ₃	82

Table 1.16: Suzuki coupling of a few heterogeneous catalysts using Et₃N or Na₂CO₃; Reaction conditions: Pd (2 mol%), μw-oven assisted reactions (26-89 °C).

These examples underline the high reactivities of such heterogeneous Pd catalysts in a variety of organic solvents under mild reaction conditions, of which a few even exhibited appreciable activities at ambient temperature. These promising results generated interest in using these insoluble Pd complexes in green media for the purpose of room temperature Suzuki-Miyaura cross-coupling reactions.¹⁷⁸ One of the most prominent examples of aqueous reactions of this type was the previously mentioned Bai and Wang work, in which sodium tetraphenylborate was coupled with *p*-bromoacetophenone, thereby generating the *hetero*-coupled product in 78-95% yield. Surprisingly, the polymer-supported Pd catalyst exhibited enhanced behavior in neat water rather than aqueous mixtures or pure organic solvents.¹³⁷

Uozumi designed several polymer-bound PR_3 complexes on account of their activities in aqueous media. In this work, mono- and bidentate ligands were anchored to polystyrene, followed by metalation with $[\text{PdCl}(\eta^3\text{-C}_3\text{H}_5)]_2$ (Figure 1.45). Of these complexes, PS-PEG-adppp-Pd exhibited the highest activity in water for aryl bromides with phenylboronic acids. The recyclability of these catalysts was not examined.^{179,180}

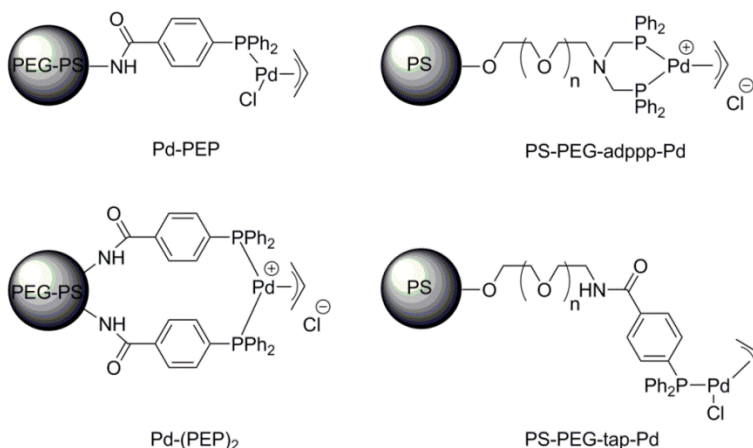


Figure 1.45: Polystyrene-supported palladium catalysts for the Suzuki reaction.

In the interest of designing new insoluble catalysts for the epoxidation of alcohols,¹⁴⁵ Yamada and co-workers developed a triphasic catalyst that also activated C–X bonds. This previously discussed catalyst self-assembled and subsequently performed a Suzuki coupling involving iodobenzene. Furthermore, this catalyst retained activity for ten consecutive trials.¹⁴⁷ On the basis of a collaboration between Yamada and Uozimi, a new 3-D Pd-phosphine network was synthesized and used under Suzuki-Miyaura reaction conditions (Figure 1.46). This catalyst exhibited remarkable reactivity at low loadings (0.05 mol%), particularly when used for the coupling of aryl bromides with various functionalized phenylboronic acids. The biphenyl products were isolated in high yields from neat water at 100 °C without the addition of organic solvents during the reaction work-up.¹⁸¹

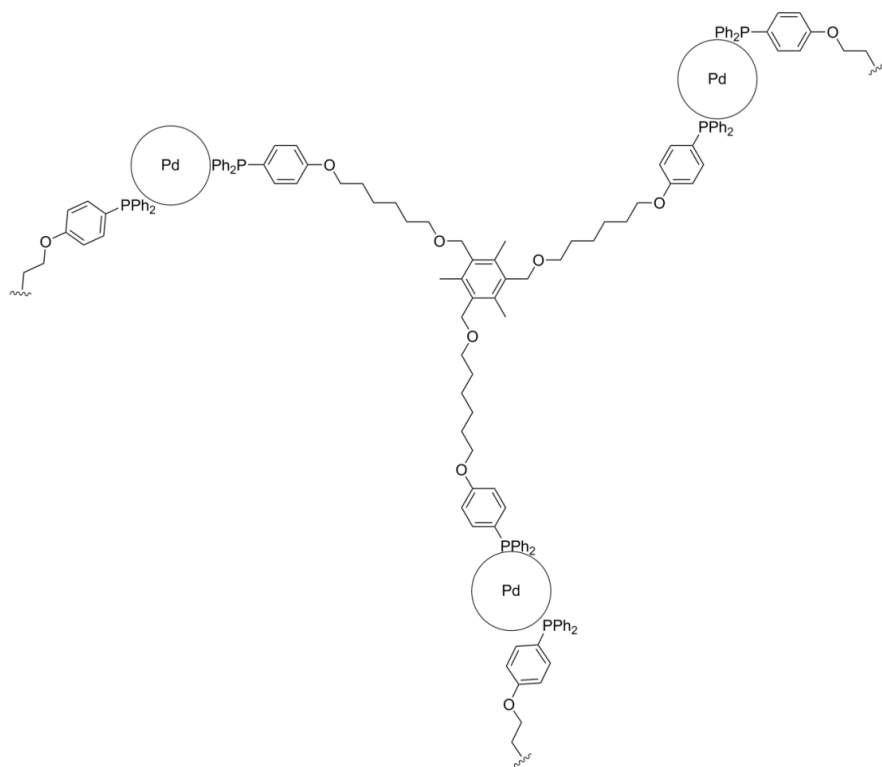


Figure 1.46: 3-D Pd-phosphine network reported by Yamada and Uozimi *et al.*

The majority of the examples of heterogeneous palladium complexes generated for use in Suzuki couplings are phosphine ligand-based. Although several of the previous Pd–NHC catalysts were employed in aqueous solutions, very few examples of Pd–NHC complexes in pure water can be found in the literature. Nevertheless, Kim and co-workers produced a PS–PEG–NHC–Pd complex that is active for both aryl iodides and bromides in pure water. Furthermore, it could be recycled five times with only a gradual reduction in the production of biphenyl compounds (Figure 1.47).¹⁵⁰ Complete conversion of unactivated aryl bromides was observed at 50 °C.

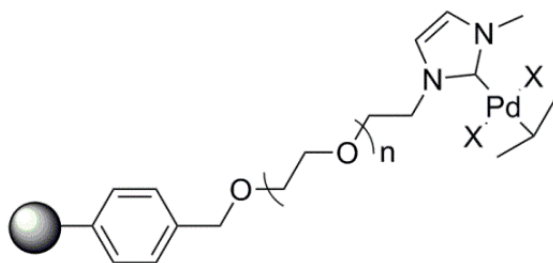


Figure 1.47: PS–PEG–NHC–Pd complex synthesized by Kim *et al.*

1.4 HOMOGENEOUS VS. HETEROGENEOUS CATALYSIS

In the past few decades, several catalysts have been designed for the activation of C–X bonds for a variety of cross-coupling reactions. These homo- and heterogeneous catalysts were synthesized and characterized in the solid state prior to being introduced into the liquid-phase. Unfortunately, these catalysts have been rarely studied post-reaction, which resulted in ambiguous assignments of the truly active catalytic species. In the case of the Suzuki-Miyaura reaction, it has been demonstrated that upon occasion the soluble palladium species can dissociate from the homo- or heterogeneous complex and generate molecular Pd species that exhibit significant catalytic activity.¹⁸² In light of

these observations, a few simple experiments were developed to eliminate the obscurity of the active palladium entity.

1.4.1 Identification of the Active Species

One of the prevalent tests was established by Sheldon and co-workers during their investigation of epoxidation reactions, with the objective of determining the active catalytic species.¹⁸³ The hot filtration test (or split test) is an efficient technique for establishing the presence of any leached soluble Pd entities. For this examination, either the homo- or heterogeneous catalyst can be employed under optimized reaction conditions and allowed to reach completion. Immediately following the completion, the hot reaction mixture was separated by means of a centrifuge into solid and liquid components. The supernatant and precipitate were then injected into separate reaction vessels containing fresh reagents. This precipitate reaction system required the addition of fresh solvent. Each entity was then monitored for evidence of any new biphenyl production in order to determine the location of the actual catalytic species. In the case of a homogeneous catalyst, the generation of the *hetero*-coupled product from the supernatant layer indicates the presence of molecular Pd complexes. On the other hand, if the precipitate exhibits reactivity toward the aryl halides, this implies that soluble Pd species have been leached from the molecular catalyst and are therefore responsible for at least some portion of the catalysis. In the case of a heterogeneous catalyst, the opposite effects would be expected. Because only 50 ppb is required for the construction of C–C bonds, a hot filtration test must be utilized in conjunction with another catalyst in order to unequivocally prove the nature of the homo- or heterogeneous catalyst.

A favored secondary analysis of the active catalyst is commonly referred to as the Mercury test. For this experiment, liquid Hg(0) is added to the pertinent reaction mixture,

hence any catalysts that might be present in a cycle containing a Pd(0) intermediate are poisoned. The experimental evidence for this examination is evident from the immediate termination of the Suzuki reaction. For example, Foley and Anton supplemented their reaction conditions with liquid mercury and observed no measurable changes in the catalytic system, thus confirming the homogenous character of their catalysts.^{10,184}

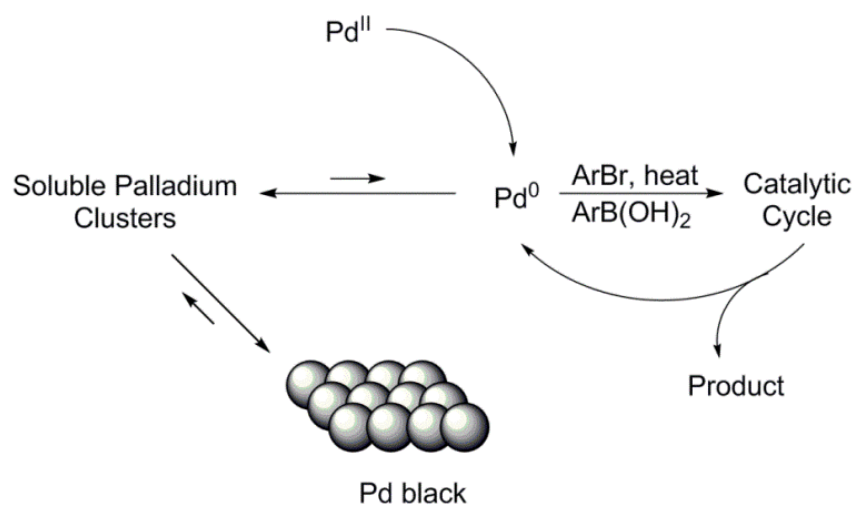
The scientific community has resisted similar proclamations for homogenous systems, since the mercury test was originally devised for the examination of heterogeneous character. As a consequence, DuPont and Phan have debated the value of a positive mercury test. In fact, DuPont asserted that a mercury test can “confirm a homogeneous catalytic system but not a heterogeneous one,”¹⁸⁵ whereas Phan contended that “the observation that Hg(0) does not affect the catalysis can confirm a mechanism that does not involve unprotected Pd(0) (soluble or supported), whereas an observation that Hg(0) quenches the activity may be consistent with a Pd(0) intermediate.”¹⁸² Ultimately, however, the addition of liquid mercury will at least indicate the nature of the active catalyst.

A few alternative methods have also been introduced for soluble catalysts. The most common catalyst poisons for homogeneous catalysts are thiophene, CS₂, DCT, and PPh₃.¹⁸⁴ If less than one equivalent of catalyst poison (relative to Pd) terminates the reaction, the catalyst is believed to operate under heterogeneous conditions. This is particularly difficult with respect to Suzuki-Miyaura cross-coupling reactions since the exact quantity of the catalyst is rarely established. On this account, a new catalyst poison was proposed recently by Phan, in which the cross-linked poly(vinylpyridine) effectively eliminates any catalysis by soluble molecular Pd species.¹⁸²

The ambiguity of the active catalysis in homo- and heterogeneous catalysis became even more problematic when Leadbeater and co-workers discovered that commercially-available sodium carbonate reagents contained trace amounts of Pd species.¹⁸⁶ DuPont expanded the study to determine the amount of residual Pd on reaction equipment that was used for moderate catalysis of the Heck reaction.¹⁸⁷ Moreover, Kashin and co-workers recently proposed the presence of several additional Pd contaminants stemming from the environment, auto catalyst exhaust, or magnetic-stirbar Pd remnants. Furthermore, they suggested that all future catalysis should be performed using clean room technology if at all possible.¹⁸⁸

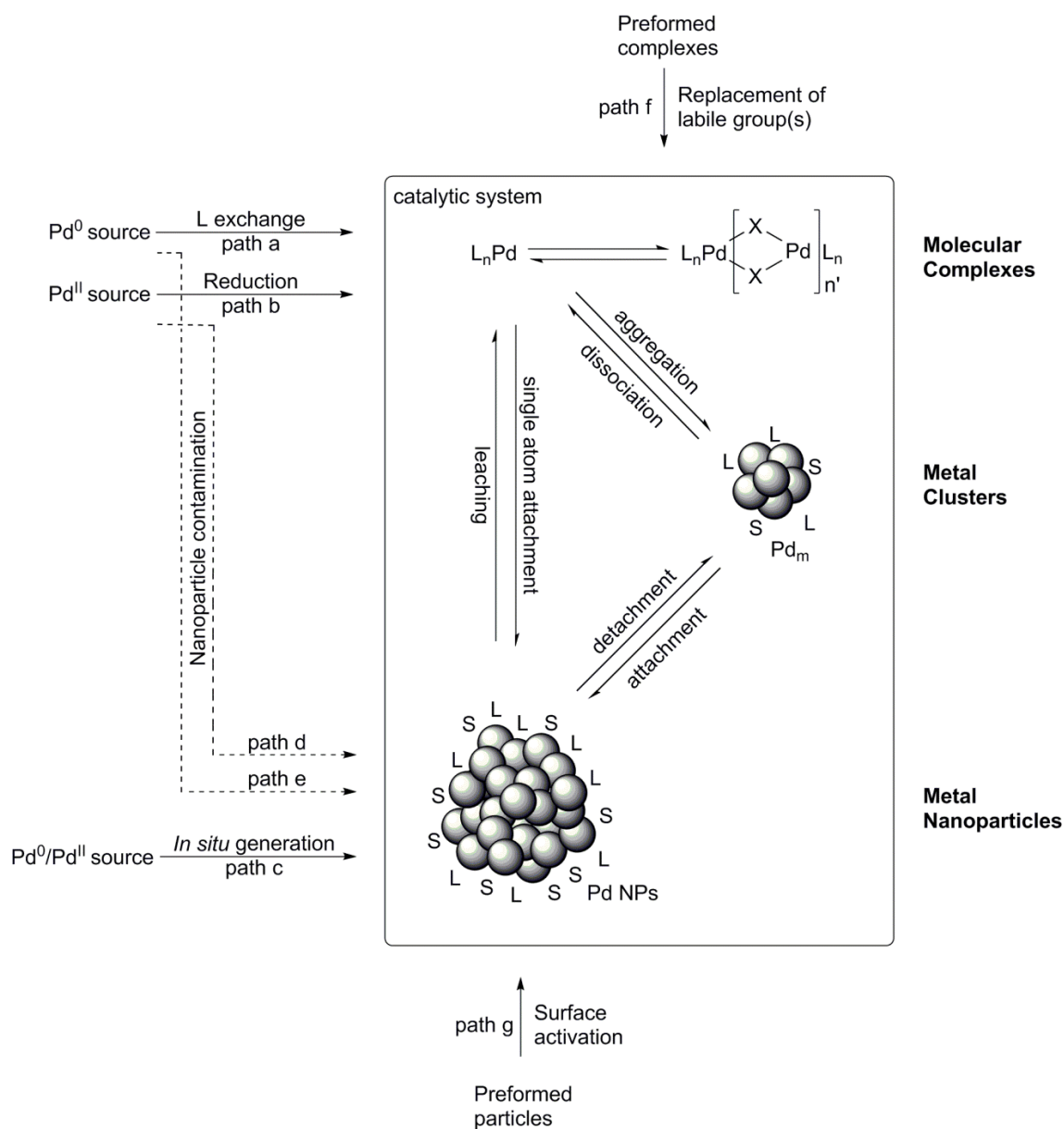
1.4.2 Homoeopathic Systems

A significant breakthrough for this difficult predicament was presented by De Vries in 2003 when the kinetic parameters of $\text{Pd}(\text{OAc})_2$ and a common palladacycle were directly compared.¹⁸⁹ Both catalysts provided comparable kinetic data for a variety of activated and deactivated aryl bromides, specifically at low catalyst loadings. Furthermore, a unique relationship between catalyst loading and turnover frequency was detected, thus indicating the establishment of equilibrium between molecular Pd species and soluble $\text{Pd}(0)$ clusters. The unusual decrease of turnover frequency with an increase of catalyst loading became a definitive characteristic of these homeopathic systems. The mechanism for such systems as proposed by De Vries is presented in Scheme 1.33.¹⁹⁰



Scheme 1.33: Homeopathic mechanism presented by De Vries *et al.*

The most recent development on these types of mixed homo- and heterogeneous catalytic systems was proposed by Ananikov *et al.*,¹⁹¹ who suggested the existence of two distinct categories of catalysis, namely single-type and cocktail-type. The former mechanism entails a fully-characterized catalyst with tightly-bound ligands that maintains its chemical structure, whereas the latter system experiences metal-ligand degradation thereby producing a “cocktail” of palladium-based clusters and nanoparticles (Scheme 1.34).¹⁸⁸ The combination of these systems represents the active Pd species for the Suzuki-Miyaura cross-coupling reaction.



Scheme 1.34: Mechanism of the cocktail of molecular complexes, metal clusters, and metal nanoparticles as presented by Ananikov *et al.*

Chapter 2: *Bis(imino)acenaphthene (BIAN)*-supported palladium(II) carbene complexes as effective C–C coupling catalysts and solvent effects in organic and aqueous media

2.1 ABSTRACT

The synthesis and catalytic properties of two new 1,2-acenaphthenyl *N*-heterocyclic carbene-supported palladium(II) catalysts are presented. The acenaphthenyl carbene has been prepared with mesityl or 2,6-diisopropyl *N*-aryl substituents. Comprehensive catalytic studies for the Suzuki coupling of aryl halides with aryl boronic acids have been conducted. In general, the diisopropyl-functionalized catalyst showed superior selectivity and reactivity. A comparison of the catalytic performances in dichloromethane, toluene and water at low temperatures (30–40 °C) is also presented. Both catalysts were proficient in the homogeneous Suzuki coupling of aryl iodides, bromides and chlorides with boronic acids in dichloromethane. Similar reactions in water led to the formation of insoluble colloidal catalytic species that still exhibited high activity in the Suzuki reaction with aryl chlorides. Reactions performed in toluene showed intermediate results; partial catalyst decomposition led to concomitant homogeneous and heterogeneous catalysis. The heterogeneous palladium precipitates could be easily recovered by filtration and reactivated for subsequent use. Activation energies determined for aryl bromide-based Suzuki reactions were found to be in the range of 159–171 kJ mol⁻¹ in organic solvents and 111–116 kJ mol⁻¹ in water. The corresponding activation energy for the aryl chloride was found to be 322 kJ mol⁻¹ in water.

****Crawford, K., Cowley, A., Humphrey, S. *Cat. Sci. Technol.* **2014**, 4, 1456. Cowley and Humphrey were co-supervisors of this work.**

2.2 INTRODUCTION

The Suzuki-Miyaura cross-coupling reaction is used extensively in industrial processes for the formation of carbon-carbon bonds.¹⁹² This reaction plays an important industrial-scale role for the production of natural products, pharmaceuticals, and agrochemicals.^{193–195} Typically, Suzuki coupling is performed in an organic solvent using homogeneous catalysts that are designed to generate exclusively the *hetero*-coupled biaryl product. The C–C coupled products are obtained by the treatment of an aryl halide with an organoborane in the presence of a suitable base (Scheme 1.3)¹⁹⁶ Complexes based on Group X metals are the most proficient in this task and can be rendered soluble in appropriate organic solvents using a range of spectator ligands such as 3-chloropyridine, triethylamine, and allyl moieties.^{197–9} Suzuki catalysts often employ bulky phosphine ligands that result in optimal catalytic activity and selectivity. However, phosphine ligands are typically susceptible to oxidation and metal-ligand degradation.^{56,67,200} As a consequence, *N*-heterocyclic carbenes (NHCs) have attracted interest as more stable supporting ligands. NHCs feature a significantly stronger electron donating character than phosphines, which enhances the stability of resulting complexes towards heat, air and moisture. The strong σ -donating ability of the NHCs also promotes oxidative addition of aryl halides and can assist in reductive elimination of biaryl products.^{85,201}

Recent advances in ‘green’ Suzuki coupling have focused on developing catalysts that are easily recoverable and can operate in environmentally benign solvents. Some pertinent examples include, heterogenised catalysts (*e.g.*, nanoparticles),^{202–204} metallopolymers,^{205–207} and single-site catalysts grafted onto insoluble support media (*e.g.*, silica or alumina).^{208–210} For example, Sekar *et al.* generated active catalysts for Suzuki, Heck, and Sonogashira cross-coupling reactions using covalently-bonded Pd–

C_(binaphthyl) nanoparticles.¹⁵ These nanoparticles formed quantitatively C–C bonds even after several cycles of catalyst use and recovery.²⁰² Meanwhile, Ma *et al.* have prepared active Pd(II) Suzuki catalysts by direct anchoring to SBA-16-type silica, which afforded an easily recoverable and recyclable heterogeneous composite catalyst that showed excellent activity even after prolonged recycling.²⁰⁸

The pursuit of greener Suzuki catalysts has also resulted in the development of molecular complexes that are catalytically active in environmentally-benign and renewable solvents, such as water. Morales-Morales *et al.* utilized water-soluble pincer ligands in aqueous media to convert *p*-substituted aryl bromides to the corresponding *hetero*-coupled biphenyl products in appreciable yields.²¹¹ Such aqueous reactions raise an important question: do homogeneous molecular catalysts remain intact during Suzuki reaction conditions, or do the catalysts decompose to generate new (presumably heterogeneous) catalyst species? A technique that is commonly employed to address this question involves the injection of excess Hg(0) into the reaction mixture to poison any leached Pd(0) species.^{184,10} Alternatively, the likely identity of the active Suzuki cross-coupling species can be determined *via* a filtration test, in which the reaction is interrupted, and then separated into a supernatant layer and a precipitate; both phases are then independently probed for the presence of trace metal species and catalytic reactivity.^{212–213.}

In the present work, two new 1,2-acenaphthenyl *N*-heterocyclic carbene-supported palladium(II) catalysts have been synthesized with the objective of assessing their comparative performance in the Suzuki reaction, when conducted in polar and nonpolar organic solvents, and in aqueous media. In general, it was found that these catalysts consistently behaved as stable homogeneous catalysts in organic solvents, and

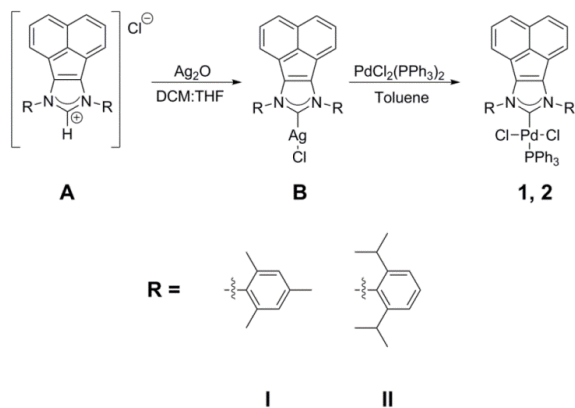
decomposed to give less well-defined, but still highly active heterogeneous catalyst species in water. In fact, reactions performed in water significantly enhanced the activity of the original Pd(II) catalysts, based on measured rate constants and activation energies. In addition, both catalysts studied here were able to activate aryl chloride feedstocks in all solvents. Consideration of the trend in activation energies for the aryl halides ($\text{C-Cl} > \text{C-Br} > \text{C-I}$; 407, 346, 280 kJ mol⁻¹, respectively) reveals that aryl chlorides are significantly the least reactive, yet they are industrially the most attractive because heavy halogenated by-products can be avoided.⁶ In this study, appreciable yields of cross-coupled products were obtained using aryl chlorides at temperatures as low as 40 °C.

2.3 RESULTS AND DISCUSSION

2.3.1 Catalyst synthesis and structures

The present work has focused on the catalytic activities of two related Pd(II)–carbene complexes with the objective of expanding the scope of this family of catalysts. The carbene ligands in question (**A-I** and **A-II**) were prepared using the previously reported route for **B-II** (Scheme 2.1).²¹⁴ The silver(I)–carbene complexes **B-I** and **B-II** were treated directly with PdCl₂(PPh₃)₂ in toluene to give the corresponding Pd(II) complexes, (IMes)PdCl₂PPh₃ (**1**) and (IPr)PdCl₂PPh₃ (**2**) by transmetalation and elimination of AgCl (Scheme 2.1; see experimental section for further synthetic details). The single crystal X-ray diffraction structure of **2** was obtained by growing suitable crystals by slow evaporation of CH₂Cl₂ in air (Figure 2.1 and Table 2.1). The metal site Pd1 in **2** displays a somewhat distorted square-planar environment, most likely imposed by the steric bulk of the *N*-diisopropyl aryl groups that are rotated approximately perpendicular to the C₃N₂ ring plane, which is commonly observed for such Brookhart-

type complexes.²¹⁵ The Pd1–C1 bond distance is 2.04 Å, while the *trans*-oriented phosphine Pd1–P1 bond is 2.32 Å. The average Pd–P bond length obtained from a survey of similar NHC-Phosphine Pd(II) structures in the CCDC is somewhat shorter, at 2.267 Å. This may be indicative of a particularly strong *trans* influence exerted by the acenaphthene carbene ligand. As expected, the fused five- and six-membered aromatic acenaphthene structure in **2** displays a distinct curvature with a maximum out-of-plane displacement of 0.18(2) Å degrees with respect to the C1–N1–C2–C3–N2 mean plane.



Scheme 2.1: Syntheses of palladium catalysts **1** and **2**.

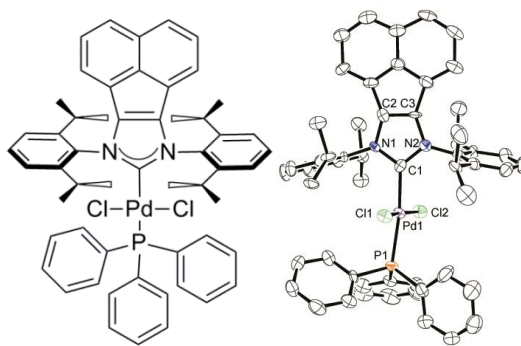


Figure 2.1: Crystal structure of **2**.

Length (Å)		Angles (°)	
Pd1–Cl1	2.295(2)	Cl1–Pd1–Cl2	172.82(10)
Pd1–Cl2	2.321(2)	C1–Pd1–Cl1	92.2(2)
Pd1–C1	2.041(7)	C1–Pd1–Cl2	90.4(2)
Pd1–P1	2.324(2)	C1–Pd1–P1	173.2(2)
C2–C3	1.356(12)	N1–Pd1–N2	107.3(7)

Table 2.1: Selected bond distances and angles of **2**.

Tu *et al.* recently reported the synthesis of a related NHC complex that was shown to be an active catalyst for Buchwald-Hartwig aminations^{216,217} and Suzuki-Miyaura coupling reactions.^[218] Merino *et al.* have developed a similar Ru-based complex that is capable of ring closing metathesis.²¹⁹

2.3.2 Suzuki coupling by catalysts **1** and **2** with aryl iodide, bromide and chloride precursors

The catalytic activities of **1** and **2** with respect to Suzuki-Miyaura cross-coupling reactions were initially explored with aryl iodides (0.216 mmol), phenylboronic acid (0.259 mmol) and K₂CO₃ (0.647 mmol) in toluene, CH₂Cl₂, or H₂O (3.0 cm³). These solvents were chosen as examples of nonpolar and polar aprotic solvents, and polar protic solvents, respectively. Prior to injection of the catalyst, all reaction mixtures were stirred at 40 °C until all solids had dissolved.

The catalyst loadings were determined using UV-vis spectrophotometry (Figures 2.2-3), and **1** or **2** was rapidly injected into the reaction mixture at *t* = 0. The reaction mixtures were then stirred at 40 °C for 20 h. A summary of the outcomes of these reactions are presented in Table 2.2. **1** and **2** both converted *p*-iodobenzaldehyde into the desired *hetero*-coupled product with greater than 91% selectivity (determined by GC analysis; Table 2.2). The observed catalytic activities revealed a significant dependence

on the nature of the solvent: the catalysts exhibited extremely low activities in CH_2Cl_2 (Table 2.2; entries 1b & 2b), but achieved 77–81% conversions in toluene (Table 2.2; entries 1a & 2a) and complete conversion in H_2O (Table 2.2; entries 1c & 2c).

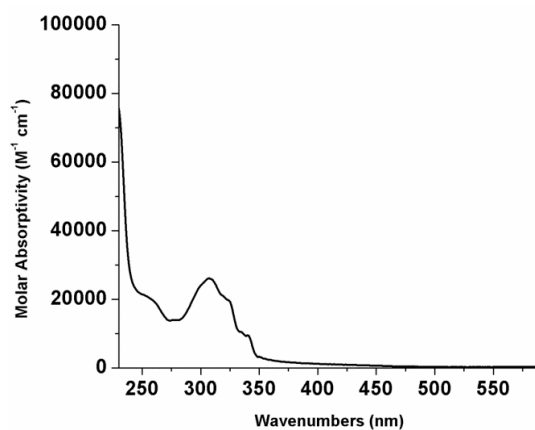


Figure 2.2: Absorption spectrum of **1** in CH_2Cl_2 with $\lambda_{\text{max}} = 308 \text{ nm}$. Beer's law was used to determine ϵ from a calibration curve created with ten data points in $10 \mu\text{L}$ increments ranging $10\text{--}100 \mu\text{L}$ ($\epsilon = 29,646 \text{ M}^{-1} \text{ cm}^{-1}$, $R^2 = 0.9918$).

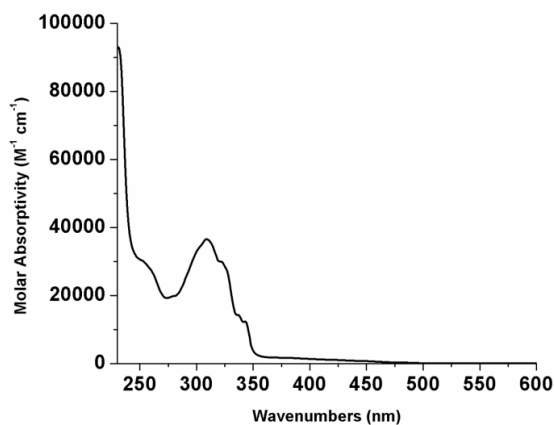
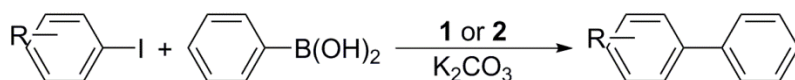


Figure 2.3: The absorption spectrum of **2** in CH_2Cl_2 with $\lambda_{\text{max}} = 309 \text{ nm}$. Beer's law was used to determine ϵ from a calibration curve created with ten data points in $10 \mu\text{L}$ increments ranging $10\text{--}100 \mu\text{L}$ ($\epsilon = 36,868 \text{ M}^{-1} \text{ cm}^{-1}$, $R^2 = 0.9997$).



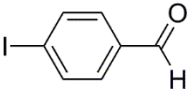
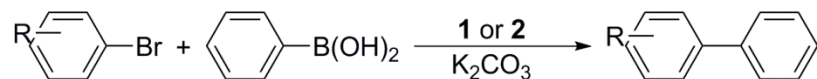
Substrate	Catalyst	Entry	Conversion [%]	S ^{hetero} [%]
	1	1a	81.5	99.7
		1b	4.6	91.2
		1c	100	97.1
	2	2a	77.3	99.6
		2b	23.3	97.3
		2c	100	97.9

Table 2.2: Suzuki-Miyaura biaryl coupling of aryl iodides by **1** and **2**; Reaction conditions: aryl iodide (0.216 mmol), phenylboronic acid (0.259 mmol), K₂CO₃ (0.647 mmol), **1** or **2** (1.0 mol % Pd), solvent (a-toluene, b-CH₂Cl₂, c-H₂O; 3.0 mL), 40 °C, 20 h; all reactions were monitored by GC.

Suzuki-Miyaura cross-coupling reactions were expanded to the use of aryl bromides under otherwise identical reaction conditions; the results of these reactions are summarized in Table 2.3. **1** and **2** exhibited comparable percentage conversions and selectivities of *p*-bromobenzaldehyde (Table 2.3; entries 3-8) to those of analogous reaction conditions with the iodo- precursor. Again, the highest conversion was obtained for H₂O. Interestingly, the catalytic activities appeared to be unaffected by the functional group position on the bromobenzaldehydes. The bromoanisoles revealed a substantial dependence on the nature of the solvent as well as on the location of the methoxy functional group. In aqueous solution, the bromoanisoles yielded slightly lower conversions and selectivities than those of the analogous bromobenzaldehydes (Table 2.3; entries 9c, 10c, 13c, & 14c). Selectivity for the desired *hetero*-coupled products was generally high (70–100%) for aldehyde-substituted precursors, regardless of the

substitution pattern, solvent or catalyst employed (Table 2.3; entries 3–8). However, much greater variation in selectivity was observed for methoxy-substituted precursors (0–99%). Most notably, catalyst **1** did not yield any of the *hetero*-coupled biphenyl products from *m*-bromoanisole in H₂O, yet catalyst **2** was highly selective under the same conditions (Table 2.3; entries 11c & 12c). It is difficult to identify clear trends in the observed reactivity; the variation in selectivities is likely due to inter-play of steric, electronic and solvation effects. In general, both catalysts were significantly less active when tested in both polar and apolar organic solvents. Less than 50% conversion to the *hetero*-coupled product was obtained when the bromoanisoles were used (Table 2.3; entries 9-14a,b) with the exception of **1** in CH₂Cl₂ (Table 2.3; entry 13b). It is of particular note that the catalysts were considerably more selective in CH₂Cl₂ than in toluene.



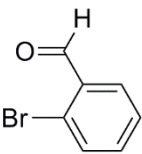
Substrate	Catalyst	Entry	Conversion [%]	S ^{hetero} [%]
	1	3a	92.3	84.4
		3b	17.4	95.9
		3c ^a	96.1	100
	2	4a	84.3	79.8
		4b	59.0	90.4
		4c ^a	92.3	100

Table 2.3 (continued)

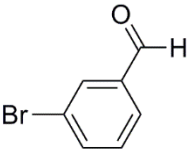
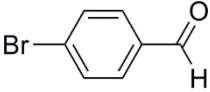
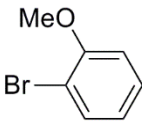
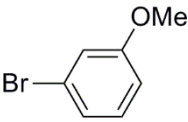
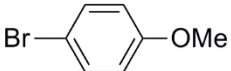
Substrate	Catalyst	Entry	Conversion [%]	S ^{hetero} [%]
	1	5a	77.8	83.4
		5b	60.4	97.6
		5c ^a	98.1	95.7
	2	6a	72.5	69.3
		6b	79.9	88.3
		6c ^a	92.9	97.1
	1	7a	87.5	92.1
		7b	82.2	99.8
		7c ^a	100	100
	2	8a	86.6	86.6
		8b	81.4	98.5
		8c ^a	99.3	96.1
	1	9a	31.7	13.4
		9b	46.4	91.5
		9c	93.6	84.6
	2	10a	37.3	14.3
		10b	43.1	67.9
		10c	91.3	95.5
	1	11a	44.9	31.0
		11b	2.8	76.3
		11c	33.1	0
	2	12a	39.8	22.5
		12b	52.9	77.3
		12c	62.9	99.1
	1	13a	47.9	24.4
		13b	60.9	95.9
		13c	100	99.5
	2	14a	46.1	22.1
		14b	34.3	78.9
		14c	90.8	89.0

Table 2.3 (continued)

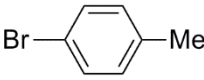
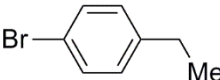
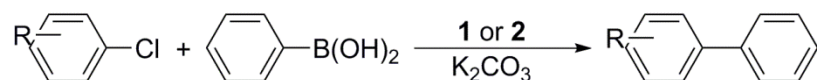
Substrate	Catalyst	Entry	Conversion [%]	S ^{hetero} [%]
	1	15a	43.9	58.5
		15b	93.0	92.4
		15c	100	100
	2	16a	50.5	54.5
		16b	100	88.5
		16c	96.6	89.1
	1	17a	44.3	39.7
		17b	68.9	90.2
		17c	100	100
	2	18a	41.2	25.5
		18b	60.1	81.6
		18c	98.6	76.7

Table 2.3: Suzuki-Miyaura biaryl coupling of aryl bromides by **1** and **2**; Reaction conditions: aryl bromide (0.270 mmol), phenylboronic acid (0.324 mmol), K₂CO₃ (0.811 mmol), **1** or **2** (1.0 mol % Pd), solvent (a-toluene, b-CH₂Cl₂, c-H₂O; 3.0 mL), 40 °C, 20 h; all reactions were monitored for conversion by GC. ^a 0.1 mol % Pd.

Interestingly, the catalysts were not only more active in reactions employing *p*-functionalized aryl halides, but they were also significantly more selective. *p*-Bromotoluene and *p*-bromoethylbenzene were selected to assist in the examination of the apparent regioselectivity (Table 2.3; entries 15c & 16c). In contrast to the bromobenzaldehydes and the bromoanisoles, high conversion completeness of the substrate to the desired *hetero*-coupled product was evident for reactions performed in both H₂O and CH₂Cl₂ (Table 2.3; entries 15-18b,c). However, these catalysts were found to be significantly less active in toluene, since **1** and **2** not only exhibited less than 50% conversion, but were also selective for the undesired *homo*-coupled product (Table 2.3; entries 15-18a). Both **1** and **2** could activate C–Br bonds in all three solvents with similar

conversions and selectivities at lower catalyst loadings (0.1–1.0 mol%). The catalysts appeared to be more active in aqueous media than either organic medium, in which the catalytic activities were only moderate. The catalytic activities in apolar toluene were generally high when halogenated benzaldehydes were employed. The overall conversion values decrease dramatically for coupling reactions performed using methoxy- and aliphatic-substituted reagents, under otherwise identical conditions. However, both catalysts were highly selective for the *homo*-coupled products. **1** and **2** activated the C–X bond most readily for *para*-substituted reagents, presumably due to a combination of preferential steric and electronic effects of the incoming precursors. The steric demands of the bulky aldehyde and methoxy- functional groups may also protect the C–Br bond from engaging in competing oxidative addition reactions.

Following the optimization of **1** and **2** for the Suzuki coupling of aryl bromides, it was decided to explore the use of aryl chlorides. Aryl chlorides are the most important industrial target, since they are both cost effective and generate significantly less harmful/corrosive by-products than the analogous aryl bromide and iodides. In our studies, the higher bond dissociation energy of the C–Cl bond resulted in the need for significantly longer reaction times than those for C–Br to achieve comparable overall conversions at the same reaction temperature (Table 2.4). Catalyst **1** activated the carbon-chloride bonds with conversions in the range of 13–42% and 76–88% for organic and aqueous solvents, respectively (Table 2.4; entries 19, 21 & 23). In contrast, **2** resulted in conversions of 40–65% and 96–100%, respectively (Table 2.4; entries 20, 22 & 24).



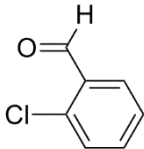
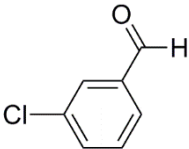
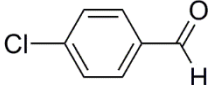
Substrate	Catalyst	Entry	Conversion [%]	S ^{hetero} [%]
	1	19a	42.1	7.2
		19b	18.0	15.8
		19c	87.8	27.0
	2	20a	44.6	23.4
		20b	59.7	100
		20c	100	92.3
	1	21a	40.6	1.4
		21b	15.5	4.7
		21c ^a	76.6	20.6 ^b
	2	22a	42.0	8.9
		22b	39.6	28.4
		22c	96.9	78.8
	1	23a	29.7	11.4
		23b	13.2	12.1
		23c	83.9	89.1
	2	24a	45.2	26.0
		24b	64.7	79.8
		24c	96.1	86.5

Table 2.4: Suzuki-Miyaura biaryl coupling of aryl chlorides by **1** and **2**; Reaction conditions: aryl chloride (0.357 mmol), phenylboronic acid (0.429 mmol), K₂CO₃ (1.07 mmol), **1** or **2** (1.0 mol % Pd), solvent (a-toluene, b-CH₂Cl₂, c-H₂O; 3.0 mL), 40 °C, 48h; all reactions were monitored by GC. ^a 2.0 mol% Pd ^b 79.3% selectivity for bifunctionalized *homo*-coupled biaryl product.

As previously observed for the use of brominated reagents (*vide supra*), a broad range of selectivity values were measured using *ortho*-, *meta*- and *para*-substituted chlorobenzaldehydes. However, catalyst **2** was consistently more selective than **1** in all solvents. In fact, catalyst **1** only gave appreciable yields of the *hetero*-coupled product

when operated in H₂O. In contrast, **2** was moderately, or highly selective in CH₂Cl₂ or H₂O. Interestingly, the rarely-observed bifunctionalized *homo*-coupled product (4,4'-biphenyldicarboxaldehyde) was obtained from a 2.0 mol% loading of **1** with 79.3% selectivity from *m*-chlorobenzaldehyde (Table 2.4; entry 21c). For *para* substituted reagents, **1** was 89.1% selective for the desired product (Table 2.4; entry 23c). Conversely, **2** always created the *hetero*-coupled product as the major product in greater than 96% conversion with selectivities of 92, 79, and 87% for the *ortho* (Table 2.4; entry 20c), *meta*- (Table 2.4; entry 22c), and *para*- (Table 2.4; entry 24c) positions, respectively. From this data, there is no obvious trend that relates total conversion (reaction rate) to the corresponding degree of product selectivity. This infers that catalyst structure and/or solvation effects play important roles in the reaction.

2.3.3 A quantitative assessment of the effect of solvent system upon Suzuki coupling by catalysts **1** and **2**

The above studies proved that catalysts **1** and **2** were able to convert a broad range of aryl iodides, bromides and chlorides into the desired functionalized biphenyl products with varying degrees of proficiency in the three contrasting solvent systems. As might be expected, the trends in activity appeared to depend in part on the electronic influence of the R group on the aryl halide precursors. For example, whereas OMe substituents greatly deactivated the C–X bond activation, aldehyde functionalized aryl halides were much more easily converted to the corresponding biphenyl aldehydes in high yields by **1** and **2**, especially for *para*-substituted precursors. However, the polarity of the solvent was clearly most highly influential in terms of both reaction selectivity and reactivity. In general, selectivity toward *hetero*-coupled biaryl products in the Suzuki reaction was significantly enhanced for both **1** and **2** in solvents with larger dielectric constants (H₂O =

80.4; CH₂Cl₂ = 9.1; toluene = 2.4). It became evident that **1** and **2** were more selective for the *hetero*-coupled product in solvents with higher polarity; therefore, further studies were made to gain a better understanding of the possible mechanistic pathways responsible for catalytic enhancement effects in certain solvent systems. In particular, a more thorough characterization of the active catalysts and *post*-catalytic species was carried out.

The stabilities of **1** and **2** were first assessed in toluene, CH₂Cl₂ and H₂O in Suzuki reactions with *p*-bromobenzaldehyde and phenylboronic acid. Immediately after cessation of the Suzuki reaction, the hot reaction mixtures were centrifuged (15 min, 8.5 krpm) to isolate any solid residues, which were then separated from the organic supernatant. After cooling, the solid and liquid phases were then analyzed by ICP-MS to determine the %Pd content of each (Table 2.5). For both **1** and **2**, the Pd elemental analysis indicated that only a minority of metal had precipitated from reactions performed in CH₂Cl₂, suggesting that the molecular catalysts retained their original structures when employed in CH₂Cl₂ (Table 2.5; entries 25b & 26b). However, both catalysts appeared to undergo significant precipitation when operated in H₂O or toluene, which is indicative of either oligomerization or decomposition due to detachment of Pd from the carbene ligands.

Catalyst	Entry	% Pd		Conversion [%]	
		sup ^a	ppt ^a	sup	ppt
1	25a	15	85	87.8	92.5
	25b	97	3	50.4	12.5
	25c	23	77	55.4	98.6
2	26a	52	48	81.0	78.3
	26b	73	27	54.5	4.1
	26c	26	74	0.2	100
Pd-PVP	27 ^b	-	-	0.06	51.5

Table 2.5: Recyclability of **1** and **2** in Suzuki-Miyaura biaryl coupling of the *p*-bromobenzaldehyde supernatant (*sup*) and precipitate (*ppt*); Reaction conditions: *p*-bromobenzaldehyde (0.270 mmol), phenylboronic acid (0.324 mmol), K₂CO₃ (0.811 mmol), Pd (1 mol%), solvent (a-toluene, b-CH₂Cl₂, c-H₂O; 3.0 mL), 40 °C, 20 h; all reactions were monitored by GC. ^a % Pd of supernatant and precipitate determined by ICP-MS. ^b *p*-bromobenzaldehyde (0.270 mmol), phenylboronic acid (0.324 mmol), K₂CO₃ (0.811 mmol), H₂O (3.0 mL), Pd-PVP (0.537 mmol), 40 °C, 20 h.

Subsequently, the isolated solid and liquid phases were employed in repeat catalytic runs under the original reaction conditions, but using newly added organic reagents. This was achieved by direct re-use of the supernatant, or by the addition of fresh solvent to dissolve/suspend the residual solids. The products of the repeat reactions were monitored by GC (Table 2.5). Interestingly, conversion was observed for both the recycled supernatant and solids in all cases. The solid residues obtained from initial reaction in H₂O or toluene each showed high catalytic activity upon re-use (Table 2.5; entries 25a,c & 26a,c), presumably due to the poorly-defined, yet catalytically-active heterogeneous (colloidal or nanoparticulate) Pd species that had been generated. This type of complex catalysis has been documented in several previous instances;^{182,189,190,220,221} a recent review by Ananikov specifically describes the inter-play of well-defined homogeneous and less defined heterogeneous catalysts in C–C coupling

reactions.¹⁸⁸ Both the supernatant and the solid residues obtained from the initial reactions in toluene converted *p*-bromobenzaldehyde to *p*-biphenylaldehyde with high selectivity upon re-use (Table 2.5; entries 25a & 26a). This indicates that the molecular catalyst species was only partially decomposed to give heterogeneous species along with molecular species. Repeat reactions in CH₂Cl₂ only showed appreciable conversion for the supernatant, suggesting that **1** and **2** remained mostly solubilized (Table 2.5; entries 25b & 26b). The reverse outcome was observed for reactions in H₂O, suggesting that the catalysts were almost completely decomposed (Table 2.5; entries 25c & 26c). For example, the relative Pd content detected by ICP-MS after catalysis by **1** in CH₂Cl₂ was 97% in the supernatant and only 3% in the precipitate. This result is in stark contrast to 23% *versus* 77% (supernatant *versus* precipitate) that was observed after catalysis had been conducted in H₂O (Table 2.5; entry 25c).

The fact that similar overall conversions and coupling selectivities were observed in the Suzuki reaction using **1** or **2** in three highly contrasting solvents is an example of how particular attention must be paid to identify the composition of the ‘real’ active species.^{28–14,213,222–225} In the present study, it could easily be incorrectly assumed from the raw conversion data that **1** and **2** were proficient in all solvent systems. However, it is very apparent from the above hot isolation tests that the predominant catalytic species are different when operated in H₂O or CH₂Cl₂. Meanwhile, an ill-defined mixture of homogeneous and heterogeneous Pd species appeared to co-exist in toluene. In an attempt to further probe the identity of the catalytically-active heterogeneous species, pre-formed 4.5 nm Pd nanoparticles (Figures 2.4-6) capped with poly(vinylpyrrolidone) as a stabilizer were employed in the Suzuki reaction under otherwise identical reaction conditions to those used in the previous reactions. The Pd-PVP nanoparticles were

employed in H₂O-based Suzuki reactions as an alternative source of pre-formed heterogeneous Pd catalysts. These results showed coupling catalysis in the presence of the Pd-PVP nanoparticles without the requirement for either **1** or **2**; the associated reactivity and product selectivity was also very similar to that observed when the molecular catalyst, **2** was employed exclusively (Table 2.5; entry 27). This is convincing additional evidence for the hypothesis that heterogeneous Pd(0) species in H₂O are indeed catalytically active for the Suzuki reaction.²¹³

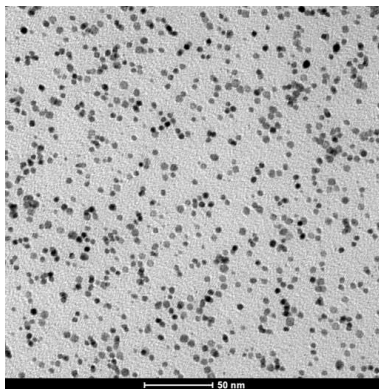


Figure 2.4: TEM images of Pd-PVP (50 nm scale).

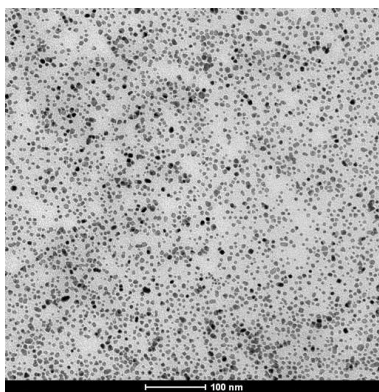


Figure 2.5: TEM images of Pd-PVP (100 nm scale).

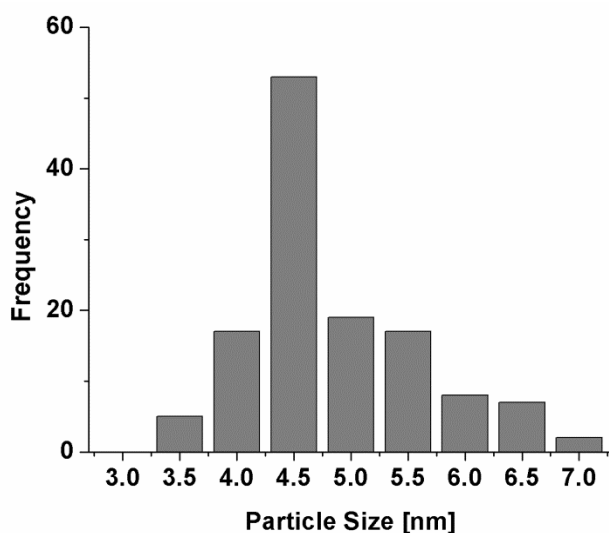


Figure 2.6: Particle size distribution of Pd-PVP.

The activation energies for **1** and **2** in H₂O, CH₂Cl₂ and toluene were also measured in order to provide kinetic insight into the nature of the different active species in each solvent. This was achieved by measuring the rate of coupling for *p*-bromobenzaldehyde as a function of catalyst loading (Table 2.6 & Figure 2.7). Complete conversion of *p*-bromobenzaldehyde with phenylboronic acid to yield the desired *hetero*-coupled product was achieved in H₂O for all catalyst loadings in the range 0.1–0.5 mol% in less than 5 h. Catalyst loading lower than 0.1 mol % usually resulted in incomplete conversion (Figure 2.8). As expected for truly catalytic systems, higher catalyst loadings required proportionately less time to reach complete conversion. Above 0.25 mol% the effect of higher loading was minimal since all reactions reached completion in less than 3 h for both **1** and **2** (Table 2.6; entries 28 & 29). The data summarized in Table 2.6 imply a *pseudo*-first order reaction with respect to the *p*-bromobenzaldehyde concentration. Also, catalyst **2** was significantly more effective than **1** in H₂O for all catalyst loadings studied.

Catalyst	Entry	0.10 mol %	0.25 mol %	0.50 mol %
1	28	0.3046	0.4407	0.5462
2	29	0.8979	0.9601	0.9667

Table 2.6: Rate constants for **1** and **2** for *p*-bromobenzaldehyde in H₂O; Reaction conditions: *p*-bromobenzaldehyde (3.24 mmol), phenylboronic acid (3.89 mmol), K₂CO₃ (9.73 mmol), H₂O (15.0 mL), 40 °C; all reactions were monitored by GC.

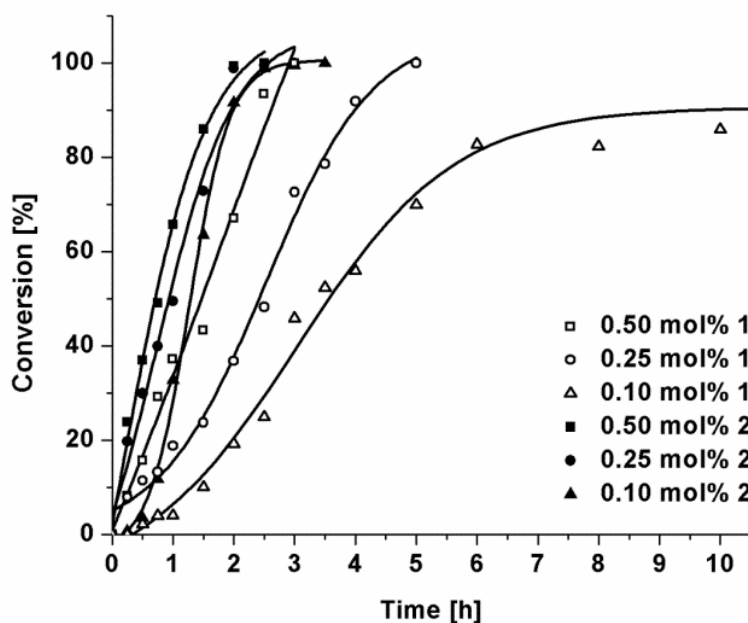


Figure 2.7: Conversion of *p*-bromobenzaldehyde with phenylboronic acid as a function of time for Suzuki-Miyaura cross-coupling reactions by **1** and **2** at 40 °C with 0.10, 0.25, and 0.50 mol % catalyst loading in H₂O; all reactions were monitored by GC.

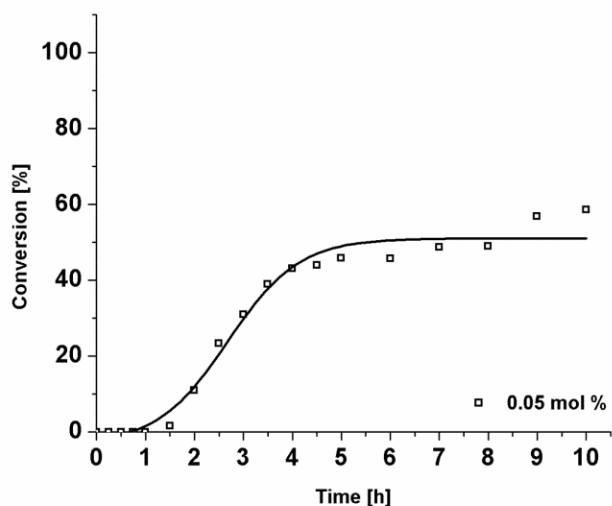


Figure 2.8: Conversion of *p*-bromobenzaldehyde with phenylboronic acid as a function of time in Suzuki-Miyaura coupling by catalyst **2** at 40 °C with 0.05 mol% catalyst loading ($k^2 = 0.8427$).

Examination of the temperature dependences for **1** and **2** at 24, 30, 35, and 40 °C were also made by means of kinetic experiments in toluene, CH₂Cl₂, and H₂O. The results are summarized in Figures 2.9-17 and the corresponding rate constants are presented in Table 2.7. This study provided some further interesting insights into the comparative identities and reactivities of the dominant active Pd species in each solvent system. Reactions performed at low temperature were most sensitive to the nature of the solvent. Specifically, both **1** and **2** affected the coupling of *p*-bromobenzaldehyde with phenylboronic acid in H₂O at 30 °C, with high coupling selectivity (Figures 2.9 & 2.12). In contrast, reactions in toluene and CH₂Cl₂ at the same temperature gave low yields for **1**, while **2** was found to be inactive. The reaction temperature was then increased in 5 °C steps to 40 °C, which resulted in increased activity for all three solvent systems, albeit with a modest reduction in coupling selectivity (Figures 2.10-11 & 2.13-14). The corresponding selectivities are presented in Figures 2.15-17.

Catalyst	Entry	24 °C	30 °C	35 °C	40 °C	45 °C
1	30a	-	0.2393	0.4091	1.8077	-
	30b	-	0.3492	1.3739	2.8619	-
	30c	0.0610	0.2144	0.2656	0.5206	-
2	31a	-	-	0.3678	1.3877	2.9481
	31b	-	0.0037	0.5999	1.7767	4.8967
	31c	0.1442	0.2183	0.2614	1.5986	-

Table 2.7: Rate constants of **1** and **2** for *p*-bromobenzaldehyde; Reaction conditions: *p*-bromobenzaldehyde (3.24 mmol), phenylboronic acid (3.89 mmol), K₂CO₃ (9.73 mmol), solvent (a-toluene, b-CH₂Cl₂, c-H₂O; 15.0 mL); all reactions were monitored by GC.

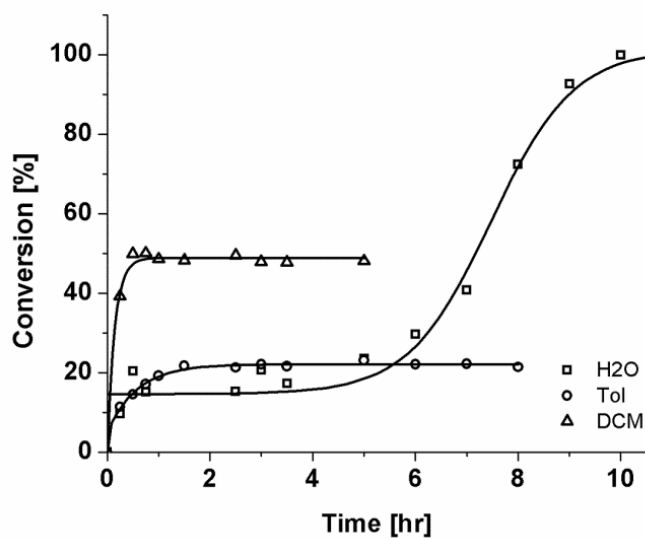


Figure 2.9: Reaction of *p*-bromobenzaldehyde with phenylboronic acid as a function of time in Suzuki-Miyaura coupling by 0.5 mol % of **1** at 30 °C.

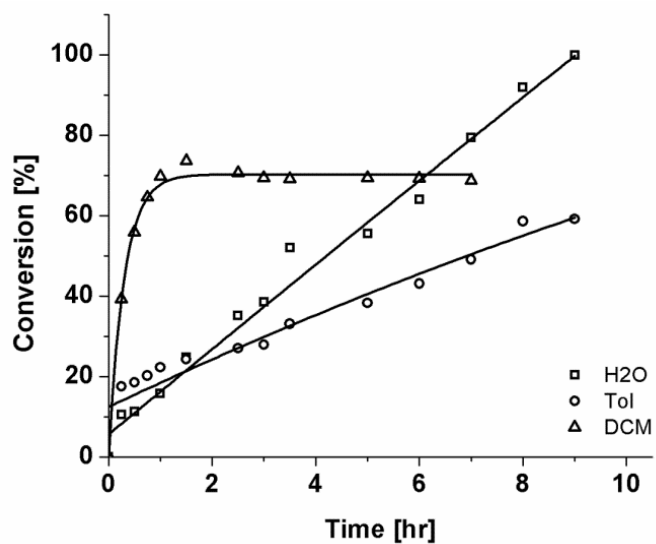


Figure 2.10: Reaction of *p*-bromobenzaldehyde with phenylboronic acid as a function of time in Suzuki-Miyaura coupling by 0.5 mol % of **1** at 35 °C.

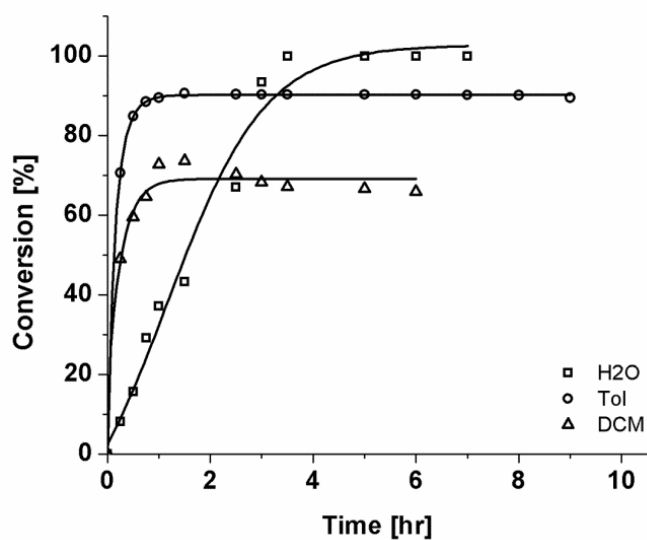


Figure 2.11: Reaction of *p*-bromobenzaldehyde with phenylboronic acid as a function of time in Suzuki-Miyaura coupling by 0.5 mol % of **1** at 40 °C.

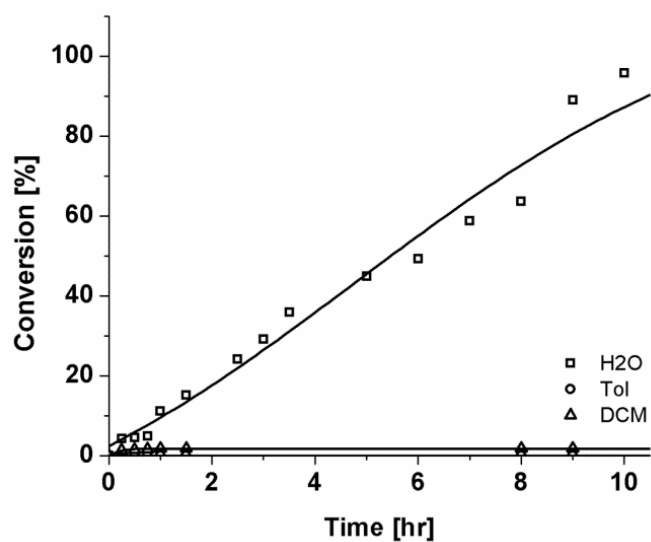


Figure 2.12: Reaction of *p*-bromobenzaldehyde with phenylboronic acid as a function of time in Suzuki-Miyaura coupling by 0.5 mol % of **2** at 30 °C.

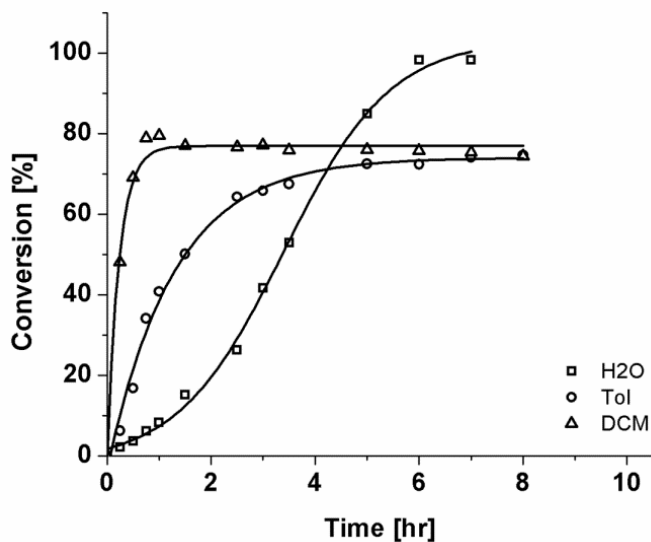


Figure 2.13: Reaction of *p*-bromobenzaldehyde with phenylboronic acid as a function of time in Suzuki-Miyaura coupling by 0.5 mol % of **2** at 35 °C.

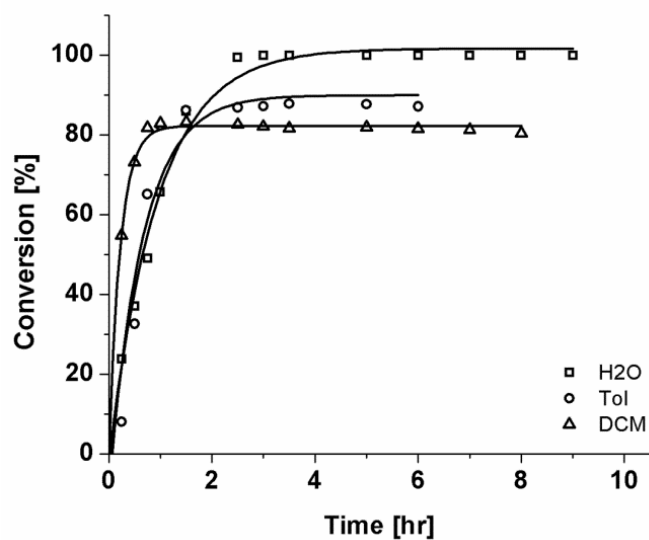


Figure 2.14: Reaction of *p*-bromobenzaldehyde with phenylboronic acid as a function of time in Suzuki-Miyaura coupling by 0.5 mol % of **2** at 40 °C.

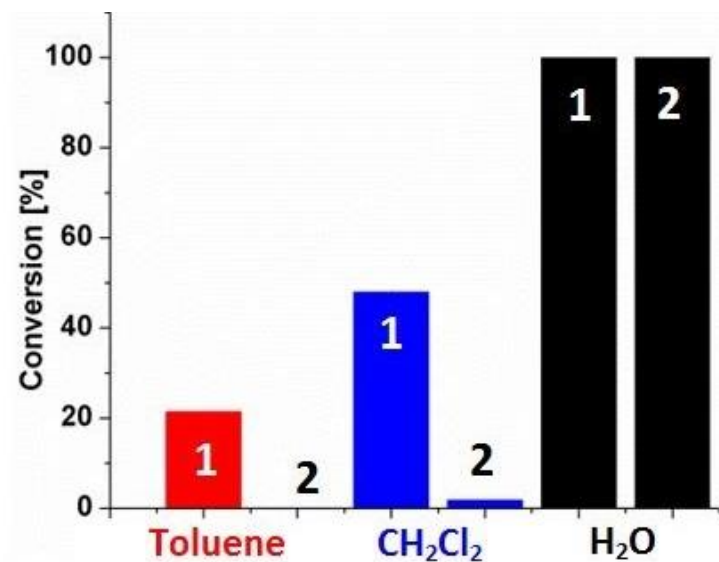


Figure 2.15: Reaction of *p*-bromobenzaldehyde with phenylboronic acid as a function of time in Suzuki-Miyaura coupling by 0.5 mol % of **1** and **2** at 30 °C. A comparison of total conversion and coupling selectivity (solid *versus* open bars).

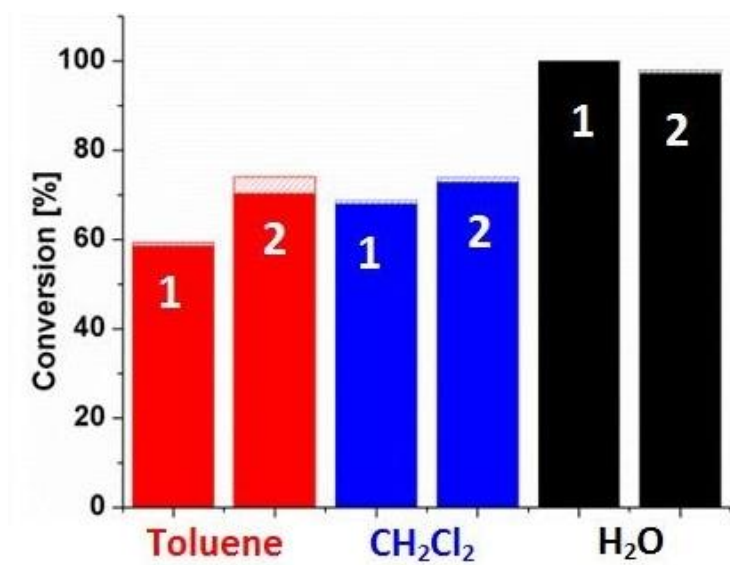


Figure 2.16: Reaction of *p*-bromobenzaldehyde with phenylboronic acid as a function of time in Suzuki coupling by 0.5 mol % of **1** and **2** at 35 °C. A comparison of total conversion and coupling selectivity (solid *versus* open bars).

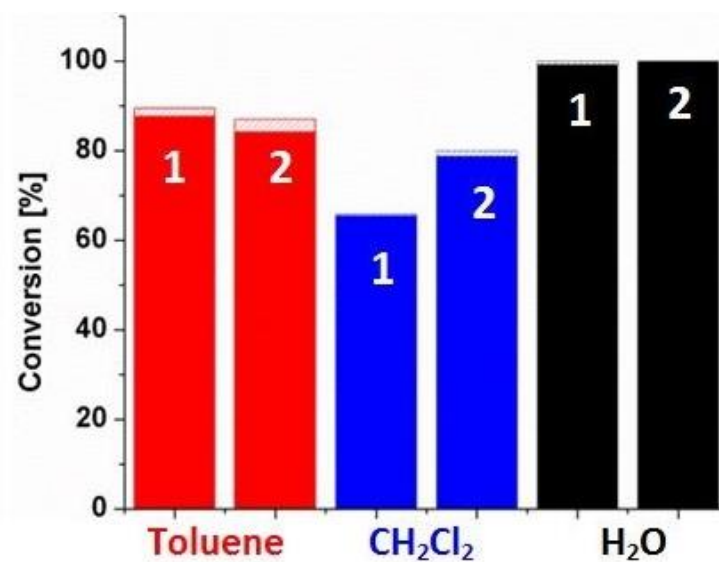


Figure 2.17: Reaction of *p*-bromobenzaldehyde with phenylboronic acid as a function of time in Suzuki coupling by 0.5 mol % of **1** and **2** at 40 °C. A comparison of total conversion and coupling selectivity (solid *versus* open bars).

The fact that no turnover was observed at 30 °C in the organic solvents, while appreciable reactivity was observed above 35 °C, suggested that a kinetic activation barrier had been overcome between 30 and 35 °C. This type of temperature-dependent behavior is commonplace for molecular species. Meanwhile, since appreciable turnover was observed in H₂O at temperatures as low as 24 °C (Figure 2.8), it is clear that a different, more easily activated catalytic species was responsible for the observed reactivity.

It is also noteworthy that distinct induction periods of *ca.* 1–5 h were observed for reactions involving **1** and **2** in H₂O at lower temperatures, resulting in s-shaped reactivity profiles (Figures 2.9-14; black data). This is presumably because at lower temperatures, the generation of the active heterogeneous Pd species occurred more slowly. Meanwhile, reactions performed at 35 or 40 °C with **1** and 40 °C with **2** did not show any appreciable induction period. These observations are also consistent with the supposition that molecular catalysis dominated in organic solvents while newly-generated heterogeneous catalysts were dominant in H₂O: single-site homogeneous species should be immediately highly active above a minimum temperature threshold, but could also become rapidly poisoned. In contrast, decomposition of the molecular species in H₂O to generate the active heterogeneous Pd species appeared to require a significant amount of time as reflected in the induction phase.

Activation energy data for the Suzuki coupling reaction was obtained in the three solvent systems using the ‘slope-ratio method’. Arrhenius plots created using the temperature-dependent activity data for **1** and **2** (Table 2.8 & Figures 2.18-19) show that the Suzuki reaction rates were faster in organic solution than in H₂O. However, the corresponding activation energies in organic solvents (159–171 kJ mol⁻¹) were

significantly larger than the comparable activation energies in H₂O (111–116 kJ mol⁻¹). This substantial difference in energy could be attributed to the different physical nature of the active catalysts, in which the homogenous molecular catalysts **1** and **2** experienced a larger energy barrier for the oxidative addition of the aryl halide precursors.

Catalyst	Entry	Activation Energy [kJ mol ⁻¹]
1	32a	159.2
	32b	166.3
	32c	111.3
2	33a	169.8
	33b	171.2
	33c	115.9

Table 2.8: Activation energies for **1** and **2** for *p*-bromobenzaldehyde; Calculated from the slope of the Arrhenius plots in Figures 2.18-19.

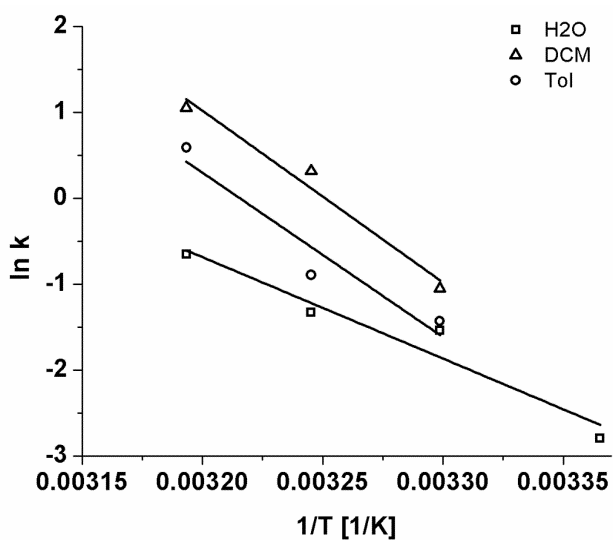


Figure 2.18: Arrhenius plot for the activation of *p*-bromobenzaldehyde by **1** in toluene, CH₂Cl₂, and H₂O.

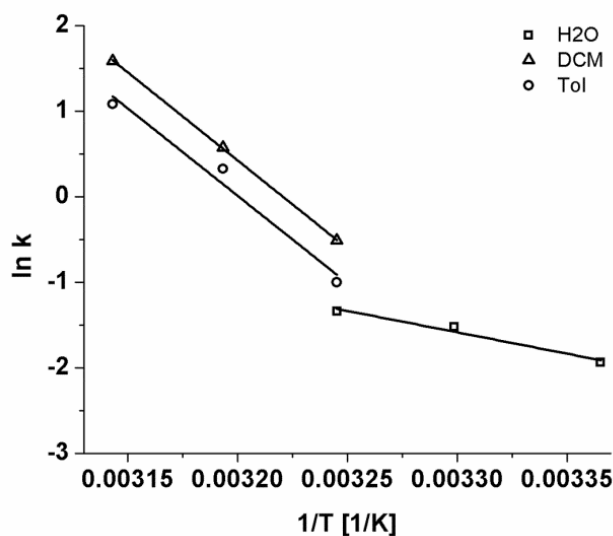


Figure 2.19: Arrhenius plot for the activation of *p*-bromobenzaldehyde by **2** in toluene, CH₂Cl₂, and H₂O.

Comparative activation energies for the Suzuki coupling of *p*-chlorobenzaldehyde in toluene, CH₂Cl₂, and H₂O solutions could not be obtained because the reactivities were minimal at lower temperatures. The C–Cl bond was most effectively activated by the supposed heterogeneous Pd(0) species in H₂O. Kinetic trials were performed in aqueous solution using *p*-chlorobenzaldehyde, in which both the catalyst mol% and the temperature were varied (Figures 2.20-21). While the reactions of both **1** and **2** resulted in complete conversion of the chlorinated precursors in H₂O, **2** was the most proficient. Accordingly, the rate constants for **2** increased drastically as the catalyst loadings increased (Table 2.9).

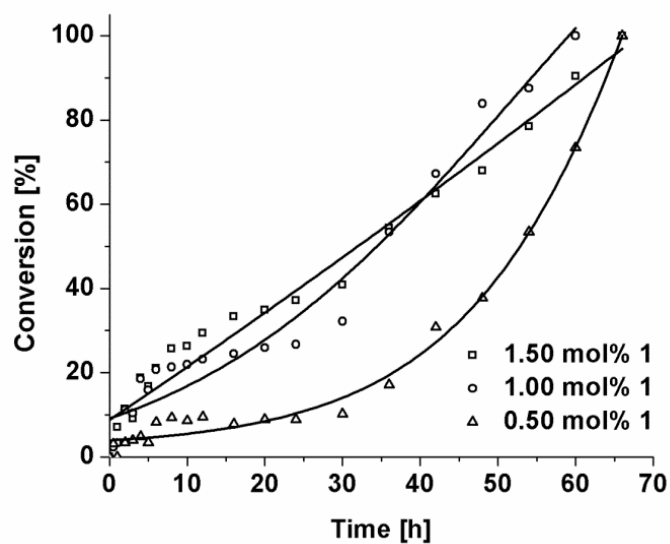


Figure 2.20: Conversion of *p*-chlorobenzaldehyde with phenylboronic acid as a function of time in Suzuki-Miyaura coupling by catalysts **1** at 40 °C in H₂O.

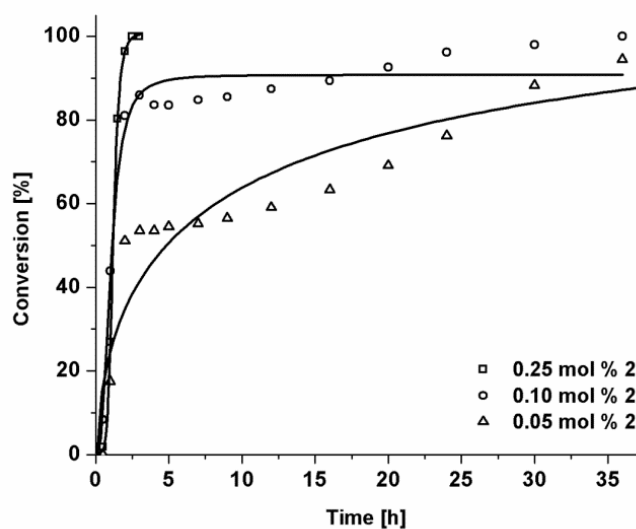


Figure 2.21: Conversion of *p*-chlorobenzaldehyde with phenylboronic acid as a function of time in Suzuki-Miyaura coupling by catalysts **2** at 40 °C in H₂O.

Catalysts	Entry	0.05 ^a	0.10 ^a	0.25 ^a	0.50 ^a	1.0 ^a	1.5 ^a
1	34	-	-	-	0.0141	0.0193	0.0206
2	35	0.0598	0.0919	2.2459	0.0270	0.0547	-

Table 2.9: Rate constants of **1** and **2** of *p*-chlorobenzaldehyde in H₂O; Reaction conditions: *p*-chlorobenzaldehyde (4.28 mmol), phenylboronic acid (5.14 mmol), K₂CO₃ (12.86 mmol), H₂O (15.0 mL); all reactions were monitored by GC. ^amol %.

In contrast to *p*-bromobenzaldehyde, **1** and **2** were found to be initially selective for the *homo*-coupled product. As the reaction proceeded, both catalysts became more selective for production of the desired *hetero*-coupled product. After approximately 30 h, the reaction selectivity had reached a steady-state, favoring approximately 80% of the *hetero*-coupled product. The origin of this selectivity evolution over such a significant period of time is most likely due to the evolving nature of the active catalyst species, as molecular **1** or **2** are converted to eventually more stable heterogeneous catalysts. It is somewhat more difficult to determine the identity of transient intermediate Pd catalysts (such as small Pd clusters) that may exist in solution prior to steady-state selectivity being reached. A so-called ‘cocktail-type’ mixture of active Pd-based species could dominate during the first 25–30 h of reaction (Figure 2.24).^{188,191} All other selectivity curves are represented in Figures 2.22–28.

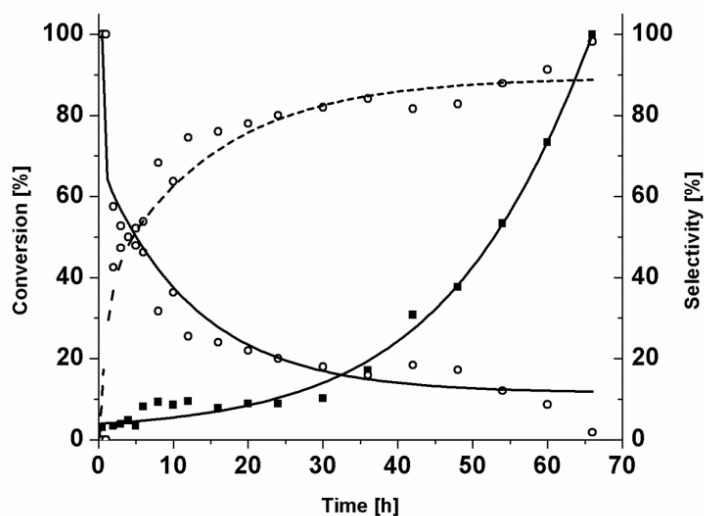


Figure 2.22: Conversion (solid squares) and selectivity (open circles) of *p*-chlorobenzaldehyde with phenylboronic acid as a function of time in Suzuki-Miyaura coupling at 40 °C with 0.5 mol % of **1** in H₂O. Dashed and solid lines through open circles denote selectivities of the *hetero*- and *homo*-coupled products, respectively.

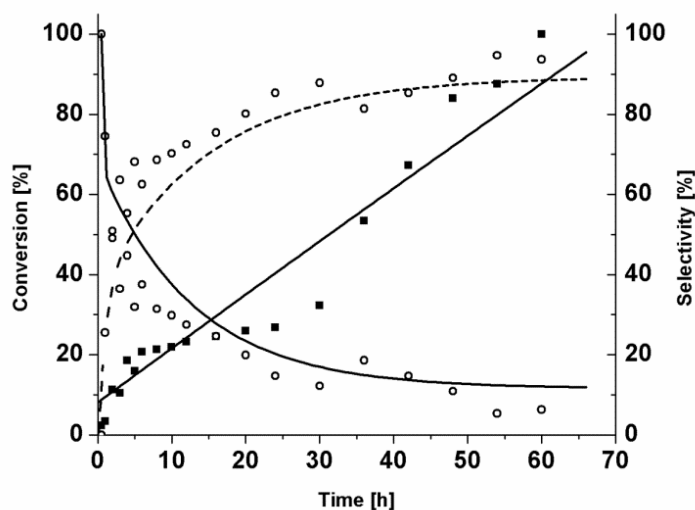


Figure 2.23: Conversion (solid squares) and selectivity (open circles) of *p*-chlorobenzaldehyde with phenylboronic acid as a function of time in Suzuki-Miyaura coupling at 40 °C with 1.0 mol % of **1** in H₂O. Dashed and solid lines through open circles denote selectivities of the *hetero*- and *homo*-coupled products, respectively.

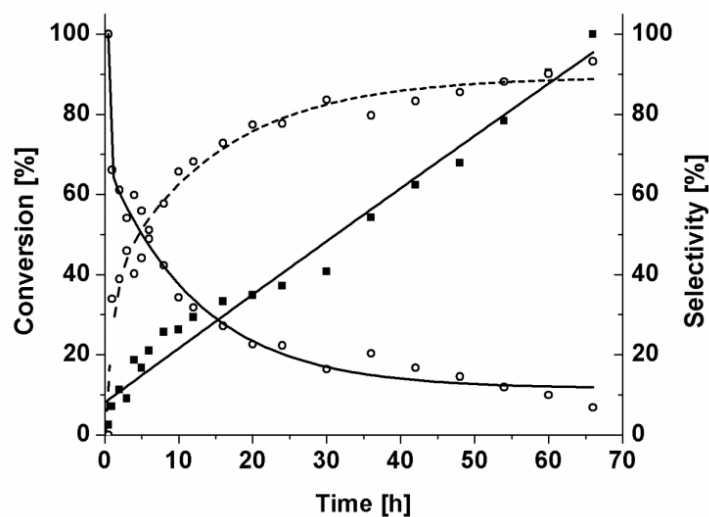


Figure 2.24: Conversion (solid squares) and selectivity (open circles) of *p*-chlorobenzaldehyde with phenylboronic acid as a function of time in Suzuki-Miyaura coupling at 40 °C with 1.5 mol % of **1** in H₂O. Dashed and solid lines through open circles denote selectivities of the *hetero*- and *homo*-coupled products, respectively.

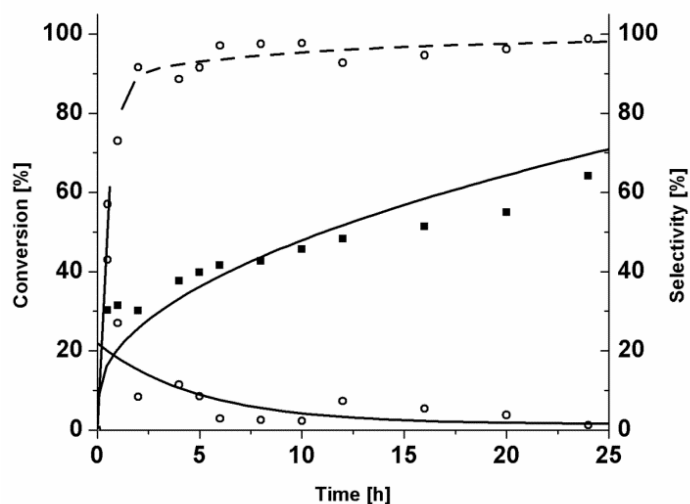


Figure 2.25: Conversion (solid squares) and selectivity (open circles) of *p*-chlorobenzaldehyde with phenylboronic acid as a function of time in Suzuki-Miyaura coupling at 40 °C with 0.5 mol % of **2** in H₂O. Dashed and solid lines through open circles denote selectivities of the *hetero*- and *homo*-coupled products, respectively.

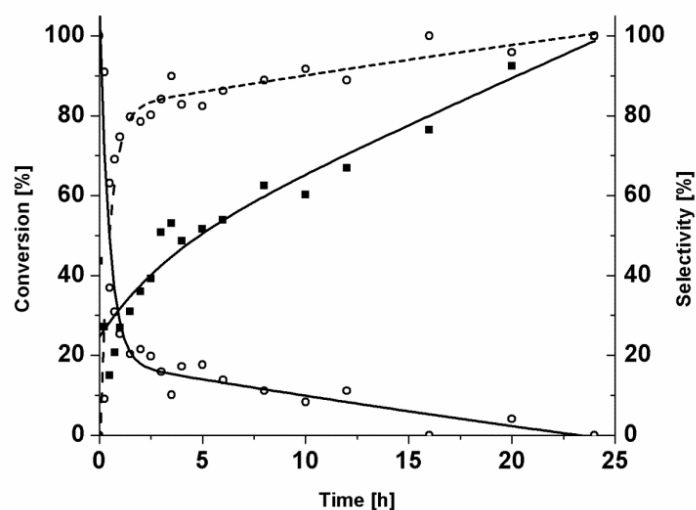


Figure 2.26: Conversion (solid squares) and selectivity (open circles) of *p*-chlorobenzaldehyde with phenylboronic acid as a function of time in Suzuki-Miyaura coupling at 40 °C with 1.0 mol % of **2** in H₂O. Dashed and solid lines through open circles denote selectivities of the *hetero*- and *homo*-coupled products, respectively.

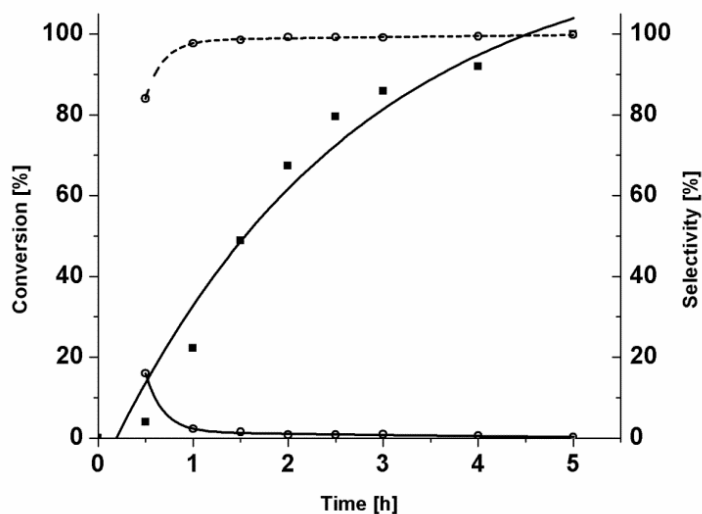


Figure 2.27: Conversion (solid squares) and selectivity (open circles) of *p*-chlorobenzaldehyde with phenylboronic acid as a function of time in Suzuki-Miyaura coupling at 35 °C with 0.25 mol % of **2** in H₂O. Dashed and solid lines through open circles denote selectivities of the *hetero*- and *homo*-coupled products, respectively.

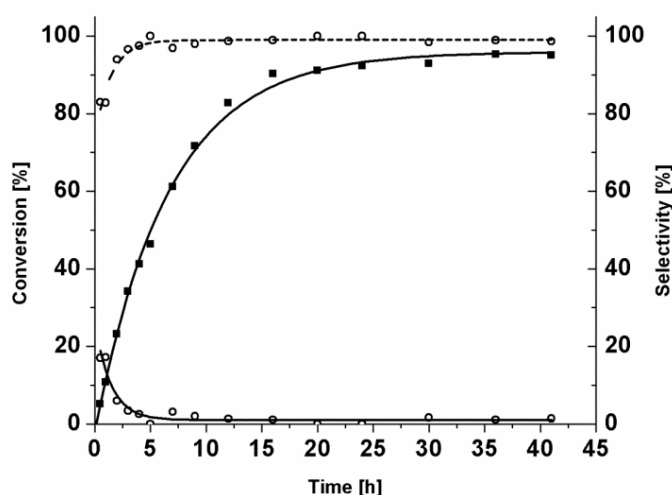


Figure 2.28: Conversion (solid squares) and selectivity (open circles) of *p*-chlorobenzaldehyde with phenylboronic acid as a function of time in Suzuki-Miyaura coupling at 30 °C with 0.25 mol % of **2** in H₂O. Dashed and solid lines through open circles denote selectivities of the *hetero*- and *homo*-coupled products, respectively.

Based on the rate constant obtained from 0.25 mol% of catalyst **2**, it was decided to double and then quadruple the catalyst loading to 0.5 and 1.0 mol% of **1** and **2**, respectively (Figures 2.29-30). As expected, the rate of **2** was significantly faster and more selective in the activation of aryl chlorides, which was consistent with the data gathered for the corresponding aryl bromides. Although these observations followed classical kinetic control, it was somewhat surprising that higher catalyst loadings resulted in lower rate constants (Table 2.9). In an attempt to understand this trend, the reaction mechanism was further investigated by varying the number of stoichiometric equivalents of phenylboronic acid and potassium carbonate, (Figure 2.31). These data suggested that the phenylboronic acid and the potassium carbonate did not affect the rate determining step of this mechanism. The temperature dependence of this system was also examined at

24, 30, 35, and 40 °C using 0.25 mol % of catalyst **2** (Figure 2.32 & Table 2.10). The *hetero*-coupled aryl product was only produced in complete conversion at 35 and 40 °C and the corresponding rate constants were found to increase with increasing temperature (Table 10).

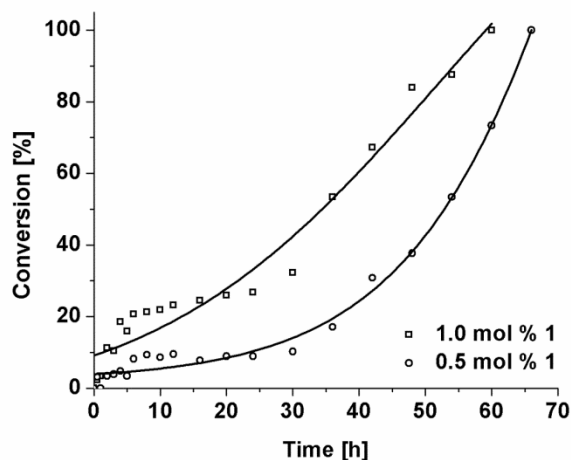


Figure 2.29: Reaction of *p*-chlorobenzaldehyde with phenylboronic acid as a function of time for Suzuki-Miyaura coupling at 40 °C with 0.5 and 1.0 mol % of **1** in H₂O.

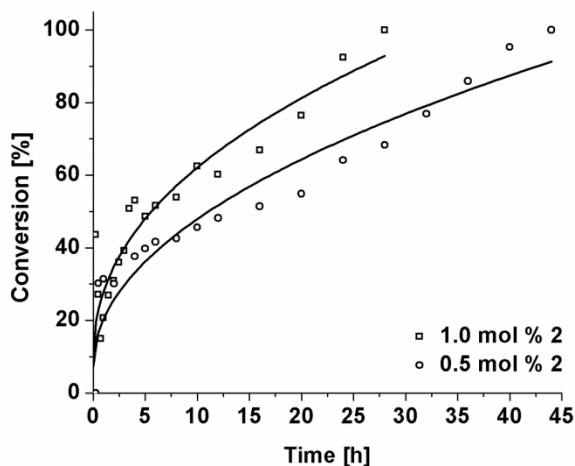


Figure 2.30: Reaction of *p*-chlorobenzaldehyde with phenylboronic acid as a function of time for Suzuki-Miyaura coupling at 40 °C with 0.5 and 1.0 mol % of **2** in H₂O.

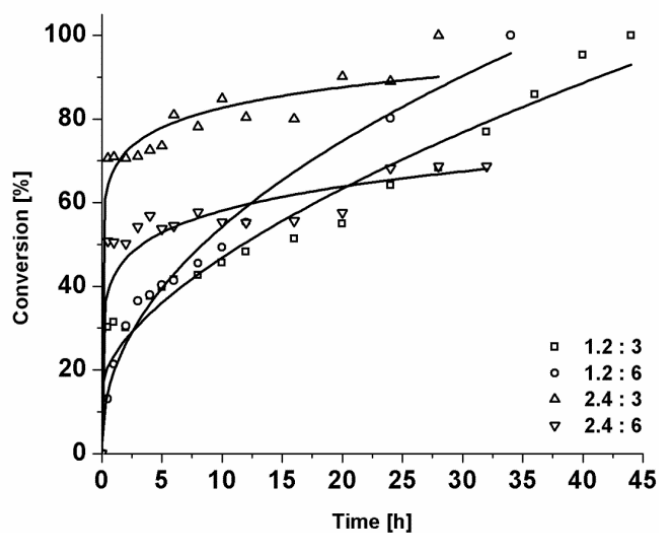


Figure 2.31: Conversion of *p*-chlorobenzaldehyde as a function of time in Suzuki-Miyaura coupling at 40 °C in H₂O with 0.5 mol % of **2** under varying conditions of phenylboronic acid and K₂CO₃ (legend denotes stoichiometric equivalents of phenylboronic acid : K₂CO₃).

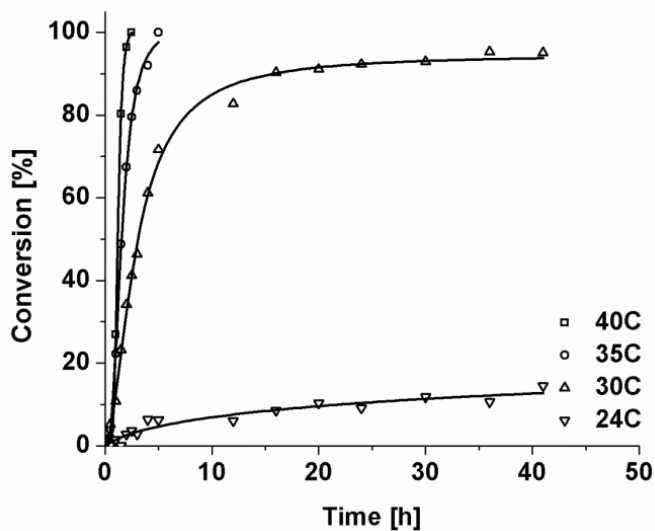


Figure 2.32: Suzuki-Miyaura coupling of *p*-chlorobenzaldehyde with phenylboronic acid as a function of time using 0.25 mol % of **2** at 24, 30, 35, and 40 °C in H₂O.

Catalyst 2	Entry 36	24 °C 0.0031	30 °C 0.1476	35 °C 1.0439	40 °C 2.2459
----------------------	-------------	-----------------	-----------------	-----------------	-----------------

Table 2.10: Rate constants for **2** using *p*-chlorobenzaldehyde in H₂O; Reaction conditions: *p*-chlorobenzaldehyde (4.28 mmol), phenylboronic acid (5.14), K₂CO₃ (12.86 mmol), H₂O (15.0 mL), 40 °C; all reactions were monitored by GC.

The activation energy for *p*-chlorobenzaldehyde in H₂O was determined on the basis of the slope of the Arrhenius plot (Figure 2.33). The activation energy was determined to be 322 kJ mol⁻¹, which is in accord with the current literature values for similar systems.

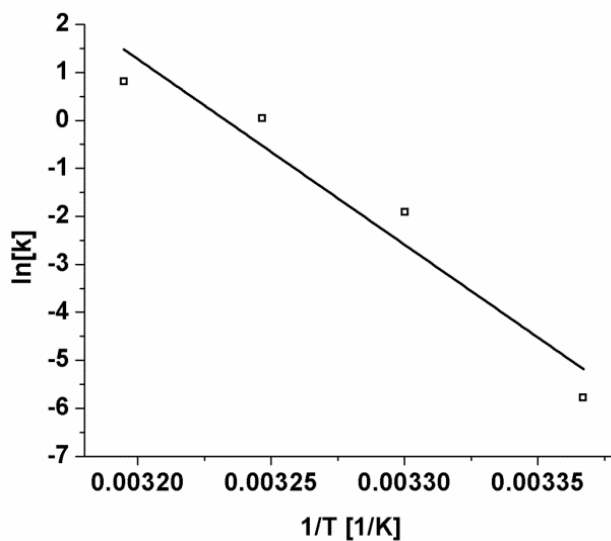


Figure 2.33: Arrhenius plot for the activation of *p*-chlorobenzaldehyde by **2** in H₂O.

2.4 CONCLUSIONS

In conclusion, two new palladium(II) carbene complexes were synthesized and studied for their catalytic activities in the Suzuki reaction. Their comparative behavior in toluene, CH₂Cl₂ and H₂O were assessed. Both **1** and **2** were able to activate C–I, C–Br, and C–Cl bonds in polar and nonpolar aprotic solvents, as well as in H₂O. The catalysts efficiently converted all aryl iodides and aryl bromides to the desired *hetero*-coupled product, whereas the analogous conversion from aryl chlorides was completed at a deterred rate. This is a direct result of the oxidative addition process of the C–X bond onto the palladium catalyst. These S_N2 reactions proceed more quickly for highly polarizable bonds, resulting in the slower oxidative addition of the aryl chlorides than analogous aryl bromides and iodides. Interestingly, it was shown that catalyst decomposition was prevalent in toluene and H₂O, yielding new, presumably heterogeneous, yet equally active catalyst species. In CH₂Cl₂, the molecular catalysts were largely stable and recyclable, presumably due to the attraction of the polar solvent to the positively charged palladium metal center. In toluene solution, both forms of the catalyst were found to co-exist. Kinetic studies revealed that the average activation energy for dissociation of the C–Br bond in organic solvents was 166 kJ mol^{–1} compared to only 113 kJ mol^{–1} for H₂O. The latter result infers that the heterogeneous species generated from the original Pd(II) carbene complexes were more reactive for the Suzuki coupling reaction, and that catalyst decomposition was not actually detrimental in the Suzuki-Miyaura cross-coupling reaction. The results of this study exemplify how well-defined molecular and less well-defined heterogeneous Pd species can provide misleadingly similar results in solution-phase catalysis.

2.5 SUMMARY OF KEY RESULTS

- **2** was significantly more active than **1**
- H₂O facilitated the highest catalytic activity, although the catalysts were proven to decompose when employed in this solvent system
- Both catalysts were more selective in CH₂Cl₂ than toluene
- Both catalysts activated the C–Cl bond in aryl chloride substrates

2.6 ACKNOWLEDGEMENTS

The authors thank Ms. Stephany Garcia for supplying the Pd-PVP catalysts and Dr. Vincent M. Lynch for assisting in X-ray crystallography, and the Robert A. Welch Foundation (F-1738, F-003) for funding.

2.7 EXPERIMENTAL

2.7.1 General Procedures

All glassware was oven-dried before use. All reagents were obtained commercially and used without further purification. Toluene and THF were dried over sodium and freshly distilled prior to use. The dichloromethane was dried over calcium hydride and freshly distilled prior to use. The starting materials IMes(BIAN) imidazolium chloride and IPr(BIAN)[AgCl] were synthesized according to published procedures.

2.7.2 Physical Measurements

Low-resolution CI mass spectra were obtained on a Thermo Scientific TSQ Quantum GC mass spectrometer and high-resolution CI mass spectra were recorded on a magnetic sector Waters Autospec Ultima instrument. ¹H and ¹³C{¹H} NMR spectra were recorded at 295 K in the indicated solvent on a Varian Unity 300 (¹H, 300 MHz; ¹³C, 75 MHz) or a Varian AS400 spectrometer (¹H, 400 MHz; ¹³C, 100 MHz) immediately

following sample preparation. Deuterated solvents were obtained from Cambridge Isotopes and stored over 4 Å molecular sieves prior to use. ^1H and $^{13}\text{C}\{^1\text{H}\}$ chemical shift values are reported in parts per million (ppm) relative to SiMe_4 (δ 0.00), using solvent resonances as internal standards. Absorption spectra were recorded on a Varian Cary 6000i UV-VIS-NIR spectrophotometer with Starna Quartz fluorometer cells with a pathlength of 10 mm. Gas chromatography (GC) was performed on an Agilent 6850 gas chromatograph (HP-1 column, $l = 30$ m, I.D. = 0.32 mm) equipped with a flame ionization detector (FID). The GC oven temperature was held at 50 °C for 3 min, then increased to 300 °C at 30 °C min^{-1} . The internal standard mesitylene was used to aid in measuring reaction conversions.

2.7.3 Preparations

2.7.3.1 *IMes(BIAN)[AgCl]*

A 1:1 dichloromethane-THF solution (20 mL) was added to an aluminum foil covered 50 mL round bottom flask. *IMes(BIAN)* imidazolium chloride (0.2 g, 0.466 mmol) and Ag_2O (0.4 g, 1.724 mmol) were added to it. The reaction mixture was stirred at ambient temperature for 48 h under argon, following which it was filtered and the solvent stripped from the filtrate under reduced pressure to afford *IMes(BIAN)[AgCl]* as an analytically pure red/orange solid (0.233 g, 88%). MS (Cl^+ , CH_4): m/z $[\text{M} - \text{Cl}]^+$; ^1H NMR (CDCl_3): δ 2.33 (s, 12H, CH_3), 2.57 (s, 6H, CH_3), 7.22 (d, 2H, Naph-H), 7.41 (s, 4H, Ar-H), 7.58 (t, 2H, Naph-H), 7.93 (d, 2H, Naph-H); ^{13}C NMR (CDCl_3): δ 17.85, 21.21, 120.98, 125.17, 127.74, 128.33, 129.86, 130.58, 133.80, 134.47, 138.40, 139.89.

2.7.3.2 (IMes)PdCl₂PPh₃ (1)

Toluene (5 mL) was added to an aluminum covered 50 mL round bottom flask that contained IMes(BIAN)[AgCl] (0.050 g, 0.0875 mmol) and PdCl₂(PPh₃)₂ (0.056 g, 0.0796 mmol). The reaction mixture was refluxed for 16 h. It was then cooled to ambient temperature and filtered over celite. The precipitate was extracted from the celite with dichloromethane, followed by removal of the solvent. Recrystallization with ethanol afforded an analytically pure yellow solid (0.044 g, 58%). MS (Cl⁺, CH₄): *m/z* 831 [M - Cl]⁺; ¹H NMR (CDCl₃): δ 2.39 (s, 12H, CH₃), 2.49 (s, 6H, CH₃), 7.00 (d, 2H, Naph-H), 7.12 (s, 4H, Ar-H), 7.21 (d, 2H, Naph-H), 7.29-7.39 (m, 11H, Naph-H, PPh₃-H), 7.69 (d, 2H, Naph-H); ¹³C NMR (CDCl₃): δ 138.67, 138.30, 137.78, 136.22, 135.98, 135.00, 134.87, 134.30, 134.16, 130.73, 130.14, 129.79, 129.64, 129.46, 129.25, 129.10, 128.02, 127.77, 127.67, 126.09, 125.89, 120.62, 120.29, 21.39, 19.18; ³¹P NMR (CDCl₃): δ 20.99.

2.7.3.3 (IPr)PdCl₂PPh₃ (2)

Toluene (5 mL) was added to an aluminum covered 50 mL round bottom flask that contained IPr(BIAN)[AgCl] (0.0514 g, 0.0785 mmol) and PdCl₂(PPh₃)₂ (0.050 g, 0.0713 mmol). The reaction mixture was refluxed for 16 h. It was then cooled to ambient temperature and filtered over celite. The precipitate was extracted from the celite with dichloromethane, followed by removal of the solvent. Recrystallization with ethanol afforded an analytically pure yellow solid (0.046 g, 62%). MS (Cl⁺, CH₄): *m/z* 915 [M - Cl]⁺; ¹H NMR (CDCl₃): δ 0.90 (d, 12H, CH₃), 1.26 (d, 12H, CH₃), 3.40 (sept, 4H, -CH(CH₃)₂), 6.86 (d, 2H, Naph-H), 7.17 (d, 6H, PPh₃-H), 7.28-7.37 (m, 11H, Naph-H, PPh₃-H), 7.48 (d, 4H, *i*Pr-Ar-H), 7.65 (d/t, 4H, Naph-H, *i*Pr-Ar-H); ¹³C NMR (CDCl₃): δ

146.94, 139.76, 134.59, 133.4, 130.35, 129.76, 129.21, 127.34, 127.16, 126.75, 125.88, 123.97, 121.57, 28.39, 35.40, 23.51; ^{31}P NMR (CDCl_3): δ 21.41.

2.7.4 General Procedure for Suzuki Cross-Coupling Reactions

Deionized water (3 mL) was added to a 20 mL scintillation vial containing aryl halide (0.267 mmol), phenylboronic acid (0.321 mmol), potassium carbonate (0.802 mmol), and the internal standard mesitylene (0.267 mmol). The scintillation vial was covered with a septum and wired down. The reaction mixture was heated to 40 °C while stirring. The catalyst concentration was determined by UV-Vis and rapidly injected into the reaction mixture (0.1-2.0 mol% of **1** or **2**). The reaction was allowed to stir for twenty hours for all aryl iodides and bromides. The aryl chlorides required 48 hours to reach complete conversion. The reaction mixture was cooled to ambient temperature, filtered over celite, and washed with ether. The solvents were evaporated from the organic layer to produce the desired product. The reactions were monitored by GC and percent conversions were calculated based on the aryl halide. The product was determined by NMR to match literature results.

Chapter 3: Direct comparison of *bis*(imino)acenaphthene (BIAN)-supported palladium(II) *mono*- and *bis*(carbene) complexes as catalysts for Suzuki-Miyaura cross-coupling reactions

3.1 ABSTRACT

Two new 1,2-acenaphthenyl *N*-heterocyclic *bis*carbene-supported palladium(II) complexes containing mesityl or 2,6-diisopropyl *N*-aryl substituents have been synthesized, characterized, and analysed for their catalytic behaviour for Suzuki coupling reactions in toluene, dichloromethane, and water. Each catalyst exhibited the highest activity when employed in aqueous media, followed in decreasing order by dichloromethane and toluene. The catalysts retained their molecular character in dichloromethane; however partial and full decomposition was observed in toluene and water, respectively.

3.2 INTRODUCTION

As already described in chapter 2, the Suzuki-Miyaura cross-coupling reaction typically employs Group X metals to form carbon–carbon bonds between aryl halides and organoboranes (Scheme 1.3).⁴ It is one of the most widely used industrial processes for the selective construction of natural products, pharmaceuticals and agrochemicals.^{193–195} Normally, the optimal reaction conditions involve a palladium-centred homogeneous catalyst along with a range of spectator ligands, such as 3-chloropyridine or triethylamine.^{104,197,198} Recently, Zhou *et al.* used 1-methylimidazole to assist in the activation of aryl chlorides in aqueous media.¹⁹⁹ However, the majority of these catalysts cannot be recycled. As a consequence, recent research in this area has been focused on the generation of greener catalysts that are capable of easy separation and recovery.^{203,204,206,207,209,210} More importantly, however, such catalysts can be

reintroduced into the catalytic cycle without a significant loss of catalytic activity.^{202,205,208} Furthermore, these new catalysts possess two industrially important properties; namely they activate inexpensive aryl chlorides and perform well in environmentally benign conditions.

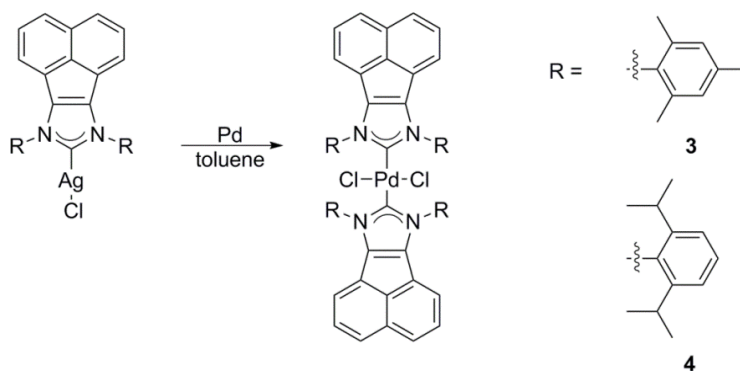
The σ -donor characteristics of the NHC ligand promote the oxidative addition of aryl halides as well as assisting in the reductive elimination of the coupled products.^{85,201} Although the homogeneous palladium catalysts are highly selective and tolerant to a wide variety of functionalities, they typically require harsh organic solvents. Accordingly, the recent focus on green chemistry has stimulated intense research activity in terms of seeking an alternative solvent that is non-toxic, cost effective and abundant.^{205,208} Water is an ideal solvent in this context. The most prominent example of this approach was reported by Karimi *et al.* with their development of a water-soluble NHC–Pd polymer that efficiently activated aryl chlorides at room temperature.²⁰⁶ However, the use of aqueous media can introduce some ambiguity with regard to the identification of the active catalyst in solution.²¹³ This predicament has often been remedied by either a hot filtration test, or *via* the injection of Hg(0) into the reaction mixture, thereby poisoning any leached Pd(0) species.^{10,14,182,184,212}

Recently, we reported the syntheses of two new palladium(II) carbene complexes [PdLCl₂(PPh₃)], along with complete studies of the catalytic activities of each catalyst in nonpolar, polar and aqueous media for the Suzuki coupling reaction. It was discovered that both catalysts decomposed to active heterogeneous species when the reactions are carried out in toluene or aqueous solution. On the other hand, they retained their molecular character when employed in dichloromethane.²²⁶ In the present work, two new *bis*(imino)acenaphthene (BIAN) supported NHC palladium complexes, [L₂PdCl₂], have

been synthesized with a view to creating more strongly-bonded Pd(II) complexes. In turn, this would permit the determination of their homogenous or heterogeneous behaviour in nonpolar, polar, and aqueous media with respect to the Suzuki coupling reaction.

3.3 RESULTS AND DISCUSSION

The preparation of the new Pd catalysts was achieved by adaptation of the previously reported methods for the syntheses of (IMes)BIAN[AgCl] and (IPr)BIAN[AgCl].²²⁶ In turn, these silver complexes were treated with Pd(OAc)₂ or PdCl₂(ACN)₂ in toluene solution, thereby producing IMes(BIAN)₂PdCl₂ (**3**) and IPr(BIAN)₂PdCl₂ (**4**), respectively. The preparative details for these complexes are summarized in Scheme 3.1 and the identities of **3** and **4** were confirmed by means of standard analytical techniques. Figures 3.1 and 3.2 illustrate the single crystal structures that were obtained for **3** and **4**, respectively, and the pertinent bond distances and angles are listed in Table 3.1. These crystal structures revealed an approximate square planar geometry around each Pd(II) centre. It was found that **3** possessed a mean plane angle of 46.3°, while that of **4** was only 0.2°. However, every asymmetric unit of **3** contained a tetrahydrofuran solvent molecule, encouraging the free rotation of the Pd–NHC bond.



Scheme 3.1: Syntheses of BIAN palladium catalysts **3** and **4**.

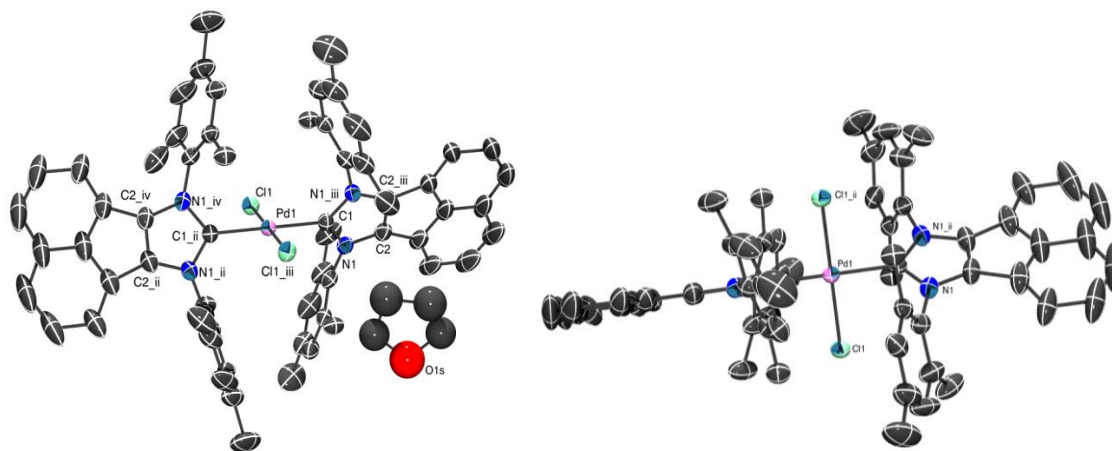


Figure 3.1: Crystal structure of **3** showing the mean plane angle of 46.3° through two different orientations.

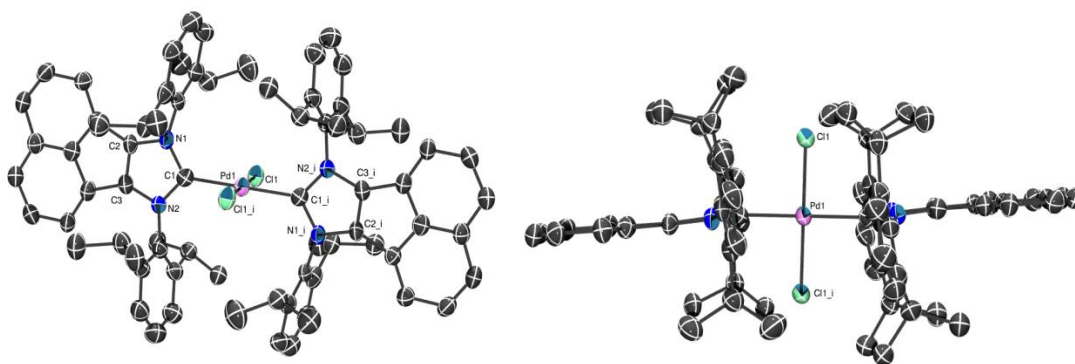


Figure 3.2: Crystal structure of **4** showing the mean plane angle of 0.2° through two different orientations.

Bond	Length (Å)	
	3	4
Pd1–C1	2.022(5)	2.043(6)
Pd1–Ci	2.022(5)	2.043(6)
Pd1–Cl1	2.3131(14)	2.314(2)
Pd1–Cli	2.3131(14)	2.314(2)
C2–C3	1.356(8)	1.360(8)

Bond	Angles (°)	
	3	4
C1–Pd1–C1i	180.0	180.0(3)
Cl1–Pd1–Cl1i	180.0	180.00(7)
C1–Pd1–Cl1	90.000(5)	89.31(17)
C1–Pd1–Cl1	90.000(5)	90.69(17)
N1–C1–N2	106.0(4)	104.5(5)

Table 3.1: Selected bond distances and angles for **3** and **4**.

The catalytic activities of **3** and **4** with respect to Suzuki-Miyaura cross-coupling reactions were investigated initially with aryl iodides (0.216 mmol), phenylboronic acid (0.259 mmol) and K₂CO₃ (0.647 mmol) in toluene, CH₂Cl₂, or H₂O solution (3.0 mL). In order to examine adequately the solvent effects on these catalysts, these three solvents were chosen as appropriate examples of nonpolar aprotic, polar aprotic, and green solvents, respectively. Each reaction mixture was stirred and heated to 40 °C until all the solids had dissolved. In each case, the catalyst loadings were determined on the basis of UV-vis spectroscopic measurements (Figures 3.3-3.4). Compound **3** or **4** was injected rapidly into the reaction mixture at $t = 0$, which was subsequently stirred at 40 °C for 20 h. A summary of the outcomes of these reactions is presented in Table 3.2.

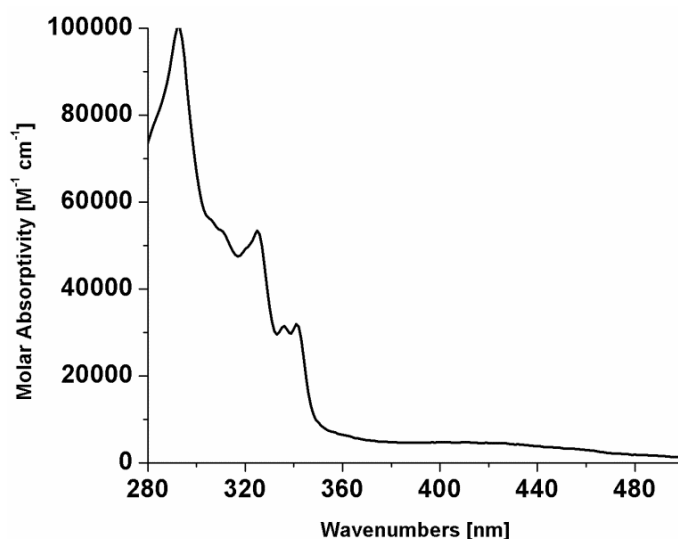


Figure 3.3: The absorption spectrum of **3** in dichloromethane with $\lambda_{\text{max}} = 293$ nm. Beer's law was used to determine the molar absorptivity from a calibration curve created with ten data points in 10 μL increments ranging 10-100 μL ($\epsilon = 102,736 \text{ M}^{-1} \text{ cm}^{-1}$, $R^2 = 0.998$).

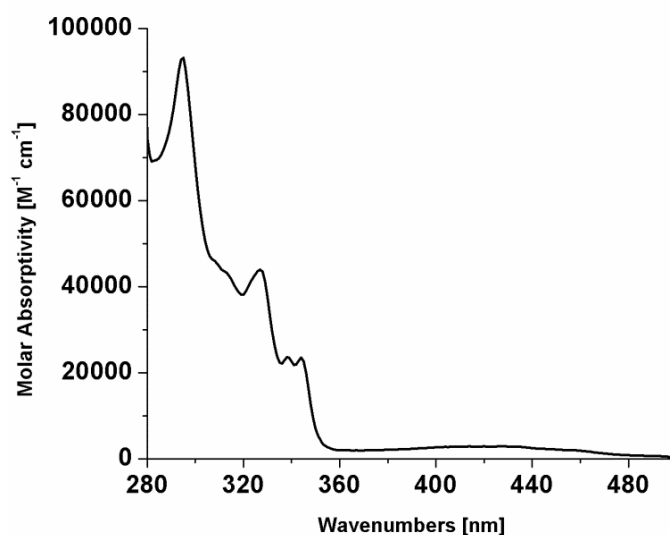
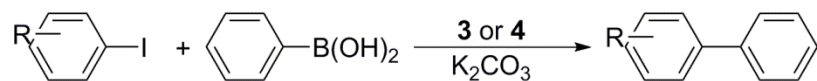


Figure 3.4: The absorption spectrum of **4** in dichloromethane with $\lambda_{\text{max}} = 295$ nm. Beer's law was used to determine the molar absorptivity from a calibration curve created with ten data points in 10 μL increments ranging 10-100 μL ($\epsilon = 100,498 \text{ M}^{-1} \text{ cm}^{-1}$, $R^2 = 0.9415$).



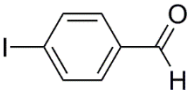
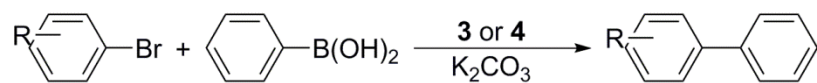
Substrate	Catalyst	Entry	Conversion [%]	S ^{hetero} [%]
	3	1a	1.0	0
		1b	1.3	42.6
		1c	3.3	0
	4	2a	16.5	99.0
		2b	0.2	51.7
		2c	88.6	91.7

Table 3.2: Suzuki-Miyaura biaryl coupling of aryl iodides by **3** and **4**; Reaction conditions: aryl iodide (0.216 mmol), phenylboronic acid (0.259 mmol), K₂CO₃ (0.647 mmol), **3** or **4** (1.0 mol % Pd), solvent (a-toluene, b-CH₂Cl₂, c-H₂O; 3.0 mL), 40 °C, 20 h; all reactions were monitored by GC.

p-Iodobenzaldehyde was converted successfully to the corresponding *p*-biphenylaldehyde by **4** in toluene and aqueous solutions with greater than 91% selectivity on the basis of GC analysis (Table 3.2; entries 2a,c). However, **3** was unable to activate the C–I bond in these solvents (Table 3.2; entries 1a-c).

In order to gain more insight into the catalytic properties of **3** and **4** in organic and aqueous media, a variety of aryl bromides were explored using otherwise identical reaction conditions (Table 3.3). Each analysis began with bromobenzaldehyde, in which the importance of the type of solvent became apparent. Both catalysts activated the C–Br bond and showed the greatest selectivity for the *hetero*-coupled product in aqueous solvent mixtures (Table 3.3; entries 3-8c). Each catalyst demonstrated higher reactivity toward *para*-aryl halides, followed in recession by *ortho*-, and *meta*-substrates.

Furthermore, in organic solvents, **3** and **4** exhibited significantly higher catalytic activities in toluene than in CH₂Cl₂ (Table 3.3; entries 3-8a,b).



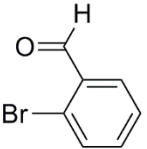
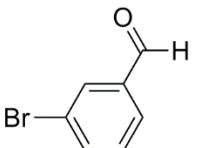
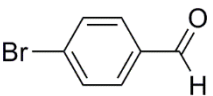
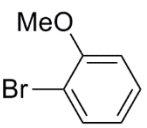
Substrate	Catalyst	Entry	Conversion [%]	S ^{hetero} [%]
	3	3a	64.1	74.7
		3b	41.1	91.7
		3c	65.4	92.6
	4	4a	2.7	53.2
		4b	1.1	73.2
		4c	22.2	95.9
	3	5a	68.1	76.1
		5b	10.8	71.7
		5c	8.3	71.5
	4	6a	16.0	69.0
		6b	4.5	73.3
		6c	11.2	83.7
	3	7a	83.2	84.3
		7b	49.5	93.7
		7c	97.9	98.1
	4	8a	89.6	93.5
		8b	11.0	97.3
		8c	9.1	91.1
	3	9a	30.5	5.7
		9b	49.9	78.4
		9c	23.5	80.9
	4	10a	15.2	0
		10b	2.4	15.9
		10c	5.0	0

Table 3.3

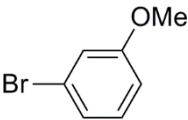
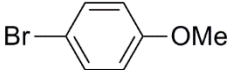
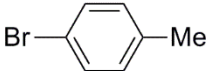
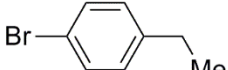
Substrate	Catalyst	Entry	Conversion [%]	S ^{hetero} [%]
	3	11a	19.0	26.0
		11b	6.7	61.1
		11c	51.3	79.9
	4	12a	0	0
		12b	0.1	100
		12c	0.1	100
	3	13a	39.4	35.5
		13b	33.0	87.9
		13c	98.5	99.0
	4	14a	0.8	0
		14b	0.3	64.5
		14c	4.7	0
	3	15a	48.5	42.7
		15b	98.9	96.2
		15c	27.0	84.9
	4	16a	15.9	38.5
		16b	20.6	0
		16c	0.8	100
	3	17a	35.5	54.8
		17b	18.7	75.5
		17c	93.3	98.1
	4	18a	15.6	33.5
		18b	0.7	54.8
		18c	0.8	52.1

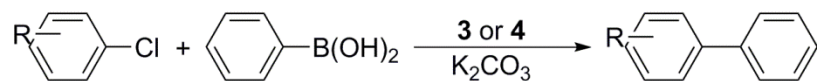
Table 3.3: Suzuki-Miyaura biaryl coupling of aryl bromides by **3** and **4**; Reaction conditions: aryl bromide (0.270 mmol), phenylboronic acid (0.324 mmol), K₂CO₃ (0.811 mmol), **3** or **4** (1.0 mol % Pd), solvent (a-toluene, b-CH₂Cl₂, c-H₂O; 3.0 mL), 40 °C, 20 h; all reactions were monitored for conversion by GC.

In the next step, the electronic characteristics of the functional groups on the aryl bromides were assessed with a family of bromoanisole reagents. In accordance with the

previous results, **3** was found to be substantially more active than **4**, especially in aqueous media (Table 3.3; entries 9-14c). For example, when **3** was treated with *p*-bromoanisole in water, the resulting *hetero*-coupled biphenyl product was formed in nearly 100% conversion (Table 3.3; entry 13c). Interestingly (and in contrast to the aforementioned results), **3** and **4** were found to be considerably more selective in polar aprotic solvent mixtures (Table 3.3; entries 9-14b). Furthermore, in nonpolar aprotic solvent mixtures, **3** selectively generated the *homo*-coupled biphenyl product.

It was particularly noteworthy that **3** was significantly more active when the functional group resided in the *para*-position relative to the carbon-halide bond (Table 3.3; entries 7c & 13c). The Suzuki reaction was further explored by using *p*-bromomethylbenzene and *p*-bromoethylbenzene as reagents (Table 3.3; entries 15-18a-c). These aqueous solvent mixtures provided the optimal media for **3** in the case of the larger, sterically demanding functional groups (Table 3.3; entry 17c), whereas the polar aprotic solvent mixture was found to be more appropriate for a simple methyl functional group (Table 3.3; entry 15b). In contrast, **4** activated the C-Br bond with a maximum of 20% conversion, regardless of the nature of the solvent (Table 3.3; entries 16a-c & 18a-c).

Upon optimization of the aryl iodides and bromides, examination of the catalytic activities of **3** and **4** were expanded to include chlorobenzaldehydes (Table 3.4). Aryl chlorides are industrially important because they are not only inexpensive, but they also permit more cost effective chemical waste procedures in comparison with the analogous aryl iodides and bromides. Unfortunately, however, the C-Cl bond is considerably more difficult to activate due to the large bond dissociation energy of 407 kJ mol⁻¹. In contrast, the bond energies for C-Br and C-I bonds are 346 and 280 kJ mol⁻¹, respectively.⁶



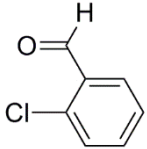
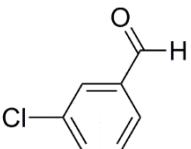
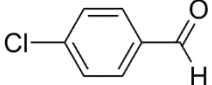
Substrate	Catalyst	Entry	Conversion [%]	S ^{hetero} [%]
	3	19a	33.5	0.4
		19b	24.7	4.6
		19c	13.9	11.4
	4	20a	19.0	17.4
		20b	4.5	81.1
		20c	13.9	38.6
	3	21a	36.6	0
		21b	31.9	0
		21c ^a	13.2	3.1
	4	22a	15.4	0
		22b	0.2	44.6
		22c	4.6	2.4
	3	23a	34.8	0.2
		23b	27.5	24.7
		23c	25.2	14.1
	4	24a	16.4	7.1
		24b	1.7	55.8
		24c	2.5	33.6

Table 3.4: Suzuki-Miyaura biaryl coupling of aryl chlorides by **3** and **4**; Reaction conditions: aryl chloride (0.357 mmol), phenylboronic acid (0.429 mmol), K₂CO₃ (1.07 mmol), **3** or **4** (1.0 mol % Pd), solvent (a-toluene, b-CH₂Cl₂, c-H₂O; 3.0 mL), 40 °C, 48h; all reactions were monitored by GC.

The aforementioned trends were confirmed by further investigation of the aryl chlorides. **3** was found to be the most selective for production of the desired *hetero*-coupled product in H₂O and CH₂Cl₂ (Table 3.4; entries 19b-c, 21b-c & 23b-c). However,

only the adverse *homo*-coupled product was produced in toluene (Table 3.4; 19a, 21a & 23a). Regrettably, neither catalyst yielded the *p*-biphenylaldehyde as the major product in the three solvents tested (Table 3.4; entries 19-24a-c).

The above results may well be a direct consequence of the strength of the Pd–C_{carbene} bonds in both **3** and **4**. It is plausible that both of the NHCs remain attached to the Pd centre when the catalysts are introduced into the reaction mixture. The inability of these catalysts to lose a carbene moiety effectively eliminates the possibility of any C–X activation, thus rendering such catalysts completely inactive. A similar trend was observed when the PCy₃ ligands in Grubbs' 1st generation catalyst were replaced with two NHC ligands.^{96,227} This 2nd generation-type catalyst exhibited less activity for ring-closing metathesis reactions than analogous catalysts containing fewer NHC ligands. These results were attributed to the labile character of the phosphine ligands, since the formation of the 14 e[−] catalytically active species forms significantly faster than that of the corresponding NHC catalysts.²²⁸ It is plausible that the previously mentioned catalytic activities of **3** and **4** may well be due to the sluggish rate of ligand dissociation. Furthermore, the demoted activity of **4** may be an immediate outcome of the stability provided by the bulky *i*-Pr groups, in which sparse dissociation of the ligand occurs, thereby generating a dormant catalyst in solution.

The final phase of the present study was concluded by means of filtration tests that were carried out in all three solvents in order to identify the nature of the catalytically active species in each system. This process began by performing the Suzuki reaction of *p*-bromobenzaldehyde and phenylboronic acid in toluene, CH₂Cl₂ or H₂O. The reaction mixtures were terminated promptly after 20 h and each hot reaction mixture was centrifuged (15 min, 8.5 krpm) in order to isolate any solid residues from the organic

supernatant. The %Pd content in the solid and liquid phases was then determined by means of ICP-MS (Table 3.5). The resulting data indicated that when **3** and **4** were employed in CH₂Cl₂ solution, the molecular catalysts retained their original structures (Table 3.5; entries 25b & 26b). In contrast, the elemental analyses implied that when the reactions were carried out in H₂O or toluene, a substantial amount of palladium metal had been detached from the carbene ligands (Table 3.5; entries 25c & 26a,c). Interestingly, **4** exhibited significantly more leaching in the nonpolar solvent than **3** (Table 3.5; entries 25a & 26a).

Catalyst	Entry	% Pd		Conversion [%]	
		sup ^a	ppt ^a	sup	ppt
3	25a	98	2	80.1	71.7
	25b	78	22	29.5	2.8
	25c	3	97	1.9	35.1
4	26a	60	40	49.0	6.6
	26b	84	16	5.5	0.7
	26c	22	78	0.1	51.9
Pd-PVP	27 ^b	-	-	0.06	51.5

Table 3.5: Recyclability of **3** and **4** in Suzuki-Miyaura biaryl coupling of the *p*-bromobenzaldehyde supernatant (*sup*) and precipitate (*ppt*); Reaction conditions: *p*-bromobenzaldehyde (0.270 mmol), phenylboronic acid (0.324 mmol), K₂CO₃ (0.811 mmol), Pd (1 mol%), solvent (a-toluene, b-CH₂Cl₂, c-H₂O; 3.0 mL), 40 °C, 20 h; all reactions were monitored by GC. ^a % Pd of supernatant and precipitate determined by ICP-MS. ^b *p*-bromobenzaldehyde (0.270 mmol), phenylboronic acid (0.324 mmol), K₂CO₃ (0.811 mmol), H₂O (3.0 mL), Pd-PVP (0.537 mmol), 40 °C, 20 h.

Finally, the original reaction conditions were repeated using fresh reagents, and either the isolated solid or the liquid phase was subsequently added to each reaction

mixture. In each case, the supernatant was injected directly into the sample. The solid phase required the addition of fresh solvent in order to dissolve/suspend the residual solids. The products of the repeated reactions were monitored by means of GC (Table 3.5). Interestingly, the supernatant and precipitate of **4** were both quite inactive, especially when employed in CH₂Cl₂ (Table 3.5; entries 26a-c). In contrast, both the supernatant and the residual solids of **3** were capable of activating the C–Br bond in each of the three solvents that were tested (Table 3.5; entries 25a-c). Thus, even though it became evident that **3** or **4** was present only in the supernatant layer, the Pd(II) metal centre remained strongly bonded to the two carbene ligands when solubilized in CH₂Cl₂. Upon subsequent re-use of the supernatant layer, a conversion of 29% was accomplished by **3**, while that for **4** was only 5% (Table 3.5; entries 25b & 26b).

In contrast, only the residual solids from the initial reaction in H₂O afforded *p*-biphenylaldehyde from *p*-bromobenzaldehyde (Table 3.5; entries 25c & 26c). This unique result confirmed that **3** and **4** had formed poorly-defined, yet catalytically-active heterogeneous (colloidal or nanoparticulate) species in aqueous media. These active Pd species are difficult to fully characterize. Ananikov and co-workers recently suggested a ‘cocktail-type’ mixture of several active Pd transient intermediate entities.^{188,191} Intriguingly, the nonpolar organic solvent also assisted in the decomposition of the molecular species, which resulted in the formation of active supernatant and precipitate layers (Table 3.5 entries 25a & 26a). It therefore became evident that organic solvents encouraged homogeneous molecular catalysis, while aqueous media caused catalyst degradation which in turn, resulted in formation of the active ‘heterogenised’ Pd species.

In comparison with recently reported catalysts (IMes)PdCl₂PPh₃ and (IPr)PdCl₂PPh₃, **3** and **4** exhibited appreciably lower reactivity toward substituted aryl

halides for the Suzuki-Miyaura cross-coupling reaction. The elevated activity of (IMes)PdCl₂PPh₃ and (IPr)PdCl₂PPh₃ may be attributed to two factors: (1) the strong σ -donation of the NHC moiety and (2) the labile character of the phosphine ligand. In the case of **3** and **4**, the NHC ligands may be too tightly bound to the Pd metal centre, supported by a strong *trans* influence, and thereby are slow to dissociate to yield the required active species. In addition, all solvent trends were confirmed by means of replicate Suzuki couplings in toluene, CH₂Cl₂, and H₂O. Reactions employed in CH₂Cl₂ enabled molecular catalysis of all catalysts, whereas partial and full decomposition occurred in toluene and aqueous solutions, respectively.

3.4 CONCLUSIONS

In conclusion, two new Pd(II) *bis*(carbene) catalysts have been synthesized and studied for their catalytic activities in toluene, CH₂Cl₂, and H₂O. **3** activated C–X bonds primarily in aqueous solvent mixtures. Due to the ease of oxidative addition of highly polarizable bonds, **3** readily generated biaryl products from all aryl iodides and most aryl bromides examined. Unfortunately, this process was discouraged for comparable aryl chlorides. The large bond dissociation energy of the C–Cl bond resulted in incomplete activation of these aryl chlorides. It was discovered that the mean plane angle and short Pd1–C1 bond distance of **3** promoted ligand dissociation and subsequent catalytic activity for the *hetero*-coupled product in polar aprotic solvents. Without either of these constraints, **4** retained two strong Pd–C_{carbene} bonds, thus rendering the catalyst completely inactive. By means of filtration tests, it was concluded that these catalysts decompose to a more active heterogenised catalyst in aqueous media, but primarily maintain their molecular structures in organic solvent mixtures.

3.6 SUMMARY OF KEY RESULTS

- **3** was significantly more active than **4**
- H₂O facilitated the highest catalytic activity, although the catalysts were proven to decompose when employed in this solvent system
- Both catalysts were more selective in CH₂Cl₂ than toluene
- Neither catalyst fully activated the C–Cl bond in aryl chloride substrates

3.6 ACKNOWLEDGEMENTS

The authors thank Ms. Stephany Garcia for supplying the Pd-PVP catalysts and Dr. Vincent M. Lynch for assisting in X-ray crystallography, and the Robert A. Welch Foundation (F-1738, F-003) for funding.

3.7 EXPERIMENTAL

3.7.1 General Procedures

All glassware was oven-dried before use. All reagents were obtained commercially and used without further purification. Toluene and THF were dried over sodium and freshly distilled prior to use. The dichloromethane was dried over calcium hydride and freshly distilled prior to use. The starting materials IMes(BIAN)[AgCl] and IPr(BIAN)[AgCl] were synthesized according to published procedures.

3.7.2 Physical Measurements

Low-resolution CI mass spectra were obtained on a Thermo Scientific TSQ Quantum GC mass spectrometer and high-resolution CI mass spectra were recorded on a magnetic sector Waters Autospec Ultima instrument. ¹H and ¹³C{¹H} NMR spectra were recorded at 295 K in the indicated solvent on a Varian Unity 300 (¹H, 300 MHz; ¹³C, 75 MHz) or a Varian AS400 spectrometer (¹H, 400 MHz; ¹³C, 100 MHz) immediately

following sample preparation. Deuterated solvents were obtained from Cambridge Isotopes and stored over 4 Å molecular sieves prior to use. ^1H and $^{13}\text{C}\{^1\text{H}\}$ chemical shift values are reported in parts per million (ppm) relative to SiMe_4 (δ 0.00), using solvent resonances as internal standards. Absorption spectra were recorded on a Varian Cary 6000i UV-VIS-NIR spectrophotometer with Starna Quartz fluorometer cells with a pathlength of 10 mm. Gas chromatography (GC) was performed on an Agilent 6850 gas chromatograph (HP-1 column, $l = 30$ m, I.D. = 0.32 mm) equipped with a flame ionization detector (FID). The GC oven temperature was held at 50 °C for 3 min, then increased to 300 °C at 30 °C min $^{-1}$. The internal standard mesitylene was used to aid in measuring reaction conversions.

3.7.3 Preparations

3.7.3.1 (*IMes*) $_2$ PdCl $_2$ (3)

Toluene (5 mL) was added to an aluminium covered 50 mL round bottom flask that contained $\text{IMes}(\text{BIAN})[\text{AgCl}]^{226}$ (0.4915 g, 0.861 mmol) and $\text{Pd}(\text{OAc})_2$ (0.092 g, 0.410 mmol). The reaction mixture was refluxed for 16 h, following which it was cooled to ambient temperature and filtered over celite. The resulting precipitate was extracted from the celite using dichloromethane, following which the solvent was removed under reduced pressure. Recrystallization from tetrahydrofuran afforded an analytically pure yellow solid (0.4785 g, 54%). MS (Cl^+ , CH_4): m/z 1057 $[\text{M}+\text{Na}]^+$; ^1H NMR (CDCl_3): δ 2.28 (s, 12H, CH_3), 2.75 (s, 6H, CH_3), 7.08 (d, 2H, Naph-H), 7.46 (s, 4H, Ar-H), 7.51 (t, 2H, Naph-H), 7.83 (d, 2H, Naph-H); ^{13}C NMR (CDCl_3): δ 137.73, 136.01, 134.32, 129.70, 129.12, 127.40, 126.15, 120.33, 21.42, 19.05.

3.7.3.2 (*IPr*)₂PdCl₂ (**4**)

Toluene (15 mL) was added to an aluminium covered 50 mL round bottom flask that contained IPr(BIAN)[AgCl] (0.3018 g, 0.461 mmol) and PdCl₂(ACN)₂ (0.0568 g, 0.219 mmol). The reaction mixture was refluxed for 16 h, following which it was cooled to ambient temperature, filtered over celite, and washed with tetrahydrofuran. The solvent was then removed from the filtrate under reduced pressure. **4** was recrystallized from toluene, followed by solvation in chloroform. The product was then filtered over celite affording an analytically pure yellow solid (0.056 g, 20%). MS (Cl⁺, CH₄): m/z 1225 [M+Na]⁺; ¹H NMR (CDCl₃): δ 0.69 (d, 24H, CH₃), 0.98 (d, 24H, CH₃), 3.20 (sept, 8H, -CH(CH₃)₂), 6.43 (d, 4H, Naph-H), 7.18-28-7.36 (d/t, 16H, Naph-H, iPr-Ar-H), 7.51 (d, 4H, iPr-Ar-H); ¹³C NMR (CDCl₃): δ 179.47, 146.70, 139.78, 135.11, 129.46, 126.95, 124.26, 121.51, 28.45, 25.42, 24.02.

3.7.4 General Procedure for Suzuki Cross-Coupling Reactions

Deionized water, dry dichloromethane or dry toluene (3 mL) was added to a 20 mL scintillation vial containing the aryl halide (0.267 mmol), phenylboronic acid (0.321 mmol), potassium carbonate (0.802 mmol) and the internal standard mesitylene (0.267 mmol). The scintillation vial was covered with a septum and wired down. The stirred reaction mixture was then heated to 40 °C. The catalyst concentration was determined by means of UV-Vis spectroscopy and injected rapidly into the reaction mixture (1.0 mol% of **3** or **4**). The resulting reaction mixture was allowed to stir for twenty hours for all the aryl iodides and bromides. On the other hand, the aryl chlorides required 48 hours to reach complete conversion. The resulting reaction mixture was cooled to ambient temperature, filtered over celite and washed with diethyl ether. The solvents were evaporated from the organic layer, thereby producing the desired product. The reactions

were monitored by GC and the percent conversions were calculated based on the aryl halide. The NMR spectra of the products matched those of literature values.

Chapter 4: Suzuki-Miyaura cross-coupling reactions performed with silica-anchored *bis*(imino)acenaphthene (BIAN)-supported palladium(II) carbene complexes

4.1 ABSTRACT

The syntheses of two novel silica-anchored BIAN heterogeneous catalysts are described, in addition to an assessment of their activities for the Suzuki-Miyaura cross-coupling reaction and full characterization by UV-vis, IR, and TGA spectroscopy. The catalysts were found to maintain 0.155–0.868 mmol g⁻¹ of palladium on the basis of ICP-MS. The catalytic activities were monitored by GC *post*-catalysis. Both catalysts exhibited C–X activation for the Suzuki reaction in toluene or water solution, specifically for aryl iodides and bromides. A direct comparison with the homogeneous analog is reported, which indicated that the heterogeneous version was found to be significantly less active. However, under optimized reaction conditions, the heterogeneous catalysts were found to be more active in tetrahydrofuran than in toluene or water under otherwise identical reaction conditions.

4.2 INTRODUCTION

The Suzuki-Miyaura cross-coupling reaction represents a pivotally important method for industrial carbon–carbon bond formation in pharmaceuticals, natural products, and agrochemicals.^{28–34} In this reaction, functionalized aryl halides and organoboranes are treated with Group X complexes, thus forming biphenyl products. Typically, a base is employed to accelerate the transmetallation step, and reductive elimination processes (Scheme 1.3).^{2,4} The catalysts for the Suzuki reaction generally contain either a phosphine ligand^{3,37,43} or an *N*-heterocyclic carbene (NHC) to assist in the C–X activation^{4,5,56,85}. The bulky nature of the phosphine ligand in conjunction with

the strong σ -donation of the NHC provides the catalyst with the necessary stability toward air and moisture.^{109–113} However, it is interesting to note that only a few examples exist in the catalyst literature of systems containing both types of ligands. This situation arises because the *trans* influence of the NHC encourages the labile phosphine ligand to dissociate, thereby generating an open site on the catalyst metal center. Nevertheless, the resulting complexes appear to be ideal candidates for the Suzuki reaction.

The catalytic activities of two such catalysts based on the *bis*(imino)acenaphthene (BIAN) carbene ligand (**1**, **2**; see chapter 2) were reported recently.²²⁶ Catalysts **1** and **2** were employed in toluene, dichloromethane, and water each as examples of nonpolar/polar organic solvents or as environmentally benign solvents, respectively. Reactions involving a variety of aryl halides were also examined, with the specific objective of activating functionalized aryl chlorides. Although C–Cl bonds are considerably less reactive than those of the analogous C–X bonds (C–Cl > C–Br > C–I; 407, 346, 280 kJ mol^{–1}, respectively), such aryl chlorides are favored for industrial use due to the relative ease of byproduct waste removal.⁶ Typically, these complexes remained intact as homogeneous catalysts in dichloromethane solution. However, in toluene or aqueous solution the production of the desired *hetero*-coupled compound was a direct result of the decomposition of **1** or **2** into more active, presumably heterogeneous, catalysts. Ananikov *et al.* attempted to explain these and similar observations based on a mechanism referred to as a “cocktail of catalysts” (Scheme 1.34).^{188,191} This hypothesis suggested that molecular complexes were in equilibrium with both metal clusters and metal nanoparticles, all of which contributed to the overall creation of the final product. Furthermore, the authors discuss the ambiguity in the identification of the actual active

catalyst(s) (homogeneous or heterogeneous in character) present in the reaction mixture.¹⁸²

In an attempt to circumvent the catalyst decomposition problem that was encountered in toluene and water, several heterogeneous catalysts were designed based on the most reactive homogeneous catalyst, **2**. These greener, insoluble catalysts were created with the objective of achieving easy separation and recovery. In turn, this permitted the addition and subsequent reuse with fresh reagents for further Suzuki couplings of activated aryl halides and phenylboronic acids.^{132,138,152} The initial catalyst design was along similar lines to those of catalysts **3** and **4**, in which two NHC ligands were directly coordinated to the palladium metal center (Figure 4.1).^{205,206} Due to the inactivity of **3** and **4**, the metallopolymer was considered not to be useful for further investigation. As a consequence, a new polymer involving organic linkers with Pd pendants was developed (Figure 4.2). However, further examination of similar systems evidenced minimal reactivity in aqueous media due to hydrophobic solvent interactions.

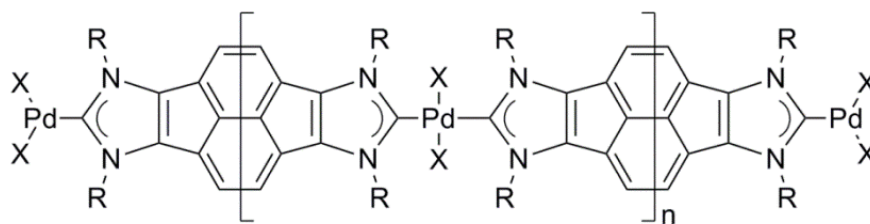


Figure 4.1: Metallopolymer based on bifunctional BIAN ligand based on the 3-D polymer presented by Karimi *et al.*

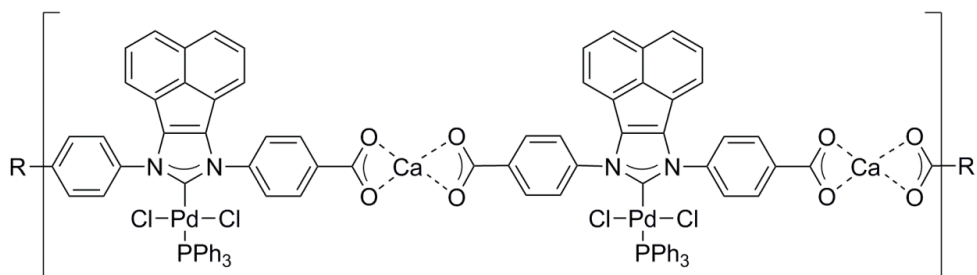


Figure 4.2: Design of 1-D metal organic polymer of Pd(II) BIAN species incorporating organic linkers.

The resulting two catalysts were developed with the objective of anchoring **2** to a solid-support, such as polystyrene, alumina, or silica.^{132,138–140,152–155} It has been determined previously that NHC ligands exhibit higher reactivities on silica supports,^{166–170} whereas phosphine ligands attached to polystyrene generate larger quantities of the biaryl products.^{133–136} As a consequence, silica was selected as the solid-support for the new catalyst; silica naturally exists as a chemically inert species, and thereby has no interference with the palladium metal centers. Although the most active NHC-anchored catalysts presented in the literature are tethered to silica by means of the aromatic groups as opposed to the NHC backbone (Figures 4.3 & 4.4, respectively), the BIAN ligand was believed to be too bulky in character to exhibit activity if tethered in this manner. Alternatively, it was considered that an elongated aliphatic tether could be employed to anchor the ligand to a solid-support *via* the BIAN backbone, thus creating an ideal candidate for the heterogeneous Suzuki-Miyaura cross-coupling reaction. Herein are reported the syntheses, characterization and catalytic activities of two new heterogeneous catalysts.

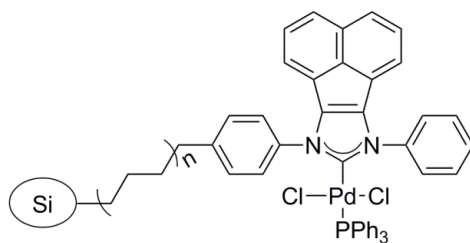


Figure 4.3: Design of asymmetrical silica-anchored BIAN catalyst.

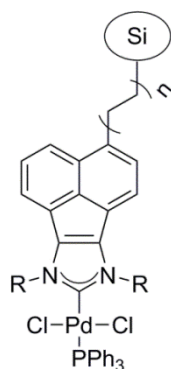


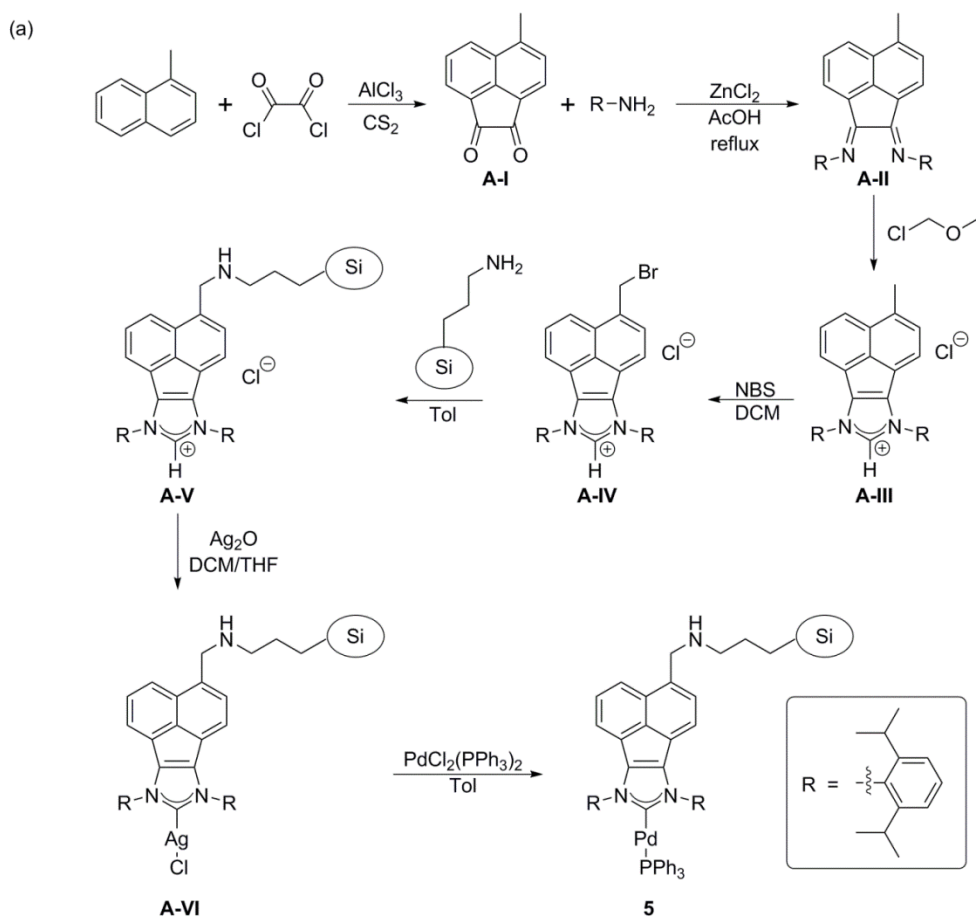
Figure 4.4: Design of silica-anchored catalyst using the BIAN backbone.

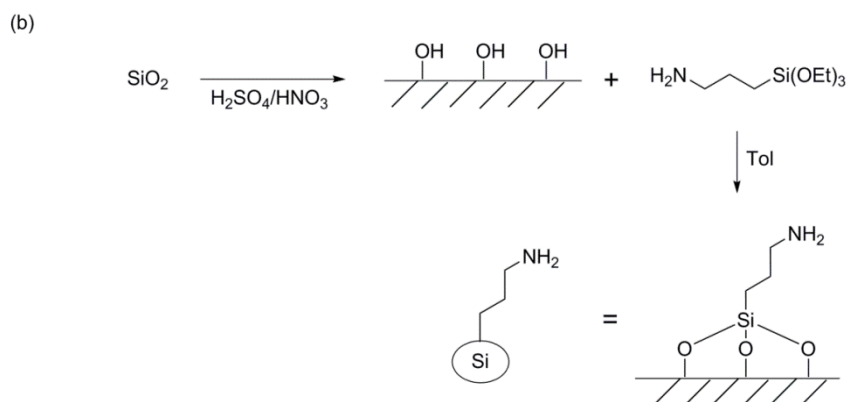
4.3 RESULTS AND DISCUSSION

4.3.1 Synthesis of **5**

The *N*-heterocyclic palladium(II) carbene catalysts presented here were developed as heterogeneous alternatives to the previously reported soluble catalysts, (IMes)PdCl₂PPh₃ and (IPr)PdCl₂PPh₃.²²⁶ The homogeneous synthetic route was proved to be impractical for the production of the methylated-BIAN ligand, and therefore an entirely new synthetic procedure was formulated (Scheme 4.1a). For this purpose, aluminum chloride was treated with oxalyl chloride and 1-methylnaphthalene in carbon disulfide, thereby producing **A-I** in low yield. Subsequently, a condensation reaction was performed on **A-I** with 2,6-diisopropylaniline in glacial acetic acid to afford **A-II** *via* the elimination of water. This reaction was followed by treatment of **A-II** with chloromethyl

methyl ether in a pressure vessel in order to obtain analytically-pure **A-III**. Following this, *N*-bromosuccinimide was added to **A-III** along with a radical initiator (benzoyl peroxide) to afford **A-IV** in moderate yields. Meanwhile, functionalized silica gel was prepared according to literature procedures (Scheme 4.1b),²²⁹ and **A-IV** was then tethered to the functionalized silica *via* a condensation reaction that produced **A-V**. The corresponding silver(I)-carbene was then created by means of the reaction of **A-V** with silver oxide in a 1:1 mixture of dichloromethane and tetrahydrofuran. Finally, the heterogeneous catalyst, **5**, was generated by means of a transmetalation reaction of **A-VI** with $\text{PdCl}_2(\text{PPh}_3)_2$ (Scheme 4.1; see experimental section for further synthetic details).





Scheme 4.1: (a) Synthesis of silica-anchored BIAN palladium catalyst **5** (b) Synthesis of functionalized silica.

4.3.2 Characterization of **5**

The heterogeneous catalyst was characterized by means of UV-vis and IR spectroscopy. The UV-vis absorption profiles for **A-V**, **2**, and **5** in dichloromethane are presented in Figure 4.5, in which **2** and **5** show similar $n \rightarrow \pi^*$ transitions [300 nm (**2**); 260 nm (**5**)], $\pi \rightarrow \pi^*$ transitions [325 nm (**2**); 275 nm (**5**)], and LMCT bands [355 nm (**2**); 350 nm (**5**)]. Furthermore, the λ_{max} for each compound was monitored for solvatochromism effects. Upon complexation of **A-V** with Pd(0) to generate **5**, a distinct blue shift was observed due to the loss of stabilizing electrostatic interactions provided by the imidazolium cations and the corresponding chloride anions. Interestingly, a much larger blue shift was observed when the analogous homogeneous and heterogeneous catalysts were compared. It is plausible that the introduction of the long aliphatic tether to the BIAN backbone destabilizes the ground state of the heterogeneous catalyst due to the increase of entropy in the system.

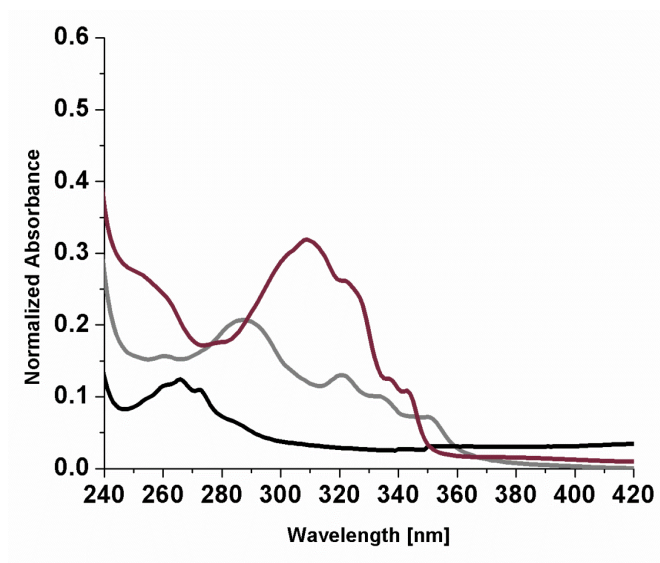


Figure 4.5: UV-vis spectra of (NHC)(PPh₃)PdCl₂ (**2**, dark grey), Imidazolium@SiO₂ (**A-V**, light grey), and (NHC)PdCl₂(PPh₃)@SiO₂ (**5**, black).

As might be expected, identical energy shifts were observed for the IR spectra that were measured (Table 4.1). The functionalized silica gel (APTES@SiO₂) exhibited higher energy absorptions than those of the analogous imidazolium salts, possibly due to the stabilizing effects of the ionic interactions in **A-V**. Once again, higher energy frequencies were observed in the case of **5** than in the corresponding compound, **A-V**.

IR	CH ₂ –CH ₂ [cm ⁻¹]	CH ₂ –NH [cm ⁻¹]
APTES@SiO ₂	1659	1554
A-V	1619	1527
5	1650	1556

Table 4.1: IR peak assignments for APTES@SiO₂, Imidazolium@SiO₂ (**A-V**), and (NHC)PdCl₂(PPh₃)@SiO₂ (**5**).

Thermogravimetric analysis (TGA) was also performed on compounds **A-V**, **2**, and **5** with the objective of differentiating the thermal stability of the homogeneous and heterogeneous systems. The resulting TGA data clearly distinguished **A-V** and **5** from **2**, since **A-V** and **5** retained 83% of their mass at 800 °C. Under identical conditions, **2** decomposed in two clear phases at 300 and 350 °C due to the loss of the phosphine and NHC ligands, respectively. In fact, the gradual increase in temperature to 800 °C resulted in decomposition of 84% of the homogeneous catalyst, whereas only 17% decomposition was observed in the case of **5**.

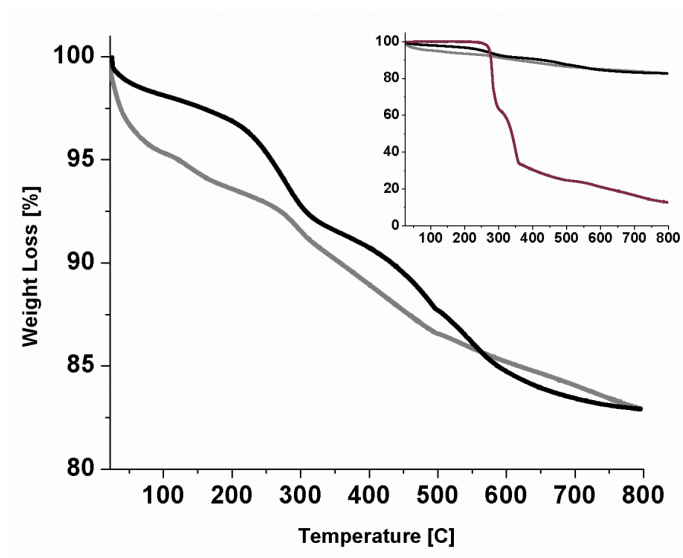
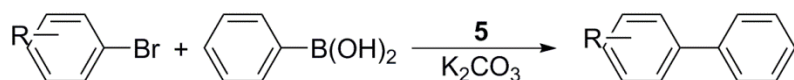


Figure 4.6: TGA for (NHC)(PPh₃)PdCl₂ (**2**, dark grey), Imidazolium@SiO₂ (**A-V**, light grey), and (NHC)PdCl₂(PPh₃)@SiO₂ (**5**, black).

4.3.3 Optimization of the catalytic activity of **5**

Catalyst **5** was probed for its reactivity in the Suzuki-Miyaura cross-coupling reaction of aryl halides with phenylboronic acid under the optimized conditions previously presented for homogeneous catalysts **1-4**. Initially, the reaction was

investigated using aryl bromides containing substituents in the *para* position relative to the C–Br bond in toluene, CH₂Cl₂, or aqueous solutions. The palladium content of **5** was determined by ICP-MS analysis (0.155–0.868 mmol g⁻¹) and the generation of the *hetero*-coupled product was monitored by GC. The aryl bromide (0.270 mmol), phenylboronic acid (0.324 mmol), K₂CO₃ (0.811 mmol), and **5** (0.0027 mmol Pd) were stirred at 40 °C for 20 h. The pertinent results are presented in Table 4.2. In all cases, very little C–Br activation occurred. The catalyst appeared to be most active in aqueous solution; however it was only selective for the undesirable *homo*-coupled product (Table 4.2; entries 1-4c). Interestingly, **5** exhibited the highest reactivity in CH₂Cl₂, and was therefore utilized as the ideal reaction medium in subsequent optimization studies. Unfortunately, when the catalyst loading was increased to 5.0 mol% Pd, the *p*-biphenyl compounds were only generated in small quantities (Table 4.3). For example, only 10% conversion was observed in the case of the activated aryl bromide (Table 4.3, entry 5).



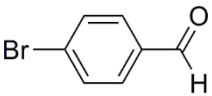
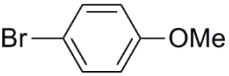
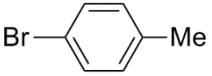
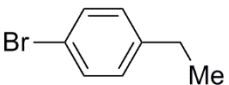
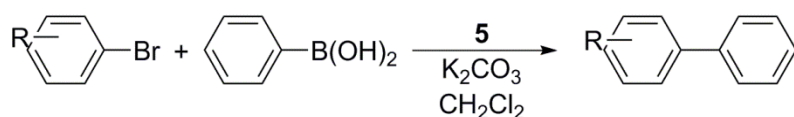
Substrate	Entry	Cat. Loading [%]	Temp. [°C]	Conv. [%]	S ^{hetero} [%]
	1a	1.0	40	0	0
	1b	1.0	40	0.2	100
	1c	1.0	40	4.1	0
	2a	1.0	40	0.7	71.6
	2b	1.0	40	0.9	66.8
	2c	1.0	40	9.2	0
	3a	1.0	40	0	0
	3b	1.0	40	0.1	23.7
	3c	1.0	40	2.5	0
	4a	1.0	40	0.01	0
	4b	1.0	40	0.4	50.7
	4c	1.0	40	0.1	0

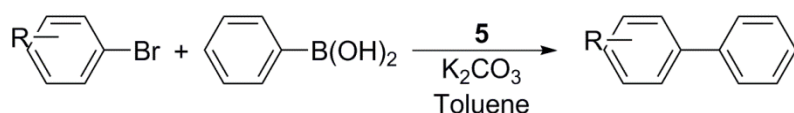
Table 4.2: Suzuki-Miyaura biaryl coupling of aryl bromides by **5**; Reaction conditions: aryl bromide (0.270 mmol), phenylboronic acid (0.324 mmol), K₂CO₃ (0.811 mmol), **5** (1.0 mol% Pd), solvent (a-toluene, b-CH₂Cl₂, c-H₂O; 3.0 mL), 40 °C, 20 h; all reactions were monitored for conversion by GC.



Substrate	Entry	Cat. Loading [mol %]	Temp. [°C]	Conv. [%]	S ^{hetero} [%]
	5	5.0	40	10.8	97.0
	6	5.0	40	2.0	56.6
	7	5.0	40	0.8	54.1

Table 4.3: Suzuki-Miyaura biaryl coupling of aryl bromides by **5**; Reaction conditions: aryl bromide (0.270 mmol), phenylboronic acid (0.324 mmol), K₂CO₃ (0.811 mmol), **5** (5.0 mol% Pd), solvent (CH₂Cl₂; 3.0 mL), 40 °C, 20 h; all reactions were monitored for conversion by GC.

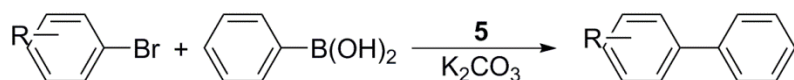
In the interest of catalyst conservation, the temperature was increased from 40 to 65 °C, and the catalytic activity of **5** was investigated at 5.0 mol% Pd catalyst loading with respect to the activated aryl bromide (Table 4.4). As a consequence of the change in temperature, CH₂Cl₂ was replaced with toluene in order to maintain the temperature of the reaction mixture adequately. However, the catalyst was found to be only slightly more active due to the increase in temperature (Table 4.4; entry 8).



Substrate	Entry	Cat. Loading [mol %]	Temp. [°C]	Conv. [%]	S ^{hetero} [%]
	8	5.0	65	19.6	97.6

Table 4.4: Suzuki-Miyaura biaryl coupling of aryl bromides by **5**; Reaction conditions: aryl bromide (0.270 mmol), phenylboronic acid (0.324 mmol), K₂CO₃ (0.811 mmol), **5** (5.0 mol% Pd), solvent (toluene; 3.0 mL), 65 °C, 20 h; all reactions were monitored for conversion by GC.

Fortunately, the increase in reaction temperature appeared to increase the yield of the desired *hetero*-coupled product. This fortuitous result led to an investigation of the original four *para*-substituted aryl bromides with 5.0 mol% Pd at 100 °C in both toluene and aqueous solutions (Table 4.5). Interestingly, the catalyst operated similarly in both reaction media; however, the catalyst exhibited higher reactivity in H₂O than in toluene. The biaryl products were formed in the highest yields from the activated aryl bromides, followed in succession by the corresponding deactivated and unactivated systems (Table 4.5; entries 9-11a,c). Surprisingly, **5** demonstrated substantially higher reactivity with *p*-bromoethylbenzene in toluene compared with water (Table 4.5; entries 12a,c).

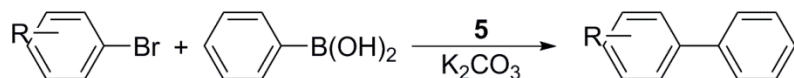


Substrate	Entry	Cat. Loading [mol %]	Temp. [°C]	Conv. [%]	S ^{hetero} [%]
	9a	5.0	100	83.1	96.4
	9c	5.0	100	98.7	99.8
	10a	5.0	100	46.1	81.3
	10c	5.0	100	60.4	90.8
	11a	5.0	100	32.4	79.1
	11c	5.0	100	49.8	78.3
	12a	5.0	100	31.9	76.0
	12c	5.0	100	14.2	84.6

Table 4.5: Suzuki-Miyaura biaryl coupling of aryl bromides by **5**; Reaction conditions: aryl bromide (0.270 mmol), phenylboronic acid (0.324 mmol), K₂CO₃ (0.811 mmol), **5** (5.0 mol% Pd), solvent (a-toluene, c-H₂O; 3.0 mL), 100 °C, 20 h; all reactions were monitored for conversion by GC.

Although the reactivity of **5** improved at elevated temperatures, it was decided to increase the catalyst loading to 10.0 mol% Pd in an attempt to enhance the reactivities of the aryl bromides containing electron withdrawing or neutral substituents. A summary of the outcomes of these reactions is presented in Table 4.6. With the presence of a larger Pd content in the reaction mixture, the *hetero*-coupled product was generated in significantly higher yields than those with only 5.0 mol% Pd (Tables 4.5 & 4.6). For example, **5** coupled *p*-bromoanisole to phenylboronic acid in the Suzuki reaction in 46 and 60% conversions at 5.0 mol% Pd and 68 and 83% conversion at 10.0 mol% Pd in toluene and water, respectively (Tables 4.5 & 4.6; entries 10a,c & 14a,c). The optimized

heterogeneous reaction conditions required 10.0 mol% Pd at 100 °C for the experiments carried out in toluene and aqueous media.



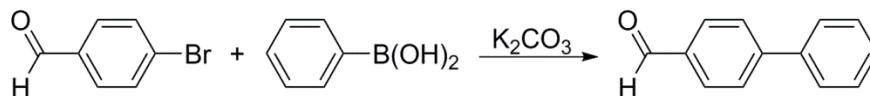
Substrate	Entry	Cat. Loading [mol %]	Temp. [°C]	Conv. [%]	S ^{hetero} [%]
	13a	10.0	100	89.6	94.6
	13c	10.0	100	100	99.9
	14a	10.0	100	68.0	76.3
	14c	10.0	100	83.0	89.9
	15a	10.0	100	63.2	75.0
	15c	10.0	100	67.0	86.5
	16a	10.0	100	49.1	70.8
	16c	10.0	100	20.9	87.4

Table 4.6: Suzuki-Miyaura biaryl coupling of aryl bromides by **5**; Reaction conditions: aryl bromide (0.270 mmol), phenylboronic acid (0.324 mmol), K₂CO₃ (0.811 mmol), **5** (10.0 mol% Pd), solvent (a-toluene, c-H₂O; 3.0 mL), 100 °C, 20 h; all reactions were monitored for conversion by GC.

4.3.4 Catalytic activity of **5**

After the optimal reaction conditions had been established, a thorough investigation of the reactivity of **5** was completed. Control studies were performed with *p*-bromobenzaldehyde and phenylboronic acid utilizing SiO₂, APTES@SiO₂, or **A-V** instead of **5**, in order to confirm the identity of the catalyst. Fortunately, no conversion to

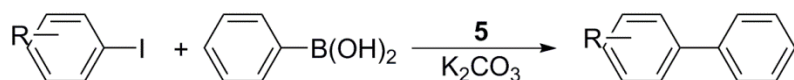
the *p*-biphenylaldehyde was observed by GC and therefore it was confirmed that **5** was the actual active catalyst species. (Table 4.7)



Compound	Entry	Temperature [°C]	Conversion [%]	S ^{hetero} [%]
SiO ₂	17a	100	0	0
	17b	80	0	0
	17c	100	0	0
APTES@SiO ₂	18a	100	0	0
	18b	80	0	0
	18c	100	0	0
A-V	19a	100	0	0
	19b	80	0	0
	19c	100	0	0

Table 4.7: Suzuki-Miyaura biaryl coupling of *p*-bromobenzaldehyde by SiO₂, APTES@SiO₂ or **A-V**; Reaction conditions: aryl bromide (0.270 mmol), phenylboronic acid (0.324 mmol), K₂CO₃ (0.811 mmol), compound (10.0 mol% Pd), solvent (a-toluene, b-THF, c-H₂O; 3.0 mL), 100 °C, 20 h; all reactions were monitored for conversion by GC.

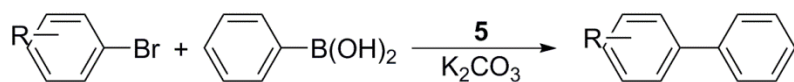
The analysis of **5** began with the examination of *p*-iodobenzaldehyde, for which complete conversion was attained when the reaction was carried out in aqueous media (Table 4.8; entry 20c). By contrast, the desired compound was only produced in 60% yield in toluene solutions (Table 4.8; entry 20a).



Substrate	Catalyst	Entry	Conversion [%]	S ^{hetero} [%]
	5	20a	60.6	99.3
		20c	100	100

Table 4.8: Suzuki-Miyaura biaryl coupling of aryl iodides by **5**; Reaction conditions: aryl iodide (0.216 mmol), phenylboronic acid (0.259 mmol), K₂CO₃ (0.647 mmol), **5** (10.0 mol% Pd), solvent (a-toluene, c-H₂O; 3.0 mL), 40 °C, 20 h; all reactions were monitored by GC.

The optimized Suzuki reaction conditions were then expanded to include the *ortho*- and *meta*-substituted aryl bromides of the *para*-substituted families of aryl bromide substrates in Table 4.6 that had been examined previously. A summary of the catalytic activity of **5** toward all the aryl bromides that were tested is presented in Table 4.9. In general, each catalyst exhibited significantly higher activity in aqueous solutions than the corresponding organic media, except in the case of *p*-bromoethylbenzene (Table 4.9; entries 28a,c). Moreover, **5** consistently demonstrated higher activity toward aryl bromides with substituents in the *para*-position than was the case with analogous *ortho*- or *meta*-substituted substrates (Table 4.9; entries 23c & 26c). It was particularly interesting to find that within a family of aryl bromides, catalyst **5** showed essentially the same reactivity toward *ortho*- or *meta*-reagents. It should be noted, however, that the selectivities varied widely (Table 4.9; entries 21c & 22c, 24c & 25c).



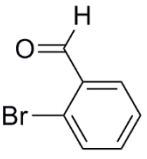
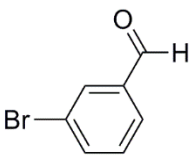
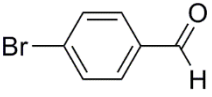
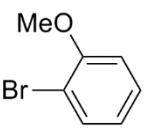
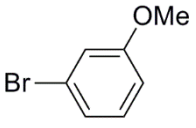
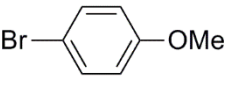
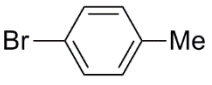
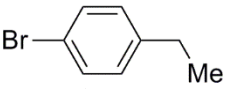
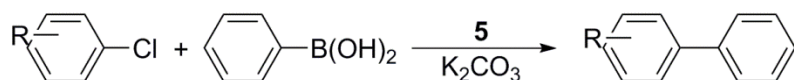
Substrate	Catalyst	Entry	Conversion [%]	S ^{hetero} [%]
	5	21a	77.9	95.6
		21c	84.8	95.3
	5	22a	65.1	87.5
		22c	83.3	40.0
	5	23a	89.6	94.6
		23c	100	99.9
	5	24a	29.3	72.4
		24c	67.3	19.0
	5	25a	51.6	85.4
		25c	68.2	28.7
	5	26a	68.0	76.3
		26c	83.0	89.9
	5	27a	63.2	75.0
		27c	67.0	86.5
	5	28a	49.1	70.8
		28c	20.9	87.4

Table 4.9: Suzuki-Miyaura coupling by **5**; Reaction conditions: aryl bromide (0.270 mmol), phenylboronic acid (0.324 mmol), K₂CO₃ (0.811 mmol), **5** (10.0 mol% Pd), solvent (a-toluene, c-H₂O; 3.0 mL), 40 °C, 20 h; all reactions were monitored for conversion by GC.

It was difficult to identify any clear trends for the reactions that were carried out in toluene solutions: the catalyst selectively activated the C–Br bond in *para*-substituted substrates, followed in succession by the *ortho*- and *meta*- aryl bromides (Table 4.9; entries 21a & 22a). Conversely, **5** was found to be more reactive with *meta*-substituted, deactivated systems than with the corresponding *ortho*-reagents (Table 4.9; entries 24a & 25a). This difference in reactivity trends may be attributed to a stronger steric influence in the case of the deactivated aryl bromides, whereas electronic effects may be more important for the analogous activated systems.

The final investigation of the catalytic activity of **5** for the Suzuki-Miyaura cross-coupling reaction was carried out by the exploration of the reactivities of the chlorobenzaldehyde family. It was decided to probe this particular family of aryl chlorides due to their previously measured high reactivity toward activated aryl chlorides using the analogous homogenous catalyst (**2**). Unfortunately, under these reaction conditions, it was discovered that **5** selectively generated the *homo*-coupled product (Table 4.10), thus rendering the catalyst inactive toward C–Cl activation. Optimization of the reaction conditions for aryl chloride systems is currently ongoing.



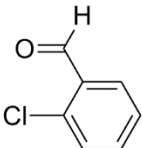
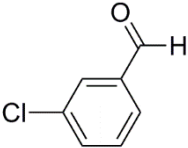
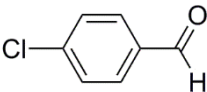
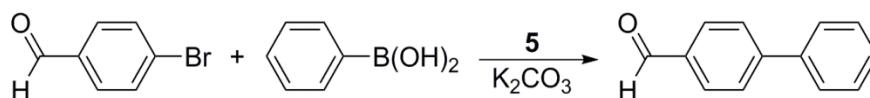
Substrate	Catalyst	Entry	Conversion [%]	S ^{hetero} [%]
	5	29a	13.5	5.8
		29c	74.4	12.3
	5	30a	10.1	2.5
		30c	12.2	0
	5	31a	9.5	17.4
		31c	1.2	0

Table 4.10: Suzuki-Miyaura biaryl coupling of aryl chlorides by **5**; Reaction conditions: aryl chloride (0.357 mmol), phenylboronic acid (0.429 mmol), K₂CO₃ (1.07 mmol), **5** (10.0 mol% Pd), solvent (a-toluene, c-H₂O; 3.0 mL), 40 °C, 48h; all reactions were monitored by GC.

4.3.5 Recyclability of **5**

Although **5** was unable to activate the C–Cl bond for the Suzuki-Miyaura cross-coupling reaction of aryl chlorides with phenylboronic acid, the catalyst exhibited substantial reactivity toward *p*-bromobenzaldehyde in both toluene and water. The reactivity was found to be comparable to that observed for the analogous homogeneous catalyst (**2**). It was determined subsequently that **2** operated in a combined homogeneous/heterogeneous manner in toluene solutions and only heterogeneously in aqueous media by means of hot filtration tests and ICP-MS analysis. In order to compare

the homogeneous and heterogeneous catalysts directly, a hot filtration test was performed on **5** in an effort to establish the active Pd species in solution. This was achieved by terminating a Suzuki reaction after 20 h in either toluene or H₂O solution, followed by immediate centrifugation (15 min, 8.5 krpm) of the hot reaction mixture in order to separate the supernatant and the precipitate. Each reaction layer was then analyzed by ICP-MS to measure the Pd content of each sample (Table 4.11). In both media, the majority of Pd was found in the precipitate, which is typical of the behavior of insoluble heterogeneous catalysts. It was particularly noteworthy that significantly more Pd metal was present in the supernatant layer of the toluene solution (Table 4.11; entry 32a), thus indicating that slight decomposition of **5** had taken place when toluene was employed.



Catalyst	Entry	% Pd		Conversion [%]	
		sup ^a	ppt ^a	sup	ppt
1	32a	7	93	36.1	14.5
	32c	<1	>99	64.4	23.1
Pd-PVP	33 ^b	-	-	0.06	51.5

Table 4.11: Recyclability of **5** in Suzuki-Miyaura biaryl coupling of the *p*-bromobenzaldehyde supernatant (*sup*) and precipitate (*ppt*); Reaction conditions: *p*-bromobenzaldehyde (0.270 mmol), phenylboronic acid (0.324 mmol), K₂CO₃ (0.811 mmol), Pd (10 mol%), solvent (a-toluene, c-H₂O; 3.0 mL), 40 °C, 20 h; all reactions were monitored by GC. ^a % Pd of supernatant and precipitate determined by ICP-MS. ^b *p*-bromobenzaldehyde (0.270 mmol), phenylboronic acid (0.324 mmol), K₂CO₃ (0.811 mmol), H₂O (3.0 mL), Pd-PVP (0.537 mmol), 40 °C, 20 h.

The supernatant and precipitate were separated and injected into fresh reaction mixtures containing new reagents. Each system was heated to 40 °C and stirred vigorously for 20 h. The resulting reaction mixtures were monitored by GC for conversion to *p*-biphenylaldehyde (Table 4.11). Interestingly, even though small amounts of Pd existed in the aqueous supernatant layer, it proved to have the highest reactivity toward the new *p*-bromobenzaldehyde reagent (Table 4.11; entry 32c). Furthermore, the insoluble Pd species activated the C–Br bond in less than 25% conversion in both toluene and water (Table 4.11; entry 32a,c). The recyclability of **5** was further explored by performing the hot filtration test consecutively two additional times. The fast deactivation of the catalyst is pictorially represented by Figure 4.7, and the corresponding activity data is summarized in Table 4.12. The catalyst rapidly became inactive following the second trial in toluene, whereas approximately 20% conversion was realized when the reaction was carried out in H₂O.

In conclusion, these results indicate that the catalyst experienced slight decomposition in toluene solutions, yet remained intact as a heterogeneous species in aqueous media. Although metallic Pd was present in the supernatant layer of each solvent, the Pd species in H₂O was significantly more active than the related catalyst entities in toluene. This outcome can be attributed to the decomposition of the catalyst into different types of soluble Pd species, dependent upon the nature of the reaction medium. Furthermore, the precipitate was unsuccessfully recycled in both toluene and H₂O, thus rendering the heterogeneous catalyst essentially useless. Taken collectively, the previous examples demonstrate that the performance of the heterogeneous catalyst (**5**) is inadequate in comparison with that of the analogous homogeneous catalyst (**2**).

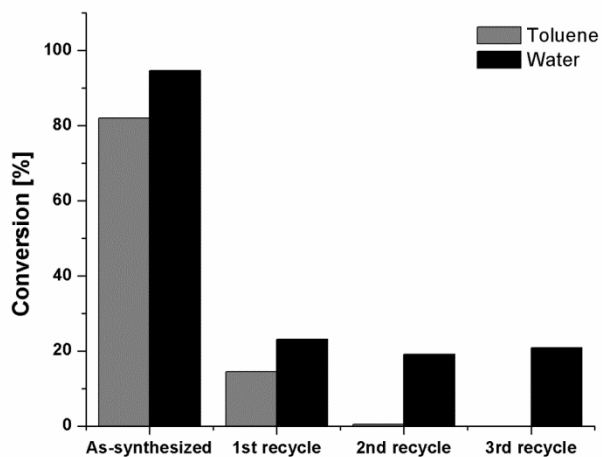
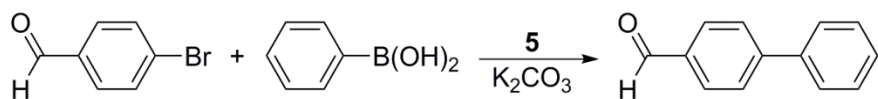
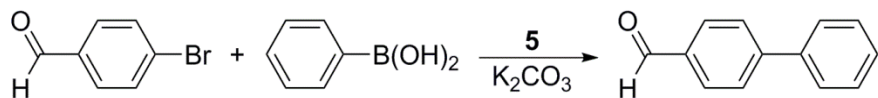


Figure 4.7: Recyclability for (NHC)PdCl₂(PPh₃)@SiO₂ (**5**) in toluene (grey) and H₂O (black) over four consecutive trials.

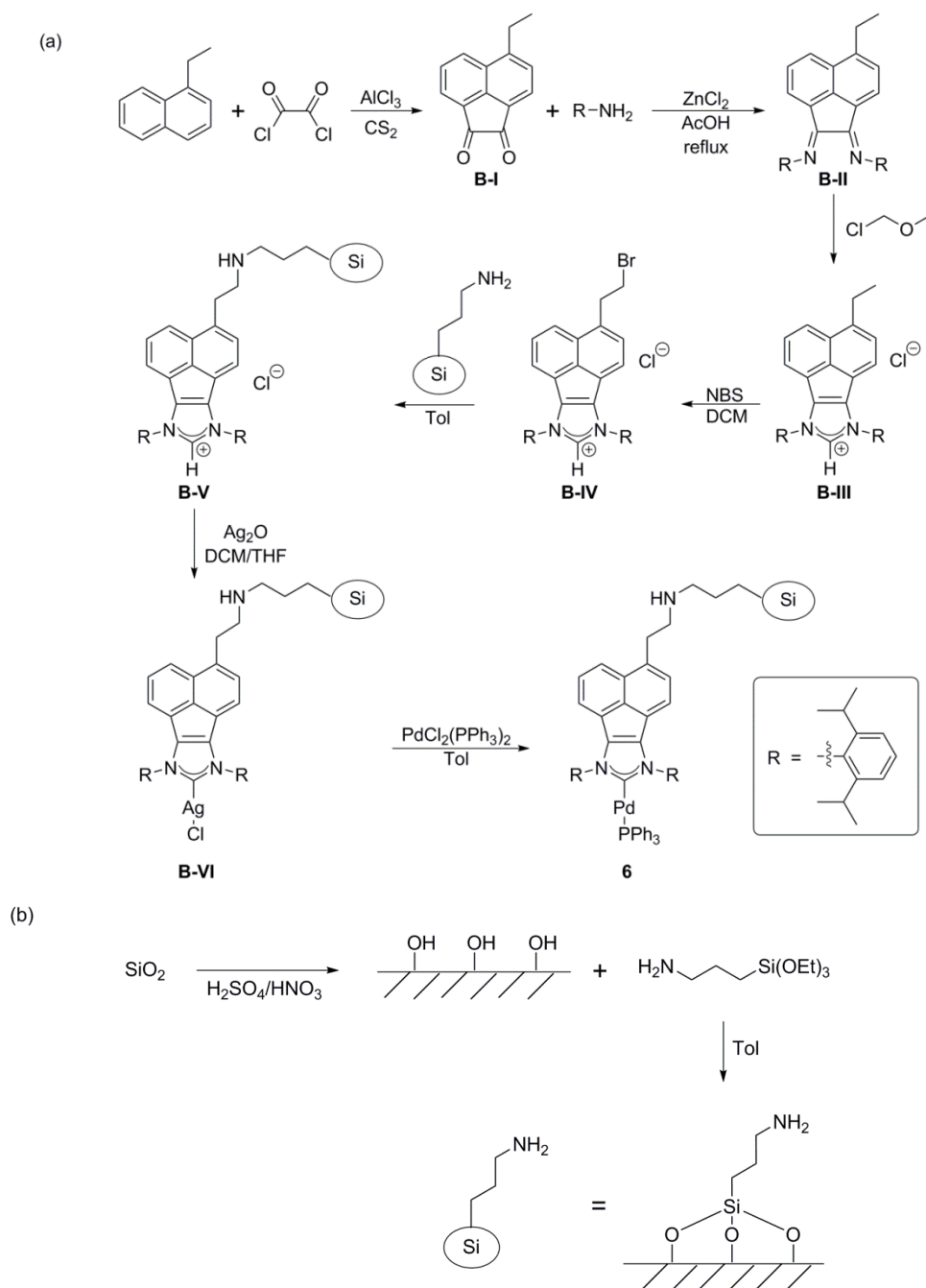


Entry	Solvent	Trial 1 [%]	Trial 2 [%]	Trial 3 [%]	Trial 4 [%]
34	Toluene	82.0	14.5	0.5	0
35	H ₂ O	94.6	23.1	19.1	20.8

Table 4.12: Recyclability of **5** in Suzuki-Miyaura biaryl coupling of the *p*-bromobenzaldehyde supernatant (*sup*) and precipitate (*ppt*); Reaction conditions: *p*-bromobenzaldehyde (0.270 mmol), phenylboronic acid (0.324 mmol), K₂CO₃ (0.811 mmol), Pd (10 mol%), solvent (toluene, H₂O; 3.0 mL), 40 °C, 20 h; all reactions were monitored by GC.

4.3.6 Synthesis and characterization of **6**

In an attempt to design a more effective heterogeneous catalyst, the tether length of **5** was altered by utilizing alternative substituted-naphthalene reagents. In the case of 1-ethylnaphthalene, a similar synthetic route was used for the generation of catalyst **6** as used to prepare **5** (Scheme 4.2; see experimental section for further synthetic details). These starting materials are more expensive than those used to obtain **5**, in addition to a low overall yield of 2.7%. Catalyst **6** was characterized by means of UV-vis, IR, and TGA and comparable trends were observed to those for **5**. However, **B-V** exhibited peaks at lower energy due to the stability provided by the electrostatic interactions of the imidazolium and counteranions, whereas a blue shift was observed following the complexation of **B-V** with Pd metal (Figure 4.8 and Table 4.13). TGA data for **6** revealed a total weight loss of 19%, which suggests that the ligand is in fact tethered onto the silica surface. Furthermore, this observation also indicated that two separate decompositions occur, correlating to the sequential loss of a phosphine ligand, followed by the NHC ligand (Figure 4.9).



Scheme 4.2: (a) Synthesis of silica-anchored BIAN palladium catalyst **6** (b) Synthesis of functionalized silica.

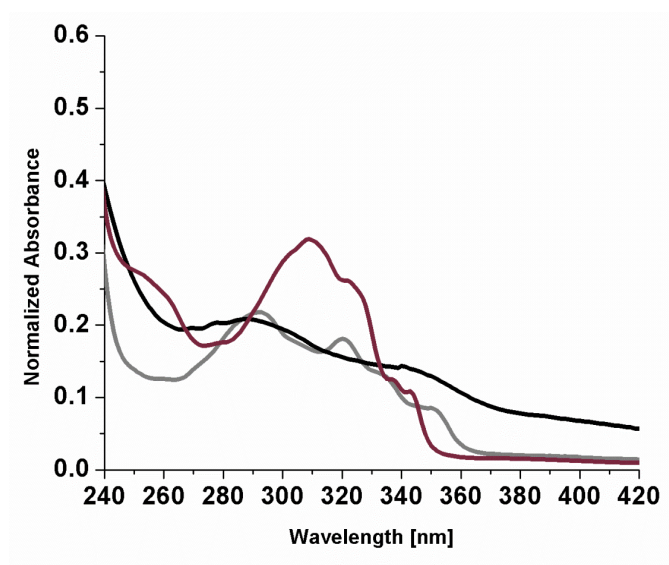


Figure 4.8: UV-vis spectra of (NHC)(PPh₃)PdCl₂ (**2**, dark grey), Imidazolium@SiO₂ (**B-V**, light grey), and (NHC)PdCl₂(PPh₃)@SiO₂ (**6**, black).

IR	CH ₂ -CH ₂ [cm ⁻¹]	CH ₂ -NH [cm ⁻¹]
APTES@SiO ₂	1659	1554
B-V	1633	1480
6	1650	1556

Table 4.13: IR peak assignments for APTES@SiO₂, Imidazolium@SiO₂ (**B-V**), and (NHC)PdCl₂(PPh₃)@SiO₂ (**6**).

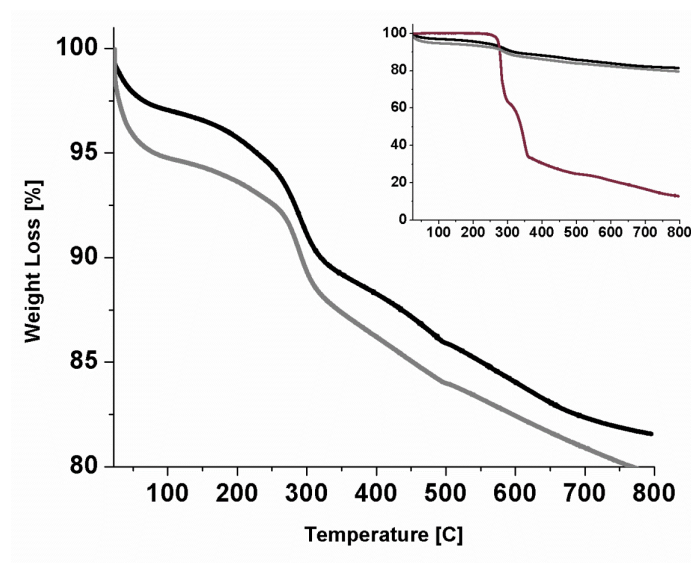
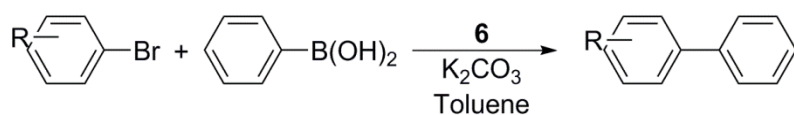


Figure 4.9: TGA for (NHC)(PPh₃)PdCl₂ (**2**, dark grey), Imidazolium@SiO₂ (**B-V**, light grey), and (NHC)PdCl₂(PPh₃)@SiO₂ (**6**, black).

4.3.7 Catalytic activity of **6**

The catalytic activity of **6** for the Suzuki-Miyaura reaction was probed by repeating the experiments that were performed with *p*-aryl bromides and **5** in toluene at 100 °C. The initial experiments were carried out using 5.0 mol% Pd. The reactions were terminated after twenty hours and analyzed for conversion to the *p*-biphenyl products by GC. As might be expected, the low catalyst loading only afforded minor quantities of the desired *hetero*-coupled product (Table 4.14). Interestingly, **6** was found to be the most reactive toward the activated and deactivated systems (Table 4.14; entries 36 & 37); however the *homo*-coupled product was selectively generated in the case of the activated systems (Table 4.14; entry 36).

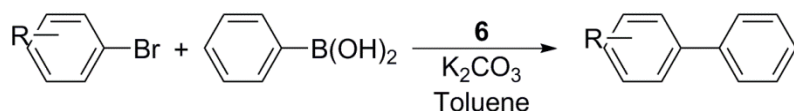


Substrate	Entry	Cat. Loading [mol %]	Temp. [°C]	Conv. [%]	S ^{hetero} [%]
	36	5.0	100	21.9	12.0
	37	5.0	100	20.2	77.6
	38	5.0	100	6.8	87.5
	39	5.0	100	11.9	83.1

Table 4.14: Suzuki-Miyaura biaryl coupling of aryl bromides by **6**; Reaction conditions: aryl bromide (0.270 mmol), phenylboronic acid (0.324 mmol), K₂CO₃ (0.811 mmol), **6** (5.0 mol% Pd), solvent (toluene; 3.0 mL), 100 °C, 20 h; all reactions were monitored for conversion by GC.

In an attempt to improve the activity of **6**, the catalyst loading was increased to 10.0 mol% Pd. The catalytic activity increased substantially from 21% to 78% conversion, simply by doubling the catalyst loading (Table 4.6 & Table 4.15; entries 13a & 40). Furthermore, the selectivity also increased dramatically from 12% to 93% for generation of the *hetero*-coupled product. These results were promising, yet at otherwise identical reaction conditions, **5** activated *p*-bromobenzaldehyde with 89% conversion and

94% selectivity. In conclusion, the extended tether of **6** was used to promote C–Br activation in toluene at 100 °C, but the catalyst appeared to be less active than that of the corresponding catalyst **5**.

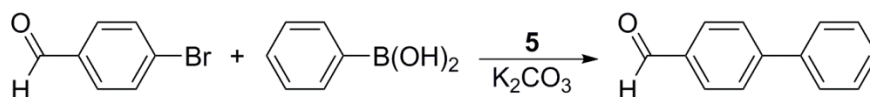


Substrate	Entry	Cat. Loading [mol %]	Temp. [°C]	Conv. [%]	S ^{hetero} [%]
	40	10.0	100	78.6	92.9

Table 4.15: Suzuki-Miyaura biaryl coupling of aryl bromides by **6**; Reaction conditions: aryl bromide (0.270 mmol), phenylboronic acid (0.324 mmol), K₂CO₃ (0.811 mmol), **6** (10.0 mol% Pd), solvent (toluene; 3.0 mL), 100 °C, 20 h; all reactions were monitored for conversion by GC.

4.3.8 Final optimization of **5**

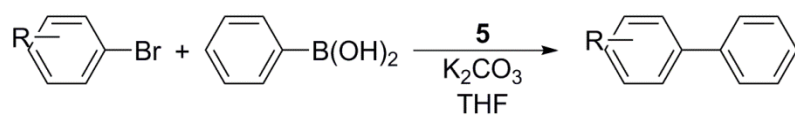
Catalyst **5** exhibited suitable reactivity toward C–X bonds at moderate catalyst loadings and high temperatures. The previously discussed reaction conditions were optimized with an objective of making direct comparison of catalysts **1-4** and **5**. However, it was later determined that the catalyst displayed much higher reactivity when employed in alternative polar solvents (Table 4.16). In particular, the catalyst was found to operate extremely well in THF at 80 °C (Table 4.16; entry 42).



Entry	Solvent	Cat. Loading [mol %]	Temp. [°C]	Conv. [%]	S ^{hetero} [%]
41	NMP	10.0	80	0.3	85.8
42	THF	10.0	80	100	100
43	DME	10.0	80	30.1	97.4
44	EtOH:H ₂ O	10.0	80	36.4	25.1

Table 4.16: Optimization of **5** in N-methyl-2-pyrrolidone (NMP), tetrahydrofuran (THF), dimethoxyethane (DME), and ethanol:water (EtOH:H₂O 1:1); Reaction conditions: *p*-bromobenzaldehyde (0.270 mmol), phenylboronic acid (0.324 mmol), K₂CO₃ (0.811 mmol), **5** (10 mol%), solvent (3.0 mL), 100 °C, 20 h; all reactions were monitored by GC.

Catalyst **5** exhibited the highest activity in THF at 80 °C, and therefore additional experiments were performed on *p*-bromoanisole, *p*-bromotoluene, and *p*-bromoethylbenzene (Table 4.17). Interestingly, **5** selectively constructed the *p*-biphenyl compound from both *p*-bromoanisole and *p*-bromoethylbenzene (Table 4.17; entries 46 & 48). However, only the *homo*-coupled product was formed in the presence of *p*-bromotoluene (Table 4.17; entries 47). Similar trends were observed in toluene and water for otherwise identical reaction conditions (Table 4.9; entries 26-28). **5** was also used in THF along with *p*-chlorobenzaldehyde in order to determine its reactivity toward C–Cl bonds (Table 4.18). This resulted in 84% conversion with 62% selectivity in the case of the *hetero*-coupled product. The investigation of aryl chlorides is currently ongoing.



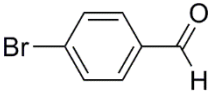
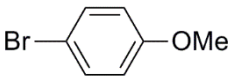
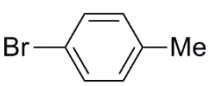
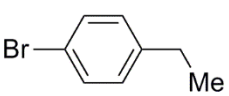
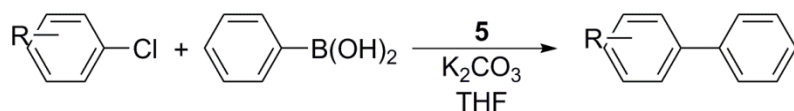
Substrate	Entry	Cat. Loading [mol %]	Temp. [°C]	Conv. [%]	S ^{hetero} [%]
	45	10.0	80	100	100
	46	10.0	80	95.1	98.3
	47	10.0	80	100	11.2
	48	10.0	80	93.5	96.6

Table 4.17: Suzuki-Miyaura biaryl coupling of aryl bromides by **5**; Reaction conditions: aryl bromide (0.270 mmol), phenylboronic acid (0.324 mmol), K₂CO₃ (0.811 mmol), **5** (10.0 mol % Pd), THF (3.0 mL), 80 °C, 48 h; all reactions were monitored for conversion by GC.



Substrate	Entry	Cat. Loading [mol %]	Temp. [°C]	Conv. [%]	S ^{hetero} [%]
	49	10.0	80	84.4	62.5

Table 4.18: Suzuki-Miyaura biaryl coupling of aryl bromides by **5**; Reaction conditions: aryl chloride (0.357 mmol), phenylboronic acid (0.429 mmol), K₂CO₃ (1.07 mmol), **5** (10.0 mol % Pd), THF (3.0 mL), 80 °C, 48h; all reactions were monitored by GC.

4.4 CONCLUSIONS

In conclusion, two new heterogeneous catalysts have been synthesized and characterized by means of UV-vis, FT-IR, TGA, and ICP-MS spectroscopy. The complexes contained 0.155–0.868 mmol g⁻¹ of Pd and were able to activate C–X bonds for the Suzuki reaction. Both catalysts exhibited reactivity toward aryl iodides and bromides, however, very little C–Cl activation was observed. As observed with catalysts **3** and **4**, **5** and **6** were unable to overcome the energy barrier in order to completely oxidatively add the aryl chloride substrates to the palladium catalysts. The S_N2 mechanism is dependent on the dissociation of the C–X bond and only catalysts **1** and **2** were able to facilitate such transformations. In comparison with catalyst **2**, catalyst **5** was found to be significantly less active and was recycled fewer times than the analogous homogeneous catalyst. Furthermore, **5** displayed a clear solvent dependence, in which higher conversion to the biphenyl product was observed in THF than in toluene or water

under otherwise identical reaction conditions. These results may be correlated with the tendency of catalysts to leach in highly polar solvents, such as THF. Further exploration of the active catalyst in THF is ongoing.

4.5 SUMMARY OF KEY RESULTS

- **5** and **6** were considerably less active than **2**
- THF facilitated the highest catalytic activity, followed in succession by toluene and H₂O
- Neither catalyst effectively activated the C–Cl bond in aryl chloride substrates

4.6 ACKNOWLEDGEMENTS

The authors thank Ms. Stephany García for supplying the Pd-PVP catalysts, Alisha Bohnsack for performing TGA measurements, and the Robert A. Welch Foundation (F-1738, F-003) for funding.

4.7 EXPERIMENTAL

4.7.1 General Procedures

All glassware was oven-dried before use. All reagents were obtained commercially and used without further purification. Toluene and THF were dried over sodium and freshly distilled prior to use. The dichloromethane was dried over calcium hydride and freshly distilled prior to use.

4.7.2 Physical Measurements

Low-resolution CI mass spectra were obtained on a Thermo Scientific TSQ Quantum GC mass spectrometer and high-resolution CI mass spectra were recorded on a magnetic sector Waters Autospec Ultima instrument. ¹H and ¹³C{¹H} NMR spectra were

recorded at 295 K in the indicated solvent on a Varian Unity 300 (^1H , 300 MHz; ^{13}C , 75 MHz) or a Varian AS400 spectrometer (^1H , 400 MHz; ^{13}C , 100 MHz) immediately following sample preparation. Deuterated solvents were obtained from Cambridge Isotopes and stored over 4 Å molecular sieves prior to use. ^1H and $^{13}\text{C}\{^1\text{H}\}$ chemical shift values are reported in parts per million (ppm) relative to SiMe_4 (δ 0.00), using solvent resonances as internal standards. Absorption spectra were recorded on a Varian Cary 6000i UV-VIS-NIR spectrophotometer with Starna Quartz fluorometer cells with a pathlength of 10 mm. Gas chromatography (GC) was performed on an Agilent 6850 gas chromatograph (HP-1 column, l = 30 m, I.D. = 0.32 mm) equipped with a flame ionization detector (FID). The GC oven temperature was held at 50 °C for 3 min, then increased to 300 °C at 30 °C min^{-1} . The internal standard mesitylene was used to aid in measuring reaction conversions.

4.7.3 Preparations

4.7.3.1 1-methylacenaphthenequinone (A-I)

Oxalyl chloride (17.5 g, 0.139 mol) was added to a 250 mL Schlenk flask containing aluminum chloride (23.2 g, 0.177 mol) in degassed carbon disulfide (100 mL) at -78 °C. 1-methylnaphthalene (7.05 g, 0.0496 mol) was added to the solution, after which the reaction mixture was allowed to warm to -10 °C for three hours, followed by one hour at ambient temperature. The reaction was terminated by the dropwise addition of water and the solvent was removed. Activated carbon (1.0 g) and urea (1.0 g) were added to the resulting yellow solid, and were dispersed in aqueous sodium bisulfite. The reaction mixture was heated to 80 °C for an hour, after which it was immediately filtered (note: both filtrate and precipitate contain product). Concentrated hydrochloric acid was

added to the filtrate and rapidly heated to 80 °C until yellow needle-type crystals precipitated out of solution. Meanwhile, the resulting black precipitate and additional activated carbon (1.0 g) were re-dispersed in aqueous sodium bisulfite and heated to 80 °C. This procedure was repeated until the analytically pure yellow crystals ceased to appear (2.39, 25%). MS (Cl^+ , CH_4): m/z 197.1 $[\text{M} + \text{H}]^+$, 219.0 $[\text{M} + \text{Na}]^+$, 415.1 $[2\text{M} + \text{Na}]^+$; ^1H NMR (CDCl_3): δ 2.85 (s, 3H, Naph- CH_3), 7.66 (d, 1H, Naph-H), 7.84 (t, 1H, Naph-H), 8.03 (d, 1H, Naph-H), 8.07 (d, 1H, Naph-H), 8.32 (d, 1H, Naph-H); ^{13}C NMR (CDCl_3): 145.93, 142.63, 129.84, 129.49, 128.72, 128.56, 128.01, 122.26, 121.98, 121.65, 19.25

4.7.3.2 1-ethylacenaphthenequinone (B-I)

Oxalyl chloride (22.8 g, 0.181 mol) was added to a 250 mL Schlenk flask containing aluminum chloride (30.19 g, 0.230 mol) in degassed carbon disulfide (150 mL) at -78 °C. 1-ethylnaphthalene (10.1 g, 0.06474 mol) was added to the solution, after which the reaction mixture was allowed to warm to -10 °C for three hours, followed by one hour at ambient temperature. The reaction was terminated by the dropwise addition of water and the solvent was removed. Activated carbon (1.0 g) and urea (1.0 g) were added to the resulting yellow solid, and were dispersed in aqueous sodium bisulfite. The reaction mixture was heated to 80 °C for 1 h, after which it was immediately filtered (note: both filtrate and precipitate contain product). Concentrated hydrochloric acid was added to the filtrate and rapidly heated to 80 °C until yellow needle-type crystals precipitated out of solution. Meanwhile, the resulting black precipitate and additional activated carbon (1.0 g) were re-dispersed in aqueous sodium bisulfite and heated to 80 °C. This procedure was repeated until the analytically pure yellow crystals ceased to appear (3.275, 12%). MS (Cl^+ , CH_4): m/z 211.1 $[\text{M} + \text{H}]^+$, 228.1 $[\text{M} + \text{NH}_4]^+$, 233.1 $[\text{M} +$

$\text{Na}]^+$ 443.1 $[2\text{M} + \text{Na}]^+$; ^1H NMR (CDCl_3): δ 1.44 (t, 3H, Naph- CH_2CH_3), 3.25 (q, 2H, Naph- CH_2CH_3), 7.68 (d, 1H, Naph-H), 7.84 (t, 1H, Naph-H), 8.04-8.08 (d/d, 2H, Naph-H), 8.38 (d, 1H, Naph-H); ^{13}C NMR (CDCl_3): 148.16, 142.32, 129.12, 127.57, 126.63, 122.06, 121.22, 25.62, 14.24

4.7.3.3 1-methyl(dipp)BIAN (A-II)

A-I (5.0 g, 25.5 mol), 2,6-diisopropylaniline (10.38 g, 58.67 mol), and zinc chloride (9.36 g, 68.87 mol) were placed into a 100 mL round bottom flask equipped with a condenser. Glacial acetic acid (150 mL) was added *via* the condenser and the reaction mixture was heated to reflux overnight. The reaction mixture was cooled to ambient temperature and filtered, after which the orange precipitate was dissolved in dichloromethane (50 mL). The zinc was removed from the complex through an extraction with aqueous $\text{K}_2\text{C}_2\text{O}_4$. The resulting organic layer was dried in a crystallization dish overnight, producing an analytically pure orange solid (5.087 g, 39%). MS (Cl^+ , CH_4): m/z 515.3 $[\text{M} + \text{H}]^+$, 537.3 $[\text{M} + \text{Na}]^+$, 1051.7 $[2\text{M} + \text{Na}]^+$; ^1H NMR (CDCl_3): δ 0.94 (d, 12H, CH_3), 1.23 (d, 12H, CH_3), 2.61 (s, 3H, Naph- CH_3), 3.03 (sept, 4H, $-\text{CH}(\text{CH}_3)_2$), 6.55 (d, 1H, Naph-H), 6.64 (d, 1H, Naph-H), 7.16 (d, 1H, Naph-H), 7.19-7.26 (d/t, 6H, Ar-H), 7.34 (t, 1H, Naph-H), 7.94 (d, 1H, Naph-H); ^{13}C NMR (CDCl_3): 147.44, 135.39, 128.17, 127.45, 125.82, 124.21, 123.60, 123.40, 28.58, 23.45, 23.11.

4.7.3.4 1-ethyl(dipp)BIAN (B-II)

B-I (0.259 g, 1.23 mmol), 2,6-diisopropylaniline (0.501 g, 2.83 mmol), and zinc chloride (0.446 g, 3.28 mmol) were placed into a 50 mL round bottom flask equipped with a condenser. Glacial acetic acid (10 mL) was added *via* the condenser and the reaction mixture was heated to reflux overnight. The reaction mixture was cooled to

ambient temperature and filtered, after which the orange precipitate was dissolved in dichloromethane (15 mL). The zinc was removed from the complex through an extraction with aqueous $K_2C_2O_4$. The resulting organic layer was dried in a crystallization dish overnight, producing an analytically pure orange solid (0.402 g, 32%). MS (Cl^- , CH_4): m/z 529.4 $[M + H]^+$, 551.3 $[M + Na]^+$, 1079.7 $[2M + Na]^+$; 1H NMR ($CDCl_3$): δ 0.95 (d, 12H, CH_3), 1.24 (d, 12H, CH_3), 1.31 (t, 3H, Naph- CH_2CH_3), 2.91 (q, 2H, Naph- CH_2CH_3), 3.02 (sept, 4H, $-CH(CH_3)_2$), 6.57 (d, 1H, Naph-H), 6.63 (d, 1H, Naph-H), 7.03 (d, 1H, Naph-H), 7.16-7.25 (d/t, 6H, Ar-H), 7.34 (t, 1H, Naph-H), 7.99 (d, 1H, Naph-H); ^{13}C NMR ($CDCl_3$): 141.11, 135.59, 130.82, 129.87, 127.74, 127.48, 126.41, 125.73, 124.22, 123.41, 28.58, 23.43, 23.13.

4.7.3.5 [1-methyl(IPr)BIAN]Cl (A-III)

Chloromethyl methyl ether (3.0 mL) was added to a pressure vessel containing **A-II** (2.335 g, 4.54 mmol), and was heated to 100 °C overnight. The reaction mixture was then cooled to room temperature and dispersed in diethyl ether. The solvents were removed *in vacuo* and the resulting precipitate was dissolved in toluene. An aqueous extraction was then performed on the solution, in which the analytically pure yellow product was obtained from the aqueous layer upon solvent removal (1.263 g, 49%). MS (Cl^- , CH_4): m/z 527.3 $[M - Cl]^+$, 1089.7 $[2M - Cl]^+$; 1H NMR ($CDCl_3$): δ 1.15 (d, 12H, CH_3), 1.34 (d, 12H, CH_3), 2.67 (sept, 4H, $-CH(CH_3)_2$), 2.79 (s, 3H, Naph- CH_3), 7.09 (d, 1H, Naph-H), 7.20 (d, 1H, Naph-H), 7.33 (d, 1H, Naph-H), 7.47 (d, 4H, Ar-H), 7.56 (t, 1H, Naph-H), 7.68 (t, 2H, Ar-H), 8.14 (d, 1H, Naph-H), 11.39 (s, 1H, imid-H); ^{13}C NMR ($CDCl_3$): 144.55, 131.91, 127.98, 128.34, 128.56, 124.61, 122.74, 121.54, 28.98, 24.21, 23.07.

4.7.3.6 [1-ethyl(*IPr*)*BIAN*]/Cl (**B-III**)

Chloromethyl methyl ether (3.0 mL) was added to a pressure vessel containing **B-II** (0.402 g, 0.763 mmol), and was heated to 100 °C overnight. The reaction mixture was then cooled to room temperature and dispersed in diethyl ether. The solvents were removed *in vacuo* and the resulting precipitate was dissolved in toluene. An aqueous extraction was then performed on the solution, in which the analytically pure yellow product was obtained from the aqueous layer upon solvent removal (0.15 g, 34%). MS (Cl^+ , CH_4): m/z 541.4 [$\text{M} - \text{Cl}$] $^+$, 1117.7 [$2\text{M} - \text{Cl}$] $^+$; ^1H NMR (CDCl_3): δ 1.14 (d, 12H, CH_3), 1.37 (d, 12H, CH_3), 2.33 (s, 3H, $\text{Naph-CH}_2\text{CH}_3$), 2.70 (sept, 4H, $-\text{CH}(\text{CH}_3)_2$), 2.78 (s, 2H, $\text{Naph-CH}_2\text{CH}_3$), 7.06 (d, 1H, Naph-H), 7.21 (d, 1H, Naph-H), 7.29 (d, 1H, Naph-H), 7.44 (d, 4H, Ar-H), 7.54 (t, 1H, Naph-H), 7.64 (t, 2H, Ar-H), 8.09 (d, 1H, Naph-H), 11.99 (s, 1H, imid-H); ^{13}C NMR (CDCl_3): 144.91, 143.21, 140.29, 137.48, 136.84, 132.09, 13.21, 129.29, 128.97, 128.29, 128.16, 127.88, 127.26, 124.88, 123.03, 122.37, 121.21, 29.36, 24.68, 23.48.

4.7.3.7 [1-bromomethyl(*IPr*)*BIAN*]/Cl (**A-IV**)

N-bromosuccinimide (0.288 g, 1.62 mmol) was added to a 100 mL Schlenk flask containing **A-III** (0.8247 g, 1.47 mmol) dissolved in dry dichloromethane (40 mL). Subsequently, a catalytic amount of benzoyl peroxide was introduced to the reaction mixture as a radical initiator, and the solution was allowed to vigorously stir at ambient temperature overnight. Aqueous sodium thiosulfate was utilized to terminate the reaction, followed by an aqueous extraction with toluene. The organic layer was separated and dried *in vacuo*. Recrystallization from ether afforded the analytically pure red/brown solid (0.6695 g, 71%). MS (Cl^+ , CH_4): m/z ^1H NMR (CDCl_3): δ 1.09 (d, 12H, CH_3), 1.29 (d, 12H, CH_3), 2.65 (sept, 4H, $-\text{CH}(\text{CH}_3)_2$), 3.43 (d/d, 2H, $\text{Naph-CH}_2\text{Br}$), 7.06 (d, 1H,

Naph-H), 7.16 (d, 1H, Naph-H), 7.31 (d, 1H, Naph-H), 7.41 (d, 4H, Ar-H), 7.54 (t, 1H, Naph-H), 7.66 (t, 2H, Ar-H), 8.09 (d, 1H, Naph-H), 10.46 (s, 1H, imid-H); ^{13}C NMR (CDCl_3): 144.77, 142.19, 140.33, 137.60, 136.97, 132.42, 130.21, 129.00, 128.30, 127.89, 125.06, 123.14, 22.48, 121.20, 29.36, 24.43, 23.66.

4.7.3.8 [1-bromoethyl(IPr)BIAN]Cl (**B-IV**)

N-bromosuccinimide (0.066 g, 0.369 mmol) was added to a 100 mL Schlenk flask containing **B-III** (0.193 g, 0.335 mmol) dissolved in dry dichloromethane (15 mL). Subsequently, a catalytic amount of benzoyl peroxide was introduced to the reaction mixture as a radical initiator, and the solution was allowed to vigorously stir at ambient temperature overnight. Aqueous sodium thiosulfate was utilized to terminate the reaction, followed by an aqueous extraction with toluene. The organic layer was separated and dried *in vacuo*. Recrystallization from ether afforded the analytically pure red/brown solid (0.102 g, 47%). MS (Cl^+ , CH_4): m/z 619.3 $\{\text{M} - \text{Cl}\}^+$; ^1H NMR (CDCl_3): δ 1.22 (d, 12H, CH_3), 1.34 (d, 12H, CH_3), 2.66 (sept, 4H, $-\text{CH}(\text{CH}_3)_2$), 2.12 (t, 2H, Naph- $\text{CH}_2\text{CH}_2\text{Br}$), 3.47-3.56 (d/d, 2H, Naph- $\text{CH}_2\text{CH}_2\text{Br}$), 7.16 (d, 1H, Naph-H), 7.44 (d, 4H, Ar-H), 7.59 (t, 1H, Naph-H), 7.66 (t, 2H, Ar-H), 8.06 (d, 1H, Naph-H), 8.29 (d, 1H, Naph-H), 10.65 (s, 1H, imid-H); ^{13}C NMR (CDCl_3): 144.41, 137.28, 131.85, 129.58, 128.61, 127.70, 124.55, 122.06, 28.90, 23.95, 23.21.

4.7.3.9 Functionalized Silica (**C**)

Silica dioxide (3.1 g, 100-240 mesh) was placed into a 100 mL round bottom flask, upon which $\text{H}_2\text{SO}_4\text{:HNO}_3$ (24:4.5 mL) was added to the reaction vessel. The reaction mixture was refluxed overnight. Successively, it was cooled to ambient temperature, filtered over a fine frit, and washed with H_2O (500 mL), acetone (50 mL),

methanol (50 mL), and dichloromethane (50 mL). The resulting white solid was dried under an absence of pressure at 150 °C for 48 hours. A slurry of aminopropyltriethoxysilane (1.66 mL) and dry toluene (10 mL) was injected into the reaction mixture and heated to 110 °C for 20 h. The resulting white solid was filtered and washed with H₂O (500 mL), acetone (50 mL), and toluene (50 mL). The resulting white solid was dried under an absence of pressure at 60 °C for 48 hours.

4.7.3.10 [1-methyl(IPr)BIAN]Cl@SiO₂ (A-V)

A-IV (0.448 g, 0.699 mmol) and **C** (0.525 g, 1.334 mmol g⁻¹) were dissolved in dry toluene (30 mL) in a 100 mL round bottom equipped with a condenser. The solution was heated to 110 °C for 20 hours. Subsequently, the reaction mixture was cooled to ambient temperature and filtered over a fine frit. The resulting yellow solid was washed with H₂O (100 mL), dichloromethane (100 mL), and toluene (100 mL). **A-V** was characterized by means of FT-IR, UV-vis, and TGA.

4.7.3.11 [1-ethyl(IPr)BIAN]Cl@SiO₂ (B-V)

B-IV (0.114 g, 0.174 mmol) and **C** (0.148 g, 1.1778 mmol g⁻¹) were dissolved in dry toluene (20 mL) in a 50 mL round bottom equipped with a condenser. The solution was heated to 110 °C for 20 hours. Subsequently, the reaction mixture was cooled to ambient temperature and filtered over a fine frit. The resulting yellow solid was washed with H₂O (100 mL), dichloromethane (100 mL), and toluene (100 mL). **B-V** was characterized by means of FT-IR, UV-vis, and TGA.

4.7.3.12 [1-methyl(IPr)BIAN]AgCl@SiO₂ (A-VI)

A 100 mL Schlenk flask was covered with aluminum foil prior to the addition of **A-V** (0.414 g) and excess Ag₂O (1.0 g). The solids were dispersed in 1:1

dichloromethane:tetrahydrofuran (30 mL) and vigorously stirred at ambient temperature for 24 hours. The resulting was filtered in the dark over a fine frit, and thoroughly washed with H₂O (400 mL), dichloromethane (100 mL), and toluene (100 mL). The afforded black product (**A-VI**) was used without further purification.

4.7.3.13 [1-ethyl(IPr)BIAN]AgCl@SiO₂ (B-VI**)**

A 100 mL Schlenk flask was covered with aluminum foil prior to the addition of **A-V** (0.102 g) and excess Ag₂O (1.0 g). The solids were dispersed in 1:1 dichloromethane:tetrahydrofuran (20 mL) and vigorously stirred at ambient temperature for 24 hours. The resulting was filtered in the dark over a fine frit, and thoroughly washed with H₂O (400 mL), dichloromethane (100 mL), and toluene (100 mL). The afforded black product (**B-VI**) was used without further purification.

4.7.3.14 [1-methyl(IPr)BIAN]PdCl₂PPh₃@SiO₂ (A-VII**)**

To a 100 mL round bottom flask covered in aluminum foil was added **A-VI** (0.3141 g, 1.334 mmol g⁻¹) and PdCl₂(PPh₃)₂ (0.323 g, 0.461 mmol) in dry toluene (15 mL). The reaction mixture was heated to 110 °C for 24 hours, cooled to ambient temperature, and then filtered over a fine frit. The resulting black precipitate was thoroughly washed with H₂O (300 mL), dichloromethane (300 mL), and toluene (300 mL). Finally, the catalyst was dried under vacuum at 80 °C for two days. **A-VII** was characterized by means of FT-IR, UV-vis, TGA, and ICP-MS.

4.7.3.15 [1-ethyl(IPr)BIAN]PdCl₂PPh₃@SiO₂ (B-VII**)**

To a 100 mL round bottom flask covered in aluminum foil was added **B-VI** (0.092 g, 1.1778 mmol g⁻¹) and PdCl₂(PPh₃)₂ (0.083 g, 0.119 mmol) in dry toluene (10 mL). The reaction mixture was heated to 110 °C for 24 hours, cooled to ambient

temperature, and then filtered over a fine frit. The resulting black precipitate was thoroughly washed with H₂O (300 mL), dichloromethane (300 mL), and toluene (300 mL). Finally, the catalyst was dried under vacuum at 80 °C for two days. **B-VII** was characterized by means of FT-IR, UV-vis, TGA, and ICP-MS.

4.7.4 General Procedure for Suzuki Cross-Coupling Reactions

Deionized water or dry toluene (3 mL) was added to a 20 mL scintillation vial containing the aryl halide (0.267 mmol), phenylboronic acid (0.321 mmol), potassium carbonate (0.802 mmol), **5** or **6** (10.0 mol% Pd), and the internal standard mesitylene (0.267 mmol). The scintillation vial was covered with a septum and wired down. The stirred reaction mixture was then heated to 100 °C. The resulting reaction mixture was allowed to stir for twenty hours for all the aryl iodides and bromides. On the other hand, the aryl chlorides required 48 hours to reach complete conversion. The resulting reaction mixture was cooled to ambient temperature, filtered over celite and washed with diethyl ether. The solvents were evaporated from the organic layer, thereby producing the desired product. The reactions were monitored by GC and the percent conversions were calculated based on the aryl halide. The NMR spectra of the products matched those of literature values.

Appendix A: X-Ray Tables

Identification code	shelxl	
Empirical formula	C36.67 H36.67 Cl1.33 N1.33 P0.67 Pd0.67	
Formula weight	634.85	
Temperature	293(2) K	
Wavelength	0.71073 Å	
Crystal system	monoclinic	
Space group	P2	
Unit cell dimensions	a = 12.669(4) Å	□ = 90°.
	b = 12.248(4) Å	□ = 90.014(6)°.
	c = 31.450(10) Å	□ = 90°.
Volume	4880(3) Å ³	
Z	6	
Density (calculated)	1.296 Mg/m ³	
Absorption coefficient	0.560 mm ⁻¹	
F(000)	1976	
Crystal size	? x ? x ? mm ³	
Theta range for data collection	1.29 to 25.00°.	
Index ranges	-15 ≤ h ≤ 15, -14 ≤ k ≤ 14, -37 ≤ l ≤ 37	
Reflections collected	73170	
Independent reflections	17137 [R(int) = 0.0999]	
Completeness to theta = 25.00°	99.9 %	
Refinement method	Full-matrix least-squares on F ²	
Data / restraints / parameters	17137 / 733 / 1116	
Goodness-of-fit on F ²	1.149	
Final R indices [I > 2σ(I)]	R1 = 0.0773, wR2 = 0.1621	
R indices (all data)	R1 = 0.0830, wR2 = 0.1674	
Absolute structure parameter	0.28(4)	
Largest diff. peak and hole	0.620 and -0.796 e.Å ⁻³	

Table A1: Crystal data and structure refinement for **2**.

	x	y	z	U(eq)
C(1)	2549(6)	7419(7)	965(2)	20(2)
C(2)	2373(6)	7611(8)	256(3)	29(2)
C(3)	3096(6)	6812(8)	322(2)	27(2)
C(4)	2242(6)	7835(7)	-200(2)	26(2)
C(5)	1656(8)	8513(9)	-461(3)	40(2)
C(6)	1802(9)	8421(10)	-906(3)	52(3)
C(7)	2473(8)	7660(11)	-1085(3)	54(3)
C(8)	3076(7)	6939(10)	-826(3)	37(2)
C(9)	2939(6)	7044(8)	-392(3)	30(2)
C(10)	3804(8)	6088(10)	-960(3)	48(3)
C(11)	4291(9)	5439(10)	-661(4)	60(3)
C(12)	4132(8)	5574(10)	-214(3)	55(3)
C(13)	3486(7)	6414(8)	-77(3)	35(2)
C(14)	1176(7)	8778(8)	705(3)	29(2)
C(15)	127(8)	8407(8)	689(3)	37(2)
C(16)	-669(9)	9215(12)	723(4)	61(3)
C(17)	-437(10)	10294(11)	770(4)	64(3)
C(18)	593(9)	10628(11)	798(3)	59(3)
C(19)	1416(8)	9864(9)	766(3)	42(2)
C(20)	-123(8)	7200(9)	650(3)	46(3)
C(21)	-1083(9)	6815(13)	911(4)	86(5)
C(22)	-311(8)	6850(10)	181(3)	57(3)
C(23)	2574(8)	10281(8)	749(3)	40(2)
C(24)	2875(9)	10655(9)	312(3)	49(3)
C(25)	2771(10)	11171(10)	1090(4)	61(3)
C(26)	3824(8)	5873(10)	981(3)	50(3)
C(27)	4885(10)	6129(11)	1050(4)	59(3)
C(28)	5479(11)	5180(13)	1246(4)	80(4)
C(29)	4910(13)	4239(12)	1351(5)	86(4)
C(30)	3879(13)	4071(12)	1282(5)	92(5)
C(31)	3293(11)	4897(9)	1083(4)	57(3)

C(32)	5395(8)	7199(10)	950(3)	52(3)
C(33)	6175(8)	7592(12)	1295(3)	70(4)
C(34)	5985(9)	7162(12)	508(3)	78(4)
C(35)	2176(10)	4688(9)	984(4)	61(3)
C(36)	1617(14)	3995(12)	1334(5)	99(5)
C(37)	2044(12)	4124(11)	548(4)	83(4)
C(38)	2038(7)	9101(8)	2529(3)	30(2)
C(39)	1948(8)	9346(9)	2958(3)	43(2)
C(40)	1475(9)	10315(10)	3088(4)	52(3)
C(41)	1085(8)	11029(9)	2796(3)	44(2)
C(42)	1157(8)	10805(9)	2362(3)	44(2)
C(43)	1622(7)	9821(7)	2233(3)	31(2)
C(44)	1811(7)	6815(8)	2654(3)	33(2)
C(45)	757(7)	6984(9)	2708(3)	42(2)
C(46)	119(9)	6172(10)	2916(3)	51(3)
C(47)	577(9)	5199(9)	3054(3)	54(3)
C(48)	1662(9)	5043(9)	3005(3)	48(3)
C(49)	2284(8)	5826(8)	2802(3)	42(2)
C(50)	3925(6)	7637(8)	2510(2)	30(2)
C(51)	4437(8)	6704(8)	2350(3)	40(2)
C(52)	5493(8)	6523(9)	2464(4)	53(3)
C(53)	6016(9)	7220(10)	2736(4)	59(3)
C(54)	5535(8)	8133(10)	2881(3)	51(3)
C(55)	4474(7)	8352(8)	2769(3)	38(2)
C(56)	7267(6)	2129(7)	4038(3)	24(2)
C(57)	6685(6)	2644(8)	4693(3)	27(2)
C(58)	7530(6)	1961(9)	4749(2)	26(2)
C(59)	6311(7)	3058(8)	5110(3)	32(2)
C(60)	5576(7)	3775(7)	5251(3)	32(2)
C(61)	5484(8)	3923(8)	5700(3)	42(2)
C(62)	6105(7)	3374(9)	5980(3)	41(2)
C(63)	6907(7)	2677(10)	5846(3)	39(2)

C(64)	6986(6)	2536(9)	5401(3)	32(2)
C(65)	7684(8)	2092(9)	6091(3)	42(2)
C(66)	8415(8)	1419(8)	5906(3)	40(2)
C(67)	8479(8)	1298(9)	5449(3)	41(2)
C(68)	7766(7)	1859(10)	5205(3)	38(2)
C(69)	5812(6)	3510(7)	4058(2)	21(2)
C(70)	4736(6)	3166(7)	4010(3)	28(2)
C(71)	4049(7)	3945(7)	3850(3)	36(2)
C(72)	4379(7)	4989(8)	3734(3)	42(2)
C(73)	5456(8)	5265(8)	3777(3)	44(2)
C(74)	6186(6)	4536(7)	3942(3)	26(2)
C(75)	4349(6)	2001(8)	4131(2)	28(2)
C(76)	3571(7)	1555(7)	3795(3)	35(2)
C(77)	3832(7)	2000(9)	4572(3)	41(2)
C(78)	7338(7)	4881(8)	4005(3)	32(2)
C(79)	7770(8)	5516(8)	3627(3)	42(2)
C(80)	7442(8)	5517(8)	4429(3)	42(2)
C(81)	8861(7)	1023(7)	4270(3)	29(2)
C(82)	8743(7)	-120(8)	4215(3)	31(2)
C(83)	9653(7)	-733(8)	4185(3)	38(2)
C(84)	10631(8)	-254(7)	4230(3)	42(2)
C(85)	10719(8)	874(7)	4285(3)	39(2)
C(86)	9835(6)	1566(6)	4299(3)	24(2)
C(87)	7662(7)	-640(8)	4198(3)	31(2)
C(88)	7587(9)	-1570(9)	3882(4)	58(3)
C(89)	7365(8)	-1097(11)	4640(4)	59(3)
C(90)	9928(6)	2798(7)	4351(3)	27(2)
C(91)	10840(7)	3229(9)	4079(3)	44(2)
C(92)	10067(8)	3143(9)	4818(3)	54(3)
C(93)	5790(6)	1986(8)	2515(3)	29(2)
C(94)	5232(6)	2847(8)	2702(3)	36(2)
C(95)	4185(8)	3039(9)	2614(3)	48(3)

C(96)	3659(7)	2311(8)	2336(3)	44(3)
C(97)	4179(8)	1410(9)	2157(3)	49(3)
C(98)	5265(7)	1256(8)	2246(3)	37(2)
C(99)	7684(7)	580(8)	2444(3)	37(2)
C(100)	8022(9)	-221(10)	2726(4)	60(3)
C(101)	8515(9)	-1160(10)	2582(4)	61(3)
C(102)	8625(9)	-1352(10)	2142(4)	55(3)
C(103)	8315(9)	-582(11)	1880(4)	54(3)
C(104)	7845(9)	400(11)	2018(4)	59(3)
C(105)	7839(6)	2922(7)	2368(3)	28(2)
C(106)	7327(8)	3875(8)	2217(3)	45(2)
C(107)	7908(10)	4725(10)	2033(4)	61(3)
C(108)	8979(10)	4619(11)	1984(4)	61(3)
C(109)	9517(9)	3693(10)	2125(4)	57(3)
C(110)	8940(7)	2881(9)	2308(3)	43(2)
Cl(1)	939(2)	6626(2)	1654(1)	46(1)
Cl(2)	3868(2)	8847(2)	1582(1)	33(1)
Cl(3)	8818(2)	3010(2)	3349(1)	36(1)
Cl(4)	5965(2)	685(2)	3438(1)	32(1)
N(1)	2000(5)	7991(6)	651(2)	24(2)
N(2)	3205(6)	6717(6)	766(2)	36(2)
N(3)	6548(5)	2748(6)	4252(2)	20(1)
N(4)	7898(5)	1674(6)	4349(2)	26(2)
P(1)	2559(2)	7808(2)	2342(1)	31(1)
P(2)	7175(2)	1855(2)	2663(1)	27(1)
Pd(1)	2460(1)	7637(1)	1607(1)	27(1)
Pd(2)	7318(1)	1955(1)	3396(1)	24(1)

Table A2: Atomic coordinates ($\times 10^4$) and equivalent isotropic displacement parameters ($\text{\AA}^2 \times 10^3$) for **2**. $U(\text{eq})$ is defined as one third of the trace of the orthogonalized U^{ij} tensor.

C(1)-N(2)	1.350(11)	C(16)-H(16)	0.9300
C(1)-N(1)	1.396(9)	C(17)-C(18)	1.370(17)
C(1)-Pd(1)	2.041(7)	C(17)-H(17)	0.9300
C(2)-C(3)	1.356(12)	C(18)-C(19)	1.404(14)
C(2)-N(1)	1.410(11)	C(18)-H(18)	0.9300
C(2)-C(4)	1.467(11)	C(19)-C(23)	1.554(14)
C(3)-N(2)	1.407(10)	C(20)-C(21)	1.542(14)
C(3)-C(13)	1.435(12)	C(20)-C(22)	1.554(13)
C(4)-C(5)	1.385(12)	C(20)-H(20)	0.9800
C(4)-C(9)	1.444(12)	C(21)-H(21A)	0.9600
C(5)-C(6)	1.418(14)	C(21)-H(21B)	0.9600
C(5)-H(5)	0.9300	C(21)-H(21C)	0.9600
C(6)-C(7)	1.381(16)	C(22)-H(22A)	0.9600
C(6)-H(6)	0.9300	C(22)-H(22B)	0.9600
C(7)-C(8)	1.422(15)	C(22)-H(22C)	0.9600
C(7)-H(7)	0.9300	C(23)-C(24)	1.498(14)
C(8)-C(9)	1.384(12)	C(23)-C(25)	1.549(14)
C(8)-C(10)	1.453(16)	C(23)-H(23)	0.9800
C(9)-C(13)	1.432(12)	C(24)-H(24A)	0.9600
C(10)-C(11)	1.376(16)	C(24)-H(24B)	0.9600
C(10)-H(10)	0.9300	C(24)-H(24C)	0.9600
C(11)-C(12)	1.430(15)	C(25)-H(25A)	0.9600
C(11)-H(11)	0.9300	C(25)-H(25B)	0.9600
C(12)-C(13)	1.384(14)	C(25)-H(25C)	0.9600
C(12)-H(12)	0.9300	C(26)-C(27)	1.398(16)
C(14)-C(19)	1.378(14)	C(26)-C(31)	1.409(17)
C(14)-C(15)	1.406(13)	C(26)-N(2)	1.462(12)
C(14)-N(1)	1.432(11)	C(27)-C(32)	1.496(17)
C(15)-C(16)	1.417(14)	C(27)-C(28)	1.515(17)
C(15)-C(20)	1.517(14)	C(28)-C(29)	1.40(2)
C(16)-C(17)	1.362(18)	C(28)-H(28)	0.9300

C(29)-C(30)	1.340(19)	C(42)-C(43)	1.401(13)
C(29)-H(29)	0.9300	C(42)-H(42)	0.9300
C(30)-C(31)	1.403(17)	C(43)-H(43)	0.9300
C(30)-H(30)	0.9300	C(44)-C(45)	1.362(12)
C(31)-C(35)	1.471(17)	C(44)-C(49)	1.429(13)
C(32)-C(33)	1.545(13)	C(44)-P(1)	1.826(9)
C(32)-C(34)	1.578(15)	C(45)-C(46)	1.439(14)
C(32)-H(32)	0.9800	C(45)-H(45)	0.9300
C(33)-H(33A)	0.9600	C(46)-C(47)	1.395(15)
C(33)-H(33B)	0.9600	C(46)-H(46)	0.9300
C(33)-H(33C)	0.9600	C(47)-C(48)	1.396(16)
C(34)-H(34A)	0.9600	C(47)-H(47)	0.9300
C(34)-H(34B)	0.9600	C(48)-C(49)	1.396(15)
C(34)-H(34C)	0.9600	C(48)-H(48)	0.9300
C(35)-C(37)	1.543(16)	C(49)-H(49)	0.9300
C(35)-C(36)	1.561(17)	C(50)-C(55)	1.383(12)
C(35)-H(35)	0.9800	C(50)-C(51)	1.407(13)
C(36)-H(36A)	0.9600	C(50)-P(1)	1.821(8)
C(36)-H(36B)	0.9600	C(51)-C(52)	1.403(14)
C(36)-H(36C)	0.9600	C(51)-H(51)	0.9300
C(37)-H(37A)	0.9600	C(52)-C(53)	1.377(15)
C(37)-H(37B)	0.9600	C(52)-H(52)	0.9300
C(37)-H(37C)	0.9600	C(53)-C(54)	1.354(16)
C(38)-C(39)	1.387(13)	C(53)-H(53)	0.9300
C(38)-C(43)	1.388(12)	C(54)-C(55)	1.415(13)
C(38)-P(1)	1.813(9)	C(54)-H(54)	0.9300
C(39)-C(40)	1.391(15)	C(55)-H(55)	0.9300
C(39)-H(39)	0.9300	C(56)-N(3)	1.363(10)
C(40)-C(41)	1.361(15)	C(56)-N(4)	1.381(10)
C(40)-H(40)	0.9300	C(56)-Pd(2)	2.033(9)
C(41)-C(42)	1.395(14)	C(57)-C(58)	1.370(12)
C(41)-H(41)	0.9300	C(57)-N(3)	1.402(10)

C(57)-C(59)	1.484(12)	C(75)-C(77)	1.533(11)
C(58)-N(4)	1.387(10)	C(75)-C(76)	1.545(10)
C(58)-C(68)	1.469(11)	C(75)-H(75)	0.9800
C(59)-C(60)	1.356(12)	C(76)-H(76A)	0.9600
C(59)-C(64)	1.407(12)	C(76)-H(76B)	0.9600
C(60)-C(61)	1.430(13)	C(76)-H(76C)	0.9600
C(60)-H(60)	0.9300	C(77)-H(77A)	0.9600
C(61)-C(62)	1.358(14)	C(77)-H(77B)	0.9600
C(61)-H(61)	0.9300	C(77)-H(77C)	0.9600
C(62)-C(63)	1.392(15)	C(78)-C(79)	1.522(13)
C(62)-H(62)	0.9300	C(78)-C(80)	1.551(12)
C(63)-C(64)	1.412(12)	C(78)-H(78)	0.9800
C(63)-C(65)	1.440(13)	C(79)-H(79A)	0.9600
C(64)-C(68)	1.431(14)	C(79)-H(79B)	0.9600
C(65)-C(66)	1.369(14)	C(79)-H(79C)	0.9600
C(65)-H(65)	0.9300	C(80)-H(80A)	0.9600
C(66)-C(67)	1.445(13)	C(80)-H(80B)	0.9600
C(66)-H(66)	0.9300	C(80)-H(80C)	0.9600
C(67)-C(68)	1.371(13)	C(81)-C(86)	1.404(12)
C(67)-H(67)	0.9300	C(81)-C(82)	1.418(13)
C(69)-C(74)	1.391(11)	C(81)-N(4)	1.479(11)
C(69)-C(70)	1.435(11)	C(82)-C(83)	1.378(13)
C(69)-N(3)	1.455(9)	C(82)-C(87)	1.511(13)
C(70)-C(71)	1.386(11)	C(83)-C(84)	1.379(14)
C(70)-C(75)	1.556(12)	C(83)-H(83)	0.9300
C(71)-C(72)	1.395(13)	C(84)-C(85)	1.397(13)
C(71)-H(71)	0.9300	C(84)-H(84)	0.9300
C(72)-C(73)	1.412(14)	C(85)-C(86)	1.406(12)
C(72)-H(72)	0.9300	C(85)-H(85)	0.9300
C(73)-C(74)	1.385(12)	C(86)-C(90)	1.522(11)
C(73)-H(73)	0.9300	C(87)-C(88)	1.515(14)
C(74)-C(78)	1.533(12)	C(87)-C(89)	1.546(14)

C(87)-H(87)	0.9800	C(100)-H(100)	0.9300
C(88)-H(88A)	0.9600	C(101)-C(102)	1.412(16)
C(88)-H(88B)	0.9600	C(101)-H(101)	0.9300
C(88)-H(88C)	0.9600	C(102)-C(103)	1.313(16)
C(89)-H(89A)	0.9600	C(102)-H(102)	0.9300
C(89)-H(89B)	0.9600	C(103)-C(104)	1.411(16)
C(89)-H(89C)	0.9600	C(103)-H(103)	0.9300
C(90)-C(91)	1.532(12)	C(104)-H(104)	0.9300
C(90)-C(92)	1.539(12)	C(105)-C(110)	1.408(12)
C(90)-H(90)	0.9800	C(105)-C(106)	1.418(13)
C(91)-H(91A)	0.9600	C(105)-P(2)	1.810(9)
C(91)-H(91B)	0.9600	C(106)-C(107)	1.401(15)
C(91)-H(91C)	0.9600	C(106)-H(106)	0.9300
C(92)-H(92A)	0.9600	C(107)-C(108)	1.371(17)
C(92)-H(92B)	0.9600	C(107)-H(107)	0.9300
C(92)-H(92C)	0.9600	C(108)-C(109)	1.395(17)
C(93)-C(98)	1.400(13)	C(108)-H(108)	0.9300
C(93)-C(94)	1.399(13)	C(109)-C(110)	1.362(14)
C(93)-P(2)	1.822(7)	C(109)-H(109)	0.9300
C(94)-C(95)	1.375(12)	C(110)-H(110)	0.9300
C(94)-H(94)	0.9300	Cl(1)-Pd(1)	2.295(2)
C(95)-C(96)	1.418(14)	Cl(2)-Pd(1)	2.321(2)
C(95)-H(95)	0.9300	Cl(3)-Pd(2)	2.302(2)
C(96)-C(97)	1.403(14)	Cl(4)-Pd(2)	2.318(2)
C(96)-H(96)	0.9300	P(1)-Pd(1)	2.324(2)
C(97)-C(98)	1.416(13)	P(2)-Pd(2)	2.315(2)
C(97)-H(97)	0.9300	N(2)-C(1)-N(1)	107.3(7)
C(98)-H(98)	0.9300	N(2)-C(1)-Pd(1)	125.2(6)
C(99)-C(104)	1.371(15)	N(1)-C(1)-Pd(1)	127.4(6)
C(99)-C(100)	1.390(15)	C(3)-C(2)-N(1)	109.2(7)
C(99)-P(2)	1.825(10)	C(3)-C(2)-C(4)	111.2(8)
C(100)-C(101)	1.384(15)	N(1)-C(2)-C(4)	139.6(8)

C(2)-C(3)-N(2)	106.2(7)	C(9)-C(13)-C(3)	104.8(8)
C(2)-C(3)-C(13)	110.0(7)	C(19)-C(14)-C(15)	121.8(9)
N(2)-C(3)-C(13)	143.7(8)	C(19)-C(14)-N(1)	120.4(8)
C(5)-C(4)-C(9)	118.9(8)	C(15)-C(14)-N(1)	117.9(9)
C(5)-C(4)-C(2)	138.7(9)	C(14)-C(15)-C(16)	116.4(10)
C(9)-C(4)-C(2)	102.4(7)	C(14)-C(15)-C(20)	121.0(9)
C(4)-C(5)-C(6)	117.9(9)	C(16)-C(15)-C(20)	122.6(10)
C(4)-C(5)-H(5)	121.1	C(17)-C(16)-C(15)	122.1(11)
C(6)-C(5)-H(5)	121.1	C(17)-C(16)-H(16)	118.9
C(7)-C(6)-C(5)	122.5(10)	C(15)-C(16)-H(16)	118.9
C(7)-C(6)-H(6)	118.8	C(16)-C(17)-C(18)	120.2(11)
C(5)-C(6)-H(6)	118.8	C(16)-C(17)-H(17)	119.9
C(6)-C(7)-C(8)	121.1(10)	C(18)-C(17)-H(17)	119.9
C(6)-C(7)-H(7)	119.4	C(17)-C(18)-C(19)	120.2(12)
C(8)-C(7)-H(7)	119.4	C(17)-C(18)-H(18)	119.9
C(9)-C(8)-C(7)	116.1(10)	C(19)-C(18)-H(18)	119.9
C(9)-C(8)-C(10)	115.5(9)	C(14)-C(19)-C(18)	119.3(10)
C(7)-C(8)-C(10)	128.4(9)	C(14)-C(19)-C(23)	121.4(9)
C(8)-C(9)-C(13)	124.9(9)	C(18)-C(19)-C(23)	119.0(10)
C(8)-C(9)-C(4)	123.5(9)	C(15)-C(20)-C(21)	114.8(10)
C(13)-C(9)-C(4)	111.6(7)	C(15)-C(20)-C(22)	112.2(9)
C(11)-C(10)-C(8)	120.2(9)	C(21)-C(20)-C(22)	107.4(8)
C(11)-C(10)-H(10)	119.9	C(15)-C(20)-H(20)	107.4
C(8)-C(10)-H(10)	119.9	C(21)-C(20)-H(20)	107.4
C(10)-C(11)-C(12)	122.7(10)	C(22)-C(20)-H(20)	107.4
C(10)-C(11)-H(11)	118.7	C(20)-C(21)-H(21A)	109.5
C(12)-C(11)-H(11)	118.7	C(20)-C(21)-H(21B)	109.5
C(13)-C(12)-C(11)	118.5(10)	H(21A)-C(21)-H(21B)	109.5
C(13)-C(12)-H(12)	120.8	C(20)-C(21)-H(21C)	109.5
C(11)-C(12)-H(12)	120.8	H(21A)-C(21)-H(21C)	109.5
C(12)-C(13)-C(9)	118.1(9)	H(21B)-C(21)-H(21C)	109.5
C(12)-C(13)-C(3)	136.8(9)	C(20)-C(22)-H(22A)	109.5

C(20)-C(22)-H(22B)	109.5	C(30)-C(29)-C(28)	126.2(14)
H(22A)-C(22)-H(22B)	109.5	C(30)-C(29)-H(29)	116.9
C(20)-C(22)-H(22C)	109.5	C(28)-C(29)-H(29)	116.9
H(22A)-C(22)-H(22C)	109.5	C(29)-C(30)-C(31)	118.5(15)
H(22B)-C(22)-H(22C)	109.5	C(29)-C(30)-H(30)	120.7
C(24)-C(23)-C(25)	112.3(9)	C(31)-C(30)-H(30)	120.7
C(24)-C(23)-C(19)	111.8(8)	C(30)-C(31)-C(26)	117.5(13)
C(25)-C(23)-C(19)	111.0(9)	C(30)-C(31)-C(35)	118.6(12)
C(24)-C(23)-H(23)	107.1	C(26)-C(31)-C(35)	123.9(10)
C(25)-C(23)-H(23)	107.1	C(27)-C(32)-C(33)	113.6(10)
C(19)-C(23)-H(23)	107.1	C(27)-C(32)-C(34)	111.4(9)
C(23)-C(24)-H(24A)	109.5	C(33)-C(32)-C(34)	109.0(9)
C(23)-C(24)-H(24B)	109.5	C(27)-C(32)-H(32)	107.5
H(24A)-C(24)-H(24B)	109.5	C(33)-C(32)-H(32)	107.5
C(23)-C(24)-H(24C)	109.5	C(34)-C(32)-H(32)	107.5
H(24A)-C(24)-H(24C)	109.5	C(32)-C(33)-H(33A)	109.5
H(24B)-C(24)-H(24C)	109.5	C(32)-C(33)-H(33B)	109.5
C(23)-C(25)-H(25A)	109.5	H(33A)-C(33)-H(33B)	109.5
C(23)-C(25)-H(25B)	109.5	C(32)-C(33)-H(33C)	109.5
H(25A)-C(25)-H(25B)	109.5	H(33A)-C(33)-H(33C)	109.5
C(23)-C(25)-H(25C)	109.5	H(33B)-C(33)-H(33C)	109.5
H(25A)-C(25)-H(25C)	109.5	C(32)-C(34)-H(34A)	109.5
H(25B)-C(25)-H(25C)	109.5	C(32)-C(34)-H(34B)	109.5
C(27)-C(26)-C(31)	127.9(11)	H(34A)-C(34)-H(34B)	109.5
C(27)-C(26)-N(2)	115.4(11)	C(32)-C(34)-H(34C)	109.5
C(31)-C(26)-N(2)	116.7(9)	H(34A)-C(34)-H(34C)	109.5
C(26)-C(27)-C(32)	125.4(11)	H(34B)-C(34)-H(34C)	109.5
C(26)-C(27)-C(28)	111.7(12)	C(31)-C(35)-C(37)	111.7(11)
C(32)-C(27)-C(28)	122.9(11)	C(31)-C(35)-C(36)	112.4(11)
C(29)-C(28)-C(27)	118.1(13)	C(37)-C(35)-C(36)	109.5(11)
C(29)-C(28)-H(28)	121.0	C(31)-C(35)-H(35)	107.7
C(27)-C(28)-H(28)	120.9	C(37)-C(35)-H(35)	107.7

C(36)-C(35)-H(35)	107.7	C(45)-C(44)-P(1)	118.3(8)
C(35)-C(36)-H(36A)	109.5	C(49)-C(44)-P(1)	121.5(7)
C(35)-C(36)-H(36B)	109.5	C(44)-C(45)-C(46)	120.2(10)
H(36A)-C(36)-H(36B)	109.5	C(44)-C(45)-H(45)	119.9
C(35)-C(36)-H(36C)	109.5	C(46)-C(45)-H(45)	119.9
H(36A)-C(36)-H(36C)	109.5	C(47)-C(46)-C(45)	119.9(10)
H(36B)-C(36)-H(36C)	109.5	C(47)-C(46)-H(46)	120.0
C(35)-C(37)-H(37A)	109.5	C(45)-C(46)-H(46)	120.0
C(35)-C(37)-H(37B)	109.5	C(46)-C(47)-C(48)	119.4(10)
H(37A)-C(37)-H(37B)	109.5	C(46)-C(47)-H(47)	120.3
C(35)-C(37)-H(37C)	109.5	C(48)-C(47)-H(47)	120.3
H(37A)-C(37)-H(37C)	109.5	C(47)-C(48)-C(49)	120.9(10)
H(37B)-C(37)-H(37C)	109.5	C(47)-C(48)-H(48)	119.6
C(39)-C(38)-C(43)	119.0(9)	C(49)-C(48)-H(48)	119.6
C(39)-C(38)-P(1)	122.3(7)	C(48)-C(49)-C(44)	119.6(10)
C(43)-C(38)-P(1)	118.4(7)	C(48)-C(49)-H(49)	120.2
C(38)-C(39)-C(40)	120.4(10)	C(44)-C(49)-H(49)	120.2
C(38)-C(39)-H(39)	119.8	C(55)-C(50)-C(51)	119.5(8)
C(40)-C(39)-H(39)	119.8	C(55)-C(50)-P(1)	125.1(8)
C(41)-C(40)-C(39)	120.4(10)	C(51)-C(50)-P(1)	115.4(7)
C(41)-C(40)-H(40)	119.8	C(52)-C(51)-C(50)	118.5(8)
C(39)-C(40)-H(40)	119.8	C(52)-C(51)-H(51)	120.7
C(40)-C(41)-C(42)	120.7(10)	C(50)-C(51)-H(51)	120.8
C(40)-C(41)-H(41)	119.7	C(53)-C(52)-C(51)	121.3(10)
C(42)-C(41)-H(41)	119.7	C(53)-C(52)-H(52)	119.4
C(41)-C(42)-C(43)	118.7(9)	C(51)-C(52)-H(52)	119.4
C(41)-C(42)-H(42)	120.6	C(54)-C(53)-C(52)	120.3(10)
C(43)-C(42)-H(42)	120.6	C(54)-C(53)-H(53)	119.8
C(38)-C(43)-C(42)	120.7(8)	C(52)-C(53)-H(53)	119.8
C(38)-C(43)-H(43)	119.6	C(53)-C(54)-C(55)	119.9(10)
C(42)-C(43)-H(43)	119.7	C(53)-C(54)-H(54)	120.0
C(45)-C(44)-C(49)	119.9(9)	C(55)-C(54)-H(54)	120.0

C(50)-C(55)-C(54)	120.4(10)	C(63)-C(65)-H(65)	118.8
C(50)-C(55)-H(55)	119.8	C(65)-C(66)-C(67)	121.4(9)
C(54)-C(55)-H(55)	119.8	C(65)-C(66)-H(66)	119.3
N(3)-C(56)-N(4)	105.1(7)	C(67)-C(66)-H(66)	119.3
N(3)-C(56)-Pd(2)	124.8(6)	C(68)-C(67)-C(66)	118.0(10)
N(4)-C(56)-Pd(2)	130.1(6)	C(68)-C(67)-H(67)	121.0
C(58)-C(57)-N(3)	106.3(7)	C(66)-C(67)-H(67)	121.0
C(58)-C(57)-C(59)	110.1(7)	C(67)-C(68)-C(64)	120.2(9)
N(3)-C(57)-C(59)	143.4(8)	C(67)-C(68)-C(58)	136.4(10)
C(57)-C(58)-N(4)	107.5(7)	C(64)-C(68)-C(58)	103.4(8)
C(57)-C(58)-C(68)	109.7(8)	C(74)-C(69)-C(70)	124.2(7)
N(4)-C(58)-C(68)	142.6(8)	C(74)-C(69)-N(3)	118.2(7)
C(60)-C(59)-C(64)	119.9(8)	C(70)-C(69)-N(3)	117.6(7)
C(60)-C(59)-C(57)	136.9(9)	C(71)-C(70)-C(69)	115.6(8)
C(64)-C(59)-C(57)	103.1(8)	C(71)-C(70)-C(75)	121.5(8)
C(59)-C(60)-C(61)	117.5(9)	C(69)-C(70)-C(75)	122.9(7)
C(59)-C(60)-H(60)	121.3	C(70)-C(71)-C(72)	122.6(9)
C(61)-C(60)-H(60)	121.3	C(70)-C(71)-H(71)	118.7
C(62)-C(61)-C(60)	122.0(10)	C(72)-C(71)-H(71)	118.7
C(62)-C(61)-H(61)	119.0	C(71)-C(72)-C(73)	119.0(8)
C(60)-C(61)-H(61)	119.0	C(71)-C(72)-H(72)	120.5
C(61)-C(62)-C(63)	122.0(9)	C(73)-C(72)-H(72)	120.5
C(61)-C(62)-H(62)	119.0	C(74)-C(73)-C(72)	121.8(9)
C(63)-C(62)-H(62)	119.0	C(74)-C(73)-H(73)	119.1
C(62)-C(63)-C(64)	115.2(9)	C(72)-C(73)-H(73)	119.1
C(62)-C(63)-C(65)	130.0(9)	C(73)-C(74)-C(69)	116.9(8)
C(64)-C(63)-C(65)	114.8(9)	C(73)-C(74)-C(78)	120.4(8)
C(59)-C(64)-C(63)	123.2(9)	C(69)-C(74)-C(78)	122.6(7)
C(59)-C(64)-C(68)	113.6(8)	C(77)-C(75)-C(76)	110.2(6)
C(63)-C(64)-C(68)	123.2(9)	C(77)-C(75)-C(70)	110.8(7)
C(66)-C(65)-C(63)	122.3(9)	C(76)-C(75)-C(70)	110.9(7)
C(66)-C(65)-H(65)	118.8	C(77)-C(75)-H(75)	108.2

C(76)-C(75)-H(75)	108.2	C(86)-C(81)-C(82)	124.6(8)
C(70)-C(75)-H(75)	108.2	C(86)-C(81)-N(4)	117.2(7)
C(75)-C(76)-H(76A)	109.5	C(82)-C(81)-N(4)	117.8(8)
C(75)-C(76)-H(76B)	109.5	C(83)-C(82)-C(81)	117.2(9)
H(76A)-C(76)-H(76B)	109.5	C(83)-C(82)-C(87)	121.7(9)
C(75)-C(76)-H(76C)	109.5	C(81)-C(82)-C(87)	121.0(8)
H(76A)-C(76)-H(76C)	109.5	C(82)-C(83)-C(84)	120.9(9)
H(76B)-C(76)-H(76C)	109.5	C(82)-C(83)-H(83)	119.6
C(75)-C(77)-H(77A)	109.5	C(84)-C(83)-H(83)	119.6
C(75)-C(77)-H(77B)	109.5	C(83)-C(84)-C(85)	120.4(9)
H(77A)-C(77)-H(77B)	109.5	C(83)-C(84)-H(84)	119.8
C(75)-C(77)-H(77C)	109.5	C(85)-C(84)-H(84)	119.8
H(77A)-C(77)-H(77C)	109.5	C(84)-C(85)-C(86)	122.5(9)
H(77B)-C(77)-H(77C)	109.5	C(84)-C(85)-H(85)	118.8
C(79)-C(78)-C(74)	112.5(7)	C(86)-C(85)-H(85)	118.8
C(79)-C(78)-C(80)	112.6(8)	C(81)-C(86)-C(85)	114.4(8)
C(74)-C(78)-C(80)	109.2(8)	C(81)-C(86)-C(90)	123.0(7)
C(79)-C(78)-H(78)	107.4	C(85)-C(86)-C(90)	122.6(8)
C(74)-C(78)-H(78)	107.4	C(82)-C(87)-C(88)	113.4(8)
C(80)-C(78)-H(78)	107.4	C(82)-C(87)-C(89)	110.0(7)
C(78)-C(79)-H(79A)	109.5	C(88)-C(87)-C(89)	107.6(9)
C(78)-C(79)-H(79B)	109.5	C(82)-C(87)-H(87)	108.6
H(79A)-C(79)-H(79B)	109.5	C(88)-C(87)-H(87)	108.6
C(78)-C(79)-H(79C)	109.5	C(89)-C(87)-H(87)	108.6
H(79A)-C(79)-H(79C)	109.5	C(87)-C(88)-H(88A)	109.5
H(79B)-C(79)-H(79C)	109.5	C(87)-C(88)-H(88B)	109.5
C(78)-C(80)-H(80A)	109.5	H(88A)-C(88)-H(88B)	109.5
C(78)-C(80)-H(80B)	109.5	C(87)-C(88)-H(88C)	109.5
H(80A)-C(80)-H(80B)	109.5	H(88A)-C(88)-H(88C)	109.5
C(78)-C(80)-H(80C)	109.5	H(88B)-C(88)-H(88C)	109.5
H(80A)-C(80)-H(80C)	109.5	C(87)-C(89)-H(89A)	109.5
H(80B)-C(80)-H(80C)	109.5	C(87)-C(89)-H(89B)	109.5

H(89A)-C(89)-H(89B)	109.5	C(97)-C(96)-H(96)	119.3
C(87)-C(89)-H(89C)	109.5	C(95)-C(96)-H(96)	119.3
H(89A)-C(89)-H(89C)	109.5	C(96)-C(97)-C(98)	118.8(9)
H(89B)-C(89)-H(89C)	109.5	C(96)-C(97)-H(97)	120.6
C(86)-C(90)-C(91)	109.9(7)	C(98)-C(97)-H(97)	120.6
C(86)-C(90)-C(92)	112.5(8)	C(93)-C(98)-C(97)	119.7(9)
C(91)-C(90)-C(92)	110.6(8)	C(93)-C(98)-H(98)	120.1
C(86)-C(90)-H(90)	107.9	C(97)-C(98)-H(98)	120.1
C(91)-C(90)-H(90)	107.9	C(104)-C(99)-C(100)	117.6(10)
C(92)-C(90)-H(90)	107.9	C(104)-C(99)-P(2)	124.0(8)
C(90)-C(91)-H(91A)	109.5	C(100)-C(99)-P(2)	118.1(8)
C(90)-C(91)-H(91B)	109.5	C(101)-C(100)-C(99)	121.2(11)
H(91A)-C(91)-H(91B)	109.5	C(101)-C(100)-H(100)	119.4
C(90)-C(91)-H(91C)	109.5	C(99)-C(100)-H(100)	119.4
H(91A)-C(91)-H(91C)	109.5	C(100)-C(101)-C(102)	120.2(11)
H(91B)-C(91)-H(91C)	109.5	C(100)-C(101)-H(101)	119.9
C(90)-C(92)-H(92A)	109.5	C(102)-C(101)-H(101)	119.9
C(90)-C(92)-H(92B)	109.5	C(103)-C(102)-C(101)	117.8(11)
H(92A)-C(92)-H(92B)	109.5	C(103)-C(102)-H(102)	121.1
C(90)-C(92)-H(92C)	109.5	C(101)-C(102)-H(102)	121.1
H(92A)-C(92)-H(92C)	109.5	C(102)-C(103)-C(104)	123.0(11)
H(92B)-C(92)-H(92C)	109.5	C(102)-C(103)-H(103)	118.5
C(98)-C(93)-C(94)	119.7(7)	C(104)-C(103)-H(103)	118.5
C(98)-C(93)-P(2)	123.7(7)	C(99)-C(104)-C(103)	120.1(11)
C(94)-C(93)-P(2)	116.5(7)	C(99)-C(104)-H(104)	119.9
C(95)-C(94)-C(93)	122.2(9)	C(103)-C(104)-H(104)	119.9
C(95)-C(94)-H(94)	118.9	C(110)-C(105)-C(106)	116.0(8)
C(93)-C(94)-H(94)	118.9	C(110)-C(105)-P(2)	120.3(7)
C(94)-C(95)-C(96)	118.0(9)	C(106)-C(105)-P(2)	123.6(7)
C(94)-C(95)-H(95)	121.0	C(107)-C(106)-C(105)	120.6(10)
C(96)-C(95)-H(95)	121.0	C(107)-C(106)-H(106)	119.7
C(97)-C(96)-C(95)	121.5(9)	C(105)-C(106)-H(106)	119.7

C(108)-C(107)-C(106)	119.7(12)	C(38)-P(1)-C(44)	102.7(4)
C(108)-C(107)-H(107)	120.1	C(50)-P(1)-C(44)	105.1(4)
C(106)-C(107)-H(107)	120.1	C(38)-P(1)-Pd(1)	112.4(3)
C(107)-C(108)-C(109)	121.7(11)	C(50)-P(1)-Pd(1)	109.2(3)
C(107)-C(108)-H(108)	119.2	C(44)-P(1)-Pd(1)	116.5(3)
C(109)-C(108)-H(108)	119.2	C(105)-P(2)-C(93)	104.7(4)
C(110)-C(109)-C(108)	117.7(11)	C(105)-P(2)-C(99)	105.0(5)
C(110)-C(109)-H(109)	121.1	C(93)-P(2)-C(99)	108.6(4)
C(108)-C(109)-H(109)	121.1	C(105)-P(2)-Pd(2)	115.9(3)
C(109)-C(110)-C(105)	124.2(10)	C(93)-P(2)-Pd(2)	108.9(3)
C(109)-C(110)-H(110)	117.9	C(99)-P(2)-Pd(2)	113.2(3)
C(105)-C(110)-H(110)	117.9	C(1)-Pd(1)-Cl(1)	92.2(2)
C(1)-N(1)-C(2)	106.9(6)	C(1)-Pd(1)-Cl(2)	90.4(2)
C(1)-N(1)-C(14)	128.1(7)	Cl(1)-Pd(1)-Cl(2)	172.82(10)
C(2)-N(1)-C(14)	124.9(7)	C(1)-Pd(1)-P(1)	173.3(2)
C(1)-N(2)-C(3)	110.3(7)	Cl(1)-Pd(1)-P(1)	91.75(8)
C(1)-N(2)-C(26)	124.5(8)	Cl(2)-Pd(1)-P(1)	86.31(8)
C(3)-N(2)-C(26)	124.7(8)	C(56)-Pd(2)-Cl(3)	91.8(2)
C(56)-N(3)-C(57)	110.8(7)	C(56)-Pd(2)-P(2)	173.0(2)
C(56)-N(3)-C(69)	125.2(7)	Cl(3)-Pd(2)-P(2)	91.72(8)
C(57)-N(3)-C(69)	123.6(7)	C(56)-Pd(2)-Cl(4)	89.4(2)
C(56)-N(4)-C(58)	110.2(7)	Cl(3)-Pd(2)-Cl(4)	171.98(9)
C(56)-N(4)-C(81)	125.1(7)	P(2)-Pd(2)-Cl(4)	87.91(8)
C(58)-N(4)-C(81)	124.6(7)		
C(38)-P(1)-C(50)	110.6(4)		

Table A3: Bond lengths [Å] and angles [°] for **2**.

	U11	U22	U33	U23	U13	U12
C(1)	24(4)	25(4)	12(3)	-5(3)	-9(3)	3(3)
C(2)	34(4)	18(4)	36(4)	1(4)	-8(3)	2(4)
C(3)	44(4)	34(5)	3(3)	-2(3)	-7(3)	4(4)
C(4)	37(4)	26(4)	16(4)	-2(3)	-4(3)	1(3)
C(5)	50(5)	36(5)	33(5)	11(4)	-6(4)	10(4)
C(6)	62(6)	60(6)	33(5)	2(5)	-7(4)	8(5)
C(7)	68(6)	60(6)	32(5)	2(5)	-3(4)	-7(6)
C(8)	41(4)	42(5)	27(4)	-4(5)	-6(3)	-5(5)
C(9)	43(4)	28(4)	18(4)	-7(4)	3(3)	-7(4)
C(10)	59(6)	61(6)	23(4)	-15(4)	-1(4)	-13(5)
C(11)	68(6)	67(7)	45(5)	-27(5)	-5(5)	18(5)
C(12)	60(6)	57(6)	46(5)	-14(5)	-12(5)	17(5)
C(13)	41(5)	40(5)	23(4)	-2(4)	-8(3)	-3(4)
C(14)	28(4)	38(5)	21(4)	4(4)	-4(3)	7(3)
C(15)	43(5)	43(5)	24(4)	2(4)	-5(4)	10(4)
C(16)	39(5)	94(8)	51(6)	4(6)	2(4)	16(5)
C(17)	62(6)	70(7)	62(6)	-4(6)	5(5)	31(5)
C(18)	77(7)	61(6)	39(5)	6(5)	8(5)	30(5)
C(19)	51(5)	45(5)	31(5)	-5(4)	-2(4)	11(4)
C(20)	40(5)	59(6)	39(5)	0(4)	3(4)	-11(4)
C(21)	59(7)	133(12)	65(8)	-2(8)	-2(6)	-51(8)
C(22)	69(6)	68(7)	35(5)	-10(5)	6(5)	-31(6)
C(23)	53(5)	30(5)	38(5)	7(4)	-11(4)	-2(4)
C(24)	68(7)	45(6)	35(5)	2(5)	-9(5)	1(5)
C(25)	93(8)	49(7)	43(6)	-10(5)	-14(6)	2(6)
C(26)	51(5)	64(6)	36(5)	-10(5)	-12(4)	28(5)
C(27)	75(7)	58(6)	45(6)	-17(5)	-5(5)	24(5)
C(28)	72(7)	93(8)	76(7)	-8(6)	-28(6)	30(6)
C(29)	104(8)	53(7)	99(8)	-4(6)	-17(7)	10(6)
C(30)	107(8)	65(7)	104(8)	-5(6)	-21(7)	11(7)

C(31)	96(7)	38(5)	38(5)	-4(4)	-2(5)	17(5)
C(32)	42(5)	72(7)	42(5)	-16(5)	-17(4)	26(4)
C(33)	51(6)	107(10)	53(6)	-16(7)	-9(5)	28(7)
C(34)	58(6)	123(11)	55(7)	-40(7)	-20(5)	22(7)
C(35)	86(7)	34(5)	61(6)	0(5)	-8(6)	5(5)
C(36)	168(13)	51(8)	79(9)	15(7)	19(9)	5(9)
C(37)	129(11)	51(7)	68(8)	8(6)	-2(8)	-30(8)
C(38)	33(4)	35(5)	21(4)	5(4)	-1(3)	-2(3)
C(39)	53(5)	51(6)	26(5)	2(4)	-3(4)	5(4)
C(40)	64(6)	52(6)	40(5)	-14(5)	-5(5)	14(5)
C(41)	46(5)	44(5)	41(5)	-1(4)	1(4)	14(4)
C(42)	48(5)	45(5)	40(5)	-7(4)	-5(4)	11(4)
C(43)	45(5)	25(4)	24(4)	1(3)	0(3)	-7(3)
C(44)	47(5)	35(5)	17(4)	0(4)	-3(3)	-9(4)
C(45)	49(5)	43(5)	34(4)	16(4)	-4(4)	0(5)
C(46)	52(5)	57(6)	44(5)	8(5)	0(4)	-11(5)
C(47)	74(6)	47(6)	40(5)	12(4)	-13(5)	-22(5)
C(48)	72(6)	36(5)	36(5)	6(4)	4(5)	0(5)
C(49)	50(5)	41(5)	36(5)	1(4)	1(4)	2(4)
C(50)	50(4)	28(4)	13(3)	10(4)	-8(3)	-16(4)
C(51)	62(5)	29(5)	28(4)	-4(4)	-7(4)	-3(4)
C(52)	54(5)	42(5)	65(6)	-9(5)	-20(5)	16(4)
C(53)	57(6)	64(7)	55(6)	-1(5)	-22(5)	1(5)
C(54)	48(5)	59(6)	47(6)	-6(5)	-20(4)	0(5)
C(55)	48(5)	30(5)	35(5)	-5(4)	-7(4)	-2(4)
C(56)	18(3)	22(4)	33(4)	-1(3)	6(3)	-6(3)
C(57)	22(3)	25(4)	35(4)	5(4)	-4(3)	-6(3)
C(58)	32(4)	40(5)	8(3)	-3(4)	1(3)	0(4)
C(59)	35(4)	42(5)	20(4)	0(4)	5(3)	-11(4)
C(60)	33(4)	31(4)	32(4)	-14(4)	4(3)	-7(3)
C(61)	48(5)	40(5)	36(5)	-11(4)	0(4)	-6(4)
C(62)	44(5)	44(5)	34(5)	0(4)	13(4)	-21(4)

C(63)	48(5)	40(5)	29(4)	-6(5)	2(4)	-9(5)
C(64)	32(4)	38(5)	28(4)	2(4)	0(3)	-5(4)
C(65)	65(5)	37(5)	22(4)	-3(4)	-11(4)	-15(4)
C(66)	63(5)	23(4)	33(5)	5(4)	-22(4)	-12(4)
C(67)	55(5)	39(5)	31(5)	3(4)	-13(4)	-10(4)
C(68)	42(4)	44(5)	28(4)	0(4)	-9(3)	2(4)
C(69)	17(4)	24(4)	21(4)	-1(3)	-2(3)	6(3)
C(70)	32(4)	23(4)	29(4)	-5(3)	-3(3)	2(3)
C(71)	31(4)	33(4)	45(5)	6(4)	-2(4)	10(4)
C(72)	43(5)	31(5)	52(5)	12(4)	-11(4)	18(4)
C(73)	54(5)	31(5)	47(5)	14(4)	-10(4)	9(4)
C(74)	32(4)	17(4)	29(4)	6(3)	0(3)	2(3)
C(75)	28(4)	37(4)	18(4)	-3(4)	9(3)	-10(4)
C(76)	43(5)	41(5)	21(4)	-10(4)	-11(4)	0(4)
C(77)	44(5)	47(5)	32(5)	-6(5)	5(4)	-9(5)
C(78)	36(4)	24(4)	35(5)	-4(4)	-7(4)	-3(3)
C(79)	59(6)	24(5)	42(5)	5(4)	2(5)	-4(4)
C(80)	50(6)	32(5)	43(5)	-1(4)	-11(4)	-7(4)
C(81)	38(4)	26(4)	22(4)	3(3)	-6(3)	1(3)
C(82)	44(5)	22(4)	26(4)	8(3)	-3(4)	3(3)
C(83)	46(5)	31(5)	37(5)	7(4)	12(4)	8(4)
C(84)	50(5)	26(5)	51(5)	15(4)	9(4)	21(4)
C(85)	39(5)	30(5)	47(5)	17(4)	1(4)	-1(4)
C(86)	33(4)	14(4)	27(4)	11(3)	0(3)	8(3)
C(87)	40(5)	28(4)	25(4)	5(4)	-11(3)	3(4)
C(88)	75(7)	26(5)	73(8)	-2(5)	-16(6)	-13(5)
C(89)	39(6)	74(8)	65(7)	11(7)	-12(5)	-4(5)
C(90)	29(4)	17(4)	35(4)	-8(3)	3(3)	-3(3)
C(91)	39(5)	47(6)	45(6)	13(5)	-9(4)	-12(4)
C(92)	51(6)	58(7)	53(6)	-16(5)	-9(5)	-1(5)
C(93)	31(4)	26(4)	30(4)	3(4)	-10(3)	14(4)
C(94)	32(4)	34(5)	42(5)	6(4)	-7(4)	-3(4)

C(95)	45(5)	50(6)	48(5)	-11(4)	1(4)	17(4)
C(96)	33(4)	50(6)	50(5)	2(4)	-12(4)	4(4)
C(97)	55(5)	46(5)	45(5)	-2(4)	-18(4)	-7(4)
C(98)	45(5)	31(5)	34(5)	1(4)	-6(4)	-6(4)
C(99)	39(5)	31(5)	41(5)	-1(4)	-12(4)	3(4)
C(100)	64(6)	63(6)	53(6)	-5(5)	25(5)	19(5)
C(101)	77(6)	43(6)	62(6)	21(5)	20(5)	10(5)
C(102)	56(6)	36(5)	74(7)	-11(5)	2(5)	2(4)
C(103)	58(6)	66(6)	37(5)	-15(5)	-5(4)	11(5)
C(104)	70(6)	64(6)	41(6)	-15(5)	-12(5)	23(5)
C(105)	29(4)	32(5)	24(4)	3(3)	-2(3)	-9(3)
C(106)	49(5)	41(5)	44(5)	1(4)	-5(4)	-16(4)
C(107)	82(7)	47(6)	52(6)	2(5)	-6(5)	-15(5)
C(108)	70(6)	66(7)	47(6)	14(5)	-6(5)	-29(6)
C(109)	57(6)	66(6)	49(6)	20(5)	-8(5)	-15(5)
C(110)	40(5)	50(6)	40(5)	8(4)	1(4)	-4(4)
Cl(1)	59(2)	52(2)	26(1)	-2(1)	-1(1)	-24(1)
Cl(2)	42(1)	36(1)	21(1)	-3(1)	-3(1)	-6(1)
Cl(3)	35(1)	39(1)	35(1)	-3(1)	0(1)	-11(1)
Cl(4)	39(1)	28(1)	31(1)	2(1)	-4(1)	-10(1)
N(1)	33(3)	23(4)	14(3)	2(3)	-1(3)	6(3)
N(2)	45(4)	36(5)	28(4)	-11(3)	-11(3)	13(3)
N(3)	25(3)	18(3)	18(3)	5(3)	-4(2)	0(3)
N(4)	31(3)	20(4)	27(4)	-2(3)	-5(3)	-1(3)
P(1)	45(1)	27(1)	20(1)	2(1)	-2(1)	-3(1)
P(2)	34(1)	28(1)	20(1)	-4(1)	-4(1)	-2(1)
Pd(1)	40(1)	25(1)	17(1)	-2(1)	-5(1)	-2(1)
Pd(2)	29(1)	23(1)	20(1)	1(1)	-5(1)	-2(1)

Table A4: Anisotropic displacement parameters ($\text{\AA}^2 \times 10^3$) for **2**. The anisotropic displacement factor exponent takes the form: $-2\pi^2 [h^2 a^{*2} U_{11} + \dots + 2 h k a^* b^* U_{12}]$.

N(1)-C(2)-C(3)-N(2)	-2.1(10)	C(4)-C(9)-C(13)-C(3)	1.3(10)
C(4)-C(2)-C(3)-N(2)	176.3(7)	C(2)-C(3)-C(13)-C(12)	-172.8(11)
N(1)-C(2)-C(3)-C(13)	-179.9(7)	N(2)-C(3)-C(13)-C(12)	11(2)
C(4)-C(2)-C(3)-C(13)	-1.6(11)	C(2)-C(3)-C(13)-C(9)	0.2(10)
C(3)-C(2)-C(4)-C(5)	179.7(11)	N(2)-C(3)-C(13)-C(9)	-176.4(12)
N(1)-C(2)-C(4)-C(5)	-3(2)	C(19)-C(14)-C(15)-C(16)	2.3(14)
C(3)-C(2)-C(4)-C(9)	2.3(10)	N(1)-C(14)-C(15)-C(16)	-177.0(8)
N(1)-C(2)-C(4)-C(9)	179.9(11)	C(19)-C(14)-C(15)-C(20)	-176.1(10)
C(9)-C(4)-C(5)-C(6)	-2.3(14)	N(1)-C(14)-C(15)-C(20)	4.5(13)
C(2)-C(4)-C(5)-C(6)	-179.4(11)	C(14)-C(15)-C(16)-C(17)	-0.2(16)
C(4)-C(5)-C(6)-C(7)	2.3(16)	C(20)-C(15)-C(16)-C(17)	178.2(11)
C(5)-C(6)-C(7)-C(8)	-1.4(17)	C(15)-C(16)-C(17)-C(18)	-1.8(19)
C(6)-C(7)-C(8)-C(9)	0.6(16)	C(16)-C(17)-C(18)-C(19)	1.9(18)
C(6)-C(7)-C(8)-C(10)	179.1(11)	C(15)-C(14)-C(19)-C(18)	-2.3(15)
C(7)-C(8)-C(9)-C(13)	-178.6(9)	N(1)-C(14)-C(19)-C(18)	177.0(8)
C(10)-C(8)-C(9)-C(13)	2.6(14)	C(15)-C(14)-C(19)-C(23)	-175.3(8)
C(7)-C(8)-C(9)-C(4)	-0.6(14)	N(1)-C(14)-C(19)-C(23)	4.0(14)
C(10)-C(8)-C(9)-C(4)	-179.4(8)	C(17)-C(18)-C(19)-C(14)	0.1(16)
C(5)-C(4)-C(9)-C(8)	1.5(14)	C(17)-C(18)-C(19)-C(23)	173.4(10)
C(2)-C(4)-C(9)-C(8)	179.6(9)	C(14)-C(15)-C(20)-C(21)	141.7(9)
C(5)-C(4)-C(9)-C(13)	179.8(8)	C(16)-C(15)-C(20)-C(21)	-36.6(14)
C(2)-C(4)-C(9)-C(13)	-2.2(10)	C(14)-C(15)-C(20)-C(22)	-95.3(11)
C(9)-C(8)-C(10)-C(11)	1.0(15)	C(16)-C(15)-C(20)-C(22)	86.4(12)
C(7)-C(8)-C(10)-C(11)	-177.6(11)	C(14)-C(19)-C(23)-C(24)	92.2(12)
C(8)-C(10)-C(11)-C(12)	-1.3(18)	C(18)-C(19)-C(23)-C(24)	-80.8(12)
C(10)-C(11)-C(12)-C(13)	-2.1(18)	C(14)-C(19)-C(23)-C(25)	-141.5(10)
C(11)-C(12)-C(13)-C(9)	5.4(15)	C(18)-C(19)-C(23)-C(25)	45.4(13)
C(11)-C(12)-C(13)-C(3)	177.6(11)	C(31)-C(26)-C(27)-C(32)	-177.5(10)
C(8)-C(9)-C(13)-C(12)	-5.9(15)	N(2)-C(26)-C(27)-C(32)	4.1(16)
C(4)-C(9)-C(13)-C(12)	175.9(9)	C(31)-C(26)-C(27)-C(28)	2.3(17)
C(8)-C(9)-C(13)-C(3)	179.6(9)	N(2)-C(26)-C(27)-C(28)	-176.1(9)

C(26)-C(27)-C(28)-C(29)	-3.7(17)	C(45)-C(44)-C(49)-C(48)	-0.7(14)
C(32)-C(27)-C(28)-C(29)	176.1(12)	P(1)-C(44)-C(49)-C(48)	-174.2(8)
C(27)-C(28)-C(29)-C(30)	3(2)	C(55)-C(50)-C(51)-C(52)	0.8(13)
C(28)-C(29)-C(30)-C(31)	1(3)	P(1)-C(50)-C(51)-C(52)	179.7(8)
C(29)-C(30)-C(31)-C(26)	-2(2)	C(50)-C(51)-C(52)-C(53)	1.8(16)
C(29)-C(30)-C(31)-C(35)	176.4(13)	C(51)-C(52)-C(53)-C(54)	-3.5(19)
C(27)-C(26)-C(31)-C(30)	0.6(19)	C(52)-C(53)-C(54)-C(55)	2.6(18)
N(2)-C(26)-C(31)-C(30)	178.9(10)	C(51)-C(50)-C(55)-C(54)	-1.6(14)
C(27)-C(26)-C(31)-C(35)	-177.9(11)	P(1)-C(50)-C(55)-C(54)	179.6(8)
N(2)-C(26)-C(31)-C(35)	0.4(16)	C(53)-C(54)-C(55)-C(50)	-0.1(16)
C(26)-C(27)-C(32)-C(33)	139.0(11)	N(3)-C(57)-C(58)-N(4)	0.7(10)
C(28)-C(27)-C(32)-C(33)	-40.9(15)	C(59)-C(57)-C(58)-N(4)	-175.1(7)
C(26)-C(27)-C(32)-C(34)	-97.5(12)	N(3)-C(57)-C(58)-C(68)	176.8(8)
C(28)-C(27)-C(32)-C(34)	82.7(13)	C(59)-C(57)-C(58)-C(68)	0.9(11)
C(30)-C(31)-C(35)-C(37)	-86.8(14)	C(58)-C(57)-C(59)-C(60)	175.5(10)
C(26)-C(31)-C(35)-C(37)	91.8(14)	N(3)-C(57)-C(59)-C(60)	2(2)
C(30)-C(31)-C(35)-C(36)	36.8(16)	C(58)-C(57)-C(59)-C(64)	-1.5(10)
C(26)-C(31)-C(35)-C(36)	-144.7(12)	N(3)-C(57)-C(59)-C(64)	-174.9(11)
C(43)-C(38)-C(39)-C(40)	-2.0(15)	C(64)-C(59)-C(60)-C(61)	-3.4(13)
P(1)-C(38)-C(39)-C(40)	-175.4(9)	C(57)-C(59)-C(60)-C(61)	179.9(10)
C(38)-C(39)-C(40)-C(41)	0.8(17)	C(59)-C(60)-C(61)-C(62)	0.2(14)
C(39)-C(40)-C(41)-C(42)	-0.3(18)	C(60)-C(61)-C(62)-C(63)	3.4(15)
C(40)-C(41)-C(42)-C(43)	1.0(16)	C(61)-C(62)-C(63)-C(64)	-3.4(15)
C(39)-C(38)-C(43)-C(42)	2.7(14)	C(61)-C(62)-C(63)-C(65)	175.1(10)
P(1)-C(38)-C(43)-C(42)	176.4(7)	C(60)-C(59)-C(64)-C(63)	3.4(15)
C(41)-C(42)-C(43)-C(38)	-2.3(14)	C(57)-C(59)-C(64)-C(63)	-178.9(9)
C(49)-C(44)-C(45)-C(46)	0.5(14)	C(60)-C(59)-C(64)-C(68)	-176.1(8)
P(1)-C(44)-C(45)-C(46)	174.1(8)	C(57)-C(59)-C(64)-C(68)	1.6(11)
C(44)-C(45)-C(46)-C(47)	-1.5(15)	C(62)-C(63)-C(64)-C(59)	0.1(15)
C(45)-C(46)-C(47)-C(48)	2.8(16)	C(65)-C(63)-C(64)-C(59)	-178.7(9)
C(46)-C(47)-C(48)-C(49)	-3.1(16)	C(62)-C(63)-C(64)-C(68)	179.5(9)
C(47)-C(48)-C(49)-C(44)	2.0(16)	C(65)-C(63)-C(64)-C(68)	0.7(15)

C(62)-C(63)-C(65)-C(66)	179.0(10)	C(73)-C(74)-C(78)-C(79)	-43.7(12)
C(64)-C(63)-C(65)-C(66)	-2.5(14)	C(69)-C(74)-C(78)-C(79)	138.4(9)
C(63)-C(65)-C(66)-C(67)	3.0(15)	C(73)-C(74)-C(78)-C(80)	82.1(11)
C(65)-C(66)-C(67)-C(68)	-1.6(14)	C(69)-C(74)-C(78)-C(80)	-95.8(10)
C(66)-C(67)-C(68)-C(64)	-0.2(15)	C(86)-C(81)-C(82)-C(83)	-0.5(14)
C(66)-C(67)-C(68)-C(58)	-178.5(11)	N(4)-C(81)-C(82)-C(83)	-173.5(8)
C(59)-C(64)-C(68)-C(67)	-180.0(9)	C(86)-C(81)-C(82)-C(87)	178.5(8)
C(63)-C(64)-C(68)-C(67)	0.6(16)	N(4)-C(81)-C(82)-C(87)	5.5(13)
C(59)-C(64)-C(68)-C(58)	-1.1(12)	C(81)-C(82)-C(83)-C(84)	3.4(14)
C(63)-C(64)-C(68)-C(58)	179.4(10)	C(87)-C(82)-C(83)-C(84)	-175.6(9)
C(57)-C(58)-C(68)-C(67)	178.6(12)	C(82)-C(83)-C(84)-C(85)	-3.4(15)
N(4)-C(58)-C(68)-C(67)	-8(2)	C(83)-C(84)-C(85)-C(86)	0.4(16)
C(57)-C(58)-C(68)-C(64)	0.1(11)	C(82)-C(81)-C(86)-C(85)	-2.2(13)
N(4)-C(58)-C(68)-C(64)	173.9(13)	N(4)-C(81)-C(86)-C(85)	170.7(8)
C(74)-C(69)-C(70)-C(71)	-2.1(13)	C(82)-C(81)-C(86)-C(90)	179.0(9)
N(3)-C(69)-C(70)-C(71)	175.7(8)	N(4)-C(81)-C(86)-C(90)	-8.0(12)
C(74)-C(69)-C(70)-C(75)	178.3(8)	C(84)-C(85)-C(86)-C(81)	2.3(14)
N(3)-C(69)-C(70)-C(75)	-3.9(11)	C(84)-C(85)-C(86)-C(90)	-178.9(9)
C(69)-C(70)-C(71)-C(72)	1.4(14)	C(83)-C(82)-C(87)-C(88)	-38.6(12)
C(75)-C(70)-C(71)-C(72)	-179.0(8)	C(81)-C(82)-C(87)-C(88)	142.5(9)
C(70)-C(71)-C(72)-C(73)	0.3(15)	C(83)-C(82)-C(87)-C(89)	82.0(12)
C(71)-C(72)-C(73)-C(74)	-1.6(15)	C(81)-C(82)-C(87)-C(89)	-97.0(11)
C(72)-C(73)-C(74)-C(69)	0.9(14)	C(81)-C(86)-C(90)-C(91)	-140.0(8)
C(72)-C(73)-C(74)-C(78)	-177.1(9)	C(85)-C(86)-C(90)-C(91)	41.3(12)
C(70)-C(69)-C(74)-C(73)	1.0(13)	C(81)-C(86)-C(90)-C(92)	96.2(10)
N(3)-C(69)-C(74)-C(73)	-176.9(8)	C(85)-C(86)-C(90)-C(92)	-82.5(11)
C(70)-C(69)-C(74)-C(78)	178.9(8)	C(98)-C(93)-C(94)-C(95)	-3.3(14)
N(3)-C(69)-C(74)-C(78)	1.1(12)	P(2)-C(93)-C(94)-C(95)	179.5(8)
C(71)-C(70)-C(75)-C(77)	-80.9(10)	C(93)-C(94)-C(95)-C(96)	2.2(15)
C(69)-C(70)-C(75)-C(77)	98.8(9)	C(94)-C(95)-C(96)-C(97)	0.8(16)
C(71)-C(70)-C(75)-C(76)	41.9(11)	C(95)-C(96)-C(97)-C(98)	-2.5(16)
C(69)-C(70)-C(75)-C(76)	-138.4(8)	C(94)-C(93)-C(98)-C(97)	1.5(14)

P(2)-C(93)-C(98)-C(97)	178.5(8)	N(1)-C(1)-N(2)-C(26)	-172.1(8)
C(96)-C(97)-C(98)-C(93)	1.4(15)	Pd(1)-C(1)-N(2)-C(26)	10.9(13)
C(104)-C(99)-C(100)-C(101)	0.8(18)	C(2)-C(3)-N(2)-C(1)	1.4(10)
P(2)-C(99)-C(100)-C(101)	-173.4(9)	C(13)-C(3)-N(2)-C(1)	178.1(12)
C(99)-C(100)-C(101)-C(102)	-4.0(19)	C(2)-C(3)-N(2)-C(26)	173.3(9)
C(100)-C(101)-C(102)-C(103)	4.7(18)	C(13)-C(3)-N(2)-C(26)	-10.1(19)
C(101)-C(102)-C(103)-C(104)	-2.5(19)	C(27)-C(26)-N(2)-C(1)	-100.3(11)
C(100)-C(99)-C(104)-C(103)	1.5(17)	C(31)-C(26)-N(2)-C(1)	81.2(12)
P(2)-C(99)-C(104)-C(103)	175.3(9)	C(27)-C(26)-N(2)-C(3)	89.0(12)
C(102)-C(103)-C(104)-C(99)	-1(2)	C(31)-C(26)-N(2)-C(3)	-89.5(12)
C(110)-C(105)-C(106)-C(107)	-2.0(14)	N(4)-C(56)-N(3)-C(57)	-3.0(9)
P(2)-C(105)-C(106)-C(107)	172.7(8)	Pd(2)-C(56)-N(3)-C(57)	176.4(6)
C(105)-C(106)-C(107)-C(108)	2.4(17)	N(4)-C(56)-N(3)-C(69)	170.6(7)
C(106)-C(107)-C(108)-C(109)	-1.9(18)	Pd(2)-C(56)-N(3)-C(69)	-10.1(11)
C(107)-C(108)-C(109)-C(110)	1.0(18)	C(58)-C(57)-N(3)-C(56)	1.4(10)
C(108)-C(109)-C(110)-C(105)	-0.7(17)	C(59)-C(57)-N(3)-C(56)	174.9(11)
C(106)-C(105)-C(110)-C(109)	1.2(15)	C(58)-C(57)-N(3)-C(69)	-172.2(7)
P(2)-C(105)-C(110)-C(109)	-173.7(9)	C(59)-C(57)-N(3)-C(69)	1.3(16)
N(2)-C(1)-N(1)-C(2)	-1.0(9)	C(74)-C(69)-N(3)-C(56)	-79.9(10)
Pd(1)-C(1)-N(1)-C(2)	175.9(6)	C(70)-C(69)-N(3)-C(56)	102.2(9)
N(2)-C(1)-N(1)-C(14)	176.2(8)	C(74)-C(69)-N(3)-C(57)	92.9(10)
Pd(1)-C(1)-N(1)-C(14)	-6.9(12)	C(70)-C(69)-N(3)-C(57)	-85.1(10)
C(3)-C(2)-N(1)-C(1)	2.0(9)	N(3)-C(56)-N(4)-C(58)	3.4(9)
C(4)-C(2)-N(1)-C(1)	-175.7(11)	Pd(2)-C(56)-N(4)-C(58)	-175.9(7)
C(3)-C(2)-N(1)-C(14)	-175.3(8)	N(3)-C(56)-N(4)-C(81)	-173.6(7)
C(4)-C(2)-N(1)-C(14)	7.0(17)	Pd(2)-C(56)-N(4)-C(81)	7.1(12)
C(19)-C(14)-N(1)-C(1)	87.0(12)	C(57)-C(58)-N(4)-C(56)	-2.6(10)
C(15)-C(14)-N(1)-C(1)	-93.7(10)	C(68)-C(58)-N(4)-C(56)	-176.5(14)
C(19)-C(14)-N(1)-C(2)	-96.3(11)	C(57)-C(58)-N(4)-C(81)	174.4(8)
C(15)-C(14)-N(1)-C(2)	83.0(11)	C(68)-C(58)-N(4)-C(81)	1(2)
N(1)-C(1)-N(2)-C(3)	-0.2(10)	C(86)-C(81)-N(4)-C(56)	97.9(9)
Pd(1)-C(1)-N(2)-C(3)	-177.2(6)	C(82)-C(81)-N(4)-C(56)	-88.7(11)

C(86)-C(81)-N(4)-C(58)	-78.7(11)	C(104)-C(99)-P(2)-C(105)	-41.6(10)
C(82)-C(81)-N(4)-C(58)	94.8(11)	C(100)-C(99)-P(2)-C(105)	132.1(9)
C(39)-C(38)-P(1)-C(50)	-62.5(9)	C(104)-C(99)-P(2)-C(93)	69.9(10)
C(43)-C(38)-P(1)-C(50)	124.0(7)	C(100)-C(99)-P(2)-C(93)	-116.3(9)
C(39)-C(38)-P(1)-C(44)	49.3(9)	C(104)-C(99)-P(2)-Pd(2)	-169.0(9)
C(43)-C(38)-P(1)-C(44)	-124.2(7)	C(100)-C(99)-P(2)-Pd(2)	4.8(9)
C(39)-C(38)-P(1)-Pd(1)	175.2(7)	N(2)-C(1)-Pd(1)-Cl(1)	-102.7(7)
C(43)-C(38)-P(1)-Pd(1)	1.7(8)	N(1)-C(1)-Pd(1)-Cl(1)	80.8(7)
C(55)-C(50)-P(1)-C(38)	4.2(9)	N(2)-C(1)-Pd(1)-Cl(2)	84.0(7)
C(51)-C(50)-P(1)-C(38)	-174.6(6)	N(1)-C(1)-Pd(1)-Cl(2)	-92.5(7)
C(55)-C(50)-P(1)-C(44)	-105.9(8)	N(2)-C(1)-Pd(1)-P(1)	24(3)
C(51)-C(50)-P(1)-C(44)	75.2(7)	N(1)-C(1)-Pd(1)-P(1)	-152.7(17)
C(55)-C(50)-P(1)-Pd(1)	128.5(7)	C(38)-P(1)-Pd(1)-C(1)	135(2)
C(51)-C(50)-P(1)-Pd(1)	-50.4(7)	C(50)-P(1)-Pd(1)-C(1)	12(2)
C(45)-C(44)-P(1)-C(38)	42.5(8)	C(44)-P(1)-Pd(1)-C(1)	-107(2)
C(49)-C(44)-P(1)-C(38)	-143.9(8)	C(38)-P(1)-Pd(1)-Cl(1)	-98.3(3)
C(45)-C(44)-P(1)-C(50)	158.3(8)	C(50)-P(1)-Pd(1)-Cl(1)	138.5(3)
C(49)-C(44)-P(1)-C(50)	-28.2(9)	C(44)-P(1)-Pd(1)-Cl(1)	19.7(4)
C(45)-C(44)-P(1)-Pd(1)	-80.8(8)	C(38)-P(1)-Pd(1)-Cl(2)	74.8(3)
C(49)-C(44)-P(1)-Pd(1)	92.8(7)	C(50)-P(1)-Pd(1)-Cl(2)	-48.4(3)
C(110)-C(105)-P(2)-C(93)	-162.0(7)	C(44)-P(1)-Pd(1)-Cl(2)	-167.2(4)
C(106)-C(105)-P(2)-C(93)	23.5(9)	N(3)-C(56)-Pd(2)-Cl(3)	108.0(7)
C(110)-C(105)-P(2)-C(99)	-47.7(8)	N(4)-C(56)-Pd(2)-Cl(3)	-72.8(7)
C(106)-C(105)-P(2)-C(99)	137.8(8)	N(3)-C(56)-Pd(2)-P(2)	-12(3)
C(110)-C(105)-P(2)-Pd(2)	78.0(8)	N(4)-C(56)-Pd(2)-P(2)	166.7(15)
C(106)-C(105)-P(2)-Pd(2)	-96.5(8)	N(3)-C(56)-Pd(2)-Cl(4)	-79.9(7)
C(98)-C(93)-P(2)-C(105)	106.6(9)	N(4)-C(56)-Pd(2)-Cl(4)	99.3(7)
C(94)-C(93)-P(2)-C(105)	-76.3(8)	C(105)-P(2)-Pd(2)-C(56)	99(2)
C(98)-C(93)-P(2)-C(99)	-5.1(10)	C(93)-P(2)-Pd(2)-C(56)	-19(2)
C(94)-C(93)-P(2)-C(99)	172.0(7)	C(99)-P(2)-Pd(2)-C(56)	-140(2)
C(98)-C(93)-P(2)-Pd(2)	-128.9(7)	C(105)-P(2)-Pd(2)-Cl(3)	-21.9(3)
C(94)-C(93)-P(2)-Pd(2)	48.2(8)	C(93)-P(2)-Pd(2)-Cl(3)	-139.5(4)

C(99)-P(2)-Pd(2)-Cl(3)	99.5(3)
C(105)-P(2)-Pd(2)-Cl(4)	166.1(3)
C(93)-P(2)-Pd(2)-Cl(4)	48.5(4)
C(99)-P(2)-Pd(2)-Cl(4)	-72.5(3)

Table A5: Torsion angles [°] for **2**.

Identification code	shelxl
Empirical formula	C _{35.75} H ₂₈ Cl N ₂ O _{1.25} Pd _{0.50}
Formula weight	594.25
Temperature	100(2) K
Wavelength	0.71069 Å
Crystal system	orthorhombic
Space group	CCCa
Unit cell dimensions	a = 15.683(5) Å $\alpha = 90.000(5)^\circ$. b = 25.640(5) Å $\beta = 90.000(5)^\circ$. c = 14.820(5) Å $\gamma = 90.000(5)^\circ$.
Volume	5959(3) Å ³
Z	8
Density (calculated)	1.325 Mg/m ³
Absorption coefficient	0.452 mm ⁻¹
F(000)	2452
Crystal size	0.33 x 0.20 x 0.18 mm ³
Theta range for data collection	1.59 to 27.50°.
Index ranges	-20 ≤ h ≤ 20, -33 ≤ k ≤ 33, -19 ≤ l ≤ 19
Reflections collected	67250
Independent reflections	3434 [R(int) = 0.0555]
Completeness to theta = 27.50°	99.9 %
Max. and min. transmission	0.9231 and 0.8652
Refinement method	Full-matrix least-squares on F ²
Data / restraints / parameters	3434 / 0 / 173
Goodness-of-fit on F ²	1.098
Final R indices [I > 2sigma(I)]	R1 = 0.0602, wR2 = 0.1835
R indices (all data)	R1 = 0.0658, wR2 = 0.1905
Largest diff. peak and hole	1.265 and -0.867 e.Å ⁻³

Table A6: Crystal data and structure refinement for **3**.

	x	y	z	U(eq)
C(1)	0	1711(2)	2500	31(1)
C(1S)	2649(6)	490(4)	-1433(7)	163(4)
C(2)	159(2)	876(1)	2075(3)	44(1)
C(2S)	2772(8)	272(4)	-618(8)	188(5)
C(3)	280(3)	340(2)	1762(3)	55(1)
C(4)	592(3)	95(2)	1002(3)	68(1)
C(5)	608(5)	-458(2)	1004(4)	91(2)
C(6)	312(5)	-746(2)	1717(5)	98(2)
C(7)	0	-506(3)	2500	80(3)
C(8)	0	39(2)	2500	62(2)
C(9)	570(2)	1552(1)	941(2)	36(1)
C(10)	-9(2)	1733(1)	307(2)	35(1)
C(11)	298(3)	1864(2)	-546(2)	46(1)
C(12)	1145(3)	1814(2)	-768(3)	59(1)
C(13)	1704(3)	1626(2)	-116(3)	67(1)
C(14)	1438(2)	1489(2)	758(3)	52(1)
C(15)	-947(2)	1777(2)	495(2)	42(1)
C(16)	1449(4)	1933(3)	-1701(4)	92(2)
C(17)	2054(3)	1287(2)	1443(3)	67(1)
N(1)	255(2)	1391(1)	1817(2)	36(1)
Cl(1)	1475(1)	2500	2500	36(1)
Pd(1)	0	2500	2500	28(1)
O(1S)	2500	0	-2094(10)	224(5)

Table A7: Atomic coordinates ($\times 10^4$) and equivalent isotropic displacement parameters ($\text{\AA}^2 \times 10^3$) for **3**. U(eq) is defined as one third of the trace of the orthogonalized U_{ij} tensor.

C(1)-N(1)	1.363(4)	C(15)-H(15A)	0.9800
C(1)-N(1)#1	1.363(4)	C(15)-H(15B)	0.9800
C(1)-Pd(1)	2.022(5)	C(15)-H(15C)	0.9800
C(1S)-C(2S)	1.345(14)	C(16)-H(16A)	0.9800
C(1S)-O(1S)	1.610(11)	C(16)-H(16B)	0.9800
C(2)-C(2)#1	1.356(8)	C(16)-H(16C)	0.9800
C(2)-N(1)	1.385(4)	C(17)-H(17A)	0.9800
C(2)-C(3)	1.462(5)	C(17)-H(17B)	0.9800
C(2S)-C(2S)#2	1.63(2)	C(17)-H(17C)	0.9800
C(3)-C(4)	1.379(6)	Cl(1)-Pd(1)	2.3131(14)
C(3)-C(8)	1.409(6)	Pd(1)-C(1)#3	2.022(5)
C(4)-C(5)	1.417(6)	Pd(1)-Cl(1)#3	2.3131(14)
C(4)-H(4)	0.9500	O(1S)-C(1S)#2	1.610(11)
C(5)-C(6)	1.371(10)	N(1)-C(1)-N(1)#1	106.0(4)
C(5)-H(5)	0.9500	N(1)-C(1)-Pd(1)	127.0(2)
C(6)-C(7)	1.401(8)	N(1)#1-C(1)-Pd(1)	127.0(2)
C(6)-H(6)	0.9500	C(2S)-C(1S)-O(1S)	104.1(10)
C(7)-C(8)	1.397(9)	C(2)#1-C(2)-N(1)	107.3(2)
C(7)-C(6)#1	1.401(8)	C(2)#1-C(2)-C(3)	110.0(3)
C(8)-C(3)#1	1.409(6)	N(1)-C(2)-C(3)	142.7(4)
C(9)-C(10)	1.386(5)	C(1S)-C(2S)-C(2S)#2	106.2(8)
C(9)-C(14)	1.396(5)	C(4)-C(3)-C(8)	119.6(4)
C(9)-N(1)	1.449(4)	C(4)-C(3)-C(2)	137.1(4)
C(10)-C(11)	1.394(5)	C(8)-C(3)-C(2)	103.2(4)
C(10)-C(15)	1.502(4)	C(3)-C(4)-C(5)	117.4(5)
C(11)-C(12)	1.374(6)	C(3)-C(4)-H(4)	121.3
C(11)-H(11)	0.9500	C(5)-C(4)-H(4)	121.3
C(12)-C(13)	1.391(7)	C(6)-C(5)-C(4)	122.3(6)
C(12)-C(16)	1.494(6)	C(6)-C(5)-H(5)	118.8
C(13)-C(14)	1.405(6)	C(4)-C(5)-H(5)	118.8
C(13)-H(13)	0.9500	C(5)-C(6)-C(7)	121.3(5)
C(14)-C(17)	1.494(6)	C(5)-C(6)-H(6)	119.3

C(7)-C(6)-H(6)	119.3	H(15A)-C(15)-H(15B)	109.5
C(8)-C(7)-C(6)#1	116.0(4)	C(10)-C(15)-H(15C)	109.5
C(8)-C(7)-C(6)	116.0(4)	H(15A)-C(15)-H(15C)	109.5
C(6)#1-C(7)-C(6)	127.9(7)	H(15B)-C(15)-H(15C)	109.5
C(7)-C(8)-C(3)	123.2(3)	C(12)-C(16)-H(16A)	109.5
C(7)-C(8)-C(3)#1	123.2(3)	C(12)-C(16)-H(16B)	109.5
C(3)-C(8)-C(3)#1	113.6(5)	H(16A)-C(16)-H(16B)	109.5
C(10)-C(9)-C(14)	123.0(3)	C(12)-C(16)-H(16C)	109.5
C(10)-C(9)-N(1)	118.6(3)	H(16A)-C(16)-H(16C)	109.5
C(14)-C(9)-N(1)	118.3(3)	H(16B)-C(16)-H(16C)	109.5
C(9)-C(10)-C(11)	118.0(3)	C(14)-C(17)-H(17A)	109.5
C(9)-C(10)-C(15)	122.8(3)	C(14)-C(17)-H(17B)	109.5
C(11)-C(10)-C(15)	119.2(3)	H(17A)-C(17)-H(17B)	109.5
C(12)-C(11)-C(10)	121.9(4)	C(14)-C(17)-H(17C)	109.5
C(12)-C(11)-H(11)	119.0	H(17A)-C(17)-H(17C)	109.5
C(10)-C(11)-H(11)	119.0	H(17B)-C(17)-H(17C)	109.5
C(11)-C(12)-C(13)	118.4(4)	C(1)-N(1)-C(2)	109.7(3)
C(11)-C(12)-C(16)	120.7(5)	C(1)-N(1)-C(9)	126.5(3)
C(13)-C(12)-C(16)	120.8(4)	C(2)-N(1)-C(9)	123.7(3)
C(12)-C(13)-C(14)	122.6(4)	C(1)#3-Pd(1)-C(1)	180.0
C(12)-C(13)-H(13)	118.7	C(1)#3-Pd(1)-Cl(1)	90.000(5)
C(14)-C(13)-H(13)	118.7	C(1)-Pd(1)-Cl(1)	90.000(5)
C(9)-C(14)-C(13)	116.1(4)	C(1)#3-Pd(1)-Cl(1)#3	90.000(5)
C(9)-C(14)-C(17)	122.5(4)	C(1)-Pd(1)-Cl(1)#3	90.000(5)
C(13)-C(14)-C(17)	121.4(4)	Cl(1)-Pd(1)-Cl(1)#3	180.0
C(10)-C(15)-H(15A)	109.5	C(1S)-O(1S)-C(1S)#2	105.0(11)
C(10)-C(15)-H(15B)	109.5		

Table A8: Bond lengths [\AA] and angles [$^\circ$] for **3**. Symmetry transformations used to generate equivalent atoms: #1 -x,y,-z+1/2 #2 -x+1/2,-y,z #3 -x+0,-y+1/2,z.

	U11	U22	U33	U23	U13	U12
C(1)	28(2)	31(2)	34(2)	0	-2(1)	0
C(2)	52(2)	34(2)	44(2)	-4(2)	-13(2)	4(1)
C(3)	70(3)	37(2)	57(2)	-8(2)	-27(2)	10(2)
C(4)	95(3)	45(2)	64(3)	-18(2)	-35(2)	24(2)
C(5)	136(5)	49(3)	88(4)	-29(3)	-54(4)	33(3)
C(6)	158(6)	34(2)	102(4)	-15(3)	-71(5)	19(3)
C(7)	117(7)	30(3)	92(6)	0	-60(5)	0
C(8)	84(5)	32(3)	70(4)	0	-39(3)	0
C(9)	34(2)	39(2)	36(2)	-9(1)	2(1)	-2(1)
C(10)	37(2)	33(2)	35(2)	-4(1)	3(1)	-5(1)
C(11)	55(2)	45(2)	38(2)	-4(1)	6(2)	-11(2)
C(12)	57(2)	70(3)	51(2)	-12(2)	16(2)	-16(2)
C(13)	38(2)	91(3)	72(3)	-31(2)	23(2)	-11(2)
C(14)	35(2)	66(2)	55(2)	-22(2)	2(2)	1(2)
C(15)	37(2)	55(2)	35(2)	-1(2)	-4(1)	-1(2)
C(16)	81(4)	128(5)	66(3)	-8(3)	38(3)	-24(4)
C(17)	39(2)	86(3)	78(3)	-31(2)	-12(2)	17(2)
N(1)	37(1)	33(1)	38(1)	-3(1)	-4(1)	3(1)
Cl(1)	25(1)	39(1)	45(1)	2(1)	0	0
Pd(1)	25(1)	29(1)	29(1)	0	0	0

Table A9: Anisotropic displacement parameters ($\text{\AA}^2 \times 10^3$) for **3**. The anisotropic displacement factor exponent takes the form: $-2\pi^2 [h^2 a^{*2} U^{11} + \dots + 2 h k a^* b^* U^{12}]$.

O(1S)-C(1S)-C(2S)-C(2S)#2	-29.7(13)	C(10)-C(9)-C(14)-C(17)	-179.3(4)
C(2)#1-C(2)-C(3)-C(4)	-177.7(5)	N(1)-C(9)-C(14)-C(17)	-2.8(5)
N(1)-C(2)-C(3)-C(4)	1.8(10)	C(12)-C(13)-C(14)-C(9)	0.1(6)
C(2)#1-C(2)-C(3)-C(8)	0.5(5)	C(12)-C(13)-C(14)-C(17)	179.9(4)
N(1)-C(2)-C(3)-C(8)	180.0(5)	N(1)#1-C(1)-N(1)-C(2)	0.01(18)
C(8)-C(3)-C(4)-C(5)	0.4(6)	Pd(1)-C(1)-N(1)-C(2)	-
C(2)-C(3)-C(4)-C(5)	178.4(5)		179.99(18)
C(3)-C(4)-C(5)-C(6)	1.4(8)	N(1)#1-C(1)-N(1)-C(9)	179.1(4)
C(4)-C(5)-C(6)-C(7)	-2.1(9)	Pd(1)-C(1)-N(1)-C(9)	-0.9(4)
C(5)-C(6)-C(7)-C(8)	0.9(7)	C(2)#1-C(2)-N(1)-C(1)	0.0(5)
C(5)-C(6)-C(7)-C(6)#1	-179.1(7)	C(3)-C(2)-N(1)-C(1)	-179.5(5)
C(6)#1-C(7)-C(8)-C(3)	-179.1(4)	C(2)#1-C(2)-N(1)-C(9)	-179.1(4)
C(6)-C(7)-C(8)-C(3)	0.9(4)	C(3)-C(2)-N(1)-C(9)	1.3(7)
C(6)#1-C(7)-C(8)-C(3)#1	0.9(4)	C(10)-C(9)-N(1)-C(1)	-75.5(4)
C(6)-C(7)-C(8)-C(3)#1	-179.1(4)	C(14)-C(9)-N(1)-C(1)	107.9(4)
C(4)-C(3)-C(8)-C(7)	-1.6(5)	C(10)-C(9)-N(1)-C(2)	103.5(4)
C(2)-C(3)-C(8)-C(7)	179.84(18)	C(14)-C(9)-N(1)-C(2)	-73.1(4)
C(4)-C(3)-C(8)-C(3)#1	178.4(5)	N(1)-C(1)-Pd(1)-C(1)#3	-158(61)
C(2)-C(3)-C(8)-C(3)#1	-0.16(18)	N(1)#1-C(1)-Pd(1)-C(1)#3	22(61)
C(14)-C(9)-C(10)-C(11)	-0.7(5)	N(1)-C(1)-Pd(1)-Cl(1)	-68.42(15)
N(1)-C(9)-C(10)-C(11)	-177.2(3)	N(1)#1-C(1)-Pd(1)-Cl(1)	111.58(15)
C(14)-C(9)-C(10)-C(15)	177.1(3)	N(1)-C(1)-Pd(1)-Cl(1)#3	111.58(15)
N(1)-C(9)-C(10)-C(15)	0.7(5)	N(1)#1-C(1)-Pd(1)-Cl(1)#3	-68.42(15)
C(9)-C(10)-C(11)-C(12)	0.3(5)	C(2S)-C(1S)-O(1S)-C(1S)#2	12.9(6)
C(15)-C(10)-C(11)-C(12)	-177.6(4)		
C(10)-C(11)-C(12)-C(13)	0.2(6)		
C(10)-C(11)-C(12)-C(16)	177.2(4)		
C(11)-C(12)-C(13)-C(14)	-0.4(7)		
C(16)-C(12)-C(13)-C(14)	-177.4(5)		
C(10)-C(9)-C(14)-C(13)	0.5(5)		
N(1)-C(9)-C(14)-C(13)	177.0(3)		

Table A10: Torsion angles [°] for **3**.
Symmetry transformations
used to generate equivalent
atoms: #1 -x,y,-z+1/2 #2 -
x+1/2,-y,z #3 -x+0,-
y+1/2,z.

Identification code	shelxl	
Empirical formula	C74 H80 Cl2 N4 Pd	
Formula weight	1202.72	
Temperature	100(2) K	
Wavelength	0.71073 Å	
Crystal system	monoclinic	
Space group	P21/n	
Unit cell dimensions	a = 12.865(11) Å	∠ = 90°.
	b = 11.911(10) Å	∠ = 94.49(2)°.
	c = 20.737(17) Å	∠ = 90°.
Volume	3168(5) Å ³	
Z	2	
Density (calculated)	1.261 Mg/m ³	
Absorption coefficient	0.423 mm ⁻¹	
F(000)	1264	
Crystal size	0.15 x 0.12 x 0.11 mm ³	
Theta range for data collection	1.93 to 25.00°.	
Index ranges	-15 ≤ h ≤ 15, -14 ≤ k ≤ 14, -24 ≤ l ≤ 24	
Reflections collected	47078	
Independent reflections	5576 [R(int) = 0.0882]	
Completeness to theta = 25.00°	99.9 %	
Max. and min. transmission	0.9550 and 0.9393	
Refinement method	Full-matrix least-squares on F ²	
Data / restraints / parameters	5576 / 0 / 375	
Goodness-of-fit on F ²	1.261	
Final R indices [I > 2sigma(I)]	R1 = 0.0989, wR2 = 0.2524	
R indices (all data)	R1 = 0.1029, wR2 = 0.2562	
Largest diff. peak and hole	2.858 and -1.049 e.Å ⁻³	

Table A11: Crystal data and structure refinement for **4**.

	x	y	z	U(eq)
C(1)	5287(5)	448(5)	948(3)	37(1)
C(2)	5189(4)	452(5)	2041(3)	37(1)
C(3)	6127(5)	902(5)	1925(3)	39(1)
C(4)	5035(4)	466(5)	2739(3)	37(1)
C(5)	4284(5)	164(5)	3147(3)	45(2)
C(6)	4488(5)	372(6)	3829(3)	48(2)
C(7)	5398(5)	845(6)	4084(3)	47(2)
C(8)	6208(5)	1166(5)	3678(3)	43(1)
C(9)	5994(5)	953(5)	3017(3)	40(1)
C(10)	7184(5)	1680(5)	3869(3)	44(1)
C(11)	7851(5)	1983(5)	3403(3)	47(2)
C(12)	7626(5)	1771(5)	2728(3)	43(1)
C(13)	6690(5)	1266(5)	2536(3)	41(1)
C(14)	3578(5)	-146(5)	1395(3)	35(1)
C(15)	3336(5)	-1286(5)	1453(3)	42(1)
C(16)	2277(5)	-1581(6)	1479(3)	51(2)
C(17)	1528(5)	-743(7)	1465(3)	53(2)
C(18)	1765(5)	381(7)	1413(3)	50(2)
C(19)	2810(5)	714(6)	1364(3)	47(2)
C(20)	4172(5)	-2220(6)	1490(3)	47(2)
C(21)	4427(6)	-2637(7)	2183(3)	59(2)
C(22)	3870(7)	-3187(7)	1039(4)	72(2)
C(23)	3098(5)	1956(6)	1296(3)	46(2)
C(24)	2253(6)	2630(6)	889(3)	56(2)
C(25)	3315(5)	2540(6)	1955(3)	53(2)
C(26)	6981(5)	1564(5)	952(3)	38(1)
C(27)	6793(5)	2735(5)	902(3)	46(2)
C(28)	7565(6)	3382(6)	658(3)	52(2)
C(29)	8475(6)	2914(6)	475(4)	59(2)
C(30)	8647(6)	1763(6)	537(3)	52(2)

C(31)	7896(5)	1059(5)	783(3)	42(1)
C(32)	5828(5)	3294(5)	1127(3)	50(2)
C(33)	5294(6)	4076(6)	618(3)	56(2)
C(34)	6094(6)	3970(6)	1753(3)	60(2)
C(35)	8134(5)	-159(5)	914(3)	43(1)
C(36)	8858(5)	-679(6)	440(3)	47(2)
C(37)	8589(6)	-360(6)	1617(3)	52(2)
N(1)	4677(4)	172(4)	1447(2)	38(1)
N(2)	6193(3)	903(4)	1257(2)	34(1)
Cl(1)	5860(1)	-1679(1)	220(1)	43(1)
Pd(1)	5000	0	0	35(1)

Table A12: Atomic coordinates ($\times 10^4$) and equivalent isotropic displacement parameters ($\text{\AA}^2 \times 10^3$) for **4**. $U(\text{eq})$ is defined as one third of the trace of the orthogonalized U_{ij} tensor.

C(1)-N(1)	1.386(8)	C(17)-C(18)	1.379(11)
C(1)-N(2)	1.396(7)	C(17)-H(17)	0.9500
C(1)-Pd(1)	2.043(6)	C(18)-C(19)	1.414(9)
C(2)-C(3)	1.360(8)	C(18)-H(18)	0.9500
C(2)-N(1)	1.390(7)	C(19)-C(23)	1.534(10)
C(2)-C(4)	1.477(8)	C(20)-C(22)	1.516(10)
C(3)-N(2)	1.393(7)	C(20)-C(21)	1.531(9)
C(3)-C(13)	1.475(8)	C(20)-H(20)	1.0000
C(4)-C(5)	1.381(9)	C(21)-H(21A)	0.9800
C(4)-C(9)	1.442(8)	C(21)-H(21B)	0.9800
C(5)-C(6)	1.438(9)	C(21)-H(21C)	0.9800
C(5)-H(5)	0.9500	C(22)-H(22A)	0.9800
C(6)-C(7)	1.368(9)	C(22)-H(22B)	0.9800
C(6)-H(6)	0.9500	C(22)-H(22C)	0.9800
C(7)-C(8)	1.441(9)	C(23)-C(25)	1.539(8)
C(7)-H(7)	0.9500	C(23)-C(24)	1.547(9)
C(8)-C(9)	1.401(8)	C(23)-H(23)	1.0000
C(8)-C(10)	1.425(9)	C(24)-H(24A)	0.9800
C(9)-C(13)	1.440(8)	C(24)-H(24B)	0.9800
C(10)-C(11)	1.389(9)	C(24)-H(24C)	0.9800
C(10)-H(10)	0.9500	C(25)-H(25A)	0.9800
C(11)-C(12)	1.429(8)	C(25)-H(25B)	0.9800
C(11)-H(11)	0.9500	C(25)-H(25C)	0.9800
C(12)-C(13)	1.376(9)	C(26)-C(31)	1.392(9)
C(12)-H(12)	0.9500	C(26)-C(27)	1.418(9)
C(14)-C(15)	1.401(8)	C(26)-N(2)	1.466(7)
C(14)-C(19)	1.421(9)	C(27)-C(28)	1.384(9)
C(14)-N(1)	1.460(8)	C(27)-C(32)	1.514(10)
C(15)-C(16)	1.412(9)	C(28)-C(29)	1.376(10)
C(15)-C(20)	1.544(9)	C(28)-H(28)	0.9500
C(16)-C(17)	1.387(10)	C(29)-C(30)	1.392(10)
C(16)-H(16)	0.9500	C(29)-H(29)	0.9500

C(30)-C(31)	1.405(9)	N(2)-C(3)-C(13)	142.1(5)
C(30)-H(30)	0.9500	C(5)-C(4)-C(9)	118.6(5)
C(31)-C(35)	1.503(9)	C(5)-C(4)-C(2)	138.7(6)
C(32)-C(33)	1.531(9)	C(9)-C(4)-C(2)	102.7(5)
C(32)-C(34)	1.542(9)	C(4)-C(5)-C(6)	118.3(6)
C(32)-H(32)	1.0000	C(4)-C(5)-H(5)	120.8
C(33)-H(33A)	0.9800	C(6)-C(5)-H(5)	120.8
C(33)-H(33B)	0.9800	C(7)-C(6)-C(5)	122.4(6)
C(33)-H(33C)	0.9800	C(7)-C(6)-H(6)	118.8
C(34)-H(34A)	0.9800	C(5)-C(6)-H(6)	118.8
C(34)-H(34B)	0.9800	C(6)-C(7)-C(8)	121.3(5)
C(34)-H(34C)	0.9800	C(6)-C(7)-H(7)	119.3
C(35)-C(36)	1.538(9)	C(8)-C(7)-H(7)	119.3
C(35)-C(37)	1.546(9)	C(9)-C(8)-C(10)	116.8(6)
C(35)-H(35)	1.0000	C(9)-C(8)-C(7)	115.4(6)
C(36)-H(36A)	0.9800	C(10)-C(8)-C(7)	127.9(5)
C(36)-H(36B)	0.9800	C(8)-C(9)-C(13)	123.1(6)
C(36)-H(36C)	0.9800	C(8)-C(9)-C(4)	124.0(5)
C(37)-H(37A)	0.9800	C(13)-C(9)-C(4)	112.8(5)
C(37)-H(37B)	0.9800	C(11)-C(10)-C(8)	119.9(6)
C(37)-H(37C)	0.9800	C(11)-C(10)-H(10)	120.1
Cl(1)-Pd(1)	2.314(2)	C(8)-C(10)-H(10)	120.1
Pd(1)-C(1)#1	2.043(6)	C(10)-C(11)-C(12)	123.1(6)
Pd(1)-Cl(1)#1	2.314(2)	C(10)-C(11)-H(11)	118.4
N(1)-C(1)-N(2)	104.5(5)	C(12)-C(11)-H(11)	118.4
N(1)-C(1)-Pd(1)	125.9(4)	C(13)-C(12)-C(11)	117.8(6)
N(2)-C(1)-Pd(1)	128.7(4)	C(13)-C(12)-H(12)	121.1
C(3)-C(2)-N(1)	107.6(5)	C(11)-C(12)-H(12)	121.1
C(3)-C(2)-C(4)	111.0(5)	C(12)-C(13)-C(9)	119.4(5)
N(1)-C(2)-C(4)	141.3(5)	C(12)-C(13)-C(3)	137.4(6)
C(2)-C(3)-N(2)	107.5(5)	C(9)-C(13)-C(3)	103.2(5)
C(2)-C(3)-C(13)	110.3(5)	C(15)-C(14)-C(19)	123.0(6)

C(15)-C(14)-N(1)	117.7(5)	C(20)-C(22)-H(22C)	109.5
C(19)-C(14)-N(1)	118.9(5)	H(22A)-C(22)-H(22C)	109.5
C(14)-C(15)-C(16)	117.8(6)	H(22B)-C(22)-H(22C)	109.5
C(14)-C(15)-C(20)	123.0(6)	C(19)-C(23)-C(25)	112.5(5)
C(16)-C(15)-C(20)	119.3(6)	C(19)-C(23)-C(24)	112.7(6)
C(17)-C(16)-C(15)	119.4(7)	C(25)-C(23)-C(24)	108.6(5)
C(17)-C(16)-H(16)	120.3	C(19)-C(23)-H(23)	107.6
C(15)-C(16)-H(16)	120.3	C(25)-C(23)-H(23)	107.6
C(18)-C(17)-C(16)	122.9(6)	C(24)-C(23)-H(23)	107.6
C(18)-C(17)-H(17)	118.5	C(23)-C(24)-H(24A)	109.5
C(16)-C(17)-H(17)	118.5	C(23)-C(24)-H(24B)	109.5
C(17)-C(18)-C(19)	119.7(7)	H(24A)-C(24)-H(24B)	109.5
C(17)-C(18)-H(18)	120.1	C(23)-C(24)-H(24C)	109.5
C(19)-C(18)-H(18)	120.1	H(24A)-C(24)-H(24C)	109.5
C(18)-C(19)-C(14)	117.2(6)	H(24B)-C(24)-H(24C)	109.5
C(18)-C(19)-C(23)	121.0(6)	C(23)-C(25)-H(25A)	109.5
C(14)-C(19)-C(23)	121.8(6)	C(23)-C(25)-H(25B)	109.5
C(22)-C(20)-C(21)	111.0(6)	H(25A)-C(25)-H(25B)	109.5
C(22)-C(20)-C(15)	111.9(5)	C(23)-C(25)-H(25C)	109.5
C(21)-C(20)-C(15)	112.2(5)	H(25A)-C(25)-H(25C)	109.5
C(22)-C(20)-H(20)	107.1	H(25B)-C(25)-H(25C)	109.5
C(21)-C(20)-H(20)	107.1	C(31)-C(26)-C(27)	123.3(6)
C(15)-C(20)-H(20)	107.1	C(31)-C(26)-N(2)	120.3(5)
C(20)-C(21)-H(21A)	109.5	C(27)-C(26)-N(2)	116.1(5)
C(20)-C(21)-H(21B)	109.5	C(28)-C(27)-C(26)	116.8(6)
H(21A)-C(21)-H(21B)	109.5	C(28)-C(27)-C(32)	119.8(6)
C(20)-C(21)-H(21C)	109.5	C(26)-C(27)-C(32)	123.3(6)
H(21A)-C(21)-H(21C)	109.5	C(29)-C(28)-C(27)	121.7(7)
H(21B)-C(21)-H(21C)	109.5	C(29)-C(28)-H(28)	119.1
C(20)-C(22)-H(22A)	109.5	C(27)-C(28)-H(28)	119.1
C(20)-C(22)-H(22B)	109.5	C(28)-C(29)-C(30)	120.4(7)
H(22A)-C(22)-H(22B)	109.5	C(28)-C(29)-H(29)	119.8

C(30)-C(29)-H(29)	119.8	C(31)-C(35)-H(35)	107.1
C(29)-C(30)-C(31)	120.8(7)	C(36)-C(35)-H(35)	107.1
C(29)-C(30)-H(30)	119.6	C(37)-C(35)-H(35)	107.1
C(31)-C(30)-H(30)	119.6	C(35)-C(36)-H(36A)	109.5
C(26)-C(31)-C(30)	116.9(6)	C(35)-C(36)-H(36B)	109.5
C(26)-C(31)-C(35)	122.3(5)	H(36A)-C(36)-H(36B)	109.5
C(30)-C(31)-C(35)	120.4(6)	C(35)-C(36)-H(36C)	109.5
C(27)-C(32)-C(33)	112.9(6)	H(36A)-C(36)-H(36C)	109.5
C(27)-C(32)-C(34)	110.9(6)	H(36B)-C(36)-H(36C)	109.5
C(33)-C(32)-C(34)	108.8(5)	C(35)-C(37)-H(37A)	109.5
C(27)-C(32)-H(32)	108.0	C(35)-C(37)-H(37B)	109.5
C(33)-C(32)-H(32)	108.0	H(37A)-C(37)-H(37B)	109.5
C(34)-C(32)-H(32)	108.0	C(35)-C(37)-H(37C)	109.5
C(32)-C(33)-H(33A)	109.5	H(37A)-C(37)-H(37C)	109.5
C(32)-C(33)-H(33B)	109.5	H(37B)-C(37)-H(37C)	109.5
H(33A)-C(33)-H(33B)	109.5	C(1)-N(1)-C(2)	110.4(5)
C(32)-C(33)-H(33C)	109.5	C(1)-N(1)-C(14)	127.4(5)
H(33A)-C(33)-H(33C)	109.5	C(2)-N(1)-C(14)	121.1(5)
H(33B)-C(33)-H(33C)	109.5	C(3)-N(2)-C(1)	110.0(4)
C(32)-C(34)-H(34A)	109.5	C(3)-N(2)-C(26)	121.8(4)
C(32)-C(34)-H(34B)	109.5	C(1)-N(2)-C(26)	126.3(4)
H(34A)-C(34)-H(34B)	109.5	C(1)#1-Pd(1)-C(1)	180.0(3)
C(32)-C(34)-H(34C)	109.5	C(1)#1-Pd(1)-Cl(1)#1	89.31(17)
H(34A)-C(34)-H(34C)	109.5	C(1)-Pd(1)-Cl(1)#1	90.69(17)
H(34B)-C(34)-H(34C)	109.5	C(1)#1-Pd(1)-Cl(1)	90.69(17)
C(31)-C(35)-C(36)	113.4(5)	C(1)-Pd(1)-Cl(1)	89.31(17)
C(31)-C(35)-C(37)	112.2(5)	Cl(1)#1-Pd(1)-Cl(1)	180.00(7)
C(36)-C(35)-C(37)	109.7(5)		

Table A13: Bond lengths [Å] and angles [°] for **4**. Symmetry transformations used to generate equivalent atoms: #1 -x+1,-y,-z.

	U11	U22	U33	U23	U13	U12
C(1)	39(3)	36(3)	36(3)	3(2)	2(2)	4(2)
C(2)	39(3)	42(3)	29(3)	-6(2)	-3(2)	0(3)
C(3)	45(3)	39(3)	33(3)	-5(2)	-3(2)	0(3)
C(4)	32(3)	44(3)	32(3)	-1(2)	-1(2)	3(2)
C(5)	41(3)	57(4)	37(3)	-1(3)	2(3)	-5(3)
C(6)	55(4)	52(4)	38(3)	1(3)	13(3)	-1(3)
C(7)	56(4)	52(4)	32(3)	-7(3)	4(3)	3(3)
C(8)	48(4)	44(3)	34(3)	1(3)	-4(2)	3(3)
C(9)	42(3)	42(3)	34(3)	3(2)	-3(2)	7(3)
C(10)	47(4)	44(3)	39(3)	-7(3)	-1(3)	5(3)
C(11)	49(4)	43(4)	48(4)	-9(3)	-3(3)	-5(3)
C(12)	47(4)	48(4)	33(3)	-7(3)	2(2)	-1(3)
C(13)	50(4)	42(3)	31(3)	-2(2)	0(2)	3(3)
C(14)	36(3)	43(3)	25(3)	-4(2)	-4(2)	-3(2)
C(15)	46(4)	52(4)	28(3)	1(3)	0(2)	-4(3)
C(16)	45(4)	64(4)	43(3)	8(3)	-2(3)	-11(3)
C(17)	38(3)	78(5)	41(3)	8(3)	0(3)	3(3)
C(18)	42(4)	68(5)	38(3)	5(3)	3(3)	5(3)
C(19)	50(4)	64(4)	27(3)	2(3)	-3(2)	9(3)
C(20)	43(4)	52(4)	46(3)	2(3)	1(3)	2(3)
C(21)	50(4)	70(5)	56(4)	8(4)	-1(3)	14(4)
C(22)	73(5)	58(5)	84(6)	-19(4)	-5(4)	9(4)
C(23)	48(4)	53(4)	37(3)	-4(3)	4(3)	9(3)
C(24)	60(4)	51(4)	56(4)	-1(3)	-5(3)	8(3)
C(25)	50(4)	63(4)	47(4)	-4(3)	3(3)	1(3)
C(26)	45(3)	36(3)	32(3)	0(2)	0(2)	-3(2)
C(27)	55(4)	47(4)	34(3)	2(3)	-5(3)	-10(3)
C(28)	68(5)	41(4)	48(4)	0(3)	3(3)	-7(3)
C(29)	66(5)	54(4)	60(4)	3(3)	13(3)	-8(3)
C(30)	53(4)	49(4)	54(4)	3(3)	2(3)	-4(3)

C(31)	40(3)	49(4)	36(3)	1(3)	-4(2)	-7(3)
C(32)	61(4)	37(3)	49(4)	-2(3)	-2(3)	1(3)
C(33)	68(5)	49(4)	50(4)	-6(3)	-10(3)	12(3)
C(34)	82(5)	53(4)	45(4)	-5(3)	-5(3)	6(4)
C(35)	35(3)	53(4)	40(3)	-3(3)	0(3)	-4(3)
C(36)	50(4)	50(4)	42(3)	-3(3)	5(3)	1(3)
C(37)	59(4)	62(4)	36(3)	-2(3)	7(3)	0(3)
N(1)	38(3)	45(3)	28(2)	-6(2)	-1(2)	-1(2)
N(2)	36(3)	38(3)	29(2)	-1(2)	-1(2)	-2(2)
Cl(1)	50(1)	44(1)	34(1)	0(1)	-3(1)	10(1)
Pd(1)	38(1)	38(1)	28(1)	0(1)	-2(1)	2(1)

Table A14: Anisotropic displacement parameters ($\text{\AA}^2 \times 10^3$) for **4**. The anisotropic displacement factor exponent takes the form: $-2\pi^2 [h^2 a^{*2} U^{11} + \dots + 2 h k a^* b^* U^{12}]$.

N(1)-C(2)-C(3)-N(2)	0.2(7)	C(2)-C(3)-C(13)-C(12)	-179.1(7)
C(4)-C(2)-C(3)-N(2)	-177.5(5)	N(2)-C(3)-C(13)-C(12)	-3.4(14)
N(1)-C(2)-C(3)-C(13)	177.4(5)	C(2)-C(3)-C(13)-C(9)	1.5(7)
C(4)-C(2)-C(3)-C(13)	-0.2(7)	N(2)-C(3)-C(13)-C(9)	177.2(7)
C(3)-C(2)-C(4)-C(5)	178.8(8)	C(19)-C(14)-C(15)-C(16)	0.4(9)
N(1)-C(2)-C(4)-C(5)	2.4(14)	N(1)-C(14)-C(15)-C(16)	172.7(5)
C(3)-C(2)-C(4)-C(9)	-1.1(7)	C(19)-C(14)-C(15)-C(20)	-179.6(5)
N(1)-C(2)-C(4)-C(9)	-177.5(7)	N(1)-C(14)-C(15)-C(20)	-7.3(8)
C(9)-C(4)-C(5)-C(6)	1.3(9)	C(14)-C(15)-C(16)-C(17)	-1.9(9)
C(2)-C(4)-C(5)-C(6)	-178.6(7)	C(20)-C(15)-C(16)-C(17)	178.2(5)
C(4)-C(5)-C(6)-C(7)	-0.7(10)	C(15)-C(16)-C(17)-C(18)	1.3(9)
C(5)-C(6)-C(7)-C(8)	0.2(10)	C(16)-C(17)-C(18)-C(19)	0.7(9)
C(6)-C(7)-C(8)-C(9)	-0.3(9)	C(17)-C(18)-C(19)-C(14)	-2.1(8)
C(6)-C(7)-C(8)-C(10)	178.8(6)	C(17)-C(18)-C(19)-C(23)	179.1(5)
C(10)-C(8)-C(9)-C(13)	-2.4(9)	C(15)-C(14)-C(19)-C(18)	1.6(8)
C(7)-C(8)-C(9)-C(13)	176.9(6)	N(1)-C(14)-C(19)-C(18)	-170.6(5)
C(10)-C(8)-C(9)-C(4)	-178.2(6)	C(15)-C(14)-C(19)-C(23)	-179.7(5)
C(7)-C(8)-C(9)-C(4)	1.0(9)	N(1)-C(14)-C(19)-C(23)	8.1(8)
C(5)-C(4)-C(9)-C(8)	-1.5(9)	C(14)-C(15)-C(20)-C(22)	-132.7(7)
C(2)-C(4)-C(9)-C(8)	178.4(6)	C(16)-C(15)-C(20)-C(22)	47.2(8)
C(5)-C(4)-C(9)-C(13)	-177.8(6)	C(14)-C(15)-C(20)-C(21)	101.7(7)
C(2)-C(4)-C(9)-C(13)	2.1(7)	C(16)-C(15)-C(20)-C(21)	-78.3(7)
C(9)-C(8)-C(10)-C(11)	2.4(9)	C(18)-C(19)-C(23)-C(25)	88.1(7)
C(7)-C(8)-C(10)-C(11)	-176.8(6)	C(14)-C(19)-C(23)-C(25)	-90.6(7)
C(8)-C(10)-C(11)-C(12)	-2.0(10)	C(18)-C(19)-C(23)-C(24)	-35.1(8)
C(10)-C(11)-C(12)-C(13)	1.5(10)	C(14)-C(19)-C(23)-C(24)	146.1(6)
C(11)-C(12)-C(13)-C(9)	-1.3(9)	C(31)-C(26)-C(27)-C(28)	1.3(9)
C(11)-C(12)-C(13)-C(3)	179.3(7)	N(2)-C(26)-C(27)-C(28)	175.4(5)
C(8)-C(9)-C(13)-C(12)	1.9(9)	C(31)-C(26)-C(27)-C(32)	-175.8(5)
C(4)-C(9)-C(13)-C(12)	178.2(6)	N(2)-C(26)-C(27)-C(32)	-1.6(8)
C(8)-C(9)-C(13)-C(3)	-178.6(5)	C(26)-C(27)-C(28)-C(29)	-0.2(9)
C(4)-C(9)-C(13)-C(3)	-2.3(7)	C(32)-C(27)-C(28)-C(29)	176.9(6)

C(27)-C(28)-C(29)-C(30)	-0.5(11)	N(1)-C(1)-N(2)-C(3)	-0.1(6)
C(28)-C(29)-C(30)-C(31)	0.3(11)	Pd(1)-C(1)-N(2)-C(3)	-169.7(4)
C(27)-C(26)-C(31)-C(30)	-1.5(9)	N(1)-C(1)-N(2)-C(26)	-164.6(5)
N(2)-C(26)-C(31)-C(30)	-175.4(5)	Pd(1)-C(1)-N(2)-C(26)	25.9(8)
C(27)-C(26)-C(31)-C(35)	172.5(5)	C(31)-C(26)-N(2)-C(3)	98.1(6)
N(2)-C(26)-C(31)-C(35)	-1.5(8)	C(27)-C(26)-N(2)-C(3)	-76.2(7)
C(29)-C(30)-C(31)-C(26)	0.6(9)	C(31)-C(26)-N(2)-C(1)	-99.1(7)
C(29)-C(30)-C(31)-C(35)	-173.4(6)	C(27)-C(26)-N(2)-C(1)	86.5(7)
C(28)-C(27)-C(32)-C(33)	52.4(8)	N(1)-C(1)-Pd(1)-C(1)#1	-108(29)
C(26)-C(27)-C(32)-C(33)	-130.6(6)	N(2)-C(1)-Pd(1)-C(1)#1	59(29)
C(28)-C(27)-C(32)-C(34)	-69.9(8)	N(1)-C(1)-Pd(1)-Cl(1)#1	93.9(5)
C(26)-C(27)-C(32)-C(34)	107.1(7)	N(2)-C(1)-Pd(1)-Cl(1)#1	-98.6(5)
C(26)-C(31)-C(35)-C(36)	152.9(6)	N(1)-C(1)-Pd(1)-Cl(1)	-86.1(5)
C(30)-C(31)-C(35)-C(36)	-33.3(8)	N(2)-C(1)-Pd(1)-Cl(1)	81.4(5)
C(26)-C(31)-C(35)-C(37)	-82.1(7)		
C(30)-C(31)-C(35)-C(37)	91.6(7)		
N(2)-C(1)-N(1)-C(2)	0.2(6)		
Pd(1)-C(1)-N(1)-C(2)	170.2(4)		
N(2)-C(1)-N(1)-C(14)	168.1(5)		
Pd(1)-C(1)-N(1)-C(14)	-22.0(8)		
C(3)-C(2)-N(1)-C(1)	-0.3(7)		
C(4)-C(2)-N(1)-C(1)	176.2(7)		
C(3)-C(2)-N(1)-C(14)	-169.0(5)		
C(4)-C(2)-N(1)-C(14)	7.5(11)		
C(15)-C(14)-N(1)-C(1)	102.7(7)		
C(19)-C(14)-N(1)-C(1)	-84.6(7)		
C(15)-C(14)-N(1)-C(2)	-90.6(7)		
C(19)-C(14)-N(1)-C(2)	82.0(7)		
C(2)-C(3)-N(2)-C(1)	0.0(6)		
C(13)-C(3)-N(2)-C(1)	-175.8(7)		
C(2)-C(3)-N(2)-C(26)	165.2(5)		
C(13)-C(3)-N(2)-C(26)	-10.6(11)		

Table A15: Torsion angles [°] for **4**.
Symmetry transformations
used to generate equivalent
atoms: #1 -x+1,-y,-z.

Appendix B: UV-vis Spectroscopy

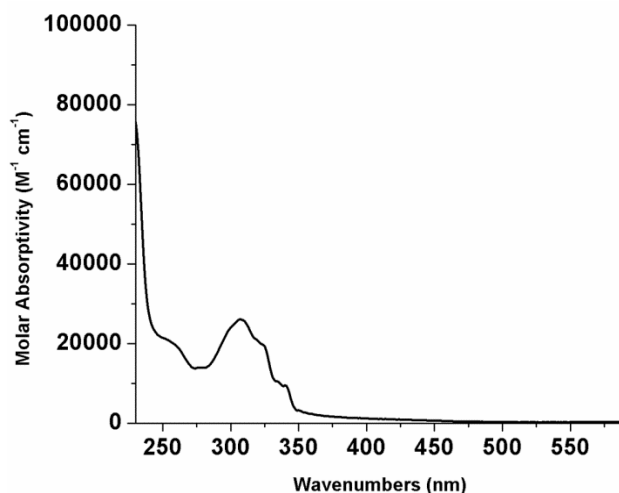


Figure B1: Absorption spectrum of **1** in dichloromethane with $\lambda_{max} = 308$ nm. Beer's law was used to determine the molar absorptivity from a calibration curve created with ten data points in 10 μL increments ranging 10-100 μL ($\epsilon = 29,646 M^{-1} cm^{-1}$, $R^2 = 0.9918$).

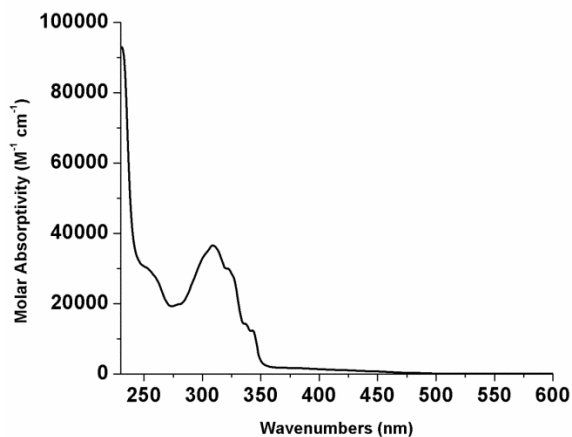


Figure B2: The absorption spectrum of **2** in dichloromethane with $\lambda_{max} = 309$ nm. Beer's law was used to determine the molar absorptivity from a calibration curve created with ten data points in 10 μL increments ranging 10-100 μL ($\epsilon = 36,868 M^{-1} cm^{-1}$, $R^2 = 0.9997$).

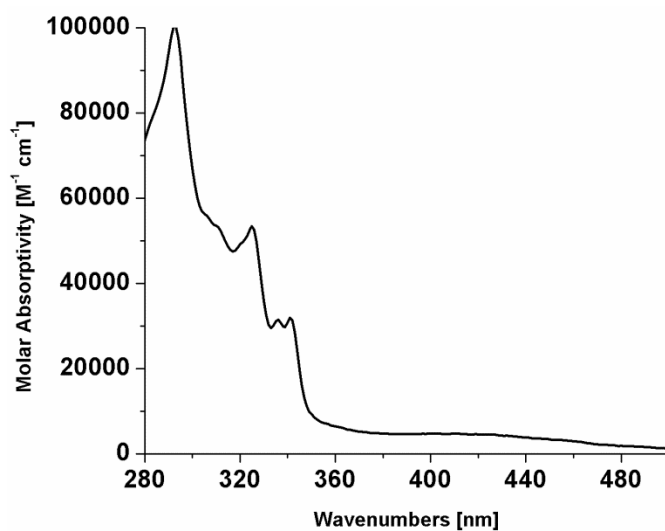


Figure B3: The absorption spectrum of **3** in dichloromethane with $\lambda_{\text{max}} = 293$ nm. Beer's law was used to determine the molar absorptivity from a calibration curve created with ten data points in 10 μL increments ranging 10-100 μL ($\epsilon = 102,736 \text{ M}^{-1} \text{ cm}^{-1}$, $R^2 = 0.998$)

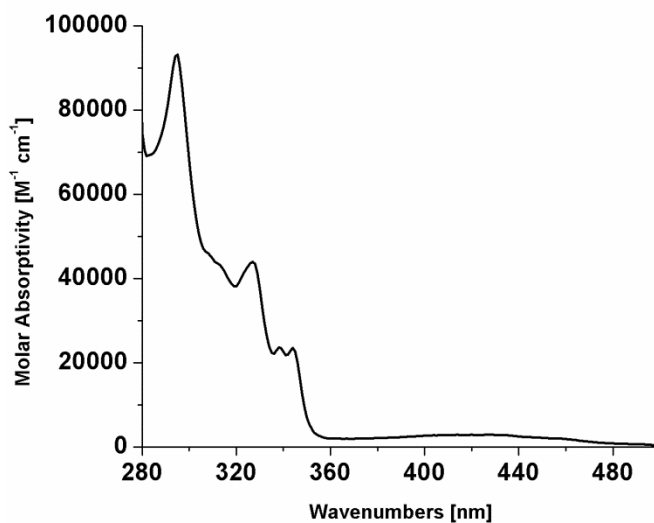


Figure B4: The absorption spectrum of **4** in dichloromethane with $\lambda_{\text{max}} = 295$ nm. Beer's law was used to determine the molar absorptivity from a calibration curve created with ten data points in 10 μL increments ranging 10-100 μL ($\epsilon = 100,498 \text{ M}^{-1} \text{ cm}^{-1}$, $R^2 = 0.9415$)

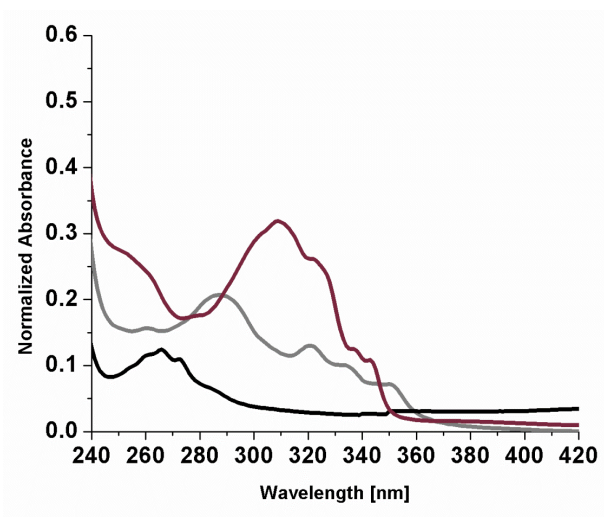


Figure B5: UV-vis spectra of (NHC)(PPh₃)PdCl₂ (**2**, dark grey), Imidazolium@SiO₂ (**A-V**, light grey), and (NHC)PdCl₂(PPh₃)@SiO₂ (**5**, black)

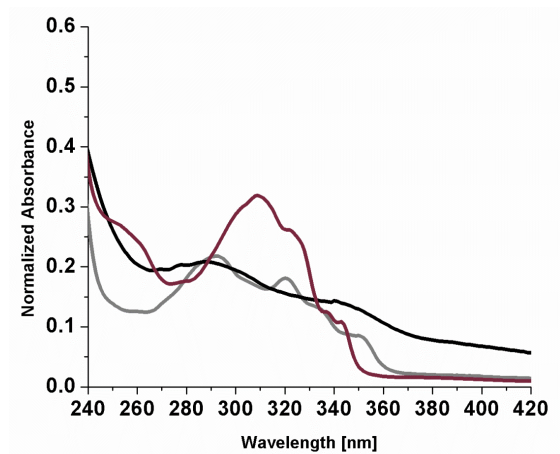


Figure B6: UV-vis spectra of (NHC)(PPh₃)PdCl₂ (**2**, dark grey), Imidazolium@SiO₂ (**B-V**, light grey), and (NHC)PdCl₂(PPh₃)@SiO₂ (**6**, black)

Appendix C: NMR spectra

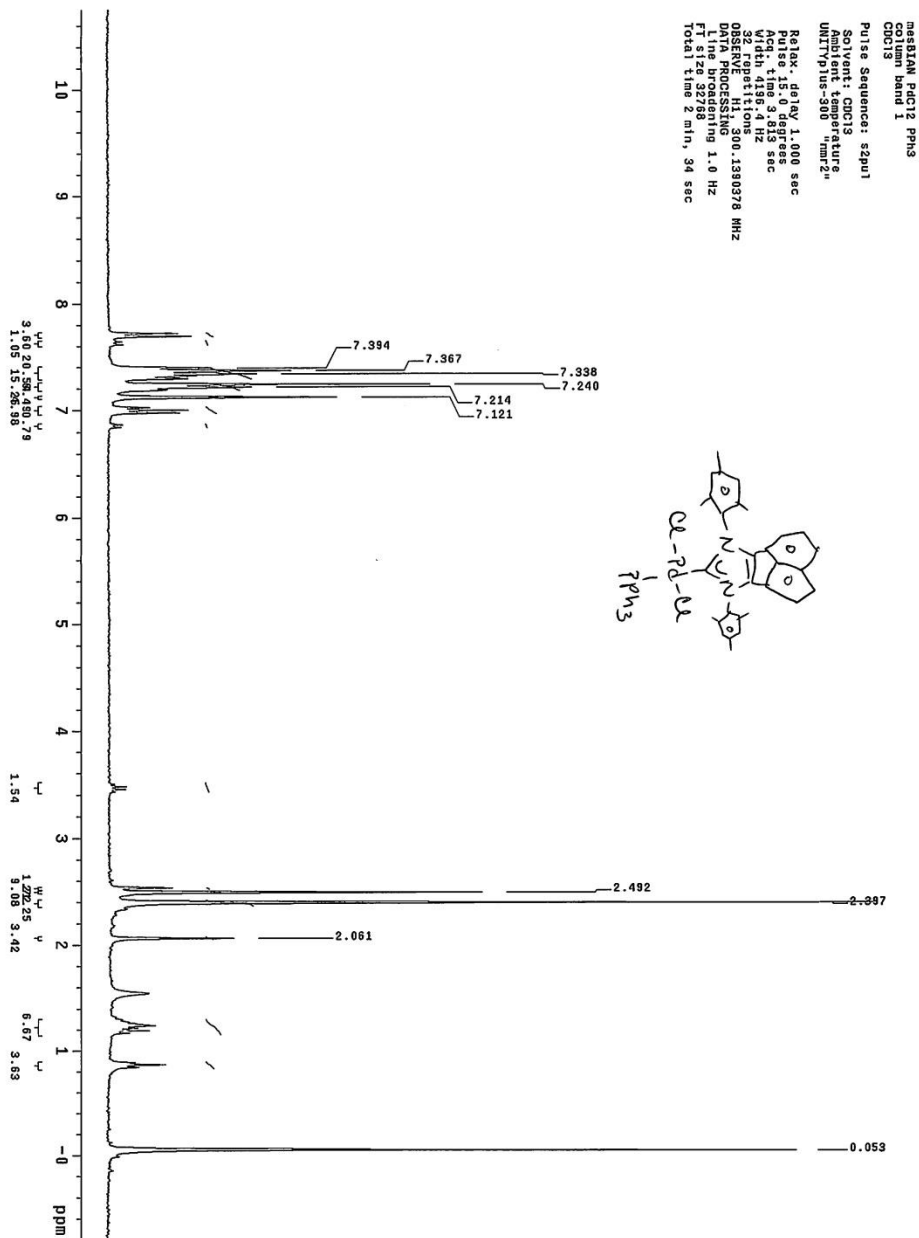
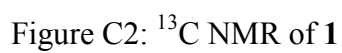


Figure C1: ^1H NMR of **1**



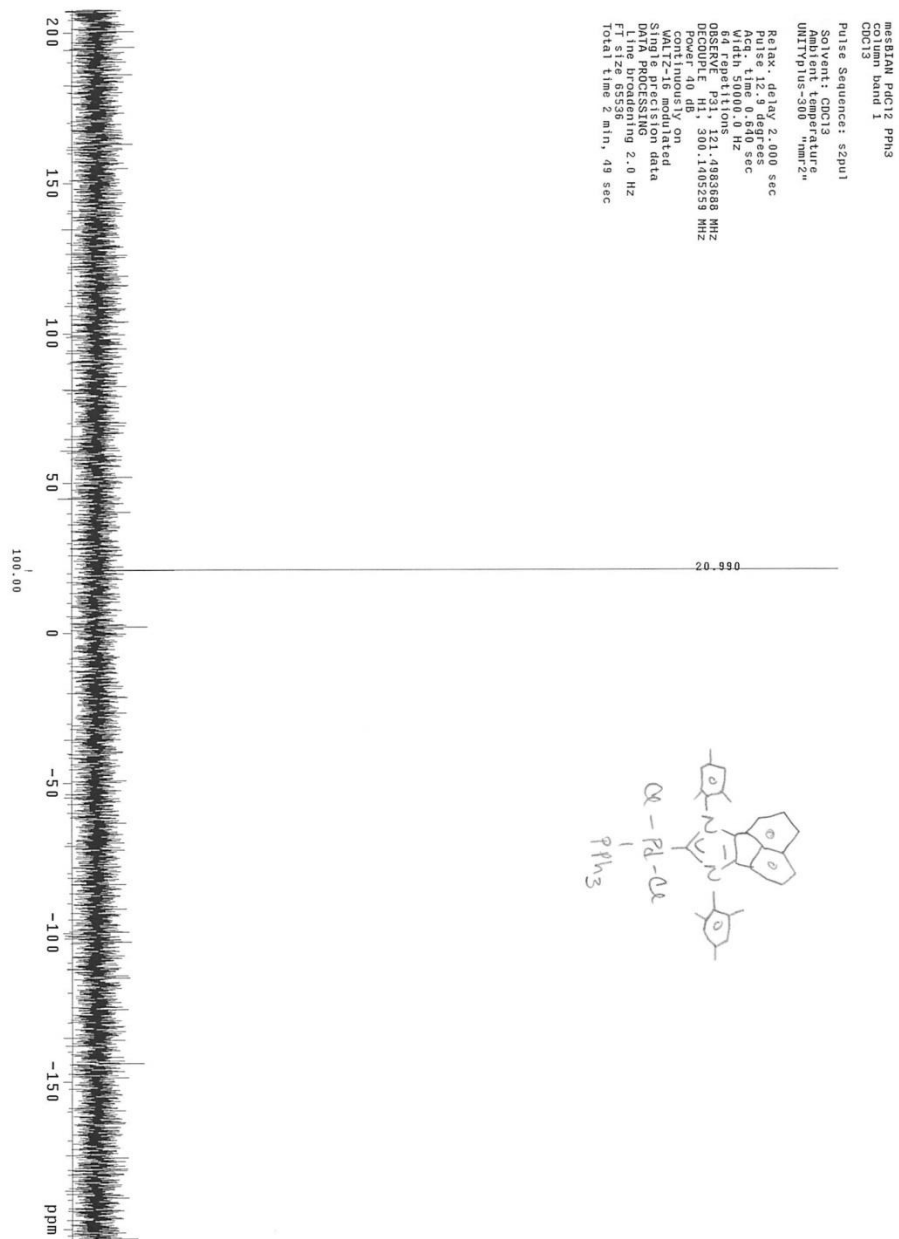


Figure C3: ³¹P NMR of **1**

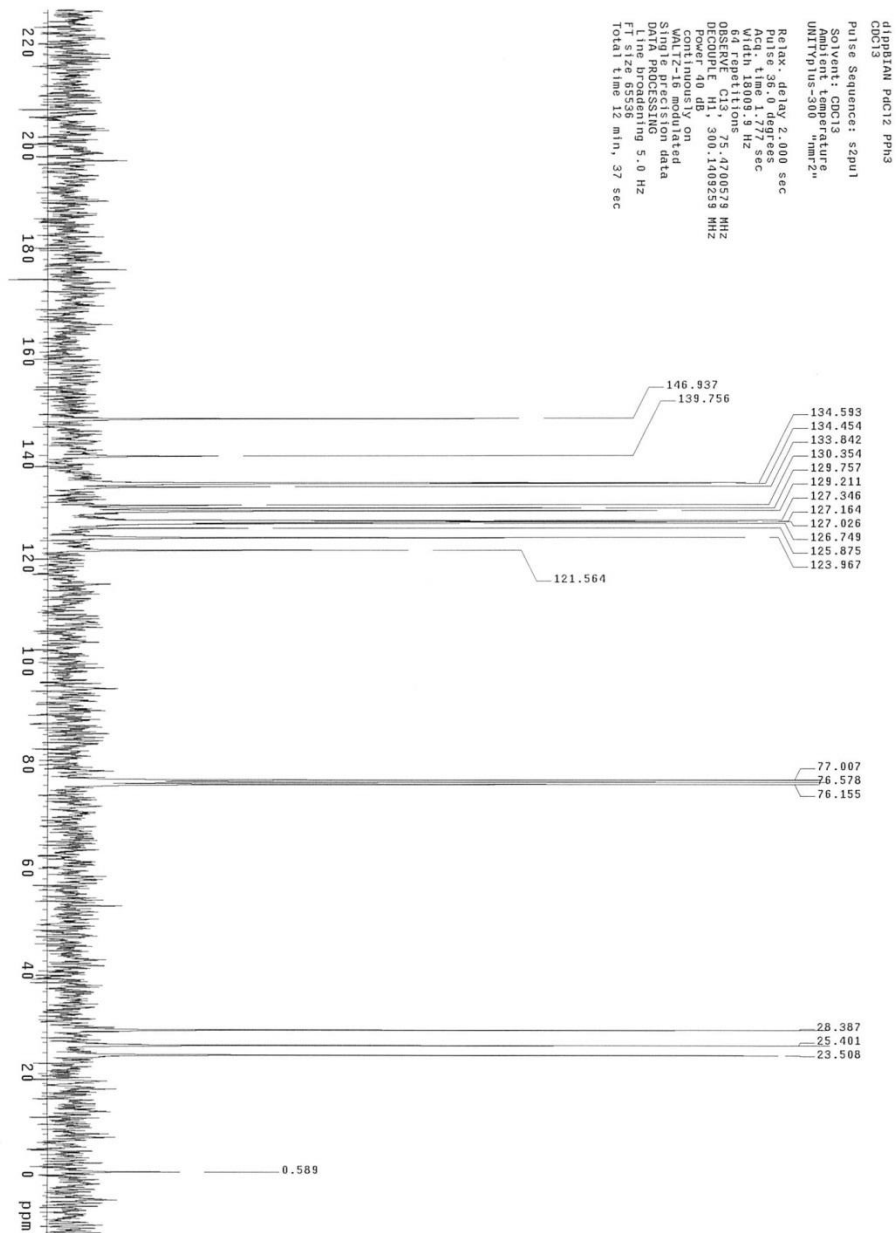


Figure C5: ^{13}C NMR of **2**

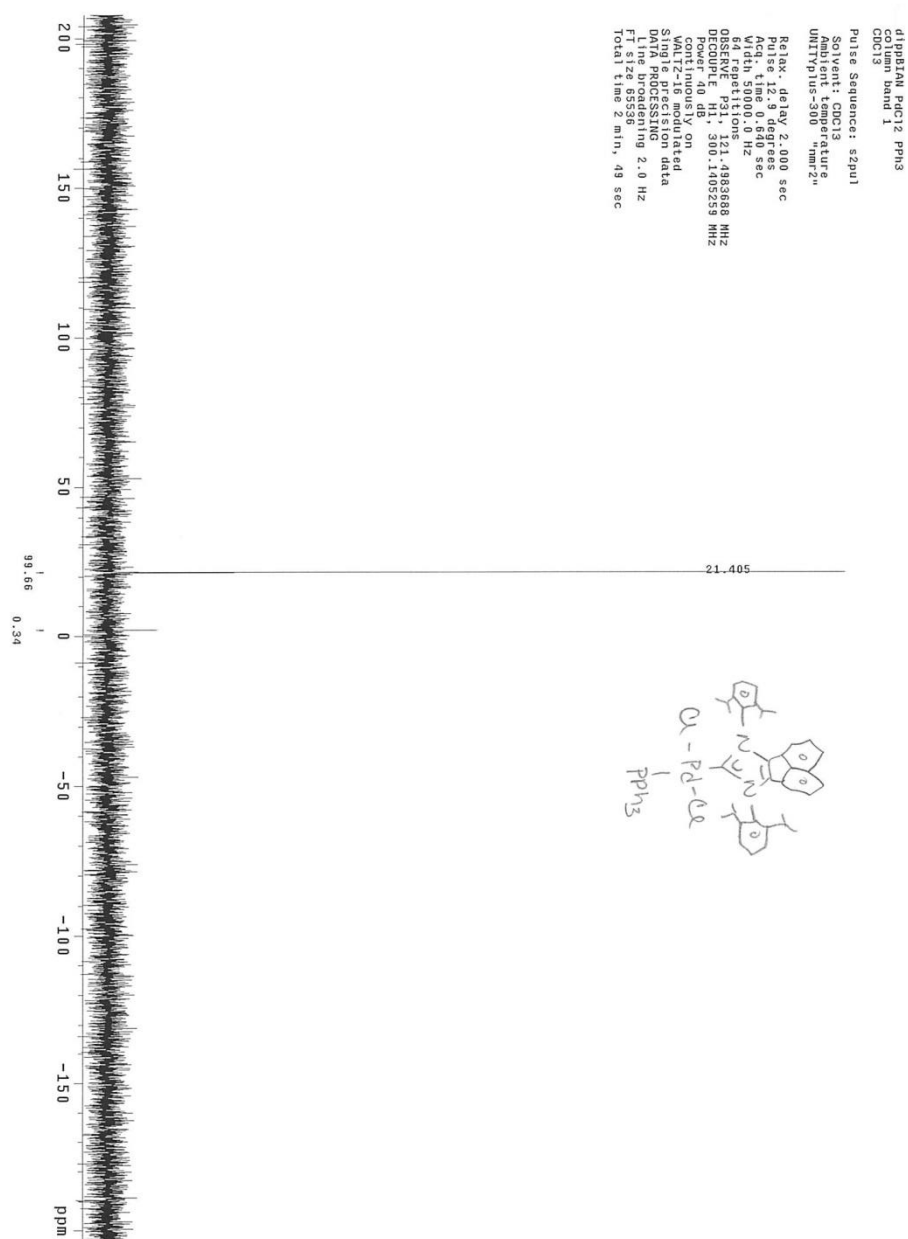


Figure C6: ^{31}P NMR of **2**

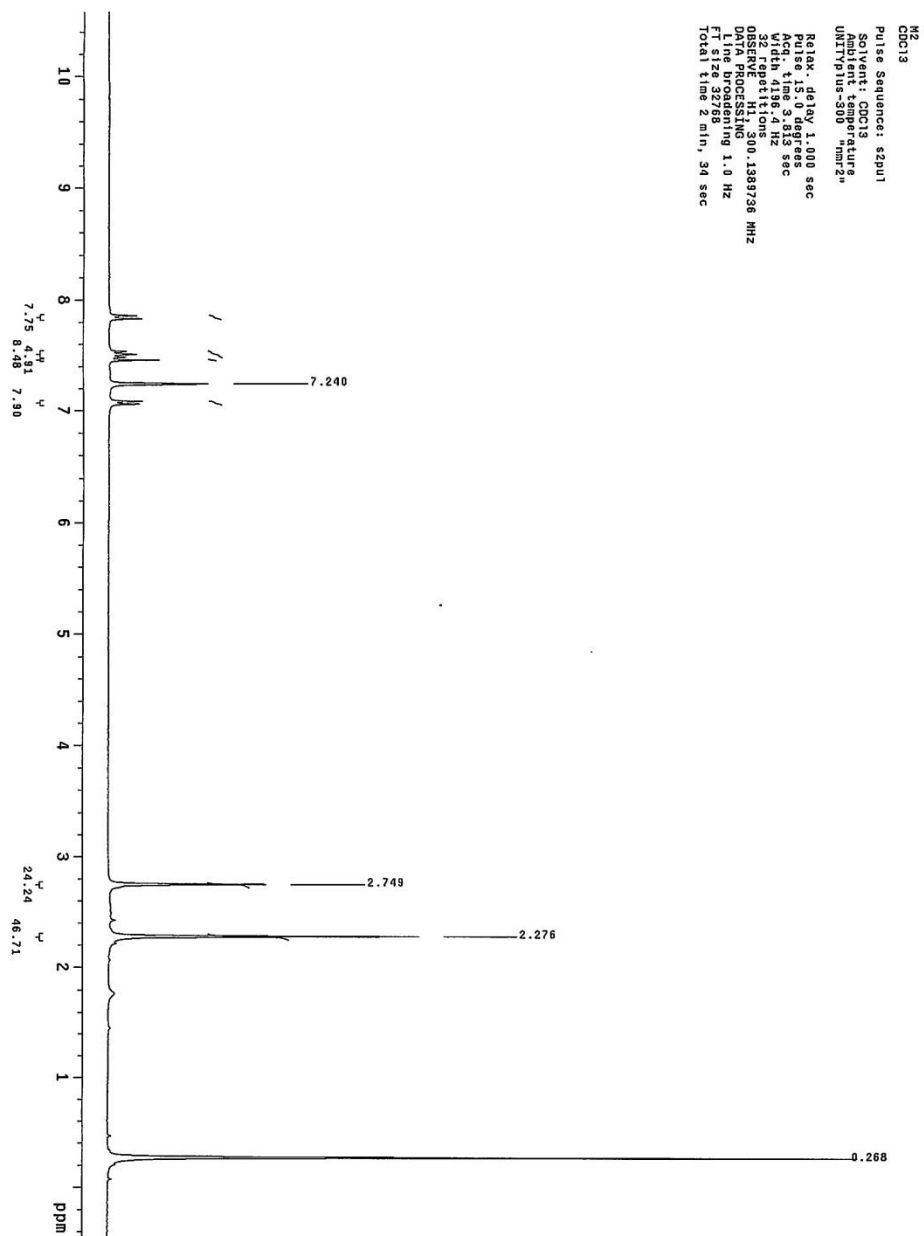


Figure C7: ¹H NMR of **3**

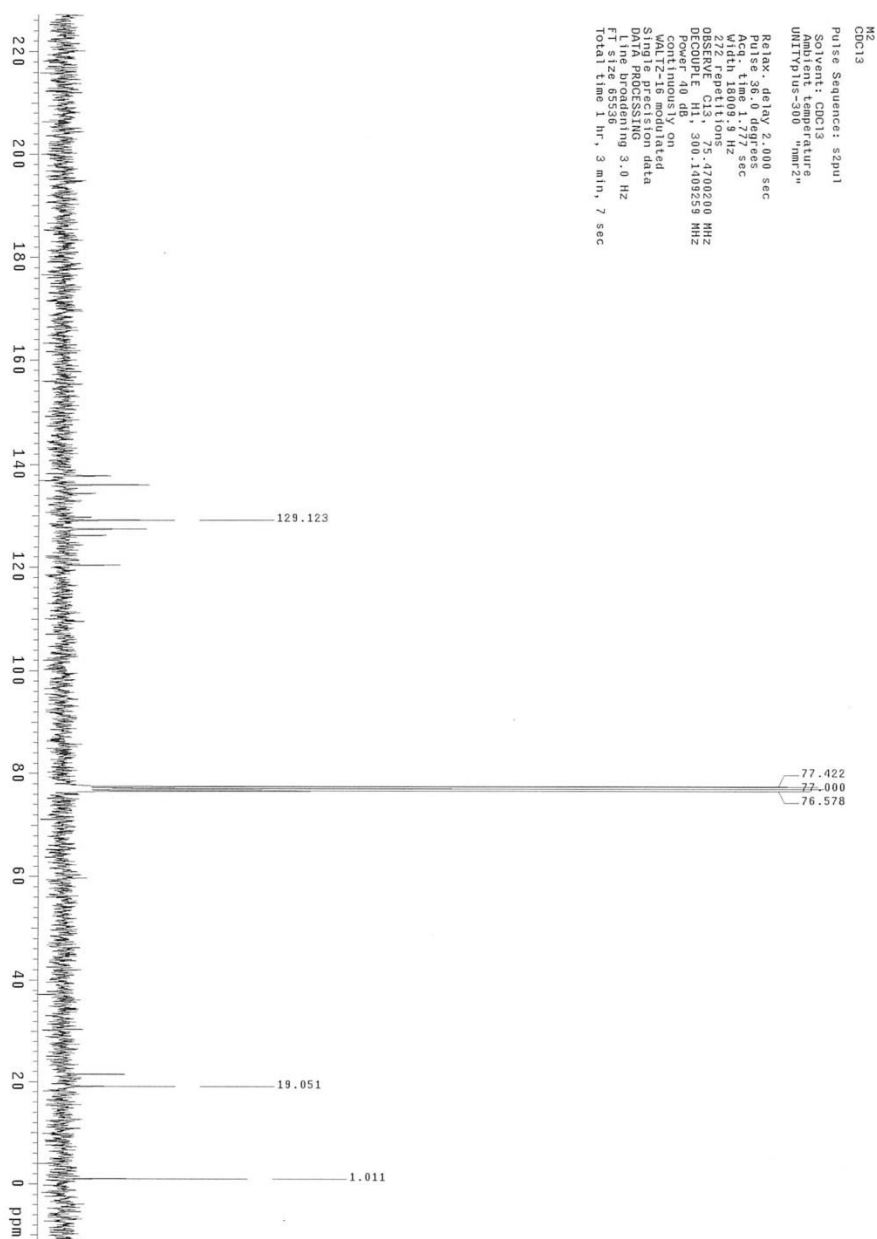


Figure C8: ¹³C NMR of **3**

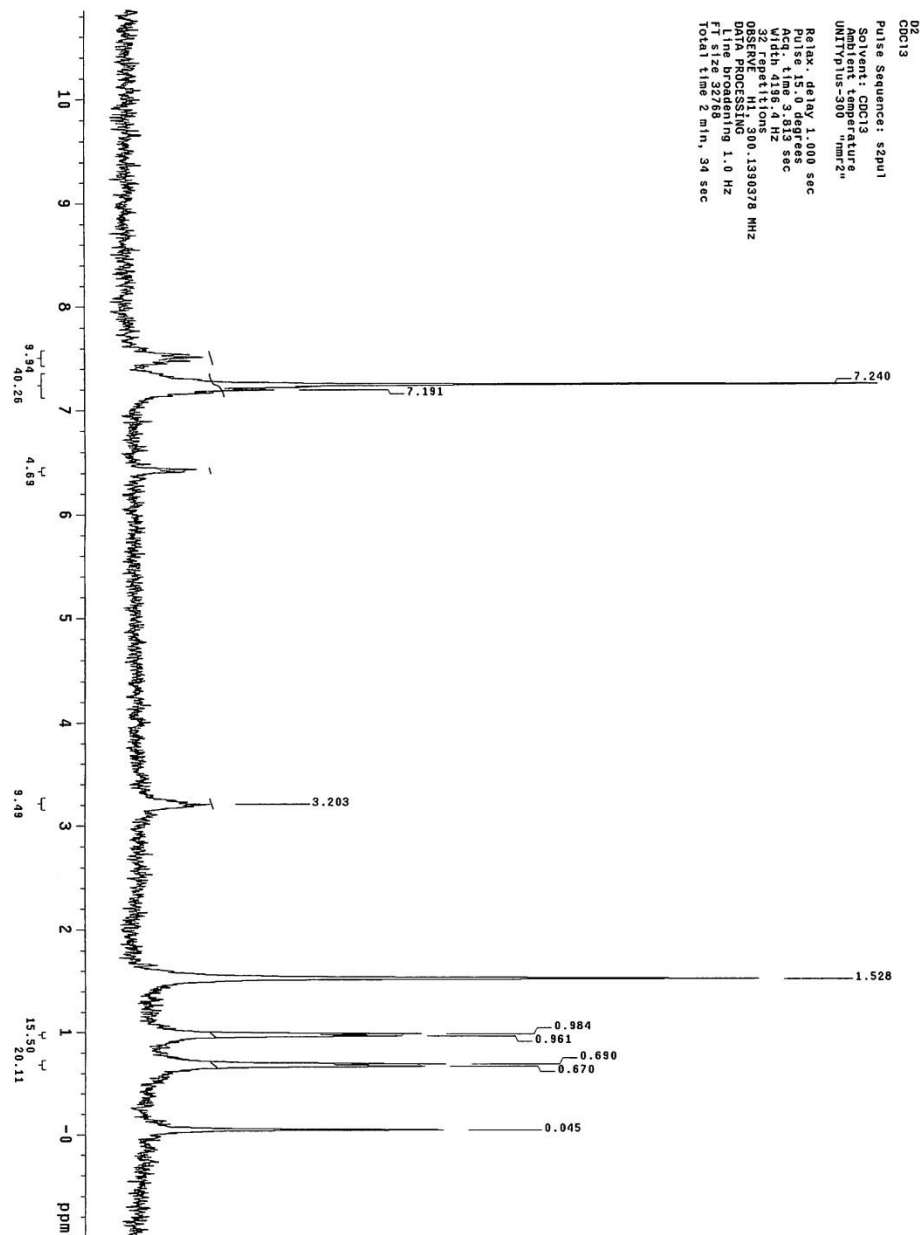


Figure C9: ¹H NMR of **4**

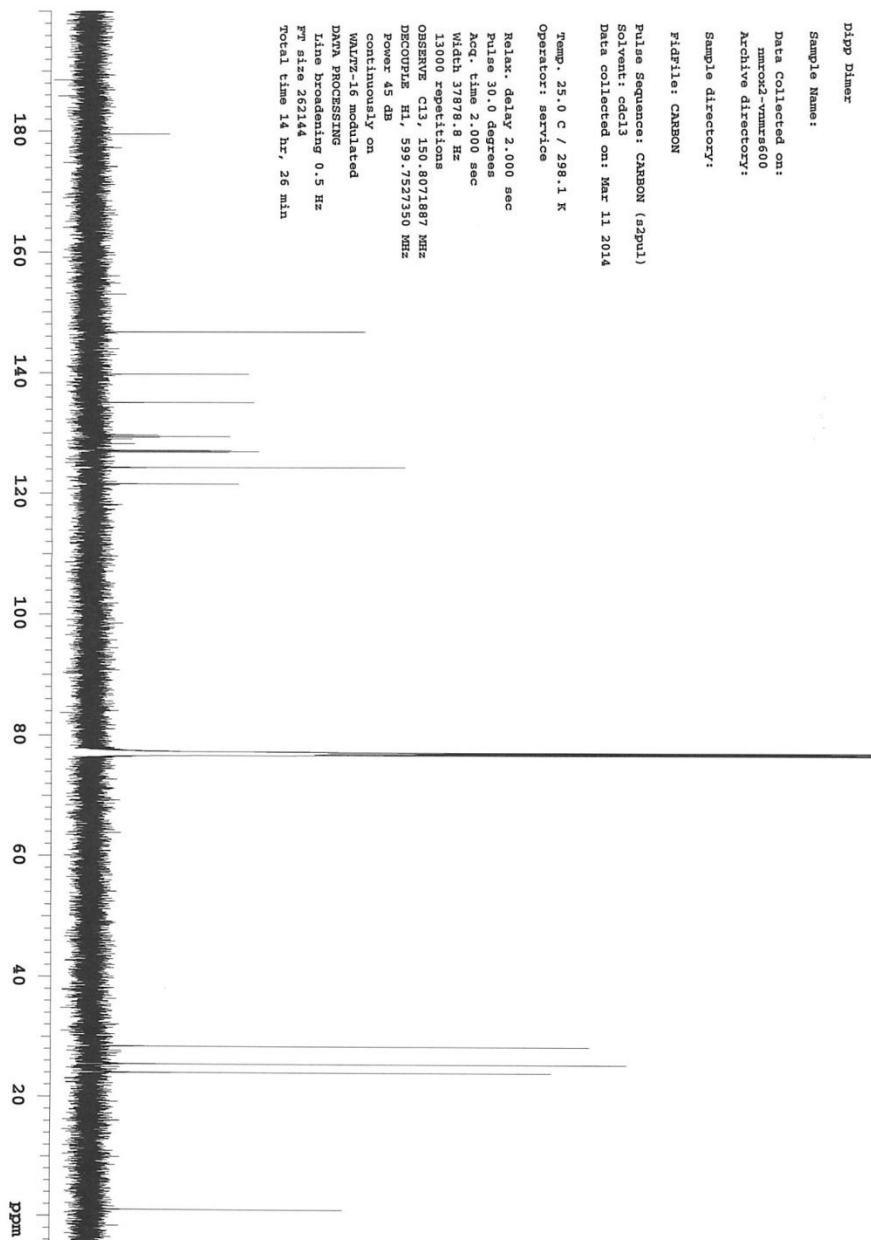


Figure C10: ^{13}C NMR of 4

Glossary

Ad	Adamantane
BIAN	<i>Bis</i> (imino)acenaphthene
Boc	<i>tert</i> -Butoxy carbamate
Dbp	Dibenzylideneacetone
Dipp	Diisopropylphenyl
Dppp	1,3- <i>bis</i> (diphenylphosphino)propane
DavePhos	2-dicyclohexylphosphino-2'-(<i>N,N</i> -dimethylamino)biphenyl
DCM	Dichloromethane
FibreCat	Polymer-bound functionalized fibre catalyst
HOMO	Highest occupied molecular orbital
JohnPhos	(2-biphenyl)di- <i>tert</i> -butylphosphine
IMes	1,3- <i>bis</i> (2,4,6-trimethylphenyl)imidazole-2-ylidene
IPA	2-propanol
IR	Infrared
ITol	1,3- <i>bis</i> (4-methylphenyl)imidazole-2-ylidene
IXy	1,3- <i>bis</i> (2,6-dimethylphenyl)imidazole-2-ylidene
LUMO	Lowest unoccupied molecular orbital
<i>m</i> -	Meta
Mes	Mesityl
MO	Molecular orbital
NUPHOS	1,4- <i>bis</i> (diphenylphosphino)-1,3-butadiene
<i>o</i> -	Ortho
<i>p</i> -	Para

ppm	Parts per million
ppb	Parts per billion
SEM	2-(trimethylsilyl)ethoxymethyl
TGA	Thermogravimetric analysis
THF	Tetrahydrofuran
Tol	Toluene
TunaCat	P(<i>t</i> -Bu ₃)-based FibreCat
UV-vis	Ultraviolet-visible
XRD	X-Ray Diffraction

References

- (1) Miyaura, N.; Yamada, K. A New Stereospecific Cross-Coupling by the Palladium-Catalyzed Reaction of 1-Alkenylboranes with 1-Alkenyl or 1-Alkynyl Halides. *Tetrahedron Lett.* **1979**, 3437–3440.
- (2) Feuerstein, M.; Doucet, H.; Santelli, M. Tetrakisphosphine/Palladium-Catalysed Suzuki Cross-Coupling with Sterically Hindered Aryl Bromides and Arylboronic Acids. *Tetrahedron Lett.* **2001**, 42, 6667–6670.
- (3) Farina, V. High-Turnover Palladium Catalysts in Cross-Coupling and Heck Chemistry: A Critical Overview. *Adv. Synth. Catal.* **2004**, 346, 1553–1582.
- (4) Miyaura, N.; Suzuki, A. Palladium-Catalyzed Cross-Coupling Reactions. *Chem. Rev.* **1995**, 95, 2457–2483.
- (5) Littke, A. F.; Fu, G. C. Palladium-Catalyzed Coupling Reactions of Aryl Chlorides. *Angew. Chemie* **2002**, 41, 4176–4211.
- (6) Sheppard, T. D. Metal-Catalysed Halogen Exchange Reactions of Aryl Halides. *Org. Biomol. Chem.* **2009**, 7, 1043–1052.
- (7) Amatore, C.; Jutand, A.; Le Duc, G. Kinetic Data for the Transmetalation/reductive Elimination in Palladium-Catalyzed Suzuki-Miyaura Reactions: Unexpected Triple Role of Hydroxide Ions Used as Base. *Chem. Eur. J.* **2011**, 17, 2492–2503.
- (8) Wu, X.-F.; Anbarasan, P.; Neumann, H.; Beller, M. From Noble Metal to Nobel Prize: Palladium-Catalyzed Coupling Reactions as Key Methods in Organic Synthesis. *Angew. Chemie* **2010**, 49, 9047–9050.
- (9) T. Crisp, G. Variations on a theme—Recent Developments on the Mechanism of the Heck Reaction and Their Implications for Synthesis. *Chem. Soc. Rev.* **1998**, 27, 427.
- (10) Foley, P. Mechanism of Thermal Decomposition of Dineopentylbis(triethylphosphine)platinum(II); Formation of Bis(triethylphosphine)-3,3-Dimethylplatinacyclobutane. *J. Am. Chem. Soc.* **1980**, 6713–6725.
- (11) Hartwig, J. F. Transition Metal Catalyzed Synthesis of Arylamines and Aryl Ethers from Aryl Halides and Triflates: Scope and Mechanism. *Angew. Chemie* **1998**, 2046–2067.

- (12) Herrmann, W. A.; Brobmer, C.; Beller, M. Coordination Chemistry and Mechanisms of Metal-Catalyzed CC- Coupling Reactions. Part 7 . Heck Vinylation of Aryl Halides with N- Butyl Acrylate : Relevance of PC Bond Cleavage to Catalyst Deactivation. *J. Mol. Catal. A Chem.* **1995**, *103*, 133–146.
- (13) Knowles, J. P.; Whiting, A. The Heck-Mizoroki Cross-Coupling Reaction: A Mechanistic Perspective. *Org. Biomol. Chem.* **2007**, *5*, 31–44.
- (14) Schmidt, A. F.; Kurokhtina, A. A.; Larina, E. V. Simple Kinetic Method for Distinguishing between Homogeneous and Heterogeneous Mechanisms of Catalysis, Illustrated by the Example of “ligand-Free” Suzuki and Heck Reactions of Aryl Iodides and Aryl Bromides. *Kinet. Catal.* **2012**, *53*, 84–90.
- (15) Amatore, C.; Le Duc, G.; Jutand, A. Mechanism of Palladium-Catalyzed Suzuki-Miyaura Reactions: Multiple and Antagonistic Roles of Anionic “Bases” and Their Counteranions. *Chem. Eur. J* **2013**, *19*, 10082–10093.
- (16) Suzuki, A. Carbon-Carbon Bonding Made Easy. *Chem. Commun.* **2005**, 4759–4763.
- (17) Miyaura, N.; Yamada, K.; Suginome, H.; Suzuki, A. Novel and Convenient Method for the Stere- and Regiospecific Synthesis of Conjugated Alkadienes and Alkynes via the Palladium-Catalyzed Cross-Coupling Reaction of 1-Alkenylboranes with Bromoalkenes and Bromoalkynes. *J. Am. Chem. Soc* **1985**, 972–980.
- (18) Matos, K.; Soderquist, J. A. Alkylboranes in the Suzuki-Miyaura Coupling: Stereochemical and Mechanistic Studies. *J. Org. Chem.* **1998**, *63*, 461–470.
- (19) Smith, G. B.; Dezeny, G. C.; Hughes, D. L.; Verhoeven, T. R. Mechanistic Studies of the Suzuki Cross-Coupling Reaction. *J. Org. Chem.* **2000**, 8151–8156.
- (20) Braga, A. A. C.; Morgon, N. H.; Ujaque, G.; Lledós, A.; Maseras, F. Computational Study of the Transmetalation Process in the Suzuki–Miyaura Cross-Coupling of Aryls. *J. Organomet. Chem.* **2006**, *691*, 4459–4466.
- (21) Glaser, R.; Knotts, N. Coordinate Covalent C → B Bonding in Phenylborates and Latent Formation of Phenyl Anions from Phenylboronic Acid. *J. Phys. Chem. A* **2006**, *110*, 1295–1304.
- (22) Jover, J.; Fey, N.; Purdie, M.; Lloyd-Jones, G. C.; Harvey, J. N. A Computational Study of Phosphine Ligand Effects in Suzuki–Miyaura Coupling. *J. Mol. Catal. A Chem.* **2010**, *324*, 39–47.

- (23) Amatore, C.; Le Duc, G.; Jutand, A. Mechanism of Palladium-Catalyzed Suzuki-Miyaura Reactions: Multiple and Antagonistic Roles of Anionic “Bases” and Their Counteranions. *Chem Eur J* **2013**, *19*, 10082–10093.
- (24) Amatore, C.; Jutand, A. Anionic Pd(0) and Pd(II) Intermediates in Palladium-Catalyzed Heck and Cross-Coupling Reactions. *Acc. Chem. Res.* **2000**, *33*, 314–321.
- (25) Adamo, C.; Amatore, C.; Ciofini, I.; Jutand, A.; Lakmini, H. Mechanism of the Palladium-Catalyzed Homocoupling of Arylboronic Acids: Key Involvement of a Palladium Peroxo Complex. *J. Am. Chem. Soc.* **2006**, *128*, 6829–6836.
- (26) Amatore, C.; Jutand, A. Formation of Anionic PdX₃(PPh₃)–Complexes by Reaction of Halide Ions. *Eur. J. Inorg. Chem.* **1999**, *3*, 1081–1085.
- (27) Amatore, C.; Jutand, A.; Le Duc, G. Mechanistic Origin of Antagonist Effects of Usual Anionic Bases (OH⁻, CO₃²⁻) as Modulated by Their Counteranions (Na⁺, Cs⁺, K⁺) in Palladium-Catalyzed Suzuki-Miyaura Reactions. *Chem. Eur. J.* **2012**, *18*, 6616–6625.
- (28) Kotha, S.; Lahiri, K.; Kashinath, D. Recent Applications of the Suzuki – Miyaura Cross-Coupling Reaction in Organic Synthesis. *Tetrahedron* **2002**, *58*, 9633–9695.
- (29) Nicolaou, K. C.; Ramanjulu, J. M.; Natarajan, S.; Br, S.; Li, H.; Christopher, N. C.; Frank, R. A Suzuki Coupling–macrolactamization Approach to the AB-COD Bicyclic System of Vancomycin. *Chem. Commun.* **1997**, *3*, 1899–1900.
- (30) Johnson, C. N.; Stemp, G.; Anand, N.; Stephen, S. C.; Gallagher, T. Palladium (0)-Catalysed Arylations Using Pyrrole and Indole 2-Boronic Acids. *Synlett* **1998**, 1025–1027.
- (31) Lee, C.-W.; Chung, Y. J. Facile Synthesis of 3-Arylpyrroles by Tandem Suzuki–dehydrogenation Reaction. *Tetrahedron Lett.* **2000**, *41*, 3423–3425.
- (32) Makavou, P. Vicinal Bromostannanes as Novel Building Blocks for the Preparation of Di- and Trisubstituted Imidazoles. *Tetrahedron Lett.* **1998**, *39*, 5171–5174.
- (33) Jones, K. A Suzuki Coupling Approach to Pyrazines Related to Coelenterazine. *Synlett* **1996**, 509–510.
- (34) Manickam, G.; Schl, A. D. New Parts for a Construction Set of Bifunctional Oligo(het)arylene Building Blocks for Modular Chemistry. *Synthesis (Stuttg.)*. **2000**, 442–446.

- (35) Heck, R. F.; Nolley, J. P. Palladium-Catalyzed Vinylic Hydrogen Substitution Reactions with Aryl, Benzyl, and Styryl Halides. *J. Org. Chem.* **1972**, *37*, 2320–2322.
- (36) Mizoroki, T.; Mori, K.; Ozaki, A. Arylation of Olefin with Aryl Iodide Catalyzed by Palladium. *Bull. Chem. Soc. Jap.* **1971**, *44*, 581.
- (37) Dieck, H. A.; Heck, F. Organophosphinepalladium Complexes as Catalysts for Vinylic Hydrogen Substitution Reactions. *J. Am. Chem. Soc.* **1974**, 1133–1136.
- (38) Sonogashira, K.; Tohda, Y.; Hagihara, N. A Convenient Synthesis of Acetylenes: Catalytic Substitutions of Acetylenic Hydrogen with Bromoalkenes, Iodoarenes, and Bromopyridines. *Tetrahedron Lett.* **1975**, 4467–4470.
- (39) Milstein, D.; Stille, J. K. A General, Selective, and Facile Method for Ketone Synthesis from Acid Chlorides and Organotin Compounds Catalyzed by Palladium. *J. Am. Chem. Soc.* **1978**, 3636–3638.
- (40) Negishi, E.; King, A. O.; Okukado, N. Selective Carbon-Carbon Bond Formation via Transition Metal Catalysis. A Highly Selective Synthesis of Unsymmetrical Biaryls and Diarylmethanes by the Nickel- or Palladium-Catalyzed Reaction of Aryl- and Benzylzinc Derivatives with Aryl Halides. *J. Org. Chem.* **1977**, *42*, 1821–1823.
- (41) Crabtree, R. H. *The Organometallic Chemistry of the Transition Metals*; 4th ed.; 2005.
- (42) Dias, P. B.; Minas, M. E.; Simoes, J. A. M. Bonding and Energetics of Phosphorus (III) Ligands in Transition Metal Complexes. *Coord. Chem. Rev.* **1994**, *135*, 737–807.
- (43) Griffiths, C.; Leadbeater, N. E. Palladium and Nickel Catalysed Suzuki Cross-Coupling of Sterically Hindered Aryl Bromides with Phenylboronic Acid. *Tetrahedron Lett.* **2000**, *41*, 2487–2490.
- (44) Littke, A. F.; Fu, G. C. A Convenient and General Method for Pd-Catalyzed Suzuki Cross-Couplings of Aryl Chlorides and Arylboronic Acids. *Angew. Chemie Int. Ed.* **1998**, *2*, 3387–3388.
- (45) Zapf, A.; Ehrentauf, A.; Beller, M. A New Highly Efficient Catalyst System for the Coupling of Nonactivated and Deactivated Aryl Chlorides with Arylboronic Acids. *Angew. Chemie Int. Ed.* **2000**, *50*, 4153–4155.

- (46) Feuerstein, M.; Doucet, H.; Santelli, M. Efficient Coupling of Heteroaryl Bromides with Arylboronic Acids in the Presence of a Palladium–tetraphosphine Catalyst. *Tetrahedron Lett.* **2001**, *42*, 5659–5662.
- (47) Feuerstein, M.; Laurenti, D.; Bougeant, C.; Doucet, H.; Santelli, M. Palladium–tetraphosphine Catalysed Cross Coupling of Aryl Bromides with Arylboronic Acids: Remarkable Influence of the Nature of the Ligand. *Chem. Commun.* **2001**, 325–326.
- (48) Feuerstein, M.; Doucet, H.; Santelli, M. Palladium Catalysed Cross-Coupling of Aryl Chlorides with Arylboronic Acids in the Presence of a New Tetraphosphine Ligand. *Synlett* **2001**, 1458–1460.
- (49) Feuerstein, R.; Doucet, H.; Santelli, M. Palladium/Tetraphosphine Catalysed Heck Reaction with Ortho-Substituted Aryl Bromides. *Synlett* **2001**, 1980–1982.
- (50) Feuerstein, M.; Doucet, H.; Santelli, M.; Herrmann, T. Efficient Heck Vinylation of Aryl Halides Catalyzed by a New Air-Stable Palladium-Tetraphosphine Complex. *J. Org. Chem.* **2001**, 5923–5925.
- (51) Laurenti, D.; Feuerstein, M.; Pèpe, G.; Doucet, H.; Santelli, M. A New Tetratertiary Phosphine Ligand and Its Use in Pd-Catalyzed Allylic Substitution. *J. Org. Chem.* **2001**, *66*, 1633–1637.
- (52) Feuerstein, M.; Laurenti, D.; Doucet, H.; Santelli, M. Dramatic Acceleration of the Catalytic Process of the Amination of Allyl Acetates in the Presence of a Tetraphosphine/palladium System. *Chem. Commun.* **2001**, 43–44.
- (53) Feuerstein, M.; Doucet, H.; Santelli, M. Efficient Coupling of Heteroaryl Halides with Arylboronic Acids in the Presence of a Palladium–tetraphosphine Catalyst. *J. Organomet. Chem.* **2003**, *687*, 327–336.
- (54) Berthiol, F.; Doucet, H.; Santelli, M. Synthesis of Polysubstituted Alkenes by Heck Vinylation or Suzuki Cross- Coupling Reactions in the Presence of a Tetraphosphane-Palladium Catalyst. *European J. Org. Chem.* **2003**, 1091–1096.
- (55) Chahen, L.; Doucet, H.; Santelli, M. Suzuki Cross-Coupling Reaction of Benzylic Halides with Arylboronic Acids in the Presence of a Tetraphosphine/Palladium Catalyst. *Synlett* **2003**, 1668–1672.
- (56) Martin, R.; Buchwald, S. L. Palladium-Catalyzed Suzuki - Miyaura Cross-Coupling Reactions Employing Dialkylbiaryl Phosphine Ligands. *Acc. Chem. Res.* **2008**, *41*, 1461–1473.

- (57) Kaye, S.; Fox, J. M.; Hicks, F. A.; Buchwald, S. L. The Use of Catalytic Amounts of CuCl and Other Improvements in the Benzyne Route to Biphenyl-Based Phosphine Ligands. *Adv. Synth. Catal.* **2001**, *343*, 789–794.
- (58) Christmann, U.; Vilar, R. Monoligated Palladium Species as Catalysts in Cross-Coupling Reactions. *Angew. Chemie* **2005**, *44*, 366–374.
- (59) Barrios-Landeros, F.; Hartwig, J. F. Distinct Mechanisms for the Oxidative Addition of Chloro-, Bromo-, and Iodoarenes to a Bisphosphine palladium(0) Complex with Hindered Ligands. *J. Am. Chem. Soc.* **2005**, *127*, 6944–6945.
- (60) Hartwig, J. F.; Paul, F. Oxidative Addition of Aryl Bromide after Dissociation of Phosphine from a Two-Coordinate Palladium(0) Complex, Bis(tri-O-tolylphosphine)palladium(0). *J. Am. Chem. Soc.* **1995**, 5373–5374.
- (61) Barder, T. E.; Buchwald, S. L. Insights into Amine Binding to Biaryl Phosphine Palladium Oxidative Addition Complexes and Reductive Elimination from Biaryl Phosphine Arylpalladium Amido Complexes via Density Functional Theory. *J. Am. Chem. Soc.* **2007**, *129*, 12003–12010.
- (62) Hartwig, J. F. Electronic Effects on Reductive Elimination to Form Carbon-Carbon and Carbon-Heteroatom Bonds from palladium(II) Complexes. *Inorg. Chem.* **2007**, *46*, 1936–1947.
- (63) Strieter, E. R.; Buchwald, S. L. Evidence for the Formation and Structure of Palladacycles during Pd-Catalyzed C-N Bond Formation with Catalysts Derived from Bulky Monophosphinobiaryl Ligands. *Angew. Chemie* **2006**, *45*, 925–928.
- (64) Old, D. W.; Wolfe, J. P.; Buchwald, S. L. A Highly Active Catalyst for Palladium-Catalyzed Cross-Coupling Reactions: Room-Temperature Suzuki Couplings and Amination of Unactivated Aryl Chlorides. *J. Am. Chem. Soc.* **1998**, *120*, 9722–9723.
- (65) Wolfe, J.; Buchwald, S. A Highly Active Catalyst for the Room-Temperature Amination and Suzuki Coupling of Aryl Chlorides. *Angew. Chemie* **1999**, *38*, 2413–2416.
- (66) Walker, S. D.; Barder, T. E.; Martinelli, J. R.; Buchwald, S. L. A Rationally Designed Universal Catalyst for Suzuki-Miyaura Coupling Processes. *Angew. Chemie* **2004**, *43*, 1871–1876.

- (67) Barder, T. E.; Walker, S. D.; Martinelli, J. R.; Buchwald, S. L. Catalysts for Suzuki-Miyaura Coupling Processes: Scope and Studies of the Effect of Ligand Structure. *J. Am. Chem. Soc.* **2005**, *127*, 4685–4696.
- (68) Billingsley, K.; Buchwald, S. L. Highly Efficient Monophosphine-Based Catalyst for the Palladium-Catalyzed Suzuki-Miyaura Reaction of Heteroaryl Halides and Heteroaryl Boronic Acids and Esters. *J. Am. Chem. Soc.* **2007**, *129*, 3358–3366.
- (69) Billingsley, K. L.; Barder, T. E.; Buchwald, S. L. Palladium-Catalyzed Borylation of Aryl Chlorides: Scope, Applications, and Computational Studies. *Angew. Chemie* **2007**, *46*, 5359–5363.
- (70) Zapf, A.; Beller, M. Palladium/Phosphite Catalyst Systems for Efficient Cross Coupling of Aryl Bromides and Chlorides with Phenylboronic Acid. *Chem Eur J* **2000**, *6*, 1830–1833.
- (71) Li, G. Y. The First Phosphine Oxide Ligand Precursors for Transition Metal Catalyzed Cross-Coupling Reactions: C-C, C-N, and C-S Bond Formation on Unactivated Aryl Chlorides. *Angew Chem Int Ed* **2001**, 1513–1516.
- (72) Li, G. Y.; Zheng, G.; Noonan, A. F.; Suzuki, C. C. Highly Active, Air-Stable Versatile Palladium Catalysts for the C-C, C-N, and C-S Bond Formations via Cross-Coupling Reactions of Aryl Chlorides. *J. Org. Chem.* **2001**, *3*, 8677–8681.
- (73) Li, G. Y. Highly Active, Air-Stable Palladium Catalysts for the C-C and C-S Bond-Forming Reactions of Vinyl and Aryl Chlorides: Use of Commercially Available [(t-Bu)(2)P(OH)](2)PdCl(2), [(t-Bu)(2)P(OH)PdCl(2)](2), and [(t-Bu)(2)PO...H...OP(t-Bu)(2)]PdCl(2) as Cat. *J. Org. Chem.* **2002**, *67*, 3643–3650.
- (74) Kayaki, Y.; Koda, T.; Ikariya, T. A Highly Effective (Triphenyl Phosphite)palladium Catalyst for a Cross-Coupling Reaction of Allylic Alcohols with Organoboronic Acids. *European J. Org. Chem.* **2004**, 4989–4993.
- (75) Clarke, M. L.; Cole-Hamilton, D. J.; Woollins, J. D. Synthesis of Bulky, Electron Rich Hemilabile Phosphines and Their Application in the Suzuki Coupling Reaction of Aryl Chlorides. *J. Chem. Soc. Dalt. Trans.* **2001**, 2721–2723.
- (76) Urgaonkar, S.; Nagarajan, M.; Verkade, J. G. Pd/P (i-BuNCH₂CH₂)₃N : An Efficient Catalyst for Suzuki Cross-Coupling of Aryl Bromides and Chlorides with Arylboronic Acids. *Tetrahedron Lett.* **2002**, *43*, 8921–8924.

- (77) Cheng, J.; Wang, F.; Xu, J.-H.; Pan, Y.; Zhang, Z. Palladium-Catalyzed Suzuki–Miyaura Reaction Using Aminophosphine as Ligand. *Tetrahedron Lett.* **2003**, *44*, 7095–7098.
- (78) Harkal, S.; Rataboul, F.; Zapf, A.; Fuhrmann, C.; Riermeier, T.; Monsees, A.; Beller, M. Dialkylphosphinoimidazoles as New Ligands for Palladium-Catalyzed Coupling Reactions of Aryl Chlorides. *Adv. Synth. Catal.* **2004**, *346*, 1742–1748.
- (79) Shen, W. Palladium Catalyzed Coupling of Aryl Chlorides with Arylboronic Acids. *Tetrahedron Lett.* **1997**, *38*, 5575–5578.
- (80) Sjövall, S.; Johansson, M. H.; Andersson, C. A New Highly Active Diphosphane-Palladium (II) Complex as a Catalyst Precursor for the Heck Reaction. *Eur. J. Inorg. Chem.* **2001**, 17–22.
- (81) Doherty, S.; Robins, E. G.; Nieuwenhuyzen, M.; Knight, J. G.; Champkin, P. A.; Clegg, W. Synthesis of a New Class of 1,4-Bis(diphenylphosphino)-1,3-Butadiene Bridged Diphosphine, NUPHOS, via Zirconium-Mediated Reductive Coupling of Alkynes and Diynes : Applications in Palladium-Catalyzed Cross-Coupling Reactions. *Organometallics* **2002**, 1383–1399.
- (82) Bei, X.; Crevier, T.; Guram, A. S.; Jandeleit, B.; Powers, T. S.; Turner, H. W.; Uno, T.; Weinberg, W. H. A Convenient Palladium/ligand Catalyst for Suzuki Cross-Coupling Reactions of Arylboronic Acids and Aryl Chlorides. *Tetrahedron Lett.* **1999**, *40*, 3855–3858.
- (83) Bei, X.; Turner, H. W.; Weinberg, W. H.; Guram, A. S.; Petersen, J. L. Palladium/P,O-Ligand-Catalyzed Suzuki Cross-Coupling Reactions of Arylboronic Acids and Aryl Chlorides. Isolation and Structural Characterization of (P,O)-Pd(dba) Complex. *J. Org. Chem.* **1999**, 6797–6803.
- (84) Mukherjee, A.; Sarkar, A. Pyrazole-Tethered Arylphosphine Ligands for Suzuki Reactions of Aryl Chlorides: How Important Is Chelation? *Tetrahedron Lett.* **2004**, *45*, 9525–9528.
- (85) Fortman, G. C.; Nolan, S. P. N-Heterocyclic Carbene (NHC) Ligands and Palladium in Homogeneous Cross-Coupling Catalysis: A Perfect Union. *Chem. Soc. Rev.* **2011**, *40*, 5151–5169.
- (86) Tolman, C. A. Steric Effects of Phosphorus Ligands in Organometallic Chemistry and Homogeneous Catalysis. *Chem. Rev.* **1976**, *1976*, 313–348.

- (87) Scott, N. M.; Nolan, S. P. Stabilization of Organometallic Species Achieved by the Use of N-Heterocyclic Carbene (NHC) Ligands. *Eur. J. Inorg. Chem.* **2005**, 1815–1828.
- (88) Clavier, H.; Nolan, S. P. Percent Buried Volume for Phosphine and N-Heterocyclic Carbene Ligands: Steric Properties in Organometallic Chemistry. *Chem. Commun.* **2010**, 46, 841–861.
- (89) Jacobsen, H.; Correa, A.; Poater, A.; Costabile, C.; Cavallo, L. Erratum to “Understanding the M-(NHC) (NHC=N-Heterocyclic Carbene) Bond.” *Coord. Chem. Rev.* **2009**, 253, 2784.
- (90) Fu, C.-F.; Lee, C.-C.; Liu, Y.-H.; Peng, S.-M.; Warsink, S.; Elsevier, C. J.; Chen, J.-T.; Liu, S.-T. Biscarbene palladium(II) Complexes. Reactivity of Saturated versus Unsaturated N-Heterocyclic Carbenes. *Inorg. Chem.* **2010**, 49, 3011–3018.
- (91) Alder, R. W.; Blake, M. E.; Chaker, L.; Harvey, J. N.; Paolini, F.; Schütz, J. When and How Do Diaminocarbenes Dimerize? *Angew. Chemie* **2004**, 43, 5896–5911.
- (92) Denk, M.K.; Thadani, A. Hatano, K. Lough, A. J. Steric Stabilization of Nucleophilic Carbenes. *Angew. Chemie* **1997**, 36, 2607–2609.
- (93) Arduengo, A. J.; Dias, H. V. R.; Harlow, R. L.; Kline, M. Electronic Stabilization of Nucleophilic Carbenes. *J. Am. Chem. Soc* **1992**, 114, 5530–5534.
- (94) Herrmann, W. A.; Elison, M.; Fischer, J.; Kocher, C.; Artus, G. R. J. N-Heterocyclic Carbenes: Generation under Mild Conditions and Formation of Group 8-10 Transition Metal Complexes Relevant to Catalysis. *Chem Eur J* **1996**, 772–780.
- (95) McGuinness, D. S.; Green, M. J.; Cavell, K. J.; Skelton, B. W.; White, A. H. Synthesis and Reaction Chemistry of Mixed Ligand Methylpalladium–carbene Complexes. *J. Organomet. Chem.* **1998**, 565, 165–178.
- (96) Weskamp, T.; Schattenmann, W. C.; Spiegler, M.; Herrmann, W. A. A Novel Class of Ruthenium Catalysts for Olefin Metathesis. *Angew Chem Int Ed* **1998**, 37, 2490–2493.
- (97) Cai, M.; Song, C.; Huang, X. Butoxycarbonylation of Aryl Halides Catalyzed by a Silica-Supported Poly [3-(2-Cyanoethylsulfanyl) Propylsiloxane Palladium] Complex. *J Chem Soc, Perkin Trans.* **1997**, 2273–2274.

- (98) Huang, J.; Stevens, E. D.; Nolan, S. P.; Petersen, J. L.; Orleans, N.; Virginia, W.; Uni, V.; September, R. V. Olefin Metathesis-Active Ruthenium Complexes Bearing a Nucleophilic Carbene Ligand. *J. Am. Chem. Soc.* **1999**, 2674–2678.
- (99) Zhang, C.; Huang, J.; Trudell, M. L.; Nolan, S. P. Palladium-Imidazol-2-Ylidene Complexes as Catalysts for Facile and Efficient Suzuki Cross-Coupling Reactions of Aryl Chlorides with Arylboronic Acids. *J. Org. Chem.* **1999**, 64, 3804–3805.
- (100) Grasa, G. A.; Viciu, M. S.; Huang, J.; Zhang, C.; Trudell, M. L.; Nolan, S. P. Suzuki - Miyaura Cross-Coupling Reactions Mediated by Palladium / Imidazolium Salt Systems. *Organometallics* **2002**, 21, 2866–2873.
- (101) Viciu, M. S.; Germaneau, R. F.; Navarro-Fernandez, O.; Stevens, E. D.; Nolan, S. P. Activation and Reactivity of (NHC)Pd(allyl)Cl (NHC = N-Heterocyclic Carbene) Complexes in Cross-Coupling Reactions. *Organometallics* **2002**, 21, 5470–5472.
- (102) Hillier, A. C.; Sommer, W. J.; Yong, B. S.; Petersen, J. L.; Cavallo, L.; Nolan, S. P.; Virginia, W.; Chimica, D. A Combined Experimental and Theoretical Study Examining the Binding of N -Heterocyclic Carbenes (NHC) to the Cp * RuCl (Cp *) η^5 -C₅Me₅) Moiety : Insight into Stereoelectronic Differences between Unsaturated and Saturated NHC Ligands. *Organometallics* **2003**, 4322–4326.
- (103) Navarro, O.; Kaur, H.; Mahjoor, P.; Nolan, S. P. Cross-Coupling and Dehalogenation Reactions Catalyzed by (N -Heterocyclic carbene)Pd(allyl)Cl Complexes. *J. Org. Chem.* **2004**, 3173–3180.
- (104) Marion, N.; Navarro, O.; Mei, J.; Stevens, E. D.; Scott, N. M.; Nolan, S. P. Modified (NHC)Pd(allyl)Cl (NHC = N-Heterocyclic Carbene) Complexes for Room-Temperature Suzuki-Miyaura and Buchwald-Hartwig Reactions. *J. Am. Chem. Soc.* **2006**, 4101–4111.
- (105) McGuinness, D. S.; Cavell, K. J. Donor-Functionalized Heterocyclic Carbene Complexes of Palladium(II): Efficient Catalysts for C–C Coupling Reactions. *Organometallics* **2000**, 19, 741–748.
- (106) McGuinness, D. S.; Cavell, K. J.; Skelton, B. W.; White, A. H. Zerovalent Palladium and Nickel Complexes of Heterocyclic Carbenes: Oxidative Addition of Organic Halides, Carbon-Carbon Coupling Processes, and the Heck Reaction. *Organometallics* **1999**, 18, 1596–1605.
- (107) Bohm, V. P. W.; Gstottmayr, C. W. K.; Weskamp, T.; Herrmann, W. A. N-Heterocyclic Carbenes Part 26 . N-Heterocyclic Carbene Complexes of Palladium

- (0): Synthesis and Application in the Suzuki Cross-Coupling Reaction. *J. Organomet. Chem.* **2000**, 595, 186–190.
- (108) Lebel, H.; Janes, M. K.; Charette, A. B.; Nolan, S. P. Structure and Reactivity of “Unusual” N-Heterocyclic Carbene (NHC) Palladium Complexes Synthesized from Imidazolium Salts. *J. Am. Chem. Soc.* **2004**, 126, 5046–5047.
- (109) Matsumara, N.; Kawano, J.; Fukunishi, N.; Inoue, H. Synthesis of New Transition Metal Carbene Complexes from Pi-Sulfurane Compounds: Reaction of 10-S-3 Tetraazapentalene Derivatives with Pd(PPh₃)₄ and RhCl(PPh₃)₃. *J. Am. Chem. Soc.* **1995**, 117, 3623–3624.
- (110) Herrmann, W. A.; Bohm, V. P. W.; Gstottmayr, C. W. K. Synthesis, Structure and Catalytic Application of Palladium (II) Complexes Bearing N-Heterocyclic Carbenes and Phosphines. *J. Organomet. Chem.* **2001**, 617, 616–628.
- (111) Liao, C.-Y.; Chan, K.-T.; Tu, C.-Y.; Chang, Y.-W.; Hu, C.-H.; Lee, H. M. Robust and Electron-Rich Cis-palladium(II) Complexes with Phosphine and Carbene Ligands as Catalytic Precursors in Suzuki Coupling Reactions. *Chem Eur J* **2009**, 15, 405–417.
- (112) Türkmen, H.; Çetinkaya, B. 1,3-Diarylimidazolidin-2-Ylidene (NHC) Complexes of Pd(II): Electronic Effects on Cross-Coupling Reactions and Thermal Decompositions. *J. Organomet. Chem.* **2006**, 691, 3749–3759.
- (113) Xu, C.; Hao, X.-Q.; Li, Z.; Dong, X.-M.; Duan, L.-M.; Wang, Z.-Q.; Ji, B.-M.; Song, M.-P. Synthesis, Structural Characterization and Catalytic Activity of Two N-Heterocyclic Carbene–phosphine palladium(II) Complexes. *Inorg. Chem. Commun.* **2012**, 17, 34–37.
- (114) Huynh, H. V.; Han, Y.; Ho, J. H. H.; Tan, G. K. Palladium(II) Complexes of a Sterically Bulky, Benzannulated N-Heterocyclic Carbene with Unusual Intramolecular C–H···Pd and Carbene ···Br Interactions and Their Catalytic Activities. *Organometallics* **2006**, 25, 3267–3274.
- (115) Mathews, C. J.; Smith, P. J.; Welton, T.; White, A. J. P.; Williams, D. J. In Situ Formation of Mixed Phosphine - Imidazolylidene Palladium Complexes in Room-Temperature Ionic Liquids. *Organometallics* **2001**, 3848–3850.
- (116) Baker, M. V.; Brown, D. H.; Hesler, V. J.; Skelton, B. W.; White, A. H. Synthesis of a Bis(N-Heterocyclic Carbene) Palladium Complex via Oxidative Addition of a C-C Bond in a Biimidazolium Ion. *Organometallics* **2007**, 26, 250–252.

- (117) Yang, W.-H.; Lee, C.-S.; Pal, S.; Chen, Y.-N.; Hwang, W.-S.; Lin, I. J. B.; Wang, J.-C. Novel Ag(I), Pd(II), Ni(II) Complexes of N,N'-Bis-(2,2-Diethoxyethyl)imidazole-2-Ylidene: Synthesis, Structures, and Their Catalytic Activity towards Heck Reaction. *J. Organomet. Chem.* **2008**, *693*, 3729–3740.
- (118) Ellul, C. E.; Reed, G.; Mahon, M. F.; Pascu, S. I.; Whittlesey, M. K. Tripodal N-Heterocyclic Carbene Complexes of Palladium and Copper: Syntheses, Characterization, and Catalytic Activity. *Organometallics* **2010**, *29*, 4097–4104.
- (119) Marshall, W. J.; Grushin, V. V. Synthesis, Structure, and Reductive Elimination Reactions of the First (σ -Aryl) Palladium Complex Stabilized by IPr N-Heterocyclic Carbene. *Organometallics* **2003**, *9*, 1591–1593.
- (120) Fantasia, S.; Egbert, J. D.; Jurčík, V.; Cazin, C. S. J.; Jacobsen, H.; Cavallo, L.; Heinekey, D. M.; Nolan, S. P. Activation of Hydrogen by palladium(0): Formation of the Mononuclear Dihydride Complex Trans-[Pd(H)₂(IPr)(PCy₃)]. *Angew. Chemie* **2009**, *48*, 5182–5186.
- (121) Zhao, F.; Bhanage, B. M.; Shirai, M.; Arai, M. Effect of Triphenylphosphine Concentration on the Kinetics of Homogeneous Heck Reaction in Different Solvents. *J. Mol. Catal. A Chem.* **1999**, *142*, 383–388.
- (122) Proutiere, F.; Schoenebeck, F. Solvent Effect on Palladium-Catalyzed Cross-Coupling Reactions and Implications on the Active Catalytic Species. *Angew Chem* **2011**, *50*, 8192–8195.
- (123) Navarro, O.; Oonishi, Y.; Kelly, R. A.; Stevens, E. D.; Briel, O.; Nolan, S. P. General and Efficient Methodology for the Suzuki–Miyaura Reaction in Technical Grade 2-Propanol. *J. Organomet. Chem.* **2004**, *689*, 3722–3727.
- (124) Casalnuovo, A. L.; Calabrese, J. C. Palladium-Catalyzed Alkylations in Aqueous Media. *J. Am. Chem. Soc.* **1990**, *112*, 4324–4330.
- (125) Genet, J. P.; Blart, E.; Savignac, M. Palladium-Catalyzed Cross-Coupling Reactions in a Homogeneous Aqueous Medium. *Synlett* **1992**, 715–717.
- (126) Genet, J.; Linquist, A.; Blart, E.; Mouri, V.; Savignac, M.; Vaultier, M.; I, U. D. R.; Recherche, G. De; Avenue, C. N. R. S. Suzuki-Type Cross Coupling Reactions Using Palladium-Water Soluble Catalyst. Synthesis of Functionalized Dienes. *Tetrahedron Lett.* **1995**, *36*, 1443–1446.

- (127) Paetzold, E.; Oehme, G. Efficient Two-Phase Suzuki Reaction Catalyzed by Palladium Complexes with Water-Soluble Phosphine Ligands and Detergents as Phase Transfer Reagents. *J. Mol. Catal. A Chem.* **2000**, *152*, 69–76.
- (128) Shaughnessy, K. H.; Booth, R. S. Sterically Demanding, Water-Soluble Alkylphosphines as Ligands for High Activity Suzuki Coupling of Aryl Bromides in Aqueous Solvents. *Org. Lett.* **2001**, *3*, 2757–2759.
- (129) Devasher, R. B.; Moore, L. R.; Shaughnessy, K. H. Bromides under Mild Conditions, Using Water-Soluble, Sterically Demanding Alkylphosphines. *J. Org. Chem.* **2004**, 7919–7927.
- (130) Najera, C.; Gil-Molto, J.; Karlstrom, S. Suzuki-Miyaura and Related Cross-Couplings in Aqueous Solvents Catalyzed by Di(2-Pyridyl)methylamine-Palladium Dichloride Complexes. *Adv. Synth. Catal.* **2004**, *346*, 1798–1811.
- (131) Anderson, K. W.; Buchwald, S. L. General Catalysts for the Suzuki-Miyaura and Sonogashira Coupling Reactions of Aryl Chlorides and for the Coupling of Challenging Substrate Combinations in Water. *Angew. Chemie* **2005**, *44*, 6173–6177.
- (132) Jang, S. Polymer-Bound Palladium-Catalyzed Cross-Coupling of Organoboron Compounds with Organic Halides and Organic Triflates. *Tetrahedron Lett.* **1997**, *38*, 1793–1796.
- (133) Fenger, I.; Le, C.; Werner, A.; Cedex, F.-M. Reusable Polymer-Supported Palladium Catalysts : An Alternative to Tetrakis(triphenylphosphine)palladium in the Suzuki Cross-Coupling Reaction. *Tetrahedron Lett.* **1998**, *39*, 4287–4290.
- (134) Akiyama, R.; Kobayashi, S. Microencapsulated Palladium Catalysts : Allylic Substitution and Suzuki Coupling Using a Recoverable and Reusable Polymer-Supported Palladium Catalyst. *Angew Chem Int Ed* **2001**, *40*, 3469–3471.
- (135) Inada, K.; Miyaura, N. The Cross-Coupling Reaction of Arylboronic Acids with Chloropyridines and Electron-Deficient Chloroarenes Catalyzed by a Polymer-Bound Palladium Complex. *Tetrahedron* **2000**, *56*, 8661–8664.
- (136) Bai, L.; Zhang, Y.; Wang, J.-X. Rapid Microwave-Promoted Cross-Coupling Reaction of Aryl Bromides with Aryl Boronic Acids and Sodium Tetrphenylborate Catalyzed by a Reusable Polymer-Supported Palladium Complex. *QSAR Comb. Sci.* **2004**, *23*, 875–882.

- (137) Bai, L.; Wang, J.-X. Reusable, Polymer-Supported, Palladium-Catalyzed, Atom-Efficient Coupling Reaction of Aryl Halides with Sodium Tetraphenylborate in Water by Focused Microwave Irradiation. *Adv. Synth. Catal.* **2008**, *350*, 315–320.
- (138) Colacot, T. J.; Gore, E. S.; Kuber, A. High-Throughput Screening Studies of Fiber-Supported Catalysts Leading to Room-Temperature Suzuki Coupling. *Organometallics* **2002**, *21*, 4295–4298.
- (139) Wang, Y.; Sauer, D. R. Use of Polymer-Supported Pd Reagents for Rapid and Efficient Suzuki Reactions Using Microwave Heating. *Org. Lett.* **2004**, *6*, 2793–2796.
- (140) Shieh, W.-C.; Shekhar, R.; Blacklock, T.; Tedesco, A. A Simple, Recyclable, Polymer-Supported Palladium Catalyst for Suzuki Coupling—an Effective Way To Minimize Palladium Contamination. *Synth. Commun.* **2002**, *32*, 1059–1067.
- (141) Parrish, C. A.; Buchwald, S. L. Use of Polymer-Supported Dialkylphosphinobiphenyl Ligands for Palladium-Catalyzed Amination and Suzuki Reactions Phenyl Ligands Has Enhanced the Efficiency of Various. *J. Org. Chem.* **2001**, 3820–3827.
- (142) an der Heiden, M.; Plenio, H. Homogeneous Catalysts Supported on Soluble Polymers: Biphasic Suzuki-Miyaura Coupling of Aryl Chlorides Using Phase-Tagged Palladium-Phosphine Catalysts. *Chem Eur J* **2004**, *10*, 1789–1797.
- (143) Datta, A.; Plenio, H.; Chemie, P.; Darmstadt, T. U. Nonpolar Biphasic Catalysis : Sonogashira and Suzuki Coupling of Aryl Bromides and Chlorides. *Chem Commun* **2003**, 1504–1505.
- (144) Datta, A.; Ebert, K.; Plenio, H. Nanofiltration for Homogeneous Catalysis Separation : Soluble Polymer-Supported Palladium Catalysts for Heck , Sonogashira , and Suzuki Coupling of Aryl Halides. *Organometallics* **2003**, 4685–4691.
- (145) Yamada, Y. M.; Ichinohe, M.; Takahashi, H.; Ikegami, S. Development of a New Triphase Catalyst and Its Application to the Epoxidation of Allylic Alcohols. *Org. Lett.* **2001**, *3*, 1837–1840.
- (146) Yamada, Y. M. A.; Takeda, K.; Takahashi, H.; Ikegami, S. An Assembled Complex of Palladium and Non-Cross-Linked Amphiphilic Polymer: A Highly Active and Recyclable Catalyst for the Suzuki-Miyaura Reaction. *Org. Lett.* **2002**, *4*, 3371–3374.

- (147) Yamada, Y. M. a; Takeda, K.; Takahashi, H.; Ikegami, S. Highly Active Catalyst for the Heterogeneous Suzuki-Miyaura Reaction: Assembled Complex of Palladium and Non-Cross-Linked Amphiphilic Polymer. *J. Org. Chem.* **2003**, *68*, 7733–7741.
- (148) Schwarz, J.; Bohm, V.; Gardiner, M.; Grosche, M.; Herrmann, W. A.; Hieringer, W.; Raudaschl-Sieber, G. Polymer-Supported Carbene Complexes of Palladium: Well-Defined, Air-Stable, Recyclable Catalysts for the Heck Reaction. *Chem. Eur. J.* **1999**, 1773–1780.
- (149) Byun, J.-W.; Lee, Y.-S. Preparation of Polymer-Supported palladium/N-Heterocyclic Carbene Complex for Suzuki Cross-Coupling Reactions. *Tetrahedron Lett.* **2004**, *45*, 1837–1840.
- (150) Kim, J.; Kim, J.; Lee, D.; Lee, Y. Amphiphilic Polymer Supported N -Heterocyclic Carbene Palladium Complex for Suzuki Cross-Coupling Reaction in Water. *Tetrahedron Lett.* **2006**, *47*, 4745–4748.
- (151) Lee, D.-H.; Kim, J.-H.; Jun, B.-H.; Kang, H.; Park, J.; Lee, Y.-S. Macroporous Polystyrene-Supported Palladium Catalyst Containing a Bulky N-Heterocyclic Carbene Ligand for Suzuki Reaction of Aryl Chlorides. *Org. Lett.* **2008**, *10*, 1609–1612.
- (152) De Vos, D. E.; Dams, M.; Sels, B. F.; Jacobs, P. A. Ordered Mesoporous and Microporous Molecular Sieves Functionalized with Transition Metal Complexes as Catalysts for Selective Organic Transformations. *Chem. Rev.* **2002**, *102*, 3615–3640.
- (153) Ranganath, K. V. S.; Onitsuka, S.; Kumar, A. K.; Inanaga, J. Recent Progress of N-Heterocyclic Carbenes in Heterogeneous Catalysis. *Catal. Sci. Technol.* **2013**, *3*, 2161.
- (154) Litschauer, M.; Neouze, M.-A. SiO₂ Units Networking through Ionic Liquid-like Bridges. *Monatshefte für Chemie* **2008**, *139*, 1151–1156.
- (155) Litschauer, M.; Neouze, M.-A. Nanoparticles Connected through an Ionic Liquid-like Network. *J. Mater. Chem.* **2008**, *18*, 640.
- (156) Cai, M.-Z.; Zhao, H.; Zhang, R. Heck Arylation of Acrylonitrile with Aryl Iodides Catlyzed by a Silica-Bound Arsine Palladium(0) Complex. *Chinese Chem. Lett.* **2005**, 449–452.

- (157) Cai, M.; Liu, G.; Zhou, J. Synthesis of Silica-Supported Poly- Ω -(methylseleno)undecylsiloxane palladium(0) Complex and Its Catalytic Properties for Heck Arylation of Alkenes. *J. Mol. Catal. A Chem.* **2005**, *227*, 107–111.
- (158) Cai, M.-Z.; Song, C.-S.; Huang, X. An Efficient Coupling of Aryl Iodides with Terminal Alkynes Catalyzed by Silica-Supported Sulfur Palladium(0) Complex. *Synth. Commun.* **1997**, *27*, 1935–1942.
- (159) Cai, M.-Z.; Song, C.-S.; Huang, X. Silica-Supported Phosphine Palladium(0) Complex Catalyzed Phenylation of Acid Chlorides and Aryl Iodides by Sodium Tetraphenylborate. *Synth. Commun.* **1998**, *28*, 693–700.
- (160) Cai, M.-Z.; Song, C.-S.; Huang, X. Silica-Supported Phosphine Palladium(0) Complex Catalysed Cross-Coupling of Organic Halides with Organotin and Organomagnesium Reagents. *J. Chem. Res.* **1998**, 264–265.
- (161) Tyrrell, E.; Al-Saardi, A.; Millet, J. A Novel Silica-Supported Palladium Catalyst for a Copper-Free Sonogashira Coupling Reaction. *Synlett* **2005**, *1*, 487–488.
- (162) Tyrrell, E.; Whiteman, L.; Williams, N. Sonogashira Cross-Coupling Reactions and Construction of the Indole Ring System Using a Robust, Silica-Supported Palladium Catalyst. *Synthesis (Stuttg.)* **2009**, *2009*, 829–835.
- (163) Chen, W.; Li, P.; Wang, L. Silica Supported Palladium-Phosphine Complex: Recyclable Catalyst for Suzuki–Miyaura Cross-Coupling Reactions at Ambient Temperature. *Tetrahedron* **2011**, *67*, 318–325.
- (164) Wang, L.; Reis, A.; Seifert, A.; Philippi, T.; Ernst, S.; Jia, M.; Thiel, W. R. A Simple Procedure for the Covalent Grafting of Triphenylphosphine Ligands on Silica: Application in the Palladium Catalyzed Suzuki Reaction. *Dalton Trans.* **2009**, 3315–3320.
- (165) Fukaya, N.; Onozawa, S.; Ueda, M.; Miyaji, T.; Takagi, Y.; Sakakura, T.; Yasuda, H. Palladium Phosphine Complex Catalysts Immobilized on Silica via a Tripodal Linker Unit for the Suzuki–Miyaura Coupling Reactions of Aryl Chlorides. *J. Mol. Catal. A Chem.* **2014**, *385*, 7–12.
- (166) Zhao, Y.; Zhou, Y.; Ma, D.; Liu, J.; Li, L.; Zhang, T. Y.; Zhang, H. Suzuki Cross-Coupling Mediated by Tetradentate N-Heterocyclic Carbene (NHC)-Palladium Complexes in an Environmentally Benign Solvent. *Org. Biomol. Chem.* **2003**, *1*, 1643–1646.

- (167) Gurbuz, N.; Ozdemir, I.; Cetinkaya, B.; Seckin, T. Silica-Supported 3-4,5-Dihydroimidazol-1-yl-propyltriethoxysilanedichloropalladium(II) Complex: Heck and Suzuki Cross-Coupling Reactions. *Appl. Organomet. Chem.* **2003**, *17*, 776–780.
- (168) Gurbuz, N.; Seckin, T.; Cetinkaya, B.; Ozdemir, I. Surface Modification of Inorganic Oxide Particles with a Carbene Complex of Palladium : A Recyclable Catalyst for the Suzuki Reaction. *J. Inorg. Organomet. Polym.* **2004**, *14*, 149–159.
- (169) Karimi, B.; Enders, D. New N-Heterocyclic Carbene Palladium Complex/ionic Liquid Matrix Immobilized on Silica: Application as Recoverable Catalyst for the Heck Reaction. *Org. Lett.* **2006**, *8*, 1237–1240.
- (170) Aksin, Ö.; Türkmen, H.; Artok, L.; Çetinkaya, B.; Ni, C.; Büyükgüngör, O.; Özkal, E. Effect of Immobilization on Catalytic Characteristics of Saturated Pd-N-Heterocyclic Carbenes in Mizoroki–Heck Reactions. *J. Organomet. Chem.* **2006**, *691*, 3027–3036.
- (171) Qiu, H.; Sarkar, S. M.; Lee, D.-H.; Jin, M.-J. Highly Effective Silica Gel-Supported N-Heterocyclic carbene–Pd Catalyst for Suzuki–Miyaura Coupling Reaction. *Green Chem.* **2008**, *10*, 37–40.
- (172) Lee, S.-M.; Yoon, H.-J.; Kim, J.-H.; Chung, W.-J.; Lee, Y.-S. Highly Active Organosilane-Based N-Heterocyclic Carbene-Palladium Complex Immobilized on Silica Particles for the Suzuki Reaction. *Pure Appl. Chem.* **2007**, *79*, 1553–1559.
- (173) Tandukar, S.; Sen, A. N-Heterocyclic Carbene–palladium Complex Immobilized on Silica Nanoparticles. *J. Mol. Catal. A Chem.* **2007**, *268*, 112–119.
- (174) Polshettiwar, V.; Varma, R. S. Pd–N-Heterocyclic Carbene (NHC) Organic Silica: Synthesis and Application in Carbon–carbon Coupling Reactions. *Tetrahedron* **2008**, *64*, 4637–4643.
- (175) Tyrrell, E.; Whiteman, L.; Williams, N. The Synthesis and Characterisation of Immobilised Palladium Carbene Complexes and Their Application to Heterogeneous Catalysis. *J. Organomet. Chem.* **2011**, *696*, 3465–3472.
- (176) Gruber-Woelfler, H.; Radaschitz, P. F.; Feenstra, P. W.; Haas, W.; Khinast, J. G. Synthesis, Catalytic Activity, and Leaching Studies of a Heterogeneous Pd-Catalyst Including an Immobilized Bis(oxazoline) Ligand. *J. Catal.* **2012**, *286*, 30–40.

- (177) Wolfson, A.; Dlugy, C. Palladium-Catalyzed Heck and Suzuki Coupling in Glycerol. *Chem. Pap.* **2007**, *61*, 228–232.
- (178) Lamblin, M.; Nassar-Hardy, L.; Hierso, J.-C.; Fouquet, E.; Felpin, F.-X. Recyclable Heterogeneous Palladium Catalysts in Pure Water: Sustainable Developments in Suzuki, Heck, Sonogashira and Tsuji-Trost Reactions. *Adv. Synth. Catal.* **2010**, *352*, 33–79.
- (179) Uozumi, Y.; Danjo, H.; Hayashi, T. Cross-Coupling of Aryl Halides and Allyl Acetates with Arylboron Reagents in Water Using an Amphiphilic Resin-Supported Palladium Catalyst. *J. Org. Chem.* **1999**, 3384–3388.
- (180) Uozumi, Y.; Nakai, Y. An Amphiphilic Resin-Supported Palladium Catalyst for High-Throughput Cross-Coupling in Water. *Org. Lett.* **2002**, *4*, 2997–3000.
- (181) Yamada, Y. M. A.; Maeda, Y.; Uozumi, Y. Novel 3D Coordination Palladium-Network Complex: A Recyclable Catalyst for Suzuki-Miyaura Reaction. *Org. Lett.* **2006**, *8*, 4259–4262.
- (182) Phan, N. T. S.; Van Der Sluys, M.; Jones, C. W. On the Nature of the Active Species in Palladium Catalyzed Mizoroki–Heck and Suzuki–Miyaura Couplings – Homogeneous or Heterogeneous Catalysis, A Critical Review. *Adv. Synth. Catal.* **2006**, *348*, 609–679.
- (183) Sheldon, R. a.; Wallau, M.; Arends, I. W. C. E.; Schuchardt, U. Heterogeneous Catalysts for Liquid-Phase Oxidations: Philosophers’ Stones or Trojan Horses? *Acc. Chem. Res.* **1998**, *31*, 485–493.
- (184) Anton, D. R.; Crabtree, R. H. Dibenzo[a,e]cyclooctatetraene in a Proposed Test for Heterogeneity in Catalysts Formed from Soluble Platinum-Group Metal Complexes. *Organometallics* **1983**, *2*, 855–859.
- (185) Consorti, C. S.; Flores, R.; Dupont, J.; Alegre, P.; Brazil, R. S. Kinetics and Mechanistic Aspects of the Heck Reaction Promoted by a CN - Palladacycle Most Important and Investigated Classes of Organometallic. *J. Am. Chem. Soc* **2005**, 12054–12065.
- (186) Arvela, R. K.; Leadbeater, N. E.; Sangi, M. S.; Williams, V. A.; Granados, P.; Singer, R. D. A Reassessment of the Transition-Metal Free Suzuki-Type Coupling Methodology. *J. Org. Chem.* **2005**, *70*, 161–168.

- (187) Gruber, A. S.; Pozebon, D.; Monteiro, A. L. On the Use of Phosphine-Free $\text{PdCl}_2(\text{SEt}_2)_2$ Complex as Catalyst Precursor for the Heck Reaction. *Tetrahedron Lett.* **2001**, *42*, 7345–7348.
- (188) Kashin, A. S.; Ananikov, V. P. Catalytic C-C and C-Heteroatom Bond Formation Reactions: In Situ Generated or Preformed Catalysts? Complicated Mechanistic Picture behind Well-Known Experimental Procedures. *J. Org. Chem.* **2013**, *78*, 11117–11125.
- (189) Vries, H. M. De; Parlevliet, F. J.; De, L. S.; Mommers, J. H. M.; Henderickx, H. J. W.; Monique, A. M.; Vries, G. De. A Practical Recycle of a Ligand-Free Palladium Catalyst for Heck Reactions. *Adv. Synth. Catal.* **2002**, 996–1002.
- (190) De Vries, A. H. M.; Mulders, J. M. C. a; Mommers, J. H. M.; Henderickx, H. J. W.; de Vries, J. G. Homeopathic Ligand-Free Palladium as a Catalyst in the Heck Reaction. A Comparison with a Palladacycle. *Org. Lett.* **2003**, *5*, 3285–3288.
- (191) Ananikov, V. P.; Beletskaya, I. P. Toward the Ideal Catalyst: From Atomic Centers to a “Cocktail” of Catalysts. *Organometallics* **2012**, *31*, 1595–1604.
- (192) Miyaura, N.; Suzuki, A. Palladium-Catalyzed Cross-Coupling Reactions. *Chem Rev* **1995**, *95*, 2457–2483.
- (193) Magano, J.; Dunetz, J. R. Large-Scale Applications of Transition Metal-Catalyzed Couplings for the Synthesis of Pharmaceuticals. *Chem. Rev.* **2011**, *111*, 2177–2250.
- (194) Torborg, C.; Beller, M. Recent Applications of Palladium-Catalyzed Coupling Reactions in the Pharmaceutical, Agrochemical, and Fine Chemical Industries. *Adv. Synth. Catal.* **2009**, *351*, 3027–3043.
- (195) Corbet, J.-P.; Mignani, G. Selected Patented Cross-Coupling Reaction Technologies. *Chem. Rev.* **2006**, *106*, 2651–2710.
- (196) Nicolaou, K. C.; Bulger, P. G.; Sarlah, D. Palladium-Catalyzed Cross-Coupling Reactions in Total Synthesis. *Angew. Chemie* **2005**, *44*, 4442–4489.
- (197) Chen, M.; Vicic, D. A.; Turner, M. L.; Navarro, O. (N-Heterocyclic Carbene) $\text{PdCl}_2(\text{TEA})$ Complexes : Studies on the Effect of the “Throw-Away” Ligand in Catalytic Activity. *Organometallics* **2011**, *30*, 5052–5056.
- (198) Organ, M. G.; Avola, S.; Dubovyk, I.; Hadei, N.; Kantchev, E. A. B.; O’Brien, C. J.; Valente, C. A User-Friendly, All-Purpose Pd-NHC (NHC=N-Heterocyclic

Carbene) Precatalyst for the Negishi Reaction: A Step towards a Universal Cross-Coupling Catalyst. *Chem Eur J* **2006**, *12*, 4749–4755.

- (199) Zhou, X.-X.; Shao, L.-X. N-Heterocyclic Carbene/Pd(II)/1-Methylimidazole Complex Catalyzed Suzuki-Miyaura Coupling Reaction of Aryl Chlorides in Water. *Synthesis (Stuttg)*. **2011**, *2011*, 3138–3142.
- (200) Miura, M. Rational Ligand Design in Constructing Efficient Catalyst Systems for Suzuki-Miyaura Coupling. *Angew. Chemie* **2004**, *43*, 2201–2203.
- (201) Li, H.; Johansson Seechurn, C. C. C.; Colacot, T. J. Development of Preformed Pd Catalysts for Cross-Coupling Reactions, Beyond the 2010 Nobel Prize. *ACS Catal.* **2012**, *2*, 1147–1164.
- (202) Ganapathy, D.; Sekar, G. Palladium Nanoparticles Stabilized by Metal–carbon Covalent Bond: An Efficient and Reusable Nanocatalyst in Cross-Coupling Reactions. *Catal. Commun.* **2013**, *39*, 50–54.
- (203) Samarasimhareddy, M.; Prabhu, G.; Vishwanatha, T.; Sureshbabu, V. PVC-Supported Palladium Nanoparticles: An Efficient Catalyst for Suzuki Cross-Coupling Reactions at Room Temperature. *Synthesis (Stuttg)*. **2013**, *45*, 1201–1206.
- (204) Shendage, S. S.; Patil, U. B.; Nagarkar, J. M. Electrochemical Synthesis and Characterization of Palladium Nanoparticles on Nafion–graphene Support and Its Application for Suzuki Coupling Reaction. *Tetrahedron Lett.* **2013**, *54*, 3457–3461.
- (205) Karimi, B.; Fadavi Akhavan, P. A Novel Water-Soluble NHC-Pd Polymer: An Efficient and Recyclable Catalyst for the Suzuki Coupling of Aryl Chlorides in Water at Room Temperature. *Chem. Commun.* **2011**, *47*, 7686–7688.
- (206) Karimi, B.; Akhavan, P. F. A Study on Applications of N-Substituted Main-Chain NHC-Palladium Polymers as Recyclable Self-Supported Catalysts for the Suzuki-Miyaura Coupling of Aryl Chlorides in Water. *Inorg. Chem.* **2011**, *50*, 6063–6072.
- (207) Langecker, J.; Rehahn, M. Iridium-Functionalized Polyfluorenes: Advantages and Limitations of the Suzuki and Yamamoto Approaches. *Macromol. Chem. Phys.* **2008**, *209*, 258–271.
- (208) Wei, S.; Ma, Z.; Wang, P.; Dong, Z.; Ma, J. Anchoring of Palladium (II) in Functionalized SBA-16: An Efficient Heterogeneous Catalyst for Suzuki Coupling Reaction. *J. Mol. Catal. A Chem.* **2013**, *370*, 175–181.

- (209) Flapper, J.; Reek, J. N. H. Templated Encapsulation of Pyridyl-Bian Palladium Complexes: Tunable Catalysts for CO/4-Tert-Butylstyrene Copolymerization. *Angew. Chemie* **2007**, *46*, 8590–8592.
- (210) Khalafi-Nezhad, A.; Panahi, F. Immobilized Palladium Nanoparticles on Silica–starch Substrate (PNP–SSS): As a Stable and Efficient Heterogeneous Catalyst for Synthesis of P-Teraryls Using Suzuki Reaction. *J. Organomet. Chem.* **2012**, *717*, 141–146.
- (211) Crisóstomo-Lucas, C.; Toscano, R. A.; Morales-Morales, D. Synthesis and Characterization of New Potentially Hydrosoluble Pincer Ligands and Their Application in Suzuki–Miyaura Cross-Coupling Reactions in Water. *Tetrahedron Lett.* **2013**, *54*, 3116–3119.
- (212) Yu, K.; Sommer, W.; Richardson, J.; Weck, M.; Jones, C. Evidence That SCS Pincer Pd(II) Complexes Are Only Precatalysts in Heck Catalysis and the Implications for Catalyst Recovery and Reuse. *Adv. Synth. Catal.* **2005**, *347*, 161–171.
- (213) Kyriakou, G.; Beaumont, S. K.; Humphrey, S. M.; Antonetti, C.; Lambert, R. M. Sonogashira Coupling Catalyzed by Gold Nanoparticles: Does Homogeneous or Heterogeneous Catalysis Dominate? *ChemCatChem* **2010**, *2*, 1444–1449.
- (214) Butorac, R. R.; Al-Deyab, S. S.; Cowley, A. H. Antimicrobial Properties of Some Bis(iminoacenaphthene (BIAN)-Supported N-Heterocyclic Carbene Complexes of Silver and Gold. *Molecules* **2011**, *16*, 2285–2292.
- (215) Svejda, S. A.; Brookhart, M.; Hill, C.; Carolina, N. Ethylene Oligomerization and Propylene Dimerization Using Cationic (r-Diimine) Nickel (II) Catalysts. *Organometallics* **1999**, *18*, 65–74.
- (216) Tu, T.; Fang, W.; Jiang, J. A Highly Efficient Precatalyst for Amination of Aryl Chlorides: Synthesis, Structure and Application of a Robust Acenaphthoimidazolylidene Palladium Complex. *Chem. Commun.* **2011**, *47*, 12358–12360.
- (217) Fang, W.; Jiang, J.; Xu, Y.; Zhou, J.; Tu, T. Novel Robust Benzimidazolylidene Palladium Complexes: Synthesis, Structure, and Catalytic Applications in Amination of Chloroarenes. *Tetrahedron* **2013**, *69*, 673–679.
- (218) Tu, T.; Sun, Z.; Fang, W.; Xu, M.; Zhou, Y. Robust Acenaphthoimidazolylidene Palladium Complexes: Highly Efficient Catalysts for Suzuki–Miyaura Couplings with Sterically Hindered Substrates. *Org. Lett.* **2012**, *14*, 4250–4253.

- (219) Merino, E.; Poli, E.; Díaz, U.; Brunel, D. Synthesis and Characterization of New Ruthenium N-Heterocyclic Carbene Hoveyda II-Type Complexes. Study of Reactivity in Ring Closing Metathesis Reactions. *Dalton Trans.* **2012**, *41*, 10913–10918.
- (220) Schmidt, A. F.; Smirnov, V. V. Simple Method for Enhancement of the Ligand-Free Palladium Catalyst Activity in the Heck Reaction with Non-Activated Bromoarenes. *J. Mol. Catal. A Chem.* **2003**, *203*, 75–78.
- (221) Schmidt, A. F.; Smirnov, V. V. Concept of “Magic” Number Clusters as a New Approach to the Interpretation of Unusual Kinetics of the Heck Reaction with Aryl Bromides. *Top. Catal.* **2005**, *32*, 71–75.
- (222) Widegren, J. A.; Finke, R. G. A Review of the Problem of Distinguishing True Homogeneous Catalysis from Soluble or Other Metal-Particle Heterogeneous Catalysis under Reducing Conditions. *J. Mol. Catal. A Chem.* **2003**, *198*, 317–341.
- (223) Pröckl, S. S.; Kleist, W.; Gruber, M. A.; Köhler, K. In Situ Generation of Highly Active Dissolved Palladium Species from Solid Catalysts-a Concept for the Activation of Aryl Chlorides in the Heck Reaction. *Angew. Chemie* **2004**, *43*, 1881–1882.
- (224) Köhler, K.; Kleist, W.; Pröckl, S. S. Genesis of Coordinatively Unsaturated Palladium Complexes Dissolved from Solid Precursors during Heck Coupling Reactions and Their Role as Catalytically Active Species. *Inorg. Chem.* **2007**, *46*, 1876–1883.
- (225) Nobre, S. M.; Wolke, S. I.; da Rosa, R. G.; Monteiro, A. L. Simple and Efficient Protocol for Catalyst Recycling and Product Recovery in the Pd-Catalyzed Homogeneous Suzuki Reaction. *Tetrahedron Lett.* **2004**, *45*, 6527–6530.
- (226) Crawford, K. A.; Cowley, A. H.; Humphrey, S. M. Bis(imino)acenaphthene (BIAN)-Supported Palladium(ii) Carbene Complexes as Effective C–C Coupling Catalysts and Solvent Effects in Organic and Aqueous Media. *Catal. Sci. Technol.* **2014**.
- (227) Scholl, M.; Ding, S.; Lee, C. W.; Grubbs, R. H. Synthesis and Activity of a New Generation of Ruthenium-Based Olefin Metathesis Catalysts Coordinated with 1,3-Dimesityl-4,5-Dihydroimidazol-2-Ylidene Ligands. *Org. Lett.* **1999**, *1*, 953–956.

- (228) Samojłowicz, C.; Bieniek, M.; Grela, K. Ruthenium-Based Olefin Metathesis Catalysts Bearing N-Heterocyclic Carbene Ligands. *Chem. Rev.* **2009**, *109*, 3708–3742.
- (229) Paul, S.; Clark, J. H. A Highly Active and Reusable Heterogeneous Catalyst for the Suzuki Reaction: Synthesis of Biaryls and Polyaryls. *Green Chem.* **2003**, *5*, 635.

Vita

Katherine Alexis Crawford was born in Kalamazoo Michigan on June 2, 1986 as the daughter of Craig and Teresa Crawford. She graduated from Portage Central High School in May 2004 and then moved to Ann Arbor, Michigan to attend the University of Michigan. She graduated in May 2008 with a Bachelor of Science in Chemistry and German. In August 2008, she entered the Graduate School of the University of Texas at Austin.

Permanent e-mail address: ktcrawfs@gmail.com

This dissertation was typed by the author.